

**Human peripheral $\gamma\delta$ T cell phenotypic and
functional shift in response to stimulation
with *E.coli***

Marta Barisa

Infection, Immunity and Inflammation Programme
Great Ormond Street Institute of Child Health

A thesis submitted for the degree of Doctor of Philosophy
August 2017

ABSTRACT

It is known that $\gamma\delta$ T cells provide immune-surveillance and host defense against infection and cancer. Our understanding of $\gamma\delta$ T cell functionality and antimicrobial immunity, however, remains poor. Limited data suggests that $\gamma\delta$ T cells can phagocytose particles and act as professional antigen-presenting cells (pAPCs). In order to examine $\gamma\delta$ T cell bacterial interactions, an *ex vivo* co-culture model of human peripheral blood mononuclear cell (PBMC) responses to *Escherichia coli* was employed. Following PBMC stimulation with *E.coli*, V γ 9V δ 2 cells underwent rapid T cell receptor (TCR)-dependent proliferation and functional transition from cytotoxic, inflammatory cytokine immunity, to cell expansion with diminished cytokine but increased costimulatory molecule expression, and capacity for professional phagocytosis. Phagocytosis was augmented by IgG opsonization, and inhibited by TCR-blockade, suggesting a licensing interaction involving the TCR and Fc γ R. V γ 9V δ 2 cells displayed potent cytotoxicity through TCR-dependent and independent mechanisms. V γ 9V δ 2 cell cytokine responses and cytotoxicity further presented with variable sensitivity to blocking of host butyrophilin 3A (BTN3A), in response to both, self and non-self, stimuli. We conclude that i) V γ 9V δ 2 T cells transition from early inflammatory cytotoxic killers to myeloid-like pAPCs in response to infectious stimuli, and that ii) V γ 9V δ 2 T cell recognition of targets is predominantly governed by TCR recognition of self stress markers in a BTN3A-dependent manner.

DECLARATION

I, Marta Barisa, confirm that the work presented in this thesis is my own. Where information has been derived from other sources, I confirm that this has been indicated as such in the thesis.

ACKNOWLEDGEMENTS

Thank you, Kenth, John and Mona, for your support and bottomless patience. Under your watchful eye and the safety of your wing, my pursuit of a career in research commences.

Paldies arī maniem mīļajiem vecākiem!

Paldies par ticību maniem spēkiem, par pacietību, par padomu, par plecu un smaidu. Šis ceļš, ko eju, ir bijis iespējams dēļ jūsu mīlestības un atbalsta. Varu tikai cerēt, ka došu jums ar ko lepoties.

TABLE OF CONTENTS

ABSTRACT.....	2
DECLARATION	3
ACKNOWLEDGEMENTS	4
TABLE OF CONTENTS.....	5
LIST OF TABLES	8
ABBREVIATIONS.....	9
1. INTRODUCTION.....	12
1.1. Introduction to $\gamma\delta$ T cells.....	12
1.2. $\gamma\delta$ T cells in health and disease	16
1.3. $\gamma\delta$ T cells as professional antigen presenting cells	18
1.4. Phagocytosis	21
1.5. $\gamma\delta$ T cell recall and memory	24
1.6. Categorisation of $\gamma\delta$ T cell subsets	31
1.7. Role of the TCR in $\gamma\delta$ T cell physiology.....	33
1.8. Role of the BTN3A in $\gamma\delta$ T cell physiology.....	42
1.9. $\gamma\delta$ T cells as a tool in immunotherapy	52
1.10. Aims of the project	53
2. MATERIALS AND METHODS.....	54
2.1. Study Design	54
2.2. Statistical analysis	55
2.3. Sample acquisition and preparation.....	55
2.4. Growth and preparation of <i>E.coli</i> DH5 α	57
2.5. <i>E.coli</i> opsonisation	57
2.6. PBMC stimulation with UV-irradiated <i>E.coli</i>	57
2.7. PBMC stimulation with zoledronate	58
2.8. FACS staining and processing.....	58
2.9. Confocal imaging of $\gamma\delta$ T cell uptake of <i>E.coli</i>	61
2.10. Confocal imaging of $\gamma\delta$ T cell uptake of <i>E.coli</i>	61

2.11.	<i>E.coli</i> FITC uptake assay	62
2.12.	<i>E.coli</i> pHrodo acidification assay	63
2.13.	Meso Scale Discovery electrochemiluminescence assay	64
2.14.	Sequencing of $\gamma\delta$ TCR CDR3	65
2.15.	Spectratyping of $\gamma\delta$ TCR CDR3	65
2.16.	Confocal imaging of <i>E.coli</i> -expanded $\gamma\delta$ T cell morphology	65
2.17.	$\gamma\delta$ T cell sorting by flow cytometry	66
2.18.	$\gamma\delta$ T cell antigen presentation assay	66
2.19.	Expanded $\gamma\delta$ T cell re-stimulation with <i>E.coli</i> in the presence of autologous 'helper' cells	68
2.20.	$\gamma\delta$ T cell bactericidal activity against <i>E.coli</i>	69
2.21.	$\gamma\delta$ T cell bead phagocytosis assay	70
2.22.	$\gamma\delta$ TCR blocking	70
2.23.	BTN3A staining and blocking	70
2.24.	PBMC responder stimulation with autologous cells in the presence of BTN3A and $\gamma\delta$ TCR blocking	71
2.25.	PBMC responder stimulation with THP-1 cells in the presence of BTN3A and $\gamma\delta$ TCR blocking	73
3.	$\gamma\delta$ T CELL ACQUISITION OF PHAGOCYTOTIC CAPACITY	75
3.1.	Aims	75
3.2.	Zoledronate-expanded $\gamma\delta$ T cells take up IgG-opsonized 1.0 μ m beads and <i>E.coli</i> 75	
3.3.	<i>E. coli</i> -expanded, but not freshly-isolated $\gamma\delta$ T cells, take up IgG-opsonized <i>E.coli</i> 79	
3.4.	Discussion	87
3.5.	Summary	92
4.	<i>E.COLI</i> AND ZOLEDRONATE PROMOTE EXPANSION OF PHENOTYPICALLY EQUIVALENT $\gamma\delta$ T CELL POPULATIONS	93
4.1.	Aims	93
4.2.	<i>E.coli</i> and zoledronate stimulation induces sustained $\gamma\delta$ T cell upregulation of HLA-DR and CD86	94
4.3.	<i>E.coli</i> and zoledronate stimulation induces transient $\gamma\delta$ T cell upregulation of CCR7 and downregulation of CD62L	97
4.4.	<i>E.coli</i> and zoledronate stimulation lead to expansion of similar populations of $\gamma\delta$ T cells, as well as $\alpha\beta$ T cells and CD3 ^{neg} cells	103
4.5.	<i>E.coli</i> and zoledronate induce significantly different early cytokine environments within stimulated PBMC	111

4.6.	<i>E.coli</i> and zoledronate induce similar V γ 9V δ 2 TCR repertoires	115
4.7.	Discussion.....	119
4.8.	Summary.....	127
5.	$\gamma\delta$ T CELL ACQUISITION OF pAPC PHENOTYPE IS CONCURRENT TO A LOSS OF Th1 INFLAMMATORY PHENOTYPE	128
5.1.	Aims	128
5.2.	$\gamma\delta$ T cells expanded with <i>E.coli</i> or zoledronate display a pAPC effector phenotype	129
5.3.	$\gamma\delta$ T cell expansion leads to a loss of a Th1 inflammatory phenotype.....	136
5.4.	Discussion.....	144
5.5.	Summary.....	147
6.	V δ 2 $\gamma\delta$ T CELL EFFECTOR FUNCTION DEPENDENCE ON THE TCR	148
6.1.	Aims	148
6.2.	Phagocytosis by expanded $\gamma\delta$ T cells is TCR-dependent	148
6.3.	$\gamma\delta$ T cell cytokine production and proliferation in response to <i>E.coli</i> are TCR-dependent, whereas TCR dependence of cytotoxicity appears only partial.....	151
6.4.	Discussion.....	154
6.5.	Summary.....	158
7.	V γ 9 δ 2 $\gamma\delta$ T CELL EFFECTOR FUNCTION DEPENDENCE ON BTN3A	159
7.1.	Aims	159
7.2.	BTN3A is ubiquitously expressed on PBMC.....	159
7.3.	$\gamma\delta$ T cells are activated by autologous pAg-stimulated PBMC.....	162
7.4.	V γ 9V δ 2 cell effector responses to autologous stimulator PBMC are differentially sensitive to blocking of the $\gamma\delta$ TCR and BTN3A	165
7.5.	V γ 9V δ 2 cell effector responses to stimulator THP-1 cells are differentially sensitive to blocking of the $\gamma\delta$ TCR and BTN3A	171
7.6.	Discussion.....	177
7.7.	Summary.....	183
8.	DISCUSSION	184
	REFERENCES.....	194
	SUPPLEMENTARY MEDIA MATERIAL.....	215
	Fig. 5.4. V δ 2 cell expansion leads to their acquisition of a phagocyte-like morphology and probing behaviour.....	215
	APPENDIX	216
	<i>E.coli</i> promotes human V γ 9 δ 2 T cell transition from cytokine-producing bactericidal effectors to professional phagocytic killers in a TCR-dependent manner	216

LIST OF TABLES

Table 1.1 Features of human $\gamma\delta$ T, $\alpha\beta$ T and B cells.....	15
Table 1.2 Features of human $\gamma\delta$ T cell subsets.....	16
Table 1.3 Types of phagocytic receptors.....	24
Table 1.4 Activating ligands for human $\gamma\delta$ T cells	26
Table 1.5 Characteristics of human $\gamma\delta$ T cell clones.....	40
Table 1.6 Characteristics of published anti-BTN3A mAbs	44
Table 2.1 Recipe for complete $\gamma\delta$ T cell culture media.....	57
Table 4.1 Homing receptors of interest to $\gamma\delta$ T cell APC function.....	125

ABBREVIATIONS

APC – antigen presenting cell

APC (in the context of FACS staining only, in the Materials and Methods sections) –

Allophycocyanin

pAPC – professional antigen presenting cell

α - - anti

$\alpha\beta$ T cell – alpha beta T cell

BTN - butyrophilin

BTN3A – butyrophilin 3A

CCR – chemokine receptor

CD – cluster of differentiation

CDR – complementarity-determining region

CFU – colony forming unit

Ctrl – control

CyD – Cytochalasin D

Cy5.5 – Cyanine 5.5

Cy7 – Cyanine 7

C. albicans – *Candida albicans*

C. jejuni – *Campylobacter jejuni*

DAPI - 4',6-diamidino-2-phenylindole

DMSO - Dimethyl sulfoxide

D1-D14 – day 1 to day 14

E.coli – *Eschericia coli*

FITC - Fluorescein isothiocyanate

FcR – Fc receptor

Fc γ R – Fc gamma receptor

GFP – Green Fluorescent Protein

GM-CSF – granulocyte macrophage colony stimulating factor

$\gamma\delta$ T cell – gamma delta T cell

HMBPP - (E)-4-Hydroxy-3-methyl-but-2-enyl pyrophosphate
HCMV – human cytomegalovirus
HLA – human leukocyte antigen
IEL – intraepithelial lymphocyte
IFN – Interferon
Ig - immunoglobulin
IgG – immunoglobulin G
IL – Interleukin
iNKT – invariant natural killer T cell
IPP – isopentenyl pyrophosphate
IPTG - Isopropyl β -D-1-thiogalactopyranoside
Iso – isotype control
ITAM - Immunoreceptor tyrosine-based activation motif
LCK – lymphocyte-specific protein tyrosine kinase
L. monocytogenes – *Lysteria monocytogenes*
MFI – median fluorescence intensity
MHC – major histocompatibility complex
MICA - MHC class I chain-related A
M. morganii - *Morganella morganii*
M. tuberculosis – *Mycobacterium tuberculosis*
neg – negative
NK – natural killer cell
NKG2D - Natural Killer Group 2D receptor
NKT – natural killer T cell
Ops. – opsonized (usually IgG-opsonized)
O/N – overnight
OD – optical density
pAg – phosphoantigen
PBMC – peripheral blood mononuclear cells
PE – Phycoerythrin
PMN – polymorphonuclear cells
pos – positive
PRR – pattern recognition receptor
P. falciparum – *Plasmodium falciparum*

S. typhimurium - *Salmonella typhimurium*

S. aureus – *Staphylococcus aureus*

TB – Trypan Blue

TCR – T cell receptor

Th1- Th1 T helper cell

Th2 – Th2 T helper cell

Th17 – Th17 T helper cell

TLR – toll-like receptor

TM – transmembrane region

TNF – tumour necrosis factor

Treg – regulatory T cell

T. gondii – *Toxoplasma gondii*

UV - ultraviolet radiation

w/ - with

Zol. - zoledronate

1. INTRODUCTION

Gamma delta T ($\gamma\delta$ T) cells are an atypical subset of CD3^{pos} lymphocytes with heterogeneous phenotypic patterns, effector functions and anatomical distribution that differ significantly from canonical alpha beta T ($\alpha\beta$ T) cells. Recent immunotherapeutic insights have highlighted $\gamma\delta$ T cells as an attractive putative tool against malignancy and infectious disease. Particular attention in this context has been given to the unusual capacity of $\gamma\delta$ T cells to act as both cytotoxic effectors against target cells and professional antigen presenting cells (pAPCs) to $\alpha\beta$ T cells. The following thesis presents an *ex vivo* experimental investigation of peripheral human $\gamma\delta$ T cell cytokine, cytotoxic and pAPC effector phenotype in response to various antigenic challenges, and the molecular factors that regulate it, therein.

A significant portion of the data contained within this thesis has been published in a June 2017 issue of *Scientific Reports* journal. The article, titled “*E. coli* promotes human V γ 9V δ 2 T cell transition from cytokine producing bactericidal effectors to professional phagocytic killers in a TCR-dependent manner”, can be viewed in the Appendix section.

1.1. Introduction to $\gamma\delta$ T cells

Expressing a T cell receptor (TCR) composed of γ and δ chains, $\gamma\delta$ T cells comprise between 1% and 20% of the human peripheral T cell compartment, and up to 50% of epithelial lymphocytes. Often referred to in the literature as “innately-adaptive” lymphocytes (1), $\gamma\delta$ T cells are characterized by potent and rapid pro-inflammatory cytokine release and cytotoxicity upon stimulation, which is nonetheless paired with a lymphoid-like capacity for extensive clonal expansion (2–4). Some 70% of $\gamma\delta$ T cells are CD4^{neg}CD8^{neg}; the remainder are largely CD4^{neg}CD8^{pos}, with a CD4^{pos}CD8^{neg} phenotype

a rarity. Whilst their baseline clonality remains controversial, it is thought that $\gamma\delta$ T cells have a predominantly oligoclonal rather than polyclonal TCR repertoire, which may underlie their swift and potent responses to primary antigenic stimulation (5,6).

$\gamma\delta$ T cells undergo a distinct developmental process. Unlike their classic, well-characterized counterparts – peripheral $\alpha\beta$ T cells - $\gamma\delta$ T cells appear to develop in several waves, the first of which is already evident in the prenatal thymus (reviewed by Vantourout and Hayday(7)). “Innate-like” CD27^{pos} and CD27^{neg} $\gamma\delta$ T cells, possibly derived from foetal liver progenitors and characterized by secretion of interferon- γ (IFN- γ) and interleukin 17 (IL-17), respectively, have been detected in the prenatal thymus of both, mouse and man (7). A second wave of bone marrow-derived “lymphoid-like” $\gamma\delta$ T cells appears to emerge postnatally with a proposed default potential for the production of IFN- γ . In a significant deviation from $\alpha\beta$ T cell development, some $\gamma\delta$ T cells then migrate to distinct anatomical locations, rather than entering lymphatic re-circulation; human and mouse “innate-like” $\gamma\delta$ T cells have a particular propensity for epithelial sites, such as the gastrointestinal mucosa and skin, whilst “lymphoid-like” $\gamma\delta$ T cells reside mostly within systemic circulation (7).

A summary of the basic features, shared and divergent, between the main human adaptive lymphocyte cell types - $\gamma\delta$ T cells, $\alpha\beta$ T cells and B cells – can be viewed in Table 1.1. Anatomical distribution, surface marker expression, cytokine secretion and proliferative behaviour have been used as a basis for differential $\gamma\delta$ T cell investigation and discussion in the literature. Perhaps the most basic and frequently used of these divisions relies on anatomical localization, with relatively scarce “lymphoid-like” $\gamma\delta$ T cells residing in suspension within the circulatory system, and highly abundant “innate-like” $\gamma\delta$ T cells residing at mucosal epithelial sites, largely as intraepithelial lymphocytes (IELs) (7).

Table 1.1 | Features of human $\gamma\delta$ T, $\alpha\beta$ T and B cells

Characteristic	$\alpha\beta$ T cells	$\gamma\delta$ T cells	B cells
Antigen-receptor configuration	CD3 complex + $\alpha\beta$ TCR	CD3 complex + $\gamma\delta$ TCR	Immunoglobulin (Ig)
Theoretical receptor number	$\sim 10^{15}$	$\sim 10^{20}$	$\sim 10^{11}$
Antigen recognition	Peptide + MHC	Protein and non-protein	Protein and non-protein
Antigen restriction	Yes	Rare	No
Phenotype	CD4 ^{pos} or CD8 ^{pos}	Mostly CD4 ^{neg} CD8 ^{neg} ; some IEL are CD8(α) ^{pos}	CD19 ^{pos} CD20 ^{pos}
Frequency in blood	65-75%	1-10% (25-60% in gut)	5-10%
Distribution	Blood and lymphoid tissue	Blood, lymphoid and epithelial/mucosal tissue	Blood and lymphoid tissue
Effector capability	Cytotoxicity (CD8 ^{pos}), Cytokine release (Th1/Th2/Th17)	Cytotoxicity, Cytokine release (Th1>Th17>Th2)	Ig production
Function	Immune protection and pathogen eradication	Immunoregulation and immunosurveillance	Humoral immunity

Adapted from Carding and Egan (2002) (8)

Human $\gamma\delta$ T cells are further often denoted based on their respective use of V δ TCR chains. In most healthy human adults the peripheral $\gamma\delta$ T cell compartment is dominated by V δ 2 cells, whereas the predominant $\gamma\delta$ TCR^{pos} IEL population are V δ 1 cells. There are a number of further V δ chains employed by both peripheral and tissue-resident, $\gamma\delta$ T cells, but these rare populations are poorly understood and are often referred to simply as V δ 1⁻ V δ 2⁻ $\gamma\delta$ T cells (for a basic subset summary refer to Table 1.2). Meaningful discussion of $\gamma\delta$ T cell physiological functions and therapeutic potential must note that the subdivision of $\gamma\delta$ T cells into “innate-like” and “lymphoid-like” subsets has been disputed. Significant further investigation is required for the establishment of well-defined, reproducible physiological differences between the multiple $\gamma\delta$ T cell compartments, regardless of subset definition.

Table 1.2 | Features of human $\gamma\delta$ T cell subsets

Subset	Most common V γ V δ pairs	Tissue distribution	Key cytokines	Cytotoxicity
V δ 1 ^{pos}	Not defined	Epithelia, dermis, spleen and liver	IFN- γ and TNF; can produce IL-17	Potent
V δ 2 ^{pos}	V γ 9V δ 2	Blood	IFN- γ and TNF; can produce IL-17	Potent
V δ 1 ^{neg} V δ 2 ^{neg}	Not defined	Liver and gut epithelium	Not defined	Not defined

Adapted from Silva-Santos, et al. (2015) (9)

A majority of our insight into human $\gamma\delta$ T cell physiology derives from the study of the peripheral blood mononuclear cell (PBMC) compartment. The peripherally dominant V δ 2 $\gamma\delta$ T cells – with a V γ 9V δ 2 TCR - are the most-studied and best understood of the many, apparently heterogeneous $\gamma\delta$ T cell subsets. While data from peripheral V δ 2 $\gamma\delta$ T cell investigations in the context of immunotherapy remain promising (reviewed recently by Casetti, Martino and others (10,11)), it is crucial to achieve a broader understanding of all $\gamma\delta$ T cell subsets, and to establish whether inferences of $\gamma\delta$ T cell physiology from the human peripheral circulation are relevant to the more enigmatic tissue-resident lymphocyte compartments. It is, moreover, crucial to note that it remains, as of yet, unclear

to what extent human and murine $\gamma\delta$ T cell physiology is related. A significant portion of $\gamma\delta$ T cell literature examines murine $\gamma\delta$ T cells, which lack a homologous population to the human V γ 9V δ 2 cells, and possess oligoclonal, highly tissue-specific $\gamma\delta$ T cell populations such as dendritic epidermal T cells. While the overall differences between mouse and human $\gamma\delta$ T cell functionality and significance remain inconveniently obscure (reviewed recently by Pang, Pennington, et al. (12)), I make an effort in this thesis to focus my attention on human $\gamma\delta$ T cells and clinical scenarios.

1.2. $\gamma\delta$ T cells in health and disease

Current thought prevails that the predominant V γ 9V δ 2 human peripheral $\gamma\delta$ T cell subset mediates immuno-surveillance of stress signals emanating from endogenous and microbial pyrophosphates, sourced from *e.g.* tumour cells and infected cells, respectively (13). A significant increase in systemic and mucosal $\gamma\delta$ T cell numbers is seen in acute systemic bacterial and parasitic (as well as viral) infections. These include *Brucella*, *Streptococci*, *Coxiella*, *Listeria*, *Francisella*, *Escherichia*, *Campylobacter*, *Shigella*, *Leptospira*, *Plasmodium* and *Mycobacterium*, among others (14–24). While further exploration into the functionality of these expanded $\gamma\delta$ T cells is necessary, data indicate an activated phenotype, as measured by high cell surface CD69, and significantly increased expression of MHC class II (*e.g.* HLA-DR) and CD86 (21,22,24–26). The presence of such CD69^{pos}HLA-DR^{pos} $\gamma\delta$ T cells during sepsis and systemic inflammatory response syndrome appears to correlate negatively with mortality (25,27). The natural or experimental elevation of functional, activated $\gamma\delta$ T cell numbers has, moreover, been shown to correlate with improved prognosis and even protection from such chronic infections as *M. tuberculosis*, human cytomegalovirus (HCMV), *Toxoplasma gondii*, *Listeria monocytogenes* and a number of intestinal infections, among others, in murine, non-human primate and human models (28–36). Particularly important in a clinical setting – and when considering $\gamma\delta$ T cells as an immunotherapeutic tool - $\gamma\delta$ T cells are routinely shown to infiltrate and play a role in such common human tumour types as breast, colon, ovarian and lung cancers, as well as melanoma (37–41). Strikingly, the presence of $\gamma\delta$ T

cells was recently identified as the single most favourable lymphocytic predictive factor in human malignancy in a meta-analysis of 18,000 human tumours of 25 different types; $\gamma\delta$ T cells were shown to correlate with positive outcomes in both pan-cancer analysis, which included multiple myeloma and various leukaemias, as well as solid tumour analysis (42).

Explanations of the protective properties of $\gamma\delta$ T cells are extremely varied, and illustrate the expansive immune arsenal of these “innately-adaptive” lymphocytes in limiting or preventing the onset of disease. The most commonly discussed mechanisms of $\gamma\delta$ T cell effector function include potent, en-masse release of Interferon- γ (IFN- γ) and other Th1 cytokines for the resolution of intracellular infections, secretion of IL-17 for rapid mobilization of innate immunity at epithelial sites during bacterial invasion, upregulation of tumor necrosis factor- α (TNF- α) during systemic infection, effective cytotoxicity against transformed or infected self-cells and pathogens, mobilization and maturation of dendritic cells (DCs) as well as the antibody response in systemic and intestinal disease, priming and regulation of the $\alpha\beta$ T cell response in infectious or malignant scenarios through professional antigen presentation, maintenance of the integrity of epithelial barriers and even direct suppression of $\alpha\beta$ T cell-mediated inflammation in immunopathological settings (30,37,40,41,43–54). A simplified summary of the six main ways in which $\gamma\delta$ T cells contribute to the human immune response can be viewed in Figure 1.1, adapted from Vantourout and Hayday (7).

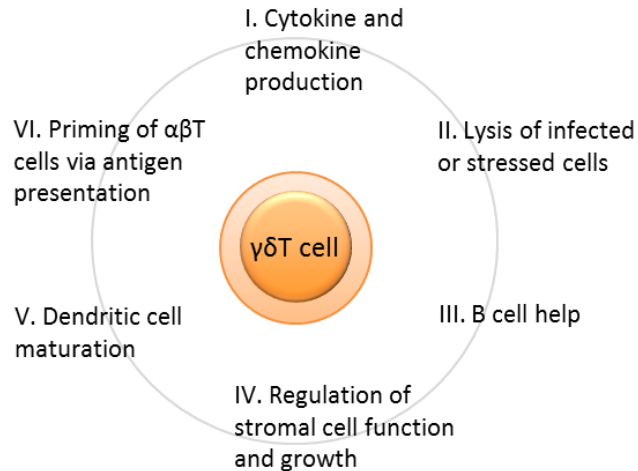


Fig. 1.1. $\gamma\delta$ T cell contribution to the human immune response. Literature documents that $\gamma\delta$ T cells have a central role in defending the host against a range of infectious and sterile stresses through six main mechanisms: I) Production of a diverse set of cytokines and chemokines to regulate other immune and non-immune cells. II) Direct lysis and, consequently, elimination of infected or stressed cells through the production of, e.g. granzymes. III) Help for B cells and promotion of IgE production. IV) Regulation stromal cell function through the production of growth factors. V) Triggering of dendritic cell maturation. VI) Antigen presentation to $\alpha\beta$ T cells, resulting in priming.

1.3. $\gamma\delta$ T cells as professional antigen presenting cells

While a T cell pAPC is by no means an accepted concept in mainstream immunology, there are multiple lines of evidence suggesting that $\gamma\delta$ T cells may indeed act as pAPCs to classic $\alpha\beta$ T cells, which range from functional studies to expression of antigen presenting and co-stimulatory molecules, to apparent phagocytic capacity - aspects of which have been explored in humans, mice and other mammals (49,50,55–59). While the seminal publication on the pAPC capacity of human $\gamma\delta$ T cells may be attributed to Brandes and Moser, *et al.* (60), our own laboratory has previously published work documenting the phagocytic capacity of human $\gamma\delta$ T cells and their ability to act as pAPC even in the context of cross-presentation to cytotoxic CD8 $\alpha\beta$ T cells (49,50).

Further to their documented oncolytic properties, $\gamma\delta$ T cells also have recorded pro-tumorigenic roles. It appears that the very effector functions which confer them with the ability to recruit and shape myeloid, as well as lymphoid immunity, and affect the growth and development of epithelial/stromal tissue, enable $\gamma\delta$ T cells to aid and even protect tumour development and survival (37,39–41). IL-17-producing $\gamma\delta$ T cells have, for example, been shown to aid development of breast cancer metastases (61). If we consider, however, the central aetiological role of epithelial site integrity in infectious and malignant disease, the restoration or, more artificially, boosting of appropriate $\gamma\delta$ T cell function emerges as a key tool in the maintenance and restoration of human health. As outlined above, overall solid and non-solid tumour meta-analysis identifies $\gamma\delta$ T cells as a factor strongly favorable to tumour clearance and recovery (42). The plethora of functional outcomes upon $\gamma\delta$ T cell stimulation illuminates the potential of their use in therapy, and highlights our lack of understanding regarding their functionality. Basic investigation of factors determining the development of $\gamma\delta$ T cell phenotypes is crucial if we hope to harvest and manipulate their vast array of effector functions in a reproducible and clinically viable manner.

V δ 2 $\gamma\delta$ T cell *in vitro* responses to different bacterial stimuli have been explored by various groups and laboratories. IFN- γ production and expansion in response to exposure have been described for *M. tuberculosis*, *L. monocytogenes*, *S. aureus* and *E.coli*, as well as products from *Morganella morganii* and *Salmonella typhimurium*, among others (35,62–66). Potent V δ 2 $\gamma\delta$ T cell responses have, thus, been described to Gram-negative, Gram-positive bacteria as well as intracellular bacteria. The significance of $\gamma\delta$ T cells for *in vivo* resolution of infectious disease has remained ambiguous, largely due to the highly complex nature of events that occur during bacterial infection at epithelial surfaces. This complexity emanates from the multitude of intricate relationships between the highly populous, poorly understood and often intra-redundant mucosal immune compartment, epithelia and commensal as well as invading microorganisms.

Recent studies have finally provided unambiguous experimental evidence for the protective antibacterial properties of human $\gamma\delta$ T cells *in vivo*. Wang *et al.* were able to

provide effective infectious control and resolution of both Gram-positive (*S. aureus*) and Gram-negative (*M. morganii*) infections in severe combined immuno-deficiency mice by adoptive transfer of human V δ 2 cells (14). Curiously, however, these were not V γ 9V δ 2 cells, but rather V γ 2V δ 2 cells. Successful *in vivo* experimental control of intracellular infection, such as *M.tuberculosis*, has meanwhile been achieved by adoptive transfer of V γ 9V δ 2 cells in non-human primate models (35). IFN- γ is of central importance in these anti-microbial responses. It does, however, remain unclear whether IFN- γ production is the only significant effector response of bacteria-exposed $\gamma\delta$ T cells, and whether the anti-microbial effects observed are the result of direct V δ 2 cell killing of free bacteria or infected cells, or an indirect activation of other immune components / bystander effects.

An area of ongoing debate in the fields of basic $\gamma\delta$ T cell biology and immunotherapy concerns the capacity of $\gamma\delta$ T cells – often V δ 2 cells, specifically – to act as pAPCs to $\alpha\beta$ T cells. As described, the controversy stems largely from the significant unorthodoxy of a T cell pAPC, and the well-founded concern of myeloid contamination of the experimental setups. Evidence for the role and significance of *in vivo* human V γ 9V δ 2 cell pAPC function is, as of yet, lacking. Compelling, if not direct, evidence can be sourced from numerous studies on mouse *TCR δ ^{-/-}* knockout models. The observations on the immune outcome in the absence of $\gamma\delta$ T cells in these models vary with disease model and experimental question being asked. A common thread emerges, however, of increased sensitivity to infection and dysregulated, aberrant lymphoid responses – including $\alpha\beta$ T cell responses - particularly at epithelial sites (45–48,67). Significantly, induction of oral tolerance could not be achieved in *TCR δ ^{-/-}* knockout mice (46). Re-introduction of $\gamma\delta$ T cells restored suppression of both CD4+ and CD8+ $\alpha\beta$ T cell responses. Further models examining $\alpha\beta$ T cell knockout mice and $\gamma\delta$ T cell knockout mice in parallel found that *TCR α ^{-/-}* mice present with defects in protective immunity, while *TCR δ ^{-/-}* mice present with exaggerated intestinal damage as an apparent consequence of a lack of immune regulation at the site of infection (45). $\gamma\delta$ T cell-deficient mice have further been found to present with substantially increased sensitivity to chemically-induced malignancy (68).

Any discussion of the *in vivo* pAPC role of $\gamma\delta$ T cells would be incomplete sans mention of mouse dendritic epidermal T cells (DETC). Described for the first time decades ago,

DETC were, in fact, found to express a distinctly oligoclonal, tissue-specific $\gamma\delta$ TCR (69). Multiple lines of compelling evidence highlight the antigen presenting and tissue homeostatic roles of DETC (56,70–72). It is important to note, however, that a human homologue to mouse DETC has not thus far been identified, nor one for Skint1 -the ligand that the DETC TCR appears to recognize (69). Nor, as mentioned earlier - a human pAg-activated V γ 9V δ 2 cell homologue in mice. I, therefore, refrain from in-depth discussion of the plethora of available $\gamma\delta$ T cell APC data generated in mouse models. The differences between mouse and human immune responses are a fascinating field of study and warrant significantly more attention from medical researchers, given how reliant we have grown on the extrapolation of mouse-generated data to human physiology and pathophysiology. A recent *Nature* editorial, based on work by Moss and group, outlines various reasons as to why murine models don't always translate easily to relevant human settings, and how these issues may be addressed, including the use of humanized mouse models (73). Reviews on the specific physiological differences between the mouse and human immune response, including $\gamma\delta$ T cells, have been compiled by Zschaler *et al.* and Mestas, *et al.* (74,75).

1.4. Phagocytosis

An important aspect of antigen presentation that necessitates consideration in the context of a $\gamma\delta$ T cell pAPC is the uptake of antigenic material destined for presentation. Cell internalization of material can take many forms and serves multiple physiologically important roles. Recent reviews by Flannagan *et al.* (76) and Underhill *et al.* (77) summarize what is known about the complex networks of information processing that occur during cell uptake of extracellular particles. While some forms of uptake serve a crucial immunological function, others are a part of routine cell homeostasis – and others still can be both, depending on the physiological context and cell type.

Endocytosis, the process by which cells internalize small molecules of *e.g.* nutritional value, is actin dependent, and occurs via multiple mechanisms. These include

internalization via clathrin-coated pits or cholesterol-rich caveolae. Macropinocytosis - sometimes referred to as “cell drinking” - involves extensive utilization of the actin cytoskeleton. It occurs via an eruption of membrane ruffles at the cell surface, which collapse back and fuse back with the cell membrane engulfing extracellular liquid in the process. The resulting vacuole, or macropinosome, is then shuttled down the normal endocytic pathway (78). Macropinocytosis is a normal part of all cell physiology. Via autophagy a cell may engulf organelles, soluble factors or microorganisms within its own cytosol. Trophocytosis describes the intracellular transfer of membrane patches from an APC to a lymphocyte (79). Cells can further engage in ‘cannibalism’, consuming whole, healthy self-cells, which are then degraded; such cannibalism has been seen with, for example, tumour cell ‘eating’ of lymphocytes (80). The unusual phenomenon of cell ‘burrowing’ is called entosis; the cell burrowing into another cell can die or re-emerge from its temporary host (80).

Phagocytosis – perhaps the most studied mode of material internalization – is actin and receptor-dependent uptake of specifically particulate targets $>0.5\mu\text{m}$ in size (81). Potential targets range from dead or dying cells to microorganisms, to environmental debris. The ability to phagocytose material is restricted to specialized cells, which are predominantly immune effectors. There are multiple known mechanisms of phagocytosis, and these include i) receptor-mediated phagocytosis, mediated by *e.g.* Fc receptors or dectin 1, ii) triggered phagocytosis, which may occur if large particulate antigens are taken up during macropinocytosis, iii) sinking phagocytosis that is mediated by complement, and iv) macroautophagy, which involves cell ‘eating’ of large cytosolic material. All of these uptake routes result in the formation of a mature phagosome, and consequential killing and degradation of phagocytosed particles (77).

A wide range of receptors has been implicated in mediating phagocytosis, categorized broadly into opsonic, non-opsonic and triggered (non-specific) receptors and phagocytosis, therein. A brief summary, adapted from Underhill and Goodridge (77) can be seen in Table 1.3.

Table 1.3 | **Types of phagocytic receptors**

Type of receptor	Receptor	Ligand	Refs
Opsonic	Fc gamma family (FcγRI, FcγRIIA and FcγRIIA)	Antibody-opsonized targets	(85)
	Complement receptors (C1, C3, C4)	Complement-opsonized targets	(86)
	α5β1 integrin	Fibronectin	(87)
Non-opsonic	Dectin 1	β-glucan	(88)
	Macrophage receptor MARCO	Bacteria (undefined)	(89)
	Scavenger receptor A	Bacteria (diverse charged molecules)	(90)
	αVβ5 integrin	Apoptotic cells	(87)
Triggered	Toll like receptors	Various, including lipopolysaccharides and lipopeptides	(91)

Phagocytosis proceeds through a number of stages, all of which involve tight control and multiple possible signaling events. Initial contact of cell and target is known as *tasting*, and involves receptor-mediated identification of target chemical identity by the cell. *Feeling*, the next step, occurs through dynamic membrane interactions between particle and cell; this permits the cell to identify the physical shape of the target. The specifics of subsequent *swallowing* are determined by signaling through the particular phagocytic receptor that was engaged. The phagocytic receptor(s) engaged further form a part of the phagosome membrane and inform phagosome handling and maturation, which result in *digesting* of the phagocytosed particle. The phagocytic process concludes with triggering of the *inflammatory response* within the cell. The inflammatory response involves secretion of specific inflammatory mediators from the cell, recruitment and activation of other cells, as well as professional antigen presentation of digested target peptides on MHC to αβT cells if the phagocyte is a pAPC.

Definitions of what exactly constitutes a *professional* APC may vary, but there is general agreement that these cells are efficient phagocytes (or in the case of B cells – efficient at

B cell receptor-mediated endocytosis), efficient at processing internalized material for presentation on MHC and express both, MHC class II and co-stimulatory molecules such as CD80 and CD86 (89). Occasionally, the ability to cross-present exogenous antigen on MHC class I is also included as a pre-requisite for a cell to be deemed a pAPC. In brief, pAPCs are cells which specialize in presenting antigen to T cells.

Some distinction as to ‘professional’ and ‘non-professional’ has also been made in reference to phagocytosis. Fibroblasts and epithelial cells have been shown to take up, for example, latex beads $>0.5\mu\text{m}$ in size or red blood cells in a receptor-mediated manner, in a process which was enhanced by opsonization of the target. What prevents their categorization as professional phagocytes by those who venture to define the difference (90) is the limited range of particles that fibroblasts and epithelial cells appear to be capable of phagocytosing. The limited range of targets is attributable to the limited range of phagocytic receptors on the cell surface. Compared to professional phagocytes, non-professional phagocytes further lack the ability to produce a range of microbicidal molecules or mount a diverse cytokine response.

1.5. $\gamma\delta$ T cell recall and memory

An important aspect of $\gamma\delta$ T cell physiology in the context of their use as immunotherapeutics that has remained impervious to conclusive debate is “memory”. In order to avoid semantic misunderstanding, the intended meaning of “memory” further in the text implies the phenomenon described by Janeway, *et al.* as: “... the ability of the immune system to respond more rapidly and effectively to pathogens that have been encountered previously, and reflects the preexistence of a clonally expanded population of antigen-specific lymphocytes”, adding that “a long-standing debate about whether specific memory is maintained by distinct populations of long-lived memory cells that can

persist without residual antigen, or by lymphocytes that are under perpetual stimulation by residual antigen, appears to have been settled in favour of the former hypothesis.” (91)

While a number of publications, disease models and research groups have suggested that $\gamma\delta$ T cells can confer residual protection from recurring disease, whether this protection is antigen-specific has been heavily contested. Publications have reported antigen-specific $\gamma\delta$ T cell memory responses to *M.tuberculosis* in humans, macaques, mice and cattle, as well as murine intestinal *L. monocytogenes* or imiquimod-induced inflammation-specific skin-resident $\gamma\delta$ T cells with indications of the hallmarks of canonical $\alpha\beta$ T cell memory: i) trafficking to draining lymph nodes, ii) migration through blood to distant tissue sites and peripheral lymph nodes, iii) persistence in these locations and iv) increased proliferative, and cytokine-producing capacity upon re-challenge (31,62,63,92). These findings are, however, inconsistent across various labs and have, importantly, struggled to find support in the patchy $\gamma\delta$ TCR sequencing data available in the literature. The number of known $\gamma\delta$ TCR antigen specificities is limited, and traditional T cell vaccination approaches have largely failed to induce reproducible, meaningful $\gamma\delta$ T cell memory to infectious re-challenge. It is, moreover, unclear to what extent the $\gamma\delta$ TCR plays a role in $\gamma\delta$ T cell activation, how it is modulated by a range of agonistic and antagonistic co-receptors, how this may differ between various $\gamma\delta$ T cell subsets or across species, such as mouse and human, and what resemblance exactly this bears to the central, tightly-regulated and non-redundant role of the TCR in canonical $\alpha\beta$ T cells.

A detailed understanding of the mode of $\gamma\delta$ TCR-antigen interaction remains elusive. As alluded to earlier in the text, it is known that $\gamma\delta$ T cells are capable of responding to antigen in the absence of major histocompatibility complex (MHC) and classic APC antigen processing and presentation. Instead, in what has been described as an “antibody-like breadth in antigen recognition” (7), $\gamma\delta$ T cells are capable of recognizing antigen presented on atypical MHC-like molecules (*e.g.* the CD1 family), altered or absent antigen presenting molecules themselves, and even free antigen (54,93–95). The notion that the $\gamma\delta$ TCR may be capable of binding free antigen is supported by the exceedingly high

$\gamma\delta$ TCR CDR3 diversity – found largely in the *TCRD* locus - which suggests a lack of restriction by the $\gamma\delta$ TCR for any particular antigen delivery structure (reviewed by Chien and Konigshofer (96)). The classes of antigen engaged by the $\gamma\delta$ TCR are consequently varied, and range from phosphoantigens (pAg) to peptide and lipid antigens. Some have suggested that $\gamma\delta$ T cells are further capable of responding to antigen in the absence of direct TCR stimulation, depending instead on the aforementioned pattern recognition receptors (PRRs) (3,44,97–99). A number of studies argue that $\gamma\delta$ T cells may be capable of engaging a single antigen through several different receptors, as is the case - in a foreign-antigen context - with bacterial lipopolysaccharide (LPS)-derived Lipid A, which triggers both the $\gamma\delta$ TCR and TLR-4 or, in a self-antigen context, with MHC class I-homologue MICA that is recognized by the $\gamma\delta$ TCR and NK-like receptor, NKG2D (93,95).

The question of $\gamma\delta$ T cell memory is hugely complicated by the popular hypothesis that $\gamma\delta$ T cells may, in fact, be largely auto-reactive, whence their responses are triggered primarily by recognition of self-stress markers, such as self-phospholipid cargos or aberrantly expressed antigen presenting molecules themselves, rather than foreign antigens (for a limited list of known $\gamma\delta$ T cell activating ligands refer to Table 1.4). These self-stress markers can be specific and induced by infection, transformation or other injury to tissue; $\gamma\delta$ T cells may thus mount a potent pro-inflammatory response to, for example, *E.coli* invasion, and yet remain entirely self-reactive. Such an explanation to the divergence between the rapid, potent, en-masse $\gamma\delta$ T cell responses and the delayed, highly antigen-specific, canonical $\alpha\beta$ T cell responses is intriguing. It may shed light on the ability of $\gamma\delta$ T cells to react so effectively to seemingly heterogeneous stimuli with what has been stipulated to be a relatively oligoclonal TCR repertoire.

Table 1.4 | **Activating ligands for human $\gamma\delta$ T cells**

Subset	Antigen
Vδ1^{pos}	MICA, CD1c, CD1d tetramers loaded with sulphatide, lipohexapeptides, phycoerythrin
Vδ2^{pos}	ULBP4, phosphoantigens, F1-ATPase, histidyl-tRNA synthetase, phycoerythrin, HMBPP
Vδ1^{neg}Vδ2^{neg}	Endothelial protein C receptor, phycoerythrin

Adapted from Hayday, et al. (2013) (7)

Here again, however, $\gamma\delta$ T cells elude simplicity and categorization; some of the most potent documented $\gamma\delta$ T cell stimuli, such as (E)-4-hydroxy-3-methyl-but-2-enyl pyrophosphate (or HMBPP), are of microbial origin (31). Some have proposed that the mechanism of HMBPP-induced activation of V δ 2 $\gamma\delta$ T cells may, in fact, be mediated via HMBPP induction of self-stress responses through dysregulation of the host mevalonate pathway, manifested as conformational changes in host cell surface butyrophilin (BTN) - BTN3A specifically - molecules (100). BTN changes through a similar mechanism have further been implicated as activatory to $\gamma\delta$ T cells, upon exposure to *E.coli* and other bacterial pathogens (101,102). Curiously, BTN3A conformational alterations further appear to be the mode of V δ 2 $\gamma\delta$ T cell activation in the context of stimulation with zoledronate. Zoledronate, a clinically-relevant bisphosphonate drug, which efficiently expands V δ 2 $\gamma\delta$ T cells *in vitro*, disrupts the host mevalonate pathway and causes the accumulation of endogenous pyrophosphates (IPP), which consequently induce conformational changes in BTN3A molecules on “stressed” self-cells (103). It is, perhaps, unsurprising that IPP and HMBPP appear to exert similar effects on V δ 2 $\gamma\delta$ T cells, given their high structural homology (Fig.1.2). The striking structural similarity between IPP and HMBPP does, however, present a hurdle in discerning the differential mechanisms by which these compounds may lead to $\gamma\delta$ T cell activation, and complicates our understanding of how $\gamma\delta$ T cells may distinguish between self and non-self danger signals. It is known, for example, that HMBPP, in the absence of any further immunogenic signals, is a far more potent activator of V δ 2 cells than IPP (104).

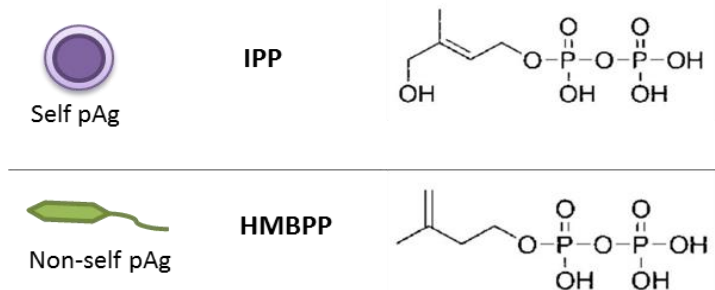


Fig. 1.2. Chemical structure of IPP and HMBPP phosphoantigens. Sourced from entirely different organisms, isopentenyl pyrophosphate (IPP), of vertebrate origin, and (E)-4-hydroxy-3-methyl-but-2-enyl pyrophosphate (HMBPP), of microbial origin, present with highly homologous chemical structures.

A simplified diagram listing the various ways in which $\gamma\delta$ T cells may recognize pAg can be viewed in figure 1.3. There are four potential modes by which $\gamma\delta$ T cells detect self and non-self pAg danger signals: i) detection of the accumulation of self pAgs within self cells, induced by self-stress, *e.g.* transformation or the application of drugs such as zoledronate (Fig.1.3A), ii) detection of non-self pAgs directly, sourced from invading pAg-expressing microorganisms, *e.g.* *E.coli* (Fig.1.3B), iii) detection of non-self pAgs directly, but in a manner that is dependent on self cells manifesting these non-self pAgs, *e.g.* via HMBPP-induced butyrophilin changes (Fig.1.3C), or iv) detection of non-self pAgs indirectly, wherein non-self stressors such as *E.coli* induce self-stress and consequent accumulation of self pAgs that are then detected by $\gamma\delta$ T cells on self cells (Fig.1.3D). It is possible that all four mechanisms play a role in $\gamma\delta$ T cell detection of immune stress signals. $\gamma\delta$ T cell recognition of pAgs is explored in significant detail in subsequent chapters of the thesis.

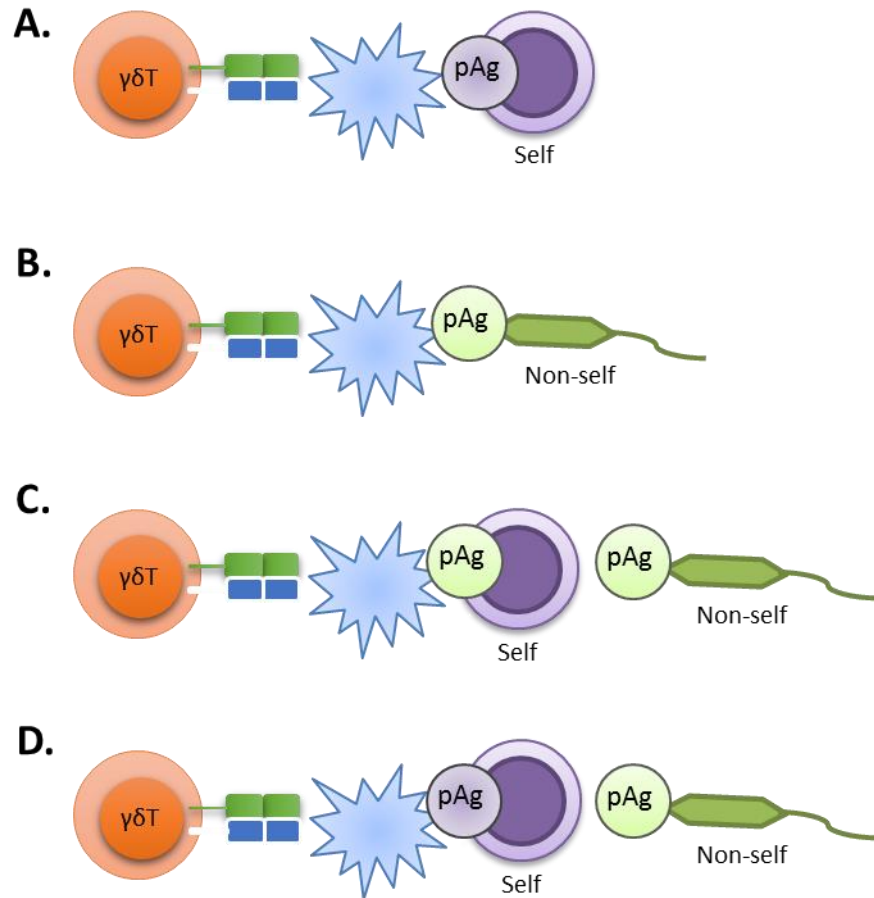


Fig. 1.3. $\gamma\delta T$ cell recognition of self and non-self phosphoantigen danger signals. It is known that $\gamma\delta T$ cells can recognise efficiently both endogenous cellular stress and invading microorganisms. While this can occur in a phosphoantigen (pAg)-dependent manner, exact mechanisms of recognition are lacking. Four different mechanisms of pAg detection in a self and non-self context are possible: **(A)** Direct detection of self pAgs, induced by self-stress, *e.g.* transformation or drugs such as zoledronate, **(B)** Direct detection of non-self pAgs, sourced from invading pAg-expressing microorganisms, *e.g.* *E.coli* **(C)** Direct detection of non-self pAgs, but in a manner that is dependent on self cells manifesting these non-self pAgs, *e.g.* via HMBPP-induced butyrophilin changes, or **(D)** Indirect detection of non-self pAgs, wherein non-self stressors such as *E.coli* induce self-stress and consequent accumulation of self pAgs that are then detected by $\gamma\delta T$ cells on self cells.

It remains important to consider in this context the extreme complexity of the immune environments that $\gamma\delta$ T cells predominantly operate in. It is conceivable that the gastrointestinal mucosa, an epithelial landscape densely populated by various immune cells and trillions of commensal microorganisms, requires effector cells sensitive to signals of self-stress as well as foreign pathogens. It is likely, thus, that $\gamma\delta$ T cells employ avenues in addition to the TCR and its machinery to fine-tune antigen recognition and determine appropriate effector function. Work to clarify the role in antigen specificity of the $\gamma\delta$ TCR *versus* the wide variety of other classically lymphoid and myeloid-associated pathogen recognition receptors (PRRs) that have been found on $\gamma\delta$ T cells, including NK-like receptors, Fc receptors (FcRs) and Toll-like receptors (TLRs) (reviewed by Hayday and Vantrout (7)), is crucial if we hope to manipulate antigen-specific $\gamma\delta$ T cell responses in a clinical setting.

The concept of a predominating $\gamma\delta$ T cell autoreactivity complicates their categorisation into traditional $\alpha\beta$ T cell memory phenotypes, such as “effector memory” or “naïve”, given that these are traditionally prescribed as resulting from various degrees of antigen exposure. As memory phenotype remains a traditionally important parameter in predicting T cell behaviour in response to antigen, numerous cell surface markers, including CD27, CD45RA, CD45RO, CD62L, CCR7, and combinations thereof, have been used to attempt $\gamma\delta$ T cell classification into memory phenotypes with homologues in the $\alpha\beta$ T cell compartment. General consensus is lacking, and, importantly, the relevance of these markers in the context of classical $\alpha\beta$ T cell memory subsets for $\gamma\delta$ T cells is unclear at best. Similar lack of clarity persists with other classic and important parameters of T cell physiology. Markers, such as CD69 for early activation or PD-1 for exhaustion, for example, are thought to represent $\gamma\delta$ T cell parallels to $\alpha\beta$ T cell behaviour, but whether these are the definitive readouts of $\gamma\delta$ T cell activation or exhaustion states remains to be established. I proceed, nonetheless, with their use in investigation for want of obviously better current alternatives.

1.6. Categorisation of $\gamma\delta$ T cell subsets

Significant efforts have been poured into establishing reproducible and clear human $\gamma\delta$ T cell functional subsets, providing more detail than merely a reference to the expression of a V δ 1 or V δ 2 TCR chain. Particularly important in the pursuit of $\gamma\delta$ T cells as immunotherapeutic tools is the classification of their effector subsets prior to and post stimulation. Expansion *ex vivo* has been a significant component of the $\gamma\delta$ T cell field since its inception. The relative scarcity of $\gamma\delta$ T cells in human peripheral blood has necessitated expansion as a means of amplifying cell number for use in functional assays, protein analyses and other experimental probes. Additionally, the promise that $\gamma\delta$ T cells have demonstrated in the clinic has created a new urgency in establishing effective, reproducible $\gamma\delta$ T cell expansion protocols, with a detailed understanding of the effector subsets of expanded cells therein. Novel approaches for $\gamma\delta$ T cell amplification are being developed as technological advances permit deepening examination of the poorly understood epithelial immune compartment, where $\gamma\delta$ T cells can constitute up to 60% of total intraepithelial lymphocytes (IEL) (7). While expansion with stimuli such as IPP, zoledronate and concanavalin A (ConA) have become a routine in basic science as well as clinical $\gamma\delta$ T cell manipulation, our understanding of specific stimuli that drive and regulate $\gamma\delta$ T cell expansion remains limited (4,103,105). Moreover, most established protocols appear only effective in expanding the peripherally dominant V γ 9V δ 2 $\gamma\delta$ T cell subset. Significant donor variation in terms of rate-expansion remains an issue in optimizing $\gamma\delta$ T cell use in the clinic; the factors, which impact V γ 9V δ 2 cell expansion rate, remain uncertain.

Fascinating insight into the functional subgroups of human V δ 2 cells has been provided by a recent publication from the group of Pennington *et. al.* (106), which describes the surprisingly stable yet heterogeneous populations of peripheral V δ 2 cells in 63 healthy individuals, which were found to be independent of donor age, sex, ethnicity or, apparently, previous pAg exposure. They were able to identify two predominant V δ 2 cell populations, which were deemed $\gamma\delta^{(28+)}$ and $\gamma\delta^{(16+)}$ based on their respective expression of either CD28 or CD16. It was observed that $\gamma\delta^{(28+)}$ cells exhibited a CCR6^{pos} phenotype,

which further correlated with increased expression of cytokine receptors (*e.g.* IL-18R) and chemokine receptors (*e.g.* CCR2 and CCR5), as well as granzyme K. $\gamma\delta^{(16+)}$ cells, meanwhile, favoured expression of CXCR1, and presented with an increased perforin/granzyme B cytotoxic potential, paired with lowered proliferative capacity. Such observations are likely to carry significant implications for the design of personalized, cell-based anti-tumour therapies, whence a match between tumour cell type (which may be *e.g.* granzyme B inhibitor, PI-9, positive) and immune effector cell killing mechanism is important.

Meanwhile, in my characterization of unstimulated or differentially-expanded V δ 2 cells, I placed a particular emphasis on their expression patterns of APC molecules, MHC class II (HLA-DR, specifically) and co-stimulatory CD86, as well as homing receptors, chemokine receptor 7 (CCR7) and CD62L (also known as L-selectin). HLA-DR and CD86 expression has been documented on human $\gamma\delta$ T cells in various contexts, ranging from *in vitro* stimulation to *in vivo* infectious disease. Both endogenous pAg and Gram-negative bacteria-stimulated $\gamma\delta$ T cells have been reported to upregulate expression of HLA-DR and CD86 (102,105). The dynamics, time scale and stability of this upregulation has, however, not been reported in detail.

CCR7, a homing receptor expressed on naïve T cells and activated APC, plays a central role in cell migration to lymphoid tissue. Its corresponding ligands, CCL19 and CCL21, are expressed strongly in the thymus and lymph nodes. Naïve CCR7^{pos} T cells continue re-circulation through blood and the lymphatic system until encountering an activating APC, at which point CCR7 is downregulated and chemokine receptors for tissue-specific migration are upregulated. Central memory T cells (T_{cm}) engage in a similar blood-to-secondary lymphoid organ re-circulation and, as naïve T cells, downregulate CCR7 and upregulate tissue-specific homing receptors upon activation (107). CD62L is a lymphoid homing receptor functionally closely related to CCR7, and mediates blood-borne T cell rolling on high endothelial venules, allowing their extravasation into lymphatic circulation. CCR7 and CD62L are both used as classic markers of T cell migration to secondary lymphoid tissue.

CCR7 upregulation on APC, such as dendritic cells (DC), is, meanwhile, a marker of cell activation. Upon encounter with appropriate stimulation (*e.g.* invading bacteria) tissue-resident DC are activated, upregulate CCR7 and migrate to secondary lymphoid tissue. Once there, DC engage in presentation of phagocytosed and processed antigen to re-circulating T cells (108,109). A similar role, although less well understood, has been ascribed to CD62L. The two main sources of DCs to lymph nodes are thought to be peripheral DCs entering via afferent lymph and monocyte-derived DCs entering via high endothelial venules. Luster *et al.* (110) have produced a comprehensive review on the plethora of chemokines and chemokine receptors involved in shaping lymphoid as well as myeloid migration during the immune response.

While CCR7 and CD62L represent but a fraction of potentially significant $\gamma\delta$ T cell homing receptors, I chose to focus on them set against the curious background that these receptors appear to follow different patterns post-activation, depending on whether expression is examined in T cells or myeloid APC. If peripheral $\gamma\delta$ T cells do indeed perform an APC function during systemic infection - such as modeled in my experimental setup - does this APC function occur in blood or in secondary lymphoid tissue? Are APC and homing marker expression patterns on $\gamma\delta$ T cells reminiscent of those on classic $\alpha\beta$ T cells or myeloid APC? Moreover, does PBMC stimulation with the highly differential stimuli of zoledronate (representing 'self') or *E.coli* (representing 'non-self') induce similar upregulation of APC molecules, MHC class II and CD86, and lymphoid homing markers, CCR7 and CD62L? Finally, are these similarities or differences in differentially-expanded $\gamma\delta$ T cell APC and homing phenotype reflected in the TCR repertoire?

1.7. Role of the TCR in $\gamma\delta$ T cell physiology

Meaningful discussion of the nature and manipulation of $\gamma\delta$ T cell effector phenotypes would be incomplete without examination of the factors that influence the development of said phenotypes. Stimulation via the TCR is central to thymocyte development and effector T cell function. It determines the deletion or maintenance of a nascent T cell, its

activation status and subsequently regulates its ‘fate decisions’. It is striking that decades after its discovery and establishment of its importance in the functioning of a healthy immune system, the exact mode of TCR engagement – even in canonical $\alpha\beta$ T cells – remains unclear. A number of models have been proposed, and their popularity in the field ebbs and flows with the income of new experimental evidence. Van der Merwe and Dushek have recently compiled a comprehensive review of various models of TCR triggering (111), accompanied by helpful diagrammatic material. In the interest of accuracy and clarity, they have defined ‘TCR triggering’ as: “[t]he process by which TCR binding to peptide-MHC molecules leads to biochemical changes in the cytoplasmic regions of the CD3 complex [...]”. These models are based on the central dogma that all TCR CD3 complex subunits contain immunoreceptor tyrosine-based activation motifs (ITAMs) in their cytoplasmic domains, which – via biochemical modification - are the central mediators of T cell activation resulting from TCR triggering. Phosphorylation by the Src family kinases, Lck and FYN, has been proposed as one of these essential biochemical ITAM changes. The models described have been organized into three main groups, depending on the primary mechanism proposed: i) aggregation, ii) conformational change and iii) segregation or re-distribution.

Models within the ‘aggregation’ group include: a) co-receptor heterodimerization and b) pseudodimerisation. Briefly, the co-receptor heterodimerisation model (arguably, the most popular and widely accepted model) proposes that co-receptors bind to the same peptide-MHC complex as the TCR, which then brings co-receptor-associated Lck into proximity with CD3 complex ITAMs, resulting in phosphorylation. A basic illustration of the heterodimerization model can be viewed in Figure 1.4. The pseudodimer model postulates that two TCRs are brought together by one of the two binding low-affinity self, and the other – binding high affinity self or non-self peptide-MHC complexes. The co-receptor associated with the low affinity TCR then engages the agonist (high affinity) peptide-MHC complex that has been bound by the high affinity TCR, thereby forming a dimer between the two TCRs. This then permits co-receptor-associated Lck phosphorylation of both TCR ITAMs.

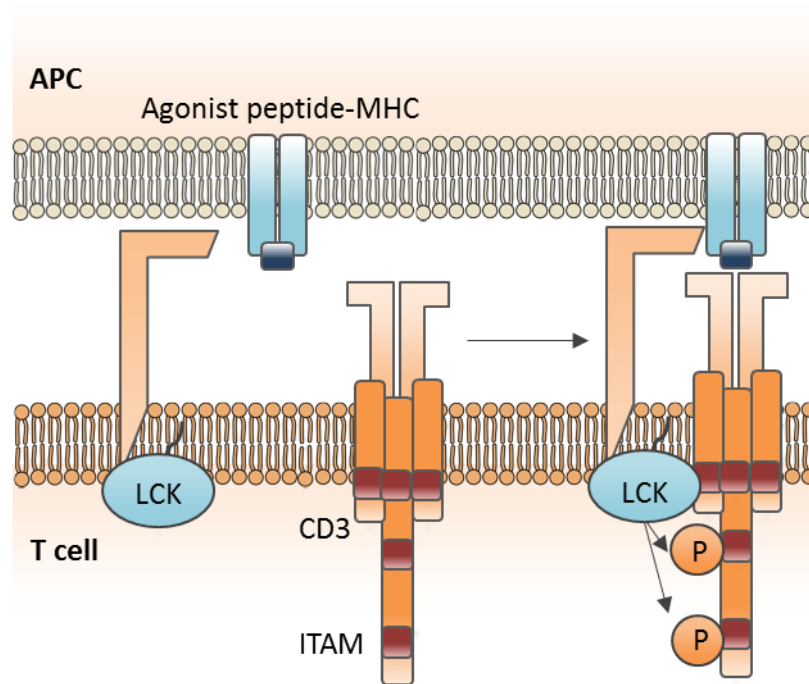


Fig. 1.4. Co-receptor heterodimerisation aggregation model of TCR triggering. The model proposes that co-receptor binding to the same peptide-MHC complex as the TCR brings co-receptor-associated Lck into proximity with TCR-CD3 ITAMs, thereby enhancing phosphorylation. Elements of this diagram have been adapted from van der Merwe and Dushek.

Models of the ‘conformational change’ group include: a) piston-like movement and b) induced clustering. The piston-like movement model describes mechanical ‘pulling’ of the TCR by cognate peptide-MHC complex, which then drives phosphorylation of the CD3 ITAMs. The induced clustering model argues that TCR clustering is induced by a conformational change in the peptide-MHC-engaged TCR-CD3 complex, which then enhances kinase activity and leads to the phosphorylation of CD3 ITAMS.

‘Segregation or re-distribution’ models include: a) kinetic segregation and b) lipid rafts. Briefly, the kinetic segregation model proposes that TCR binding to peptide-MHC ligand traps the TCR-CD3 complex in close-contact zones, thereby segregating it from inhibitory signals (*e.g.* inhibitory tyrosine phosphatase CD45) leading to stable phosphorylation of ITAMs by LCK. Lipid raft models postulate that peptide-MHC engagement results in partitioning of the TCR-CD3 complex into regions of membrane enriched in Lck and deficient in CD45.

It is conceivable that elements of all of the above-described models play a role in TCR triggering; each model applicable in a particular context, depending on, for example, the type of co-receptors a T cell expresses or the type of antigen presenting cell that is engaging the T cell at hand. It is important to note that the mechanistic aspects of TCR engagement by target do not end with triggering. Questions regarding subsequent events, such as “How is productive TCR signaling different from non-productive signaling?” and “How is productive signaling achieved?” are yet to be answered definitively. A multitude of further models that consider the mechanisms of post-triggering TCR signaling, including kinetic ‘proofreading’, segregation, sequestration of ITAMs, allosteric malleability and serial triggering, are evaluated by Chakraborty and Weiss (112). As with models of TCR triggering, their discussion of various proposed mechanisms makes several assumptions about the processes that occur. They too place importance on Lck, as well as a tyrosine kinase, Zap70. An emphasis is placed on the interactions between Lck, Zap70 and subunits of the invariant signaling protein CD3 complex, [$\alpha\beta$ TCR] co-receptors CD4 and CD8, and modulatory molecules, therein. Specifically, Chakraborty and Weiss describe a new model of TCR signaling, whereupon TCR engagement by peptide-MHC invokes basal phosphorylation of CD3, which then poises Zap70 for activation by Lck

largely via stabilization of ‘active’ Lck. A significant role is ascribed to the formation of TCR microclusters in permitting signal amplification by a triggered TCR.

Navarro and Cantrell have compiled current thought on what takes place after a TCR has been triggered and engaged productively (113). Once again, several different models persist, but most include signal transduction by serine threonine kinases. Membrane-proximal signals from TCR activation are transduced to elicit cytosolic and nuclear responses. TCR signaling triggers increased levels of second messengers (Ca^{2+} , diacylglycerol, PI3K, etc.), which facilitates activation of downstream kinases (protein kinase C, PDK1, Akt, etc.), each of which play a role in the unfolding signaling cascades. The signaling outcome of productive TCR engagement is the influencing of transcription factor activity, and, ultimately, altered gene expression and metabolic activity. Malissen *et al.* have described that Zap70 activation, downstream of productive TCR engagement, exerts an influence even on such T cell functions as rearrangements of the actin cytoskeleton and integrin affinity (114).

Canonical $\alpha\beta$ T cell TCR signaling, thus, remains an expanding, but, as of yet, contested intellectual landscape. Controversy persists regarding even basic conceptual models. A whole further level of complexity and controversy is introduced when contemplating signaling of the atypical, poorly understood $\gamma\delta$ T cell population. Rudimental understanding on $\gamma\delta$ TCR engagement of targets is lacking. It is unclear, for example, if $\gamma\delta$ TCR engagement is even necessary for the cells to exert many of their effector functions. It is unclear whether a TCR-MHC-peptide triad homologue exists for the $\gamma\delta$ TCR; some have even suggested that $\gamma\delta$ T cells are capable of recognizing free antigen, in the same way that B cells do (7). Data published by various groups, in various *in vitro* scenarios, of various donor species is frequently contradictory. As outlined in previous chapters, there are indeed significant species differences, as have been described for mouse *versus* human $\gamma\delta$ T cells. Subset and anatomical localization differences are likely additional factors explaining the heterogeneity of data generated. The recognition of ‘stressed self’ – if that is indeed what some (or all) $\gamma\delta$ T cells recognize – is particularly difficult to study. This is especially so, when considering that most $\gamma\delta$ T cells in the human body reside at epithelial surfaces, which are, as of yet, nearly impossible to replicate fully

in vitro. $\gamma\delta$ T cells are, moreover, known to express a plethora of non-TCR receptors implicated in the recognition of stressed or transformed self (*e.g.* NK cell receptors, such as NKG2D), making dissection of the unique role of the TCR exacting.

A list of documented human $\gamma\delta$ T cell clones can be viewed in Table 1.5, elements of which have been adapted from a review by Carding and Egan (8). While representing a mixture of suspected self and non-self TCR specificities, definitive evidence as to the exact mode of antigen engagement (*e.g.* crystallized TCR-antigen-antigen presenting molecule complex) is limited. It is possible that most (if not all) documented non-self ligand triggering of $\gamma\delta$ T cells in a TCR-dependent manner is merely a reflection of non-self induction of self-stress molecules, which are then ultimately what is recognized by the $\gamma\delta$ TCR. It is possible that the answer to this question is $\gamma\delta$ T cell subset-specific.

Table 1.5 | Characteristics of human $\gamma\delta$ T cell clones

$\gamma\delta$TCR composition (origin)	Antigen Specificity	Functional phenotype	Biological function	Ref.
V γ X-V δ 1 (IEL lines and clones)	MICA, MICB	Cytotoxicity	Elimination of stressed/transformed cells	(154)
V γ X-V δ 1 (synovial fluid)	Lipohexapeptides + DC + IL-2	?	Fas-mediated modulation of immune responses to infection	(155,156)
V γ X-V δ 1 (peripheral blood)	HLA-A2, HLA-A24	Cytotoxicity, Th1 cytokine release	?	(157,158)
V γ X-V δ 1 (peripheral blood)	CD1c	Cytotoxicity	?	(159,160)
V γ 9-V δ 2 (peripheral blood)	Organic phosphoesters, alkylamines, nucleotide-conjugates and cell-cell contact	Cytotoxicity, Th1 cytokine release	Unique role in immunity to infection, homeostatic control of immune and non-immune processes?	(117,161, 162)
V γ 9-V δ 2 (peripheral blood)	Pamidronate + monocytic APCs	Cytotoxicity, IFN- γ release	Elimination of myeloid-cell targets?	(163)
V γ 9-V δ 2/1 (peripheral blood)	Staphylococcal enterotoxin	Cytotoxicity	Anti-microbial immunity?	(164,165)
V γ 9-V δ 2 (synovial fluid)	Mycobacterial Hsp65 / tetanus toxoid + HLA-DR	Cytotoxicity	Elimination of autoreactive cells?	(166,167)
V γ 9-V δ 2 (peripheral blood)	GroEL heat shock protein	Cytotoxicity, cytokine release	Tumour surveillance?	(168)

The recognition of ‘self’ by the TCR has been discussed by Hogquist and Jameson (131). Their focus, in particular, was the functional consequences of TCR signaling in CD4+CD8+ double-positive thymocytes and mature T cells. They argue that all T cells (canonical $\alpha\beta$ T cells in this instance) are at least partially self-reactive, as they recognize a diverse repertoire of peptides, but only in combination with self MHC molecules. They further highlight the classic model of thymic T cell selection, whereupon thymocytes undergoing positive *versus* negative selection present with significantly different Ca^{2+} flux patterns. Strong TCR signaling in the thymus generally leads to negative selection, whereas a weaker or ‘intermediate’ signal leads to positive selection. Importantly, however, they note that multiple T cell subsets, including IELs (which constitute the majority of human $\gamma\delta$ T cells), invariant NKT cells and regulatory T cells, require strong TCR signaling for selection. It is, therefore, clear that factors other than TCR signal strength alone are involved in shaping of the TCR repertoire. What these factors may be remains poorly understood, although anatomical location of the selection process or origin of the T cell may play a role.

The sensitivity of a TCR to high- or low-affinity peptide interactions evolves as cells develop from CD4+CD8+ double positive thymocytes to mature T cells (131). Over the developmental process, T cells appear to dampen their sensitivity to self peptide-MHC complexes. This process of ‘tuning’ is parallel to alternations in the gene expression profile of the cell, as well as changes to basal intracellular Ca^{2+} concentration. Nonetheless, basal TCR signaling in response to self peptide-MHC takes place throughout the lifetime of a naïve T cell, and is likely necessary for homeostasis.

Fascinating insight into the possible TCR dependency of human $\gamma\delta$ T cells has been provided by recent investigations of the mouse $\gamma\delta$ T cell compartment. Sutton *et al.* (132) found that $\gamma\delta$ T cells rapidly produce the potent pro-inflammatory cytokine IL-17 in response solely to stimulation with IL-1 and IL-23. This stands in stark contrast to the dogma that governs our understanding of canonical T cells, which are thought to engage potent effector function only after receiving a stimulus via the TCR. The cells producing IL-17 in response to cytokine stimulation alone were negative for the co-stimulatory receptor CD27, and were subsequently deemed ‘innate-like’ $\gamma\delta$ T cells (133). Such ‘innate-

like' IL17^{pos} $\gamma\delta$ T cells are particularly abundant in murine and human neonates; their role has, thus, been postulated as one of rapid anti-microbial (anti-fungal and anti-bacterial, specifically) responders in vulnerable young animals. The same cells have further been implicated in a number of immunopathologies of both the young and adults in human and animal models, including psoriasis, rheumatoid arthritis and experimental allergic encephalomyelitis (134–139).

Mouse IL-17A-producing CD27^{neg} 'innate' $\gamma\delta$ T cells were considered to emerge by default from thymic progenitor cells that receive only weak TCR signals during development, in contrast to the strong signals received by CD27^{pos} 'lymphoid' $\gamma\delta$ T cells, delineating clearly the TCR as less important for the development and functioning of 'innate' $\gamma\delta$ T cells (133,140,141). It is known, however, that CD27^{neg} mouse $\gamma\delta$ T cells constitutively display markers associated with TCR activation (133,139,142). A recent investigation by Wencker *et al.* (143) showed that, in total contrast to previous assumption, CD27^{neg} mouse $\gamma\delta$ T cells selectively depend on strong TCR signaling, which thereafter alters and significantly mutes their TCR responsiveness. The group, thus, proposes that 'innate-like' lymphocytes reconcile their lymphoid and rapidly-responsive myeloid-like nature as follows: "During the development of innate-like T cells, a requisite activation of TCR signaling components markedly alters the antigen receptor response mode, removing it as the primary checkpoint for peripheral responsiveness. Thus freed, the cells can respond rapidly to innate signals." Wencker *et al.* further propose that this novel, atypical relationship to the TCR may permit innate T cells to utilize their TCR in novel ways. These include steady-state TCR-mediated engagement of epithelial cells by IELs or particular responses to large amounts of antigen in the context of particular cytokines (139,144). As such, TCR-expressing, 'innate' cells offer a vast expansion of the innate immune response repertoire. Indeed, $\gamma\delta$ T cells are known to express TCR repertoires that range from oligoclonal to polyclonal, depending on the subset and species of origin at hand (7). An 'innate' cell with a TCR may, moreover, provide an additional layer of quality control for lymphocytes entering the innate compartment.

While providing a fascinating insight into the workings of ‘innate’ mouse $\gamma\delta$ T cells, I emphasize that it is unclear what bearing this may have on human $\gamma\delta$ T cell counterparts. I stipulate that similar dependence on TCR may be found with human $\gamma\delta$ T IELs (largely of the V δ 1 subset). Importantly, not all mouse $\gamma\delta$ T cell subsets display TCR independence for the engagement of effector function, nor are all subsets stimulated by exposure to cytokines alone. It is possible that human $\gamma\delta$ T cells display a similar subset-specific dependence on the TCR.

1.8. Role of the BTN3A in $\gamma\delta$ T cell physiology

Detailed examination of human $\gamma\delta$ T cells function, particularly that of the peripherally dominant V γ 9V δ 2 subset, would be amiss without consideration of the role of the B7-like butyrophilins (BTN). Study of the B7 co-stimulatory immunoglobulin superfamily has expanded our understanding of the factors that regulate and fine-tune T cell activation. Classic examples of well-studied B7 member interactions include: I) activatory pairing of B7.1 (CD80) and B7.2 (CD86) on APCs to CD28 on T cells, and II) inhibitory pairing of B7.1 and B7.2 on APCs to CTLA4 on T cells. Further well-known and important members of the B7 family include PD1, PDL1 and B7RP1 (also known as ICOSL). Recent discoveries reveal that another immunoglobulin superfamily, closely related to the B7 family, may play a significant role in regulating the immune response.

The BTN immunoglobulin superfamily was first described in the 1980’s with the discovery of BTN1 (145). BTN1 (BTN1A1, specifically) was found to play a role in milk fat globule secretion and stabilization. The immune significance of the BTN family took decades to establish and is being unraveled still. With the number of known human BTN family members currently at 13, their roles appear almost entirely geared toward immune regulation. Even BTN1A1 has been ascribed a role in thymic stromal and B cell interactions with activated T cells and macrophages (146). While the exact immunomodulatory roles of BTN family members remain unclear, two main lines of evidence speak to their putative importance: i) the high phylogenetic homology of BTN

and B7 proteins, and ii) the extremely broad BTN expression on immune cells or cells that interact closely with immune cells (*e.g.* thymic stromal cells and intestinal epithelial cells). The multiple similarities between the BTN and B7 immunoglobulin superfamilies was explored recently by Arnett and Viney (147). Perhaps most obviously, the two protein families share high structural homology. Membership of the B7 family is largely defined by the presence of a small intracellular cytoplasmic tail and a transmembrane region linked to extracellular IgV and IgC domains, which then confer receptor binding specificity that is mainly for other immunoglobulin superfamily members (148). Similarly, BTNs have two extracellular IgV and IgC domains, as well as a transmembrane region. In a divergence from the B7 family, most members of the BTN family further contain an intracellular B30.2 signaling domain (illustrated in Fig 1.5).

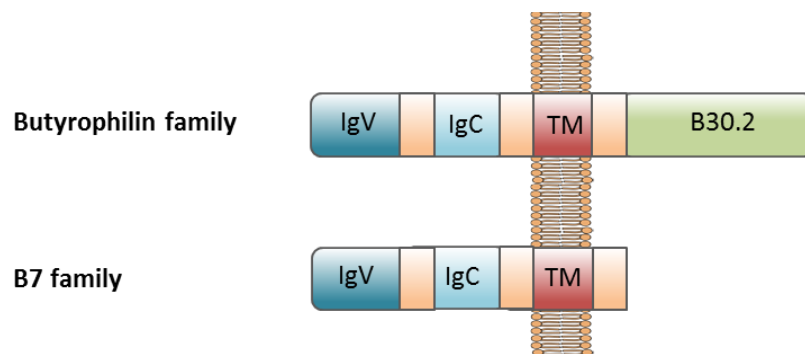


Fig. 1.5. Structural comparison of the B7 and BTN superfamilies. Both families share hallmark extracellular immunoglobulin domains, typically of IgV and IgC type. While the B30.2 domain is a common feature of BTNs, no known B7 members contain intracellular signaling domains. (TM, transmembrane domain)

Not a great deal is known about the specific cell surface binding partners of the BTN family, although it does not appear that these include the classic B7 targets of CD28, CTLA4, ICOS or PD1 (149,150). The intracellular binding interactions of BTNs are, meanwhile, governed by the B30.2 protein-binding domain. B30.2 binding partners can range from the enzyme xanthine oxidoreductase for BTN1A1 (151) to prenylated pAgs for BTN3A.1 (152). Interestingly, the B30.2 domains of these different BTNs do not appear cross-reactive in terms of binding partners. The B30.2 domain is defined by the presence of a PRY/SPRY element, which is composed of three specific sequence motifs, LDP, WEVE and LDYE. It derives its name from the inclusion of a SPRY domain, which is preceded by an amino-terminal PRY motif (153). The B30.2 domain is not exclusive to the BTN family, and has been identified in a total of 51 genes in the human genome, where it appears to play a role in mediating protein-protein interactions (154). Few specific binding partners are known.

The BTN3A (also known as CD277) subfamily of BTNs (BTNA.1, BTNA.2, BTNA.3) is expressed by most human immune cells, myeloid and lymphocytic in origin. These include T cells, B cells, NK cells, DCs and monocytes (149). A number of antibodies have been generated against all BTN3A subsets. Most of what we know about the importance of BTN3A in the functioning of $\gamma\delta$ T cells has been derived from these antibody studies, to which a significant contribution has been made by Dr. Daniel Olive's research group (Marseille, France). A summary of published anti-BTN3A antibodies can be viewed in Table 1.6.

Table 1.6 | Characteristics of published anti-BTN3A mAbs

Clone Identity	Effect on BTN3A	Known functional outcomes	Ref.
19.5	Agonistic to BTN3A.1	Binds to BTN3A directly on T cells, NK cells, monocytes and DCs, delivering an activatory signal.	(200)
20.1	Agonistic to all isoforms	Results in enhanced proliferation, survival and cytokine production, incl. IFN- γ , IL-1, IL-8 and IL-12.	(201)
103.2	Antagonistic to all isoforms	Sterically blocks association of proteins engaged by BTN3A.1 during activation. Known to block V γ 9V δ 2 T cell BTN3A.1-mediated activation.	(202)
232.5	Agonistic to BTN3A.3	Phosphorylates BTN3A.3 and initiates inhibitory signalling. Inhibits T cell function.	(203)

Observations from the various anti-BTN3A antibody clones indicate that these can be both, agonistic and antagonistic. The specific binding site and mode of engagement are what appear to govern the functional outcome of mAb engagement of BTN3A, ranging from phosphorylation to steric blocking (Table 8 and associated references). It is interesting to note that, due to the wide lymphocytic expression of BTN3A, anti-BTN3A mAb can exert dual effects on T cell activation: i) indirect effects, such as altering BTN conformation on target cells (*e.g.* monocytes) or affecting bystander cell activation with consequent pro- or anti-inflammatory effects, and ii) direct effects, such as activatory cross-linking of BTN on T cells themselves.

Comparing the different BTN3A isoforms, it is known that each contains an extracellular N-terminal IgV and a membrane-proximal IgC domain, connected to a single-pass transmembrane domain. BTN3A.1 and BTN3A.3 further contain an intracellular B30.2 domain, which is absent in BTN3A.2 (159). Importantly, while all three isoforms mediate V γ 9V δ 2 cell activation if treated with the agonistic mAb 20.1, only BTN3A.1 mediates pAg-induced activation (100,157). This alludes to i) high extracellular homology of the BTN3A isoforms, and ii) the recognition by V γ 9V δ 2 cells of extracellular BTN3A conformational changes. A basic summary of BTN3A isoform differences can be viewed in figure 1.6. Curiously, BTN3A.3 was not able to induce V γ 9V δ 2 cell activation in a pAg-dependent manner, despite containing a B30.2 domain. Sandstrom *et al.* recently demonstrated that this is due to a single amino acid difference between BTN3A.1 and BTN3A.3-associated B30.2 domains, which, in the case of BTN3A.3, impedes effective pAg binding (152).

Upon co-crystallization of pAg and BTN3A.1-associated B30.2, Sandstrom *et al.* provided definitive evidence for the importance of the B30.2 domain in acting as an intracellular pAg ‘sensor’ that communicates stress to V γ 9V δ 2 cells via its extracellular BTN3A portion (152).

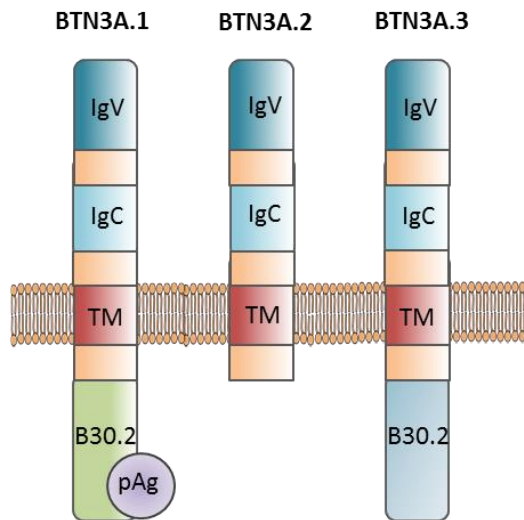


Fig. 1.6. Different isoforms of BTN3A. All isoforms share the same structure of the extracellular domain. Both BTN3A.1 and BTN3A.3 contain further intracellular B30.2 domains. Due to a single amino acid change, however, only BTN3A.1 B30.2 is capable of effectively binding pAg and, thus, transmitting the presence of intracellular pAg to V γ 9V δ 2 cells. (TM, transmembrane domain)

In contrast to the clarity of pAg-B30.2-BTN3A interactions, little is understood about how exactly the binding of pAg to BTN3A.1 B30.2 is recognized by $V\gamma 9V\delta 2$ cells. Rhodes *et al.*, who were crucial in the discovery and characterization of human BTN3A, have recently described three different scenarios by which BTN3A.1 may mediate $V\gamma 9V\delta 2$ cell activation (160). These are summarized in figure 1.7.

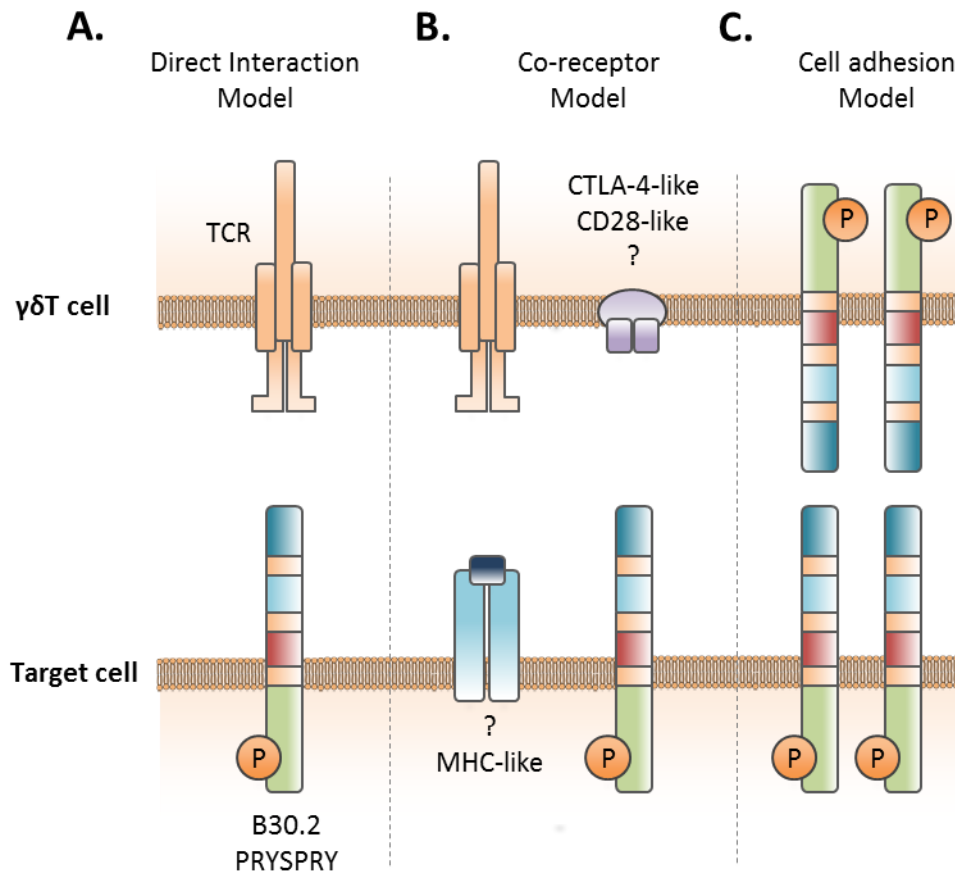


Fig. 1.7. Models of $\gamma\delta$ T cell activation by BTN3A. (A) The Direct Interaction model proposes that BTN3A.1 and its conformational changes are the ligand for the $V\gamma 9V\delta 2$ TCR. *(B)* The Co-receptor model proposes that the $V\gamma 9V\delta 2$ TCR interacts with an MHC-like molecule, while BTN3A interacts with a B7-like (e.g. CTLA-4-like or CD28-like) molecule. *(C)* The Cell-Adhesion model proposes that BTN3A engages in homotypic interactions, which promote cell contact between the $V\gamma 9V\delta 2$ and potential APC.

While all of the models described by Rhodes *et al.* are based on the finding that it is specifically BTN3A.1 that is critical for activatory signal transmission to V γ 9V δ 2 cells, they highlight that data indicates there is a role for the BTN3A.2 and BTN3A.3 isoforms and the recruitment of periplakin to stabilize the complex in the cell membrane (161). The three models they describe are, briefly: I) the Direct Interaction model, in which BTN3A.1 (or specific conformation, therein) is a ligand for the $\gamma\delta$ TCR (Fig.1.7A), II) the Co-receptor model, which assumes that $\gamma\delta$ T cell activation occurs much more along the lines of canonical T cell – APC interactions; in this model, the $\gamma\delta$ TCR recognizes an MHC-like molecule, while BTN3A acts as a co-receptor, likely binding to CD28-like or CTLA-4-like molecules; importantly, no such target molecules for the $\gamma\delta$ TCR or BTN3A have (yet) been identified (Fig.1.7B), III) the Cell Adhesion model, whereupon BTN3A molecules, in given conformation, simply act as adhesion factors promoting cell-cell interaction in a pAg-dependent manner (Fig.1.7C). Whether the $\gamma\delta$ TCR is engaged directly by BTN3A, thus, remains unclear.

In fact, so little is understood about the direct nature of BTN3A-V γ 9V δ 2 contact, that one is forced to expand the intracellular pAg-B30.2-BTN3A model. Acknowledging that pAg binding to B30.2 of BTN3A.1 is indeed activatory to V γ 9V δ 2 cells *in vitro*, Harly *et al.* hypothesize that the reality may be more complicated than that (162). One hypothesis put forth argues that extracellular pAgs are imported into target cells by unidentified transporter(s), or are produced intracellularly. Potentially, both are the case. These pAgs then bind the intracellular B30.2 domain of BTN3A.1, which induces non-exclusive key modifications in the receptor protein, which may include conformational changes, modifications of its membrane topology, recruitment or exclusion of molecular patterns, etc. Any or all of these changes can then be sensed by V γ 9V δ 2 cells. This is, perhaps, the current most popular model among researchers interested in V γ 9V δ 2 cell activation. Alternatively, Harly *et al.* argue, pAg binding could occur intracellularly *as well as* the extracellularly. Accepting that the B30.2-pAg interaction (and BTN3A.1 conformational changes, therein) are important does not exclude the possibility that also a kind of ‘antigen presentation’ occurs, whereupon the conformationally-changed BTN3A.1 can therefore present pAg to the V γ 9V δ 2 TCR. In contrast to Rhodes *et al.* and their proposed hypothetical mechanisms of activation, Harly and group appear to place significantly more

emphasis on the specific involvement of the TCR in BTN3A.1-triggered activation of V γ 9V δ 2 cells. A basic summary of Harly's different hypotheses can be viewed in figure 1.8. The idea that prenyl pyrophosphates may be presented to $\gamma\delta$ T cells on extracellular portions of BTN3A.1 has garnered experimental and intellectual support from a number of groups and researchers, including Vavassori *et al.*, Kabelitz *et al.*, De Libero *et al.* and Esser *et al.* (163–165).

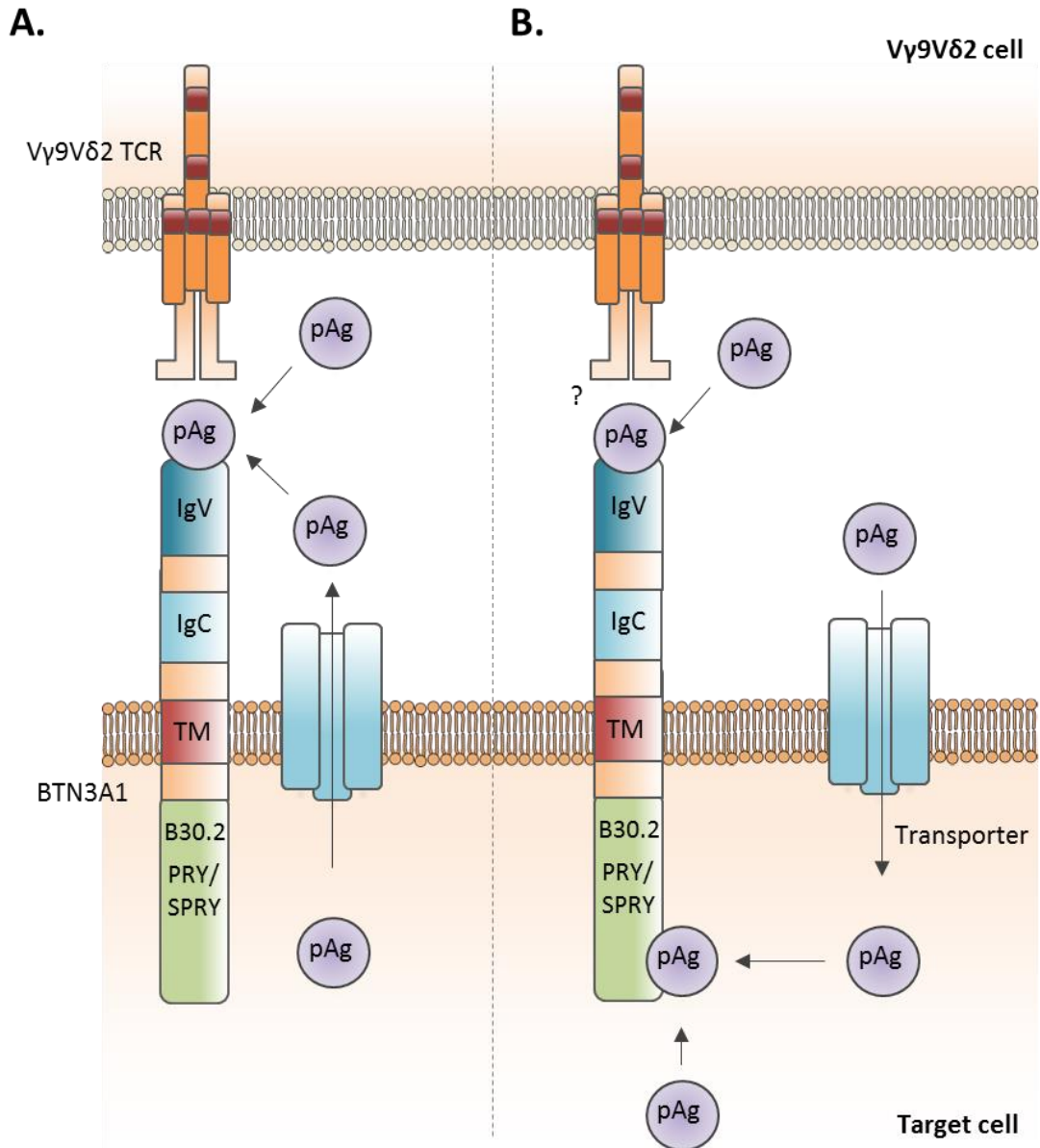


Fig. 1.8. Alternate models of pAg sourcing for Vγ9Vδ2 cell activation via BTN3A.1. Several competing and, possibly, complementary hypotheses exist of Vγ9Vδ2 cell activation by pAg via BTN3A.1 as put forth by Harley *et al.* **(A)** One hypothesis argues that intracellular pAg are exported from the cell by unidentified transporter(s), or are found in the extracellular environment, or both. These pAgs then bind BTN3A.1 on its extracellular portion (e.g. via the IgV). It is then the combination of pAg + BTN3A.1 ‘carrier’ that is recognized by the Vγ9Vδ2 TCR. **(B)** Another hypothesis stipulates that pAgs are produced intracellularly and sourced from therein or imported from the extracellular space via unknown transporters, or both. Intracellular pAg then binds the BTN3A.1 B30.2 domain, inducing key modifications to the to the receptor protein, such as changes to the membrane topology, recruitment/exclusion of molecular patterns or conformational changes to the receptor. Possibly, extracellular pAg then further binds BTN3A.1 extracellularly. These changes are then recognized by the Vγ9Vδ2 TCR.

Experimental clarification is necessary to establish whether BTN3A extracellular domains are engaged by the V γ 9V δ 2 TCR directly. Even if this is achieved, reconciliation of the various BTN3A-TCR engagement theories and the observation that cross-linking of all BTN3A isoforms with agonistic mAb (*e.g.* clone 20.1) mimics V γ 9V δ 2 cell pAg stimulation is necessary. It is possible that all proposed scenarios are true in particular settings and that significant mechanistic redundancy is in place for the activation of $\gamma\delta$ T cells by pAg. It is not inconceivable that $\gamma\delta$ T cells may be capable of sensing pAg-related cellular stress via receptors other than the TCR. As described in earlier sections, it is known that human V δ 2 cells express a range of non-TCR receptors that sense stressed or transformed self, *e.g.* NKG2D.

An important aspect of placing a pivotal role on BTNs in V γ 9V δ 2 cell activation is the consequent apparent divergence of $\gamma\delta$ T cells from other innate-like human T cells. Like invariant NKT (iNKT) cells or MAIT cells, human $\gamma\delta$ T cells appear to originate preferentially prior to birth and express semi-invariant TCRs: V γ 9V δ 2 for $\gamma\delta$ T cells, V α 24-J α 14-V β 11 for iNKT cells and V α 7.2-J α 22-oligoclonal V β for MAIT cells (166). iNKT and MAIT cells do, however, both recognize antigen presented on MHC class I-like molecules, CD1d and MR1, respectively. Thus, unlike nearly all other T cell types, including innate-like $\alpha\beta$ T cells, V γ 9V δ 2 cell activation appears independent of MHC class-like molecules. As outlined earlier, $\gamma\delta$ T cells do not appear to share the $\alpha\beta$ T cell dependence on the presence of professional antigen presentation or specific antigen presenting molecules. And when and if a dependence on a cell surface molecule for activation is observed, it may be instead on B7-like BTNs.

1.9. $\gamma\delta$ T cells as a tool in immunotherapy

As outlined above, elevated counts of activated, functional $\gamma\delta$ T cells correlate with improved health outcomes in human infection and malignancy, both solid and non-solid in nature. The physiological rationale for the apparently beneficial presence of $\gamma\delta$ T cells may derive from their production of inflammatory cytokines, direct target lysis, recruitment and activation of innate immune components, maintenance of epithelial barrier integrity and tissue healing, regulation of B cell immunity and even priming and modulation of the $\alpha\beta$ T cell response.

Such an expansive array of effector phenotypes for any one cell type carries complications in its use and manipulation in the clinic. It remains unclear whether these functions can be carried out by all human $\gamma\delta$ T cell subsets and are stimulation-dependent. Is it crucial we focus on V δ 1, V δ 2 or V δ 1-V δ 2⁻ $\gamma\delta$ T cells? Does sourcing $\gamma\delta$ T cells from peripheral blood bear consequences on their putative eventual clinical effects at epithelial surfaces? Can the same $\gamma\delta$ T cells act as pAPCs and killers simultaneously? Questions such as these, among others, need to be resolved prior to the safe and effective introduction of $\gamma\delta$ T cells into the clinic. If, however, we are able to gain a firm grasp of understanding on this complex and potentially heterogeneous set of $\gamma\delta$ TCR^{POS} cells, their clinical expediency would be significant. Perhaps the most useful property of $\gamma\delta$ T cells as an immunotherapeutic tool is the range of effector functions they may offer, uniting current clinical efforts with $\alpha\beta$ T cells, DCs and other myeloid cells under one cell type. A significant advantage of using $\gamma\delta$ T cells is their lymphoid capacity for rapid, extensive and sustained expansion *in vivo* and *in vitro*, in contrast to other pAPCs in immunotherapy development, such as DCs. We know, furthermore, that zoledronate – perhaps the most routinely used expansion stimulus for peripheral V δ 2 $\gamma\delta$ T cells – is safe to use in humans systemically. Zoledronic acid (zoledronate) is already used in the clinic as a treatment for osteoarthritis. It's proposed mechanism of action involves the reduction of osteoclast activity (167).

1.10. Aims of the project

The observations of *in vivo* $\gamma\delta$ T cell expansion upon clinical infectious disease, and the *ex vivo* work by Brandes, *et.al.* and our own laboratory on the pAPC function of human $\gamma\delta$ T cells prompted us to investigate how Gram-negative bacteria may impact the effector phenotype of this atypical T cell subset. I modeled the events that may occur during systemic infection by exposing whole, freshly-isolated PBMC to UV-irradiated *E.coli*. *E.coli* is a common cause of sepsis and bacteremia in humans, and resides as a commensal in the gastrointestinal mucosa highly populated by $\gamma\delta$ T cells. As mentioned above, *E.coli* further expresses known $\gamma\delta$ T cell targets such as HMBPP.

I ventured to document freshly-isolated $\gamma\delta$ T cell effector responses to acute *E.coli* exposure and subsequent responses to re-exposure of expanded cells. I further set out to compare $\gamma\delta$ T cell effector phenotype in response to two radically different stimuli: i) *E.coli*, representing a target-rich, complex, highly pro-inflammatory non-self stimulus, and ii) zoledronic acid, a small molecule pyrophosphate accumulation-inducing bisphosphonate drug, representing a stressed self stimulus.

2. MATERIALS AND METHODS

2.1. Study Design

This study was designed to investigate how Gram-negative bacteria may impact development of $\gamma\delta$ T cell effector phenotype. The experimental setup was modeled to reflect events that may occur during systemic infection via stimulating whole, freshly-isolated PBMC with UV-irradiated *E.coli*. $\gamma\delta$ T cell responses were recorded upon primary stimulation of fresh PBMC and subsequent re-stimulation of expanded cells. I further addressed which $\gamma\delta$ T cell effector functions are dependent on the $\gamma\delta$ T cell receptor and butyrophilin 3A.

The sample number for most expansions and experiments was five different donors; donor number is listed for all data in the corresponding figure legend. All donors used were healthy adults, between the ages of 21 and 55 years old, representing a roughly equal mixture of male and female participants. I note that recent research by Pennington and colleagues (106) indicates that gender and age of peripheral V δ 2 cell donors are unlikely to exert significant effects on observed cell behaviour. The number of five donors was chosen from previous experience in the study of known phenotypic variations between donors, in order to accurately reflect these variations. All experiments were repeated at least once, with the exception of DNA sequencing. DNA sequencing was, however, done as a separate experiment and each clonotype sequencing included in the analysis was represented by multiple individual reads. In addition, spectratyping was carried out on two donors, both of whom yielded similar results.

All experiments using peripheral blood-derived cells were performed in accordance with relevant guidelines and regulations, and were approved by UCL Research Ethics Committee. Informed consent was obtained from all volunteer blood donors.

2.2. Statistical analysis

Where relevant, acquired data was evaluated statistically with paired or unpaired t tests without assumed consistent standard deviation. Statistical significance was assessed through the Holm-Sidak method of correcting for multiple comparisons. The results referred to as “significant” further in the text entail a P value of 0.05 or lower. The statistical and graphic analysis software employed was Prism 6.0. All bar graphs indicate the mean and respective error bars indicate standard deviation of the data sets. Individual significant P values are indicated in each figure as appropriate. The individual donor number used to generate the data in each figure is indicated in accompanying figure legends. All figures are indicative of at least two experiments.

2.3. Sample acquisition and preparation

PBMCs from healthy adult donor peripheral blood were routinely extracted via Ficoll density gradient separation. Briefly, peripheral blood was obtained by venipuncture and collected in EDTA-treated containers to prevent coagulation. It was then layered onto Lymphoprep solution and centrifuged at 800g for 35min at room temperature, leading to a layer separation, according to constituent density. Plasma and red blood cell layers were discarded, while the PBMC buffy coat was processed by washing twice in phosphate-buffered saline (PBS; Invitrogen) with centrifugation at 800g for 10min. The PBMCs were then counted, suspended in complete RPMI 1640 at the desired concentration, and either stained immediately or cultured overnight for subsequent investigation.

Cells were cultured in supplemented RPMI 1640 medium at a density of 1.5×10^6 cells/mL at 37°C and 5% CO₂. Supplemented culture medium contained RPMI 1640-GlutaMax

(Life Technologies), 10% foetal calf serum, 1% Penicillin/Streptomycin (Life Technologies), 10mM HEPES buffer (Life Technologies), 1mM Sodium Pyruvate (Life Technologies) and 1x MEM non-essential amino acids (Life Technologies) (Table 2.1). All stimulation studies, unless explicitly specified, further included 100 IU/mL recombinant human IL-2 (MACS Miltenyi); medium was supplemented every two to three days.

Table 2.1 | **Recipe for complete $\gamma\delta$ T cell culture medium**

Reagent	Concentration
RPMI 1640 GlutaMax	1x
Foetal Calf Serum	10%
Penicillin / Streptomycin	100IU/mL
HEPES buffer	10mM
Sodium Pyruvate	1mM
MEM Non-Essential Amino Acids	1x

2.4. Growth and preparation of *E.coli* DH5 α

E.coli (Thermo Fisher) were grown overnight at 37°C shaking culture in 1mL ampicillin (Life Technologies)-supplemented LB medium (Sigma) from cryogenically preserved aliquots. Once grown, *E.coli* culture was washed thoroughly and assessed for colony forming unit (CFU) count via duplicate measurement of suspension optical density (OD), which typically equalled OD ~0.5 after overnight growth. With the exception of killing assays, all bacteria employed in co-culture experiments were irradiated in a trans-illuminator chamber (UVITEC), equipped with eight UV-C (250-280nm) lamps, for a period of at least 7min. Irradiation times were decided based on the minimal irradiation period necessary to prevent growth of irradiated *E.coli* in subsequent overnight liquid culture. With the exception of *E.coli*-pHrodo acidification assays, all assays employed freshly-grown *E.coli* DH5 α .

2.5. *E.coli* opsonisation

E.coli were opsonized with commercially available highly purified anti-*E.coli* rabbit serum IgG (*Escherichia coli* BioParticles Opsonizing Reagent from Thermo Fisher) according to commercial protocol. Briefly, irradiated *E.coli* were re-suspended in PBS to OD ~0.5, mixed with the recommended saturating dose of purified anti-*E.coli* rabbit serum IgG and incubated for 30min at room temperature. *E.coli* were then washed twice in 30mL of sterile PBS.

2.6. PBMC stimulation with UV-irradiated *E.coli*

Freshly isolated or expanded 1.5×10^6 cells/mL PBMC were co-cultured with *E.coli* (MOI 10) in supplemented RPMI 1640 medium, and cultured overnight (16-18h) or left to expand for 14 days. Re-stimulation of expanded PBMC with *E.coli* was carried out by mixing 14-day *E.coli*-expanded PBMC with irradiated *E.coli* at MOI 10. Re-stimulation

of expanded PBMC with *E.coli* in the presence of freshly-isolated autologous PBMC was carried out by mixing fluorescence-assisted cell sorting (FACS)-stained 14 day *E.coli*-expanded PBMC with freshly-isolated unstained autologous PBMC at a ratio of 1:10 prior to the addition of irradiated *E.coli* at MOI 10.

2.7. PBMC stimulation with zoledronate

Freshly isolated 1.5×10^6 cells/mL PBMC were cultured in $5 \mu\text{M}$ zoledronic acid monohydrate (zoledronate; Sigma-Aldrich) in supplemented RPMI 1640 medium, and cultured for 14 days. Re-stimulation of expanded PBMC with *E.coli* was carried out by mixing 14 day *E.coli*-expanded PBMC with irradiated *E.coli* at MOI 10.

2.8. FACS staining and processing

PBMC were stained for cell viability, surface markers, intracellular cytokines and cell surface CD107a throughout stimulation and expansion as indicated in supplied commercial protocols. Intracellular cytokine and CD107a staining was carried out on overnight stimulated PBMC that were cultured for a further 4h in the presence of monensin (BioLegend). Colour compensation was carried out using OneComp eBeads (eBioscience). FACS analysis was performed on the Becton Dickinson (BD) LSR II and data processing - on FlowJo vX.07 software.

The following antibody conjugates were used in PBMC staining: CD3-PE/Dazzle594 (BioLegend; clone: UCHT1), $\alpha\beta$ TCR-PE (BioLegend; clone: IP26), $\alpha\beta$ TCR-PE/Vio770 (MACS Miltenyi; clone: BW242/412), $\gamma\delta$ TCR-PE/Vio770 (MACS Miltenyi; clone: 11F2), V δ 1-FITC (Thermo Fisher; clone: TS8.2), V δ 1-APC (MACS Miltenyi; clone: REA173), V δ 2-PerCP (Biolegend; clone: B6), V δ 2-PE (Biolegend; clone: B6), IFN- γ -PE (BioLegend; clone: B27), TNF- α -APC (BioLegend; clone: MAb11), IL-17-Brilliant Violet 605 (BioLegend; clone: BL168), CD69-PerCP (BioLegend; clone: FN50), IL-10-

FITC (Affymetrix eBiosciences; clone: BT-10), granulysin-PE (BioLegend; clone DH2), CD107a-FITC (BioLegend; clone: H4A3), CCR7-PE (R&D Systems; clone: 150503), CD62L-Brilliant Violet 605 (Biolegend; DREG-56), CD4-FITC (Miltenyi Biotec; clone: M-T466), CD8-APC (Miltenyi Biotec; clone: BW135/80), CD56-PE (Biolegend; clone: MEM-188), CD14-FITC (Miltenyi Biotec; clone: TÜK4), CD16-Brilliant Violet 605 (Biolegend; clone: 3G8), CD19-PE/Cy7 (Biolegend; clone: HIB19), CD33-APC (Biolegend; WM53), CD1c-PerCP/Cy5.5 (Biolegend; clone: L161), CD27-APC/Vio770 (Miltenyi Biotec; clone: M-T271), CD45RA-FITC (BioLegend; clone: HI100), HLA-DR (MHC II)-APC/Cy7 (BioLegend; clone: L243), CD86-APC (MACS Miltenyi; clone: FM95), CD277-PE (clone: BT3.1; Biolegend), V γ 9-APC/Vio770 (clone: REA470; MACS Miltenyi). Mouse IgG1 κ of known, irrelevant, non-human specificity served as isotype control (BioLegend; clone: MG1-45). All FACS data presented subsequently is on singlet, live lymphocytes. All further references to ‘MFI’ denote median fluorescence intensity. The gating strategy employed in analysis is shown below in Fig.2.1. The use of a gating strategy that targets CD3^{pos} $\alpha\beta$ TCR^{neg} cells instead of CD3^{pos} $\gamma\delta$ T^{pos} cells is justified and examined in Fig.2.2. No significant difference in $\gamma\delta$ T cell content was found using either strategy. CD3^{pos} $\alpha\beta$ TCR^{neg} cells were used to identify $\gamma\delta$ T cells due to the much brighter expression of $\alpha\beta$ TCR *versus* $\gamma\delta$ TCR, thus permitting clearer delineation of the two cell populations, and ensuring that all $\gamma\delta$ T cells are included in the analysis.

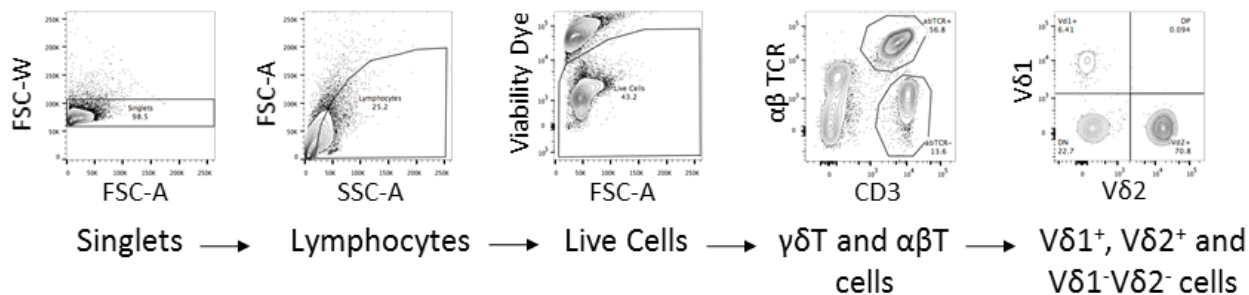


Fig. 2.1. Gating strategy. All FACS data shown for $\gamma\delta$ T cells is gated on singlet lymphocyte live $CD3^{pos} \alpha\beta TCR^{neg}$ and $V\delta$ chain-determined subsets thereof. $\alpha\beta$ T cells are designated as singlet lymphocyte live $CD3^{pos} \alpha\beta TCR^{pos}$ cells, respectively.

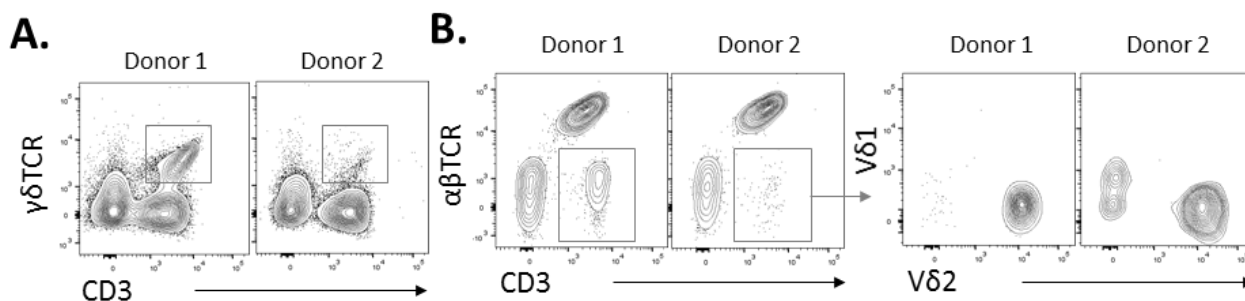


Fig. 2.2. Gating on $\gamma\delta$ T cells according to $\gamma\delta$ TCR versus $\alpha\beta$ TCR. Two methods of gating on $\gamma\delta$ T cells within whole, live PBMC, were compared. Two donor data is shown on freshly-isolated PBMC; one donor is representative of relatively high resting $\gamma\delta$ T cell content ($\sim 10\%$ of total PBMC), and the other – of relatively low resting $\gamma\delta$ T cell content ($\sim 0.5\%$ of total PBMC). The same anti-CD3 fluorochrome-antibody conjugate is used for both stains. Both anti- $\gamma\delta$ TCR and anti- $\alpha\beta$ TCR fluorochrome-antibody conjugates were purchased from the same vendor and are of the same fluorochrome (PE/Vio770). **(A)** $\gamma\delta$ T cells, gated as $CD3^{pos} \gamma\delta TCR^{pos}$ cells; **(B)** $\gamma\delta$ T cells, gated as $CD3^{pos} \alpha\beta TCR^{neg}$ cells, with a sub-gate of $CD3^{pos} \alpha\beta TCR^{neg}$ cell expression of $V\delta 1$ and $V\delta 2$.

2.9. Confocal imaging of $\gamma\delta$ T cell uptake of *E.coli*

Acknowledgement: This preliminary work was carried out by Dr. Anne Marijn Kramer, another PhD student in the laboratory, in collaboration with Dr. Dale Moulding of GOS ICH Imaging Facility. It is included in the present thesis, with her consent, to illustrate the evolution of thought that produced the experimental narrative.

Imaging was performed on a Zeiss AxioObserver LSM 710 confocal microscope. FACS-purified 14 day zoledronate-expanded $\gamma\delta$ T cells were incubated with IgG-opsonized, IPTG-inducible green fluorescent (GFP)-expressing *E.coli* (Thermo Fisher) for 60min, placed on ice and fixed. Cells were then fluorescently labeled, deposited on cleaned coverslips and mounted on glass slides using ProLong Gold antifade mountant (Thermo Fisher) and cured in the dark at room temperature for 24 hours. Images of cell conjugates were acquired with a 63 \times Plan-Apochromat oil objective, numerical aperture 1.4. Acquisition was optimized for subsequent deconvolution with Huygens software, using appropriate voxel sizes according to the Huygens Nyquist calculator.

2.10. Confocal imaging of $\gamma\delta$ T cell uptake of *E.coli*

Acknowledgement: This preliminary work was carried out by Dr. Anne Marijn Kramer. It is included in the present thesis, with her consent, to illustrate the evolution of thought that produced the experimental narrative.

Imaging was performed on an Image StreamMark II flow cytometer (Amnis). Prior to analysis, 14 day zoledronate-expanded $\gamma\delta$ T cells were incubated with protease-sensitive DQ-Green (Thermo Fisher), BSA-labelled opsonized or non-opsonized polystyrene beads 0.5 μ m or 1.0 μ m in size (Polysciences) for 60min, fixed and stained for cell surface markers. The opsonin used was Rituximab, a monoclonal, chimeric human-mouse IgG (Hoffman La Roche). The mode of opsonisation was passive adsorption of a saturating concentration of antibody to the bead, according to commercial protocol as supplied by

Thermo Fisher. Post- acquisition data analysis was performed using IDEAS software (Amnis). ImageStream internalisation scores (IS) were generated by IDEAS software as described in commercially supplied protocol. Briefly, IS is defined as the ratio of fluorescence intensity inside the cell to the intensity of the entire cell. The inside *versus* outside of the cell is judged by application of an internal mask based on the brightfield image that covers the inside of the cell, the thickness of the cell membrane in pixels and the fluorescence channel of interest, while the external region is determined by dilating the internal mask by the membrane thickness and combining this with the object mask of the channel of interest.

2.11. *E.coli* FITC uptake assay

A FITC-Trypan blue quenching assay was employed to assess PBMC uptake of *E.coli*. Briefly, UV-irradiated *E.coli* DH5 α were FITC labeled by a gentle shaking in a saturated FITC isomer I (Sigma)-PBS solution for 1h at 37°C, followed by washing prior to co-culture with fresh or expanded PBMC at MOI 10. PBMC were co-cultured in triplicate 60min at 37°C in a 5% CO₂ incubator. Cells were then fixed in cold fixation buffer (Biolegend) before quenching with 0.4% Trypan blue solution (Sigma-Aldrich) to remove extracellular FITC signal. After quenching, PBMC were washed three times in a large volume of PBS and analyzed using flow cytometry. Each sample of quenched PBMC-*E.coli* mixture was treated in parallel to a non-quenched sample of the same origin to ensure that quenching had taken place. A quenched PBMC sample incubated with non-FITCylated *E.coli* was used as a control for background FITC fluorescence. In order to determine the involvement of actin polymerization in *E.coli* uptake, PBMC were pre-incubated in 0.2mM CyD (Sigma), vessel control, DMSO (Sigma), or normal medium.

Trypan blue quenching as a method to study phagocytosis has been described previously by Busetto *et al.* (168). Figure 3.1. illustrates the effect that Trypan blue quenching exerts on green fluorescent dyes, such as FITC (ex/em at 495/519) or close homologue, 5(6)-FAM-SE (ex/em at 494/519), which Busetto *et al.* employed in the development of this

uptake assay. The principles that the assay is based upon, briefly, are that Trypan blue i) absorbs light emitted by green dyes and emits it at a far red frequency, and ii) does not penetrate into the interior of live cells. Fig.2.3A and B show a Trypan blue quenched polymorphonuclear cell (PMN)-green *Candida albicans* co-culture analyzed via confocal microscopy and flow cytometry, respectively.

2.12. *E.coli* pHrodo acidification assay

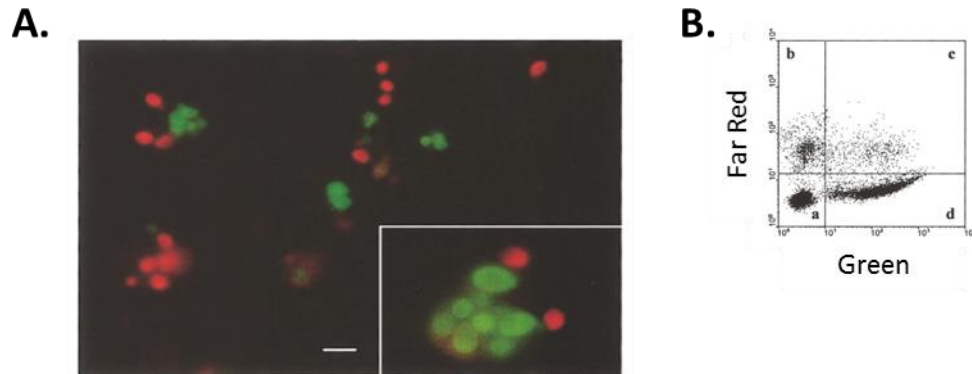


Fig. 2.3. Trypan blue (TB)-quenching as a method to study uptake of green fluorescent material. This figure is an adaptation from Busetto *et al.* (97) who describe a quantifiable assay to study uptake of fluorescently-labeled target particles, which employs Trypan blue quenching and flow cytometry. Polymorphonuclear (PMN) cells were incubated with 5(6)-FAM-SE-labeled *Candida albicans*, washed thoroughly, fixed, quenched with Trypan blue and analyzed via confocal microscopy or flow cytometry. 5(6)-FAM-SE is a FITC homologous fluorescent dye with an absorbance peak at 494nm and an excitation peak at 519nm. **(A)** PMNs were examined via confocal microscopy, following Trypan blue quenching. Extracellular *C.albicans* particles can be seen in far red, while intracellular particles – in green. A magnified single PMN is shown, with both extracellularly adherent and internalized *C.albicans*. **(B)** The same sample was analyzed via flow cytometry. Gated on PMN, one can observe: i) negative, ii) Green single positive, iii) Far Red single positive or iv) double positive cells, corresponding to i) no *C.albicans*, ii) internalized *C.albicans* only, iii) extracellularly-adherent *C.albicans* only, or iv) PMN, which have both adhered and internalized *C.albicans*.

A commercial *E.coli*-pHrodo assay was employed to assess PBMC acidification of internalized bacteria according to supplied protocol (available from “pHrodo™ Red and Green BioParticles® Conjugates for Phagocytosis” by Thermo Fisher Scientific). Briefly,

supplied PFA-fixed, pHrodo-dyed *E.coli* (strain: K-12; product code: P35366) was re-suspended via sonication in a pH neutral isotonic buffer, HBSS (Life Technologies), and co-cultured with PBMC in triplicate in a 96-well plate for 60min at 37°C and 5% CO₂. The medium used in this assay was pre-warmed, pH neutral HBSS, sans IL-2. After co-culture, the sample was removed into cold commercial fixation buffer (Biolegend). After fixation, PBMC were washed thoroughly and FACS stained for cell surface markers. Fixed and stained PBMC were then analyzed using flow cytometry. pHrodo dyes do not fluoresce at basic or neutral pH, but fluoresce strongly in proportion to pH drop below pH of 7. *E.coli*-pHrodo alone served as control for background pHrodo fluorescence. In order to determine the involvement of actin polymerization in bacterial acidification, PBMC were pre-incubated in 0.2mM CyD, DMSO or normal medium.

2.13. Meso Scale Discovery electrochemiluminescence assay

The following work was carried out in collaboration with and guidance by Dr. James Bonner and Dr. Intan Yeop, of ICH GOS Infection, Immunity and Rheumatology section. Levels of various cytokines in the medium of freshly-isolated, overnight-stimulated PBMC were measured and analyzed using a multiplex assay, the Meso Scale Discovery electrochemiluminescence assay (MSD). MSD analysis is a highly reproducible and accurate analysis platform, described by some as a more precise and reliable multiplex cytokine measurement system compared to the Cytometric Bead Array (169). Freshly-isolated PBMC were co-cultured overnight with irradiated *E.coli* (MOI 10) or zoledronate (5µM) and pelleted. Culture supernatant was removed and analyzed as described in commercial protocol. Samples were analyzed in duplicate using two MSD® Multi-Spot Assay System kits: i) V-Plex™ Cytokine Panel 1 (human) kit, which included the cytokines GM-CSF, IL-1α, IL-5, IL-7, IL-12/IL-23p40, IL-15, IL-16, IL-17A, TNF-β, VEGF, and ii) V-Plex™ Proinflammatory Panel 1 (human) kit, which included the cytokines / inflammatory mediators IFN-γ, IL-1β, IL-2, IL-4, IL-6, IL-8, IL-10, IL-12p70, IL-13 and TNF-α.

2.14. Sequencing of $\gamma\delta$ TCR CDR3

The following work was carried out in collaboration with Dr. Yvonne Majani, of ICH GOS Developmental Biology and Cancer section. RNA was extracted from 1×10^6 freshly isolated, 14 day *E.coli* or zoledronate-expanded PBMC. cDNA synthesis and PCR amplification of the gamma and delta chain sequences was performed using a commercial kit (Irepertoire Illumina human gamma delta kit; Cat. No. HTDGI-01-P). Amplified, barcoded fragments were sequenced on an Illumina MiSeq to a depth of 250 paired ends. Analysis was performed using a commercial platform provided by Irepertoire®.

2.15. Spectratyping of $\gamma\delta$ TCR CDR3

The following work was carried out in collaboration with Dr. Stuart Adams, of GOSH Department of Bone Marrow Transplantation. Spectratyping was used to determine CDR3 lengths for functional V-gamma 9 and V-delta 2 genes. RNA was extracted from 14 day *E.coli*-expanded or zoledronate-expanded PBMC. Following this, cDNA was synthesized using High Capacity RNA to cDNA (Thermo Fisher Scientific). With cDNA as the template, TCR V-delta 2 specific forward primer (TGAAAGGAGAAGCGATCGGT) or TCR V-gamma 9 specific forward primer (TGGAATGTGTGGTGTCTGGA), and a fluorescently labeled TCR C-delta (GACAAAACGGATGGTTTGG) or TCR C-gamma (GGGGAAACATCTGCATCAAG) reverse primer were used to amplify fragments of interest by PCR. Fragments were separated by size using capillary electrophoresis and analyzed by GeneMapper v3.7 software (Applied Biosystems).

2.16. Confocal imaging of *E.coli*-expanded $\gamma\delta$ T cell morphology

$\gamma\delta$ T cells were expanded from PBMC with *E.coli* for 14 days. Expanded PBMC were not purified, but were checked via FACS staining for 90+ % CD3^{pos} cell content. PBMC were

then stained with V δ 2-PE mAb (clone: B6), washed, re-suspended at 1×10^6 cells/mL in Live Cell Imaging Solution (Thermo Fisher Scientific) and plated in a 96-well glass-bottom plate (Thermo Fisher Scientific). After live imaging, cells were stained with DAPI and Hoechst dyes to visualize the cell nucleus and outer cell membrane. Imaging was performed on a Zeiss AxioObserver LSM 710 confocal microscope. Images of live cells were acquired with a 63 \times Plan-Apochromat oil objective, numerical aperture 1.4.

2.17. $\gamma\delta$ T cell sorting by flow cytometry

Day 14 expanded PBMC, with a predominantly $\gamma\delta$ T cell content, were purified further using flow sorting on the LSR II to >98% purity. Prior to the sort, PBMC were stained for expression of CD3 with CD3-PE/Dazzle594 (BioLegend; clone: UCHT1) and $\alpha\beta$ TCR with $\alpha\beta$ TCR-PE/Vio770 (MACS Miltenyi; clone: BW242/412). $\gamma\delta$ T cells were sorted for as CD3^{pos} $\alpha\beta$ TCR^{neg} PBMC, gated as shown in Fig.2.1 in the general Materials and Methods chapter (Chapter II). Bright fluorophores were used to maximize the clear separation of expanded $\alpha\beta$ T and $\gamma\delta$ T cells. Samples of purified $\gamma\delta$ T cells were stained post-sort for further $\gamma\delta$ T cell markers including V δ 2 and $\gamma\delta$ TCR to establish purity. $\gamma\delta$ T cells were sorted into 50% foetal calf serum and cultured overnight in complete RPMI 1640 prior to use in functional assays.

2.18. $\gamma\delta$ T cell antigen presentation assay

$\gamma\delta$ T cells were purified from 14 day zoledronate-expanded PBMC using FACS sorting to >98% purity; >90% of zoledronate-expanded $\gamma\delta$ T cells express a V δ 2 TCR, as described earlier in Chapter III. To mitigate the stress and potential TCR internalization in response to purification, purified $\gamma\delta$ T cells were rested overnight in supplemented, antibiotic-free RPMI 1640 medium. Zoledronate-expanded PBMC were used instead of *E.coli*-expanded PBMC to avoid the possibility that *E.coli* or debris thereof may still be present in culture medium or even intracellularly, if taken up by PBMC. Overnight rested, purified $\gamma\delta$ T cells were then incubated overnight with irradiated, IgG-opsonized *E.coli* DH5 α at MIO 10 to

allow time for phagocytosis, antigen processing and presentation at the cell surface. $\gamma\delta$ T cells were then washed thoroughly. In parallel, $\alpha\beta$ T cells were purified via positive magnetic selection (Anti- $\alpha\beta$ TCR MicroBead selection kit, Miltenyi Biotec) from autologous, freshly-isolated PBMC and rested overnight. Purified, opsonized *E.coli*-stimulated, expanded $\gamma\delta$ T cells were then co-cultured for 2 days with purified, autologous fresh $\alpha\beta$ T cells at $\alpha\beta$ T: $\gamma\delta$ T cell ratios of 5:1, 10:1 and 20:1. After 2 day co-culture, $\alpha\beta$ T cells were blocked with monensin, permeabilized and stained via FACS for intracellular IFN- γ . The experimental setup is illustrated below in figure 2.4.

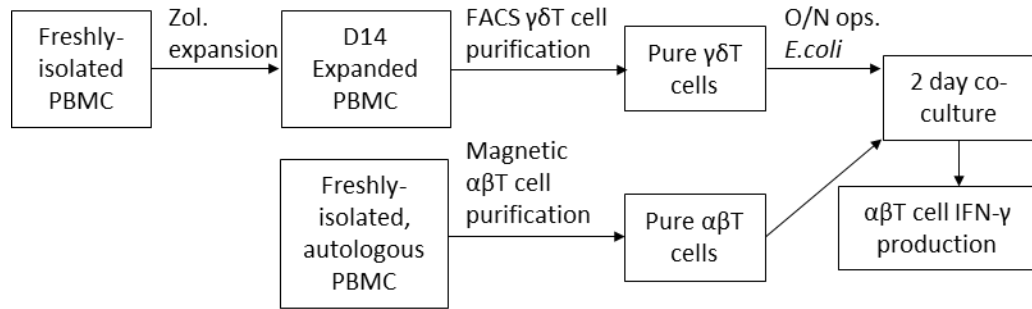
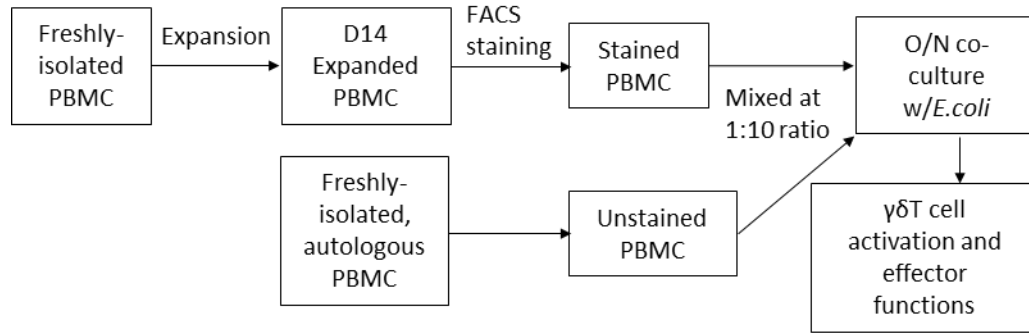


Fig. 2.4. Assay to assess expanded $\gamma\delta$ T cell antigen presentation to freshly-isolated, autologous $\alpha\beta$ T cells. $\gamma\delta$ T cells were expanded for 14 days from freshly-isolated PBMC using zoledronate ($5\mu\text{M}$). On day 14, $\gamma\delta$ T cells were purified from expanded PBMC using FACS. FACS purified $\gamma\delta$ T cells were then incubated overnight IgG-opsonized, irradiated *E.coli* at MOI 10 and washed thoroughly. In parallel, $\alpha\beta$ T cells were purified via positive magnetic selection from autologous, freshly-isolated PBMC and rested overnight. Purified, *E.coli*-stimulated, expanded $\gamma\delta$ T cells were then co-cultured for 2 days with purified, autologous fresh $\alpha\beta$ T cells. After 2 day co-culture, $\alpha\beta$ T cells were blocked with monensin, permeabilized and stained via FACS for intracellular IFN- γ .

2.19. Expanded $\gamma\delta$ T cell re-stimulation with *E.coli* in the presence of autologous 'helper' cells

Freshly-isolated or expanded 1.5×10^6 PBMC/mL were co-cultured with *E.coli* (MOI 10) or zoledronate ($5\mu\text{M}$) in supplemented RPMI 1640 medium, and left to expand for 14 days. Re-stimulation of expanded PBMC with *E.coli* in the presence of freshly-isolated autologous PBMC was carried out by mixing FACS-stained 14 day *E.coli*-expanded PBMC with freshly-isolated, unstained autologous PBMC at a ratio of expanded PBMC : freshly-isolated PBMC of 1:10 prior to the addition of irradiated *E.coli* at MOI 10. The experimental setup is illustrated below in Figure 2.5.



*Fig. 2.5. Assay to assess expanded $\gamma\delta$ T cell responses to *E.coli* in the presence of autologous, freshly-isolated PBMC. $\gamma\delta$ T cells were expanded for 14 days from freshly-isolated PBMC using zoledronate (5 μ M) or *E.coli* (at MOI 10). On day 14, expanded PBMC were FACS-stained for $\gamma\delta$ T cell surface markers. In parallel, PBMC were isolated from autologous donors. Freshly-isolated, unstained PBMC were then mixed with stained, autologous 14 day-expanded PBMC (1 expanded cell per 10 freshly-isolated cells), prior to the addition of irradiated, IgG-opsonized *E.coli* at MOI 10. After overnight co-culture, PBMC were blocked with monensin, permeabilized and stained via FACS for CD107a, CD69, as well as intracellular IFN- γ and TNF- α .*

2.20. $\gamma\delta$ T cell bactericidal activity against *E.coli*

$\gamma\delta$ T cells were purified from 14 day *E.coli* or zoledronate-expanded PBMC using FACS sorting to >98% purity. To mitigate the stress and potential TCR internalization in response to purification, purified $\gamma\delta$ T cells were rested overnight in supplemented, antibiotic-free RPMI 1640 medium. 1.5×10^6 cells/mL $\gamma\delta$ T cells were then co-cultured with live, non-irradiated *E.coli* DH5 α at MOI 10 for 15, 30, 60 or 90 minutes. At designated time points, PBMC-bacterial suspension was removed in duplicate into sterile-filtered, room temperature distilled H₂O, allowed to hypotonically lyse for 10 minutes (to account for possible uptake of bacteria by $\gamma\delta$ T cells) and then serially diluted in H₂O to 10^{-6} of the original concentration. The dilution series was plated in duplicate onto LB agar plates and grown overnight. The number of colony forming units (CFU) was as a measure of bactericidal activity.

2.21. $\gamma\delta$ T cell bead phagocytosis assay

A green fluorescent bead-Trypan Blue quenching assay was employed to assess PBMC uptake of opsonized beads. Briefly, streptavidinylated (SA) 'Dragon Green' beads (Bangs Laboratories) were incubated with anti-SA rabbit mAb (GeneScript), washed and co-cultured in triplicate with PBMC for 60min at 37°C in a 5% CO₂ incubator. Cells were then fixed in cold fixation buffer (Biolegend) before quenching with 0.4% Trypan Blue solution (Sigma-Aldrich) to reduce extracellular Dragon Green signal. After quenching, PBMC were washed three times in a large volume of PBS and analyzed using flow cytometry. Each sample of quenched PBMC-bead mixture was treated in parallel to a non-quenched sample of the same origin to ensure that quenching had taken place.

2.22. $\gamma\delta$ TCR blocking

PBMC were co-incubated for 2h with 10 μ g/mL LEAF-purified anti- $\gamma\delta$ TCR mouse IgG1 κ mAb (Biolegend; clone: B1), the blocking properties of which have been described by Correia, *et al.*(170) or isotype-matched LEAF purified mouse IgG1 κ mAb of known nonhuman specificity (BioLegend; clone: MG1-45). PBMC were then washed in PBS and utilized in the functional assay of interest.

2.23. BTN3A staining and blocking

BTN3A.1 (CD277) was stained for analysis via flow cytometry with CD277-PE (Biolegend; clone: BT3.1). BTN3A functionality was blocked using anti-BTN3A mAb (clone: 103.2), which was kindly supplied by Dr. Daniel Olive (Marseille, France). To achieve blocking, PBMC stimulator cells were co-incubated for 2h with 1.5 μ g/mL anti-BTN3A mouse IgG2a mAb or LEAF purified mouse mAb of known nonhuman specificity (BioLegend; clone: MG1-45). PBMC were then washed in PBS and utilized in the functional assay of interest.

2.24. PBMC responder stimulation with autologous cells in the presence of BTN3A and $\gamma\delta$ TCR blocking

Freshly-isolated PBMC were depleted of $\gamma\delta$ T cells using a positive magnetic selection kit for $\gamma\delta$ TCR (MACS Miltenyi). Labeled PBMC were run through two magnetic columns in sequence to ensure total $\gamma\delta$ T cell removal from PBMC. PBMC were then stimulated overnight in complete RPMI 1640 medium with one of the following stimuli: irradiated *E.coli* at MOI 10, HMBPP at 10 μ M (highly purified (E)-1-Hydroxy-2-methyl-2-butenyl 4-pyrophosphate lithium salt, dissolved for storage in ddH₂O; Sigma), IPP at 10 μ M (highly purified isopentenyl pyrophosphate lithium salt, dissolved for storage in ddH₂O; Sigma), zoledronate at 5 μ M (zoledronic acid; Sigma) or mock stimulated with medium only. After overnight stimulation PBMC were washed thoroughly in a large volume of PBS and blocked with either anti-BTN3A mAb (clone: 103.2) or isotype-matched control (clone: MG1-45). These PBMC served as BTN3A blocked or non-blocked stimulator cells. Stimulator cells were then pre-incubated with autologous, non-depleted PBMC responder cells. Responder cells were either pre-blocked for 2h with anti- $\gamma\delta$ TCR mAb (clone: B1) or isotype-matched control (clone: MG1-45). Responder cells and stimulator cells were then co-cultured at a ratio of 2:1. Responder $\gamma\delta$ T cell intracellular IFN- γ and cell surface CD107a were measured via FACS after overnight co-culture. The experimental setup is illustrated in figure 2.6.

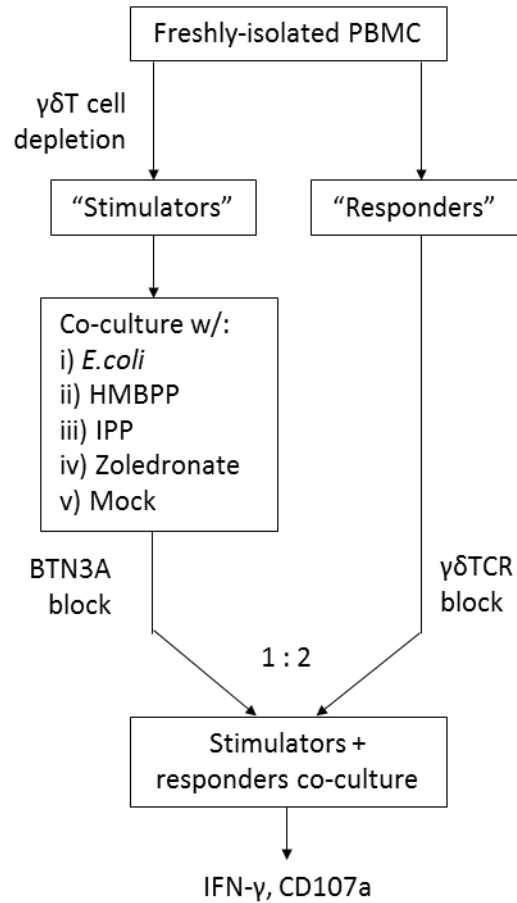
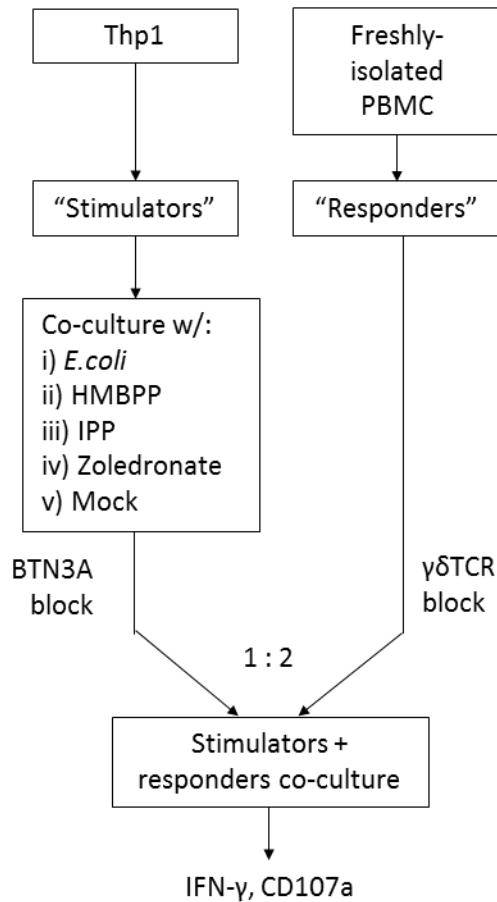


Fig. 2.6. Assay to assess $\gamma\delta$ T cell effector responses in the presence of autologous stimulator cell pre-incubation with anti-BTN3A mAb and responder cell pre-incubation with anti- $\gamma\delta$ TCR mAb. Freshly-isolated PBMC were split into “stimulator” and “responder” cells. Stimulator PBMC were depleted of $\gamma\delta$ T cells using a magnetic positive $\gamma\delta$ T cell selection kit. Stimulator cells were then co-cultured overnight with *E.coli*, HMBPP, IPP, zoledronate or mock-stimulated with media only, washed thoroughly and cultured for 2h with anti-BTN3A mAb or isotype-matched control. Responder cells were rested overnight during stimulator cell preparation, and then cultured for 2h with anti- $\gamma\delta$ TCR mAb or isotype-matched control. Stimulator and responder cells were then co-cultured at a ratio of 1 stimulator per 2 responders. Responder $\gamma\delta$ T cell intracellular IFN- γ and cell surface CD107a were measured via FACS after overnight co-culture.

2.25. PBMC responder stimulation with THP-1 cells in the presence of BTN3A and $\gamma\delta$ TCR blocking

THP-1 cells were stimulated overnight in complete RPMI 1640 medium with one of the following stimuli: irradiated *E.coli* at MOI 10, HMBPP at 10 μ M (highly purified (E)-1-Hydroxy-2-methyl-2-butenyl 4-pyrophosphate lithium salt, dissolved for storage in ddH₂O; Sigma), IPP at 10 μ M (highly purified isopentenyl pyrophosphate lithium salt, dissolved for storage in ddH₂O; Sigma), zoledronate at 5 μ M (zoledronic acid; Sigma) or mock stimulated with medium only. After overnight stimulation THP-1 cells were washed thoroughly in a large volume of PBS and blocked with either anti-BTN3A mAb (clone: 103.2) or isotype control (clone: MG1-45). These THP-1 cells served as BTN3A blocked or non-blocked “stimulator” cells. Freshly-isolated PBMC served as “responder” cells. Responder cells were either pre-blocked anti- $\gamma\delta$ TCR mAb (clone: B1) or isotype-matched control (clone: MG1-45). Stimulator THP-1 cells were incubated with freshly-isolated responder PBMC at a ratio of 1:2. Responder $\gamma\delta$ T cell intracellular IFN- γ and cell surface CD107a were measured via FACS after overnight co-culture. The experimental setup is illustrated in figure 2.7.



*Fig. 2.7. Assay to assess $\gamma\delta$ T cell effector responses in the presence of THP-1 stimulator cell pre-incubation with anti-BTN3A mAb and responder cell pre-incubation with anti- $\gamma\delta$ TCR mAb. THP-1 stimulator cells were co-cultured overnight with *E.coli*, HMBPP, IPP, zoledronate or mock-stimulated with media only, washed thoroughly and cultured for 2h with anti-BTN3A mAb or isotype-matched control. Freshly-isolated PBMC responder cells cultured for 2h with anti- $\gamma\delta$ TCR mAb or isotype-matched control. Stimulator and responder cells were then co-cultured at a ratio of 1 stimulator per 2 responders. Responder $\gamma\delta$ T cell intracellular IFN- γ and cell surface CD107a were measured via FACS after overnight co-culture.*

3. $\gamma\delta$ T CELL ACQUISITION OF PHAGOCYTOTIC CAPACITY

3.1. Aims

My intent in this chapter was to examine whether $\gamma\delta$ T cells are capable of target uptake in a fashion which bears relevance to their putative pAPC function. As described above, phagocytosis and receptor-mediated endocytosis can both contribute material to pAPC antigen processing and eventual presentation. Both processes are also dependent on actin polymerization. I shall not strive further in the text to determine the particular type of antigen uptake $\gamma\delta$ T cells may engage in, but rather to establish whether $\gamma\delta$ T cells are capable of target uptake in a pAPC function-permissive manner, and what cellular conditions are necessary for this to take place.

I set out to determine i) whether human peripheral $\gamma\delta$ T cells are capable of phagocytosis, and ii) what the optimal conditions for this phagocytosis may be. The conditions examined included single *versus* repeated exposure to antigen, cells freshly-isolated from blood *versus* cells expanded *in vitro* and target opsonisation or non-opsonisation with antibody. Various aspects of phagocytosis, such as uptake and acidification of material, were examined.

3.2. Zoledronate-expanded $\gamma\delta$ T cells take up IgG-opsonized 1.0 μ m beads and *E.coli*

We have previously reported limited phagocytosis by freshly-isolated peripheral $\gamma\delta$ T cells. Specifically, Wu *et al.* were able to induce $\gamma\delta$ T cell uptake of IgG-opsonized 1.0 μ m beads, which was inhibitable by cell pre-incubation with anti-CD16 (Fc γ R) mAb and was

sensitive to Cytochalasin D (CyD), an inhibitor of actin polymerization (50). Herein, I examined the effect of cell expansion on $\gamma\delta$ T cell phagocytic capacity in greater detail. I highlight that the data visible in Fig.3.1 and Fig.3.2 was generated predominantly by another PhD student in the Gustafsson laboratory, Anne Marijn Kramer, who has given her consent to the inclusion of the relevant data into the present thesis. This data was not further utilized by her, and is included in the present thesis to illustrate the evolution of thought and experimental narrative that lead to the completion of the work therein.

14 day zoledronate-expanded $\gamma\delta$ T cells were co-cultured with protease-activated DQ-Green fluorescent, bovine serum albumin (BSA)-labeled polystyrene beads (0.5 μ m or 1.0 μ m in size), with or without IgG opsonization. DQ-Green, BSA-labeled beads have been employed previously as an indicator of phagosome maturation and antigen processing in macrophages (171). Internalization of fluorescing, i.e. protease exposed, beads was quantified using an ImageStream internalization score (Fig.3.1A). Expanded $\gamma\delta$ T cell incubation with non-opsonized beads revealed significant uptake of 0.5 μ m, but not 1.0 μ m beads. Opsonization with Rituximab (monoclonal, chimeric human-mouse IgG against CD20) significantly enhanced 1.0 μ m bead uptake - to a level statistically indistinguishable from the uptake of beads 0.5 μ m in size (Fig.3.1B). Internalization scores indicated that ~9% of $\gamma\delta$ T cells associated with opsonized beads, of which ~86% showed internalization.

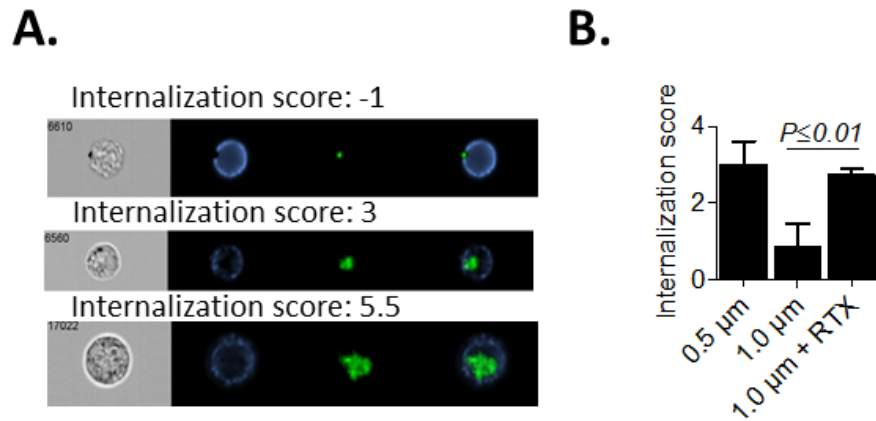


Fig. 3.1. Zoledronate-expanded $\gamma\delta$ T cells take up IgG-opsonized 1.0 μ m beads. 14 day zoledronate (5 μ M)-expanded $\gamma\delta$ T cells (n=3) were incubated with IgG-opsonized or non-opsonized protease-sensitive DQ BSA polystyrene beads, and analyzed for internalized material. $\gamma\delta$ T cell uptake of beads was assessed with an internalization score generated via ImageStream analysis. **(A)** Representative data is shown from one donor, with $\gamma\delta$ TCR in blue and beads in green. Bead fluorescence was an indicator of DQ BSA exposure to proteases. **(B)** Zoledronate-expanded PBMC (n=3) were cultured for 60min with non-opsonized 0.5 μ m and 1.0 μ m beads, as well as IgG (Rituximab; RTX)-opsonized 1.0 μ m beads. PBMC were then stained for ImageStream analysis; internalisation scores, as generated by ImageStream software, are shown for $\gamma\delta$ T cells. Bar graphs indicate the mean \pm standard deviation.

The observation that a significant portion of expanded $\gamma\delta$ T cells internalize opsonized beads into a protease-rich environment (as indicated by fluorescence of the DQ Green dye) prompted us to investigate $\gamma\delta$ T cell uptake of bacteria, such as *E.coli*. Confocal microscopy allowed detection of whole and partially-degraded *E.coli* in the interior of zoledronate-expanded $\gamma\delta$ T cells incubated with IgG-opsonized, GFP-expressing *E.coli* (Fig.3.2). As exemplified in Fig.3.2, virtually all $\gamma\delta$ T cells within the field of vision were associated with multiple adherent *E.coli*, whereupon only a minor fraction of the bacteria were found to be intracellular.

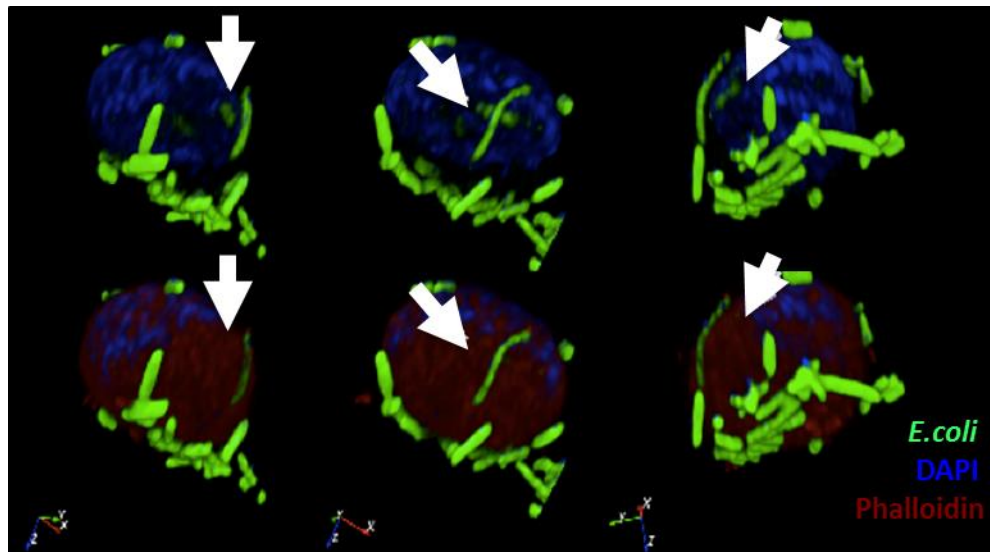


Fig. 3.2. Zoledronate-expanded $\gamma\delta$ T cells take up IgG-opsonized E.coli. 14 day zoledronate (5 μ M)-expanded, FACS-purified $\gamma\delta$ T cells were stained with phalloidin (red), DAPI (blue), incubated with IgG opsonized, GFP-expressing *E.coli*, and analyzed via confocal microscopy. Representative data is shown of a single cell in 3D-rotation with or without phalloidin. Internalised *E.coli* is indicated with white arrows.

3.3. *E. coli*-expanded, but not freshly-isolated $\gamma\delta$ T cells, take up IgG-opsinized *E. coli*

I next quantified the uptake of IgG opsonized *versus* non-opsonized *E. coli* by freshly isolated *versus* *E. coli*-expanded $\gamma\delta$ T cells. Freshly-isolated PBMC from healthy laboratory donors were co-cultured with UV-irradiated *E. coli* and left to expand for 14 days. Expansion resulted in a marked increase in CD3^{pos} cells (Fig.3.3A), with a preferential (>200-fold) expansion of $\gamma\delta$ T cells (Fig.3.3B, C). It was interesting to note that a population of $\alpha\beta$ T cells persisted with minimal expansion (Fig.3.3C).

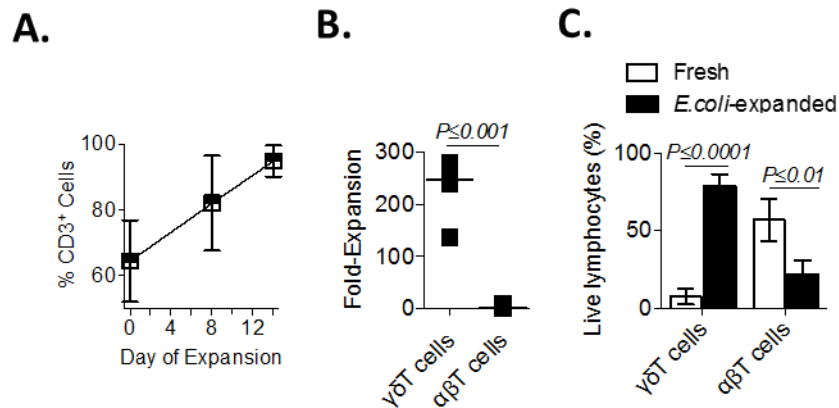


Fig. 3.3. PBMC stimulation with *E. coli* induces preferential $\gamma\delta$ T cell expansion. Freshly-isolated PBMC (n=5) were stimulated with irradiated *E. coli* at MOI 10 and left to expand in IL-2-supplemented media for 14 days. Rates of expansion were compared between $\gamma\delta$ T and $\alpha\beta$ T cells. **(A)** The proportion of CD3^{pos} cells of total live PBMC was tracked. **(B)** Fold-expansion of $\gamma\delta$ T and $\alpha\beta$ T cells, assessed by FACS and Trypan Blue exclusion, was compared. **(C)** PBMC were compared via FACS for $\gamma\delta$ T and $\alpha\beta$ T cell content of total live lymphocytes. Bar graphs indicate the mean \pm standard deviation.

V δ 2 $\gamma\delta$ T cells displayed the highest rate of expansion (~250-fold), followed by V δ 1-V δ 2-cells (~40-fold) and V δ 1 $\gamma\delta$ T cells, which instead contracted (Fig.3.4A). Donor-matched, parallel expansions of PBMC in IL-2 medium with zoledronate or *E.coli* induced similar rates of expansion of subsets (Fig.3.4B). Of note, IL-2 medium alone failed to induce expansion of $\gamma\delta$ T or $\alpha\beta$ T cells.

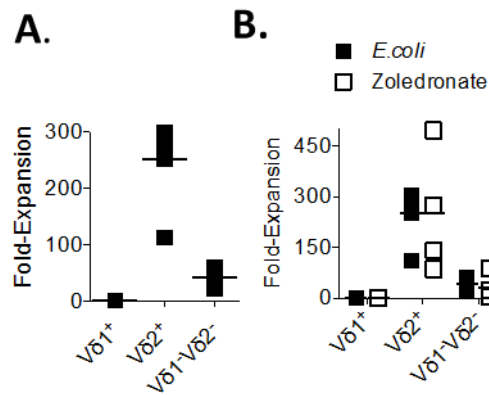


Fig. 3.4. PBMC stimulation with *E.coli* and zoledronate induces preferential V δ 2 $\gamma\delta$ T cell expansion. Freshly-isolated PBMC (n=5) were stimulated with irradiated *E.coli* at MOI 10 or zoledronate (5 μ M) and left to expand in IL-2-supplemented media for 14 days. Rates of expansion were compared between V δ 1, V δ 2 and V δ 1^{neg}V δ 2^{neg} $\gamma\delta$ T cell subsets. (A) Fold-expansion over 14 day stimulation was compared between $\gamma\delta$ T cell subsets in *E.coli*-expanded PBMC only, or (E) compared between *E.coli* and zoledronate-stimulated PBMC.

To measure phagocytosis, freshly-isolated or expanded PBMC were incubated with IgG-opsionized or non-opsionized FITCylated-*E.coli* for 60min, and analysed via Trypan Blue quenching and flow cytometry (Fig.3.5). Freshly-isolated $\gamma\delta$ T and $\alpha\beta$ T cells failed to show notable bacterial uptake; in contrast ~25% and ~45% of freshly isolated CD3^{neg} PBMC (predominantly monocytes) internalized non-opsionized and opsionized *E.coli*, respectively; both processes were found to be sensitive to CyD (Fig.3.6). More than 50% of *E.coli* expanded $\gamma\delta$ T cells took up opsionized *E.coli* in a CyD-sensitive manner. Interestingly, a subpopulation (mean 35%) of the residual $\alpha\beta$ T cells following *E.coli* expansion also took up opsionized *E.coli*, but this uptake was not significantly inhibited by CyD (Fig.3.6).

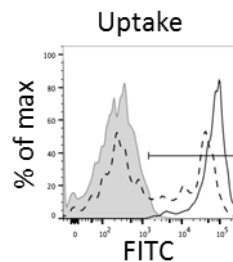


Fig. 3.5. $\gamma\delta$ T cell uptake of E.coli was investigated using a FITC-Trypan Blue quenching assay. PBMC were incubated for 60min with FITC-labeled E.coli, washed and quenched post-culture with Trypan Blue. PBMC were then stained for cell surface markers and analyzed via FACS. Shown are representative stains, gated on $\gamma\delta$ T cells: i) non-quenched co-culture indicating total FITC fluorescence (black, solid, unshaded), ii) quenched co-culture indicating intracellular FITC fluorescence (black, dotted, unshaded), iii) co-culture with non-FITCylated E.coli (gray, shaded).

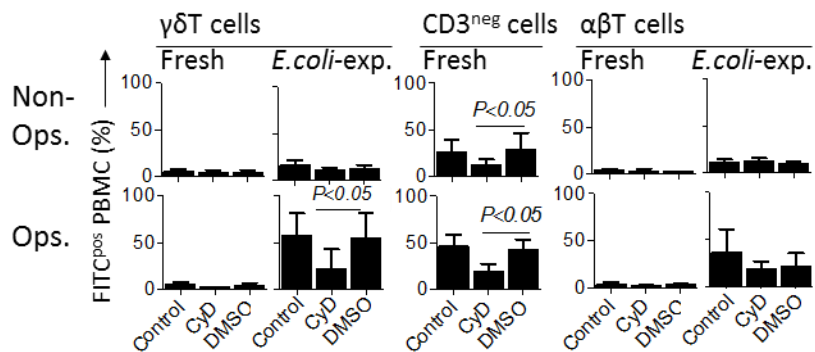


Fig. 3.6. E.coli-expanded, but not fresh, $\gamma\delta$ T cells take up IgG-opsonized E.coli. Freshly-isolated or *E.coli*-expanded PBMC (n=5) PBMC were incubated for 60min with FITC-labeled *E.coli* at MOI 10, washed and quenched post-culture with Trypan Blue. PBMC were then stained for cell surface markers and analyzed via FACS. Remaining post-quench FITC fluorescence was interpreted as intracellular in origin. The proportion of FITC^{pos} PBMC was tallied, and compared between fresh and *E.coli*-expanded $\gamma\delta$ T and $\alpha\beta$ T cells, as well as fresh $CD3^{neg}$ cells. Intracellular FITC fluorescence was evaluated in the presence of PBMC pre-culture with normal media (control), Cytochalasin D at 0.2mM (CyD) or DMSO at 0.2mM (DMSO). *E.coli* were UV-irradiated prior to co-culture with PBMC and left non-opsonized (non-ops.) or opsonized with purified rabbit anti-*E.coli* IgG (ops.). Bar graphs indicate the mean \pm standard deviation.

Phagocytosis promotes fusion of the phagosome with the lysosomal compartment. To determine whether *E.coli* uptake by *E.coli*-expanded $\gamma\delta$ T cells resulted in bacterial acidification (implying phagolysosome formation), freshly-isolated and 14 day expanded PBMC were co-cultured for 60min with IgG-opsonized pH-sensitive pHrodo-*E.coli* (Fig.3.7). *E.coli*-expanded $\gamma\delta$ T cells, but not $\alpha\beta$ T cells or freshly isolated $\gamma\delta$ T cells, showed notable acidification of *E.coli*, which increased further upon opsonization. As a positive control, freshly isolated CD3^{neg} PBMC (largely monocytes) also acidified non-opsonized and opsonized *E.coli*. Only acidification by CD3^{neg} PBMC was CyD-sensitive (Fig.3.8).

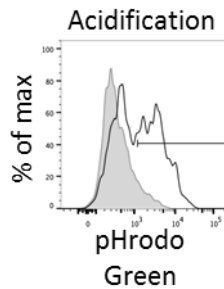


Fig. 3.7. $\gamma\delta$ T cell acidification of *E.coli* was investigated using a pHrodo-*E.coli* assay. PBMC were incubated for 60min with pH sensitive pHrodo-labeled *E.coli* and washed post-culture. PBMC were then stained for cell surface markers and analyzed via FACS. Shown are representative stains, gated on $\gamma\delta$ T cells, of: i) PBMC, gated on $\gamma\delta$ T cells, co-cultured with pHrodo-*E.coli* (black, solid, unshaded), ii) pHrodo-*E.coli* only control (gray, shaded).

It remains unclear as to why bacterial uptake but not acidification appeared CyD-sensitive. One possible explanation may be the difference in bacterial preparations employed, as fresh exponentially-grown *E. coli* were irradiated just prior to uptake studies whilst

lyophilized, *E.coli*-pHrodo conjugates were utilized to examine acidification. Lyophilisation may lead to bacterial acquisition of a spherical rather than rod shape, with consequential changes to the involvement of the actin cytoskeleton in the uptake process (172,173). Nonetheless, this series of experiments provides evidence for the first time that, upon expansion, $\gamma\delta$ T cells can phagocytose and direct bacteria to an acid-rich environment.

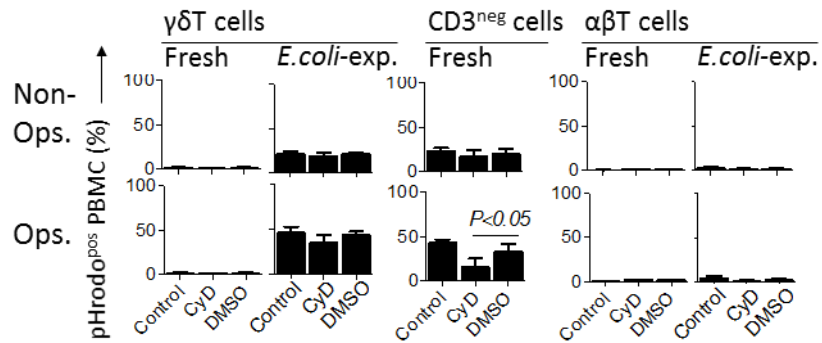


Fig. 3.8. E.coli-expanded, but not fresh, $\gamma\delta$ T cells acidify IgG-opsonized E.coli. Freshly-isolated or *E.coli*-expanded PBMC (n=5) PBMC were incubated for 60min with pHrodo-labeled *E.coli* and washed. PBMC were then stained for cell surface markers and analyzed via FACS. pHrodo positivity was interpreted as labeled *E.coli* exposure to acidic pH. The proportion of pHrodo^{pos} PBMC was tallied, and compared between fresh and *E.coli*-expanded $\gamma\delta$ T and $\alpha\beta$ T cells, as well as fresh CD3^{neg} cells. pHrodo fluorescence was evaluated in the presence of PBMC pre-culture with normal media (control), Cytochalasin D at 0.2mM (CyD) or DMSO at 0.2mM (DMSO). pHrodo-*E.coli* were left non-opsonized (non-ops.) or opsonized with purified rabbit anti-*E.coli* IgG (ops.). Bar graphs indicate the mean \pm standard deviation.

A similar degree of opsonized *E.coli* uptake and CyD-sensitivity by expanded $\gamma\delta$ T cells was seen regardless of whether PBMC were expanded with *E.coli* or zoledronate (Fig.3.9). The same was true for expanded $\gamma\delta$ T cell acidification of opsonized *E.coli* (Fig.3.10).

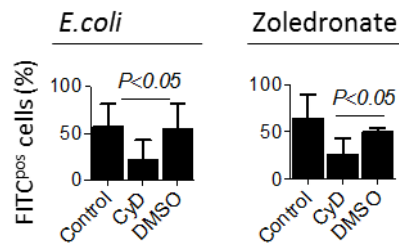


Fig. 3.9. *E.coli* and zoledronate-expanded $\gamma\delta$ T cells take up IgG-opsonized *E.coli* with similar dynamics. 14 day *E.coli* or zoledronate-expanded PBMC (n=5) PBMC were incubated for 60min with FITC-labeled *E.coli* at MOI 10, washed and quenched post-culture with Trypan Blue. PBMC were then stained for cell surface markers and analyzed via FACS. Remaining post-quench FITC fluorescence was interpreted as intracellular in origin. The proportion of FITC^{pos} PBMC was tallied, and compared between *E.coli* or zoledronate-expanded $\gamma\delta$ T cells. Intracellular FITC fluorescence was evaluated in the presence of PBMC pre-culture with normal media (control), Cytochalasin D at 0.2mM (CyD) or DMSO at 0.2mM (DMSO). *E.coli* were UV-irradiated prior to co-culture with PBMC and opsonized with purified rabbit anti-*E.coli* IgG. Bar graphs indicate the mean \pm standard deviation.

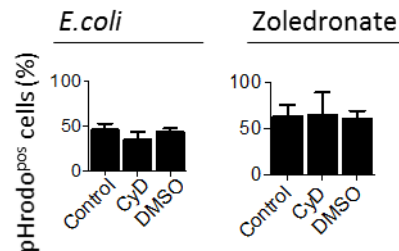


Fig.3.10. *E.coli* and zoledronate-expanded $\gamma\delta$ T cells acidify IgG-opsonized *E.coli* with similar dynamics. 14 day *E.coli* or zoledronate-expanded PBMC (n=5) PBMC were incubated for 60min with pHrodo-labeled *E.coli* and washed. PBMC were then stained for cell surface markers and analyzed via FACS. pHrodo positivity was interpreted as labeled *E.coli* exposure to acidic pH. The proportion of pHrodo^{pos} PBMC was tallied, and compared between *E.coli* or zoledronate-expanded $\gamma\delta$ T cells. pHrodo fluorescence was evaluated in the presence of PBMC pre-culture with normal media (control), Cytochalasin D at 0.2mM (CyD) or DMSO at 0.2mM (DMSO). *E.coli* were opsonized with purified rabbit anti-*E.coli* IgG. Bar graphs indicate the mean \pm standard deviation.

Interestingly, the magnitude of bacterial acidification varied between expanded $\gamma\delta$ T cells and freshly-isolated $CD3^{neg}$ PBMC (Fig.3.11), suggesting cell-specific pathways may be involved in bacterial uptake and processing.

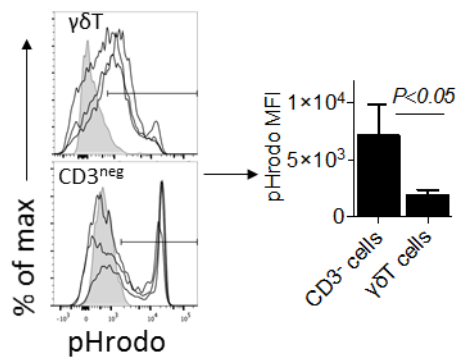


Fig. 3.11. Expanded $\gamma\delta$ T cells acidify bacteria with different dynamics than $CD3^{neg}$ fresh PBMC. Freshly-isolated or *E.coli*-expanded PBMC (n=5) were incubated with IgG-opsonized pHrodo-*E.coli* for 60min, washed and stained for cell surface markers for subsequent analysis via FACS. Shown are representative stains of three donors, gated on *E.coli*-expanded $\gamma\delta$ T cells and freshly-isolated $CD3^{neg}$ PBMC, of: i) PBMC, gated on either cell type, co-cultured with pHrodo-*E.coli* (black, solid, unshaded), ii) pHrodo-*E.coli* only control (gray, shaded). A compilation of donor pHrodo MFI is shown, comparing *E.coli*-expanded $\gamma\delta$ T cells and freshly-isolated $CD3^{neg}$ cells.

3.4. Discussion

In this chapter, I sought to address whether human peripheral $\gamma\delta$ T cells are capable of phagocytosis, to quantify this phenomenon and to establish what the conditions permissive of this phenotype may be. My findings included:

- i) Zoledronate-expanded $\gamma\delta$ T cells are capable of phagocytosing 1.0 μ m polystyrene beads, but only if the beads are opsonized with IgG, as indicated by ImageStream quantification.
- ii) Intracellular *E.coli* can be visualized using confocal microscopy after 60min zoledronate-expanded $\gamma\delta$ T cell co-culture with opsonized *E.coli*.
- iii) Freshly-isolated PBMC stimulation with *E.coli* and IL-2 leads to a preferential expansion of V δ 2 $\gamma\delta$ T cells, at rates similar to those achieved by PBMC stimulation with zoledronate and IL-2.
- iv) A novel application of a FITC-Trypan blue quenching FACS-based assay for the quantification of *E.coli* uptake by $\gamma\delta$ T cells. Some 50% of expanded, but not fresh, $\gamma\delta$ T cells can take up *E.coli* at the same rate as freshly-isolated CD3^{neg} PBMC (mostly monocytes).
 - a. This uptake is significantly enhanced if the *E.coli* is opsonized with IgG.
 - b. The uptake of opsonized *E.coli* is sensitive to cytochalasin D (CyD), an inhibitor of actin polymerization.
 - c. Expanded $\alpha\beta$ T cells appear capable of some uptake of opsonized *E.coli*, but this uptake is not CyD sensitive.
- v) A novel application of a pHrodo Green FACS-based assay for the study and quantification of *E.coli* acidification by $\gamma\delta$ T cells. Some 50% of expanded, but not fresh, $\gamma\delta$ T cells can acidify *E.coli* at the same rate as freshly-isolated CD3^{neg} PBMC (mostly monocytes).
 - a. This acidification is significantly enhanced if the *E.coli* opsonized with IgG.
 - b. In $\gamma\delta$ T cells this acidification is, curiously, not significantly sensitive to CyD, an inhibitor of actin polymerisation, but is CyD-sensitive in freshly-isolated CD3^{neg} PBMC.

- c. Expanded $\alpha\beta$ T cells appear capable of some uptake of opsonized *E.coli*, but it is not CyD sensitive.
- vi) *E.coli* and zoledronate-expanded $\gamma\delta$ T cells take up and acidify opsonized *E.coli* with similar efficiency.
- vii) $\gamma\delta$ T cell acidification of opsonized *E.coli* is different from acidification by freshly-isolated CD3^{neg} PBMC. CD3^{neg} PBMC appear to acidify opsonized *E.coli* with greater intensity to a lower pH, as indicated by higher fluorescence of the pH-sensitive pHrodo dye.

As mentioned previously, work by our lab and others has reported limited phagocytosis by freshly-isolated peripheral $\gamma\delta$ T cells. Wu *et al.* were the first to publish an account of phagocytosis by peripheral human $\gamma\delta$ T cells (50). They were able to induce CyD-sensitive $\gamma\delta$ T cell uptake of IgG-opsonized 1 μ m beads in a process that was inhibitable by cell pre-incubation with anti-CD16 (phagocytic Fc γ R) mAb. Their work further documented some uptake of opsonized *E.coli*. Himoudi *et al.* have since demonstrated that $\gamma\delta$ T cells are seemingly able to cross-present antigen from IgG-opsonized tumour cells (49), implying phagocytosis (or an alternative uptake process) of target material. While establishing that $\gamma\delta$ T cells are indeed capable of phagocytosis, these experiments crucially lacked quantification of the phenomena observed.

Important questions such as I) “What proportion of $\gamma\delta$ T cells are capable of phagocytosis?”, II) “How does $\gamma\delta$ T cell phagocytosis of targets quantifiably differ from that carried out by established myeloid phagocytes?”, III) “Are particles uptaken by $\gamma\delta$ T cells shuttled into phagolysosomes for subsequent processing?”, IV) “Does the phagocytic capacity of freshly-isolated *versus* expanded $\gamma\delta$ T cells differ significantly?” and V) “Is $\gamma\delta$ T cell phagocytosis enhanced by previous encounter with specific antigen?” have not been addressed comprehensively in published research. Therein, I carried out the experiments described in this chapter.

Preliminary ImageStream work by Anne Marijn Kramer quantified for the first time $\gamma\delta$ T cell uptake of material; she was able to perform statistical analysis on zoledronate-

expanded $\gamma\delta$ T cell uptake of pH-sensitive IgG-opsonized beads. Some 7% of expanded $\gamma\delta$ T cells presented with intracellular, pH<7-exposed beads (Fig.3.1). While this presented an advance in the examination of $\gamma\delta$ T cell phagocytic capacity, it was carried out using a highly non-physiological target - plastic beads - and used a single phagocytosis stimulus, IgG, neglecting the potential necessity TCR, TLR and other PRR stimulation (or co-stimulation) that may be necessary to stimulate $\gamma\delta$ T cell uptake of antigenic material. Using confocal microscopy, she was further able to document *E.coli* in the interior of zoledronate-expanded $\gamma\delta$ T cells. This was not quantified. The desire to quantify and explore in detail $\gamma\delta$ T cell phagocytosis of a physiologically relevant target, I set out to characterize and quantify $\gamma\delta$ T cell uptake of *E.coli*.

My initial attempts to quantify $\gamma\delta$ T cell phagocytosis of *E.coli* were via gentamicin protection assays, considered the ‘gold standard’ in classic phagocytosis literature (174–177). These assays are based on the principle that gentamicin, a potent bactericidal Gram negative antibiotic, does not penetrate the cell membrane of mammalian cells. Cells are incubated with live *E.coli* for a given time period, washed thoroughly, treated with gentamicin, washed once more and lysed with hypotonic pressure. The cell lysate is then plated and cultured on agar, providing optimal growth conditions for surviving *E.coli*. If any *E.coli* CFU are seen, one concludes that these *E.coli* must have been protected from the bactericidal effects of gentamicin by the mammalian cell membrane - therein implying intracellular location.

My attempts at $\gamma\delta$ T cell gentamicin protection assays consisted of FACS-purified *E.coli* or zoledronate-expanded $\gamma\delta$ T cells co-cultured with *E.coli* at various MOIs (ranging from 1-100). None of my attempts yielded viable *E.coli* CFU post gentamicin treatment. The obvious conclusion that $\gamma\delta$ T cells must, therefore, not engage in phagocytosis of *E.coli*, was overturned when I began examining the capacity of $\gamma\delta$ T cells to kill live *E.coli* in culture. Data on $\gamma\delta$ T cell killing of bacterial targets is further discussed in Chapter V. Briefly, expanded, FACS-purified $\gamma\delta$ T cells exhibited a surprisingly rapid and potent bactericidal phenotype: within less than an hour $\gamma\delta$ T cells reduced *E.coli* CFU by >90%. Given that a gentamicin protection assay involves hours-long incubation periods – during

which time $\gamma\delta$ T cells may have effectively killed present *E.coli* – I decided to pursue different phagocytosis quantification methodology.

As outlined in the ‘Materials and Methods’ chapter, I employed a FITC-Trypan blue quenching assay, described by Busetto *et al.* (168). In addition to permitting quantification of phagocytosis, the use of a FACS-based assay further permitted staining for cell surface markers, which omitted the need for cell purification. I could, thus, examine *E.coli* uptake by various PBMC populations simultaneously and in parallel (Fig.3.6). The pH-sensitive pHrodo dye phagocytosis assay further indicated that, within the 60min of observed *E.coli*-FITC uptake, *E.coli*-pHrodo is also acidified (Fig.3.7). Using this as an indirect readout of phagolysosome formation allowed me to state with added confidence that the phenomenon I am observing is indeed phagocytosis.

It was interesting to note the difference in the intensity of acidification between expanded $\gamma\delta$ T cells and freshly-isolated CD3^{neg} PBMC (Fig.3.11). While this may allude to cell-specific phagocytic and antigen processing mechanisms, it is important to address the possibility that - given the potent cytotoxicity that $\gamma\delta$ T cells displayed upon exposure to *E.coli* - it cannot be ruled out that *E.coli*-pHrodo may also be acidified by $\gamma\delta$ T cells extracellularly. The bactericidal mechanisms of $\gamma\delta$ T cells are poorly understood. It is conceivable that one route of killing involves $\gamma\delta$ T cell release of acidic lysosomal contents onto nearby bacteria, which may activate the pH-sensitive pHrodo dyes. Further work, involving visualizing techniques such as confocal microscopy, is necessary to determine whether pH-sensitive dyes are an adequate means of studying post-phagocytosis phagolysosomal formation in $\gamma\delta$ T cells. I stipulate that a likely scenario is that $\gamma\delta$ T cells acidify *E.coli* via cytotoxicity extracellularly *and* via phagolysosome formation intracellularly. Cytotoxicity data (Chapter V) indicated potent anti-*E.coli* CD107a-mediated degranulation by freshly-isolated $\gamma\delta$ T cells, which nonetheless failed to show acidification of *E.coli*-pHrodo. This observation lends strength to the idea that expanded $\gamma\delta$ T cells take up and subsequently acidify opsonized *E.coli* intracellularly. It is nonetheless important to clarify this question prior to drawing meaningful conclusions from data concerning $\gamma\delta$ T cell acidification intensity of internalized bacterial targets.

It is also important to further examine the CyD-insensitivity of $\gamma\delta$ T cell acidification of *E.coli*. A potential cause of this may be the different preparations of *E.coli* used. One way to address this would be to label freshly-grown *E.coli* with FITC and a pHrodo dye in parallel, ensuring that both types of labeled *E.coli* have undergone the same treatment. Thus, the two preparations could also have more closely controlled MOIs, omitting the reliance on commercially-available *E.coli*-pHrodo protocols that do not specify bacterial cell number. It is possible that the difference in CyD sensitivity between uptake of *E.coli*-FITC and acidification of *E.coli*-pHrodo was caused by differences in phagocyte-to-target ratio.

The necessity for IgG opsonisation of targets for $\gamma\delta$ T cells has been reported previously (178). What was surprising and a novel finding herein was the stark difference I found between the phagocytic capacity of expanded *versus* freshly-isolated $\gamma\delta$ T cells, whereupon expanded $\gamma\delta$ T cells phagocytosed *E.coli* at a rate statistically similar to that observed in freshly-isolated CD3^{neg} PBMC (largely monocytes and B cells). The marked difference in phagocytic capacity between freshly-isolated and *E.coli*-expanded $\gamma\delta$ T cells implies a significant phenotypic shift of $\gamma\delta$ T cells after initial exposure to *E.coli*. This prompted us to examine whether the acquired extensive phagocytic capacity for *E.coli* may be antigen specific. I enquired whether expansion with a particular antigen followed by a re-challenge by that same antigen (*E.coli* in this case) was responsible for the vast difference in phagocytic $\gamma\delta$ T cells that I observed.

I quantified the phagocytic capacity for opsonized *E.coli* of zoledronate-expanded $\gamma\delta$ T cells, and compare it to that of *E.coli*-expanded $\gamma\delta$ T cells. To my surprise, no significant difference between the two expansion conditions could be found in either uptake of *E.coli*-FITC (Fig.3.9) or acidification of *E.coli*-pHrodo (Fig.3.10). The importance of this finding lies in the different mechanisms that have been proposed by which *E.coli* and zoledronate induce $\gamma\delta$ T cell proliferation. As outlined in the thesis introduction, both stimuli are known to activate V δ 2 $\gamma\delta$ T cells. General consensus argues, however, that *E.coli* activates V δ 2 cells via HMBPP, Lipid A and other bacterial antigens via stimulation of the TCR and various PRRs (93,179). Zoledronate, meanwhile, is a small molecule aminobisphosphonate drug, which does not contain any conceivable targets for $\gamma\delta$ T cell

antigen receptors. Instead, zoledronate is thought to disrupt the mevalonate pathway during cholesterol synthesis, and lead to the accumulation of toxic intermediates, such as isoprenyl pyrophosphate (IPP). IPP accumulation then leads to cellular stress and consequent conformational changes in cell surface butyrophilin 3A (BTN3A) molecules (180). IPP itself and its effect on BTN3A conformation have both been proposed as mediators of $\gamma\delta$ TCR activation (100,181). *E.coli* and zoledronate, thus, represent two separate types of antigen: i) non-self and ii) 'stressed' self. The observation that these differential stimuli induced $\gamma\delta$ T cell populations with equivalent phagocytic capacity - which was nonetheless different from that of freshly-isolated $\gamma\delta$ T cells - prompted us to compare the effect of *E.coli* versus zoledronate expansion on freshly-isolated $\gamma\delta$ T cells in greater detail.

3.5. Summary

Analysis of the data laid out in this chapter lead us to the conclusion that *E.coli* or zoledronate-expanded $\gamma\delta$ T cells are capable of effective phagocytosis of IgG-opsonized targets, including *E.coli*, while freshly-isolated $\gamma\delta$ T cells are not.

4. *E.COLI* AND ZOLEDRONATE PROMOTE EXPANSION OF PHENOTYPICALLY EQUIVALENT $\gamma\delta$ T CELL POPULATIONS

4.1. Aims

Surprised to find that *E.coli* and zoledronate-expanded, but not fresh, $\gamma\delta$ T cells display equivalent efficiency in opsonized *E.coli* phagocytosis, I set out to compare the phenotype of these expanded $\gamma\delta$ T cells in greater detail. Particular emphasis was placed on antigen presenting cell (APC) phenotype expression and T cell receptor (TCR) repertoires.

In the characterization of *E.coli* versus zoledronate-expanded V δ 2 cells, I placed a particular emphasis on their expression patterns of APC molecules, MHC class II (HLA-DR, specifically) and co-stimulatory CD86, as well as homing receptors, chemokine receptor 7 (CCR7) and CD62L (also known as L-selectin). HLA-DR and CD86 expression has been documented on human $\gamma\delta$ T cells in various contexts, ranging from *in vitro* stimulation to *in vivo* infectious disease. Both endogenous pAgs and Gram-negative bacteria-stimulated $\gamma\delta$ T cells have been reported to upregulate expression of HLA-DR and CD86 (75,106). The dynamics, time scale and stability of this upregulation has, however, not been reported in detail.

4.2. *E.coli* and zoledronate stimulation induces sustained $\gamma\delta$ T cell upregulation of HLA-DR and CD86

In the previous chapter I outlined phagocytosis by zoledronate and *E.coli*-expanded peripheral $\gamma\delta$ T cells. Consequently, I hypothesized that opsonization-mediated phagocytosis is associated with acquisition of APC capabilities by $\gamma\delta$ T cells. To test this, expression of classic APC markers, HLA-DR and CD86, was investigated. *E.coli* mediated a steady increase in both markers, with a majority of expanding $\gamma\delta$ T cells developing an HLA-DR^{pos}CD86^{pos} phenotype within days of stimulation (Fig.4.1A and B). HLA-DR and CD86 expression on expanded $\gamma\delta$ T cells was similar to that observed on freshly-isolated monocytes (CD3^{neg}CD14^{pos} PBMC). $\alpha\beta$ T cells remained negative for both markers throughout expansion (Fig.4.1B).

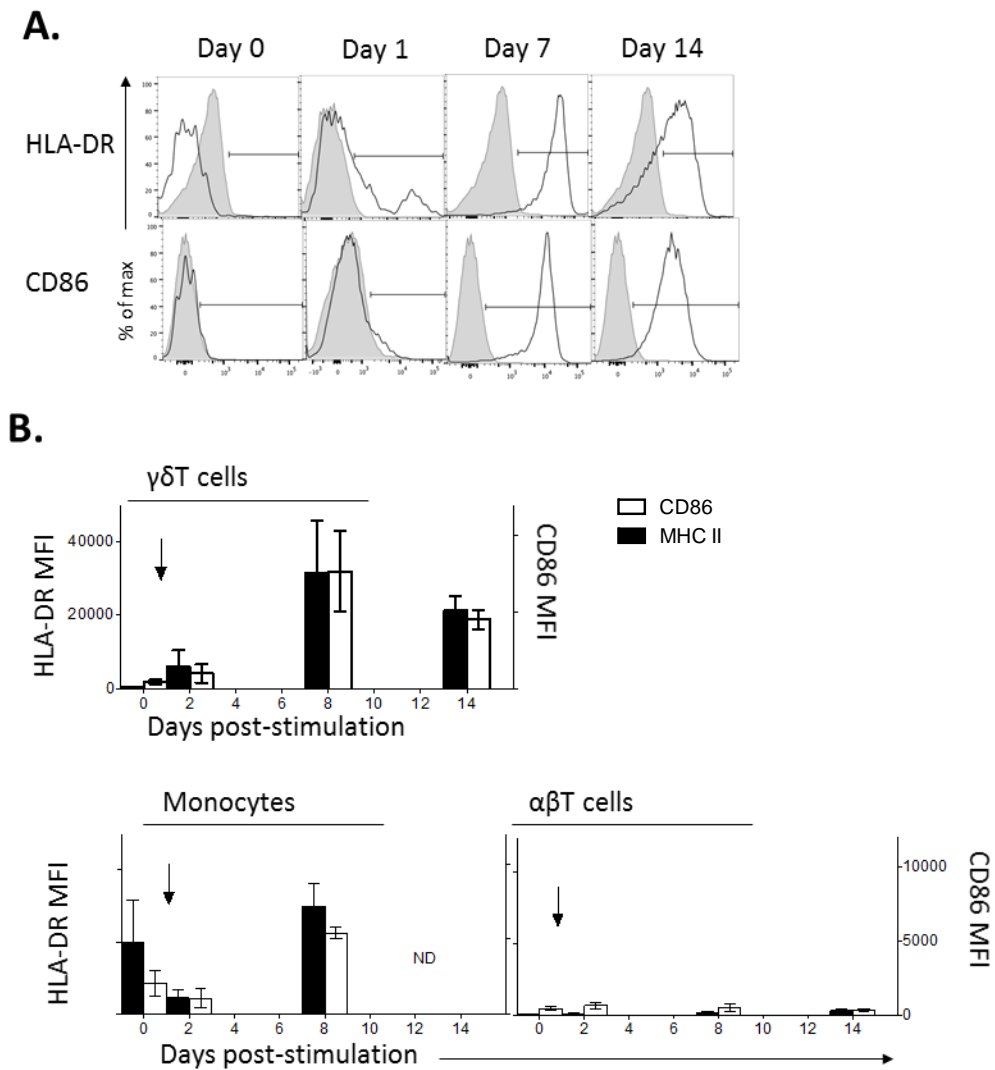


Fig. 4.1. PBMC stimulation with *E.coli* leads to $\gamma\delta$ T cell upregulation of cell surface HLA-DR and CD86. Freshly-isolated PBMC ($n=5$) were expanded for 14 days with irradiated *E.coli* at MOI 10, and FACS stained for cell surface HLA-DR and CD86 throughout expansion. **(A)** Representative stains of one donor $\gamma\delta$ T cells is shown, with specific antibody in black, unshaded, and isotype-matched control - in gray, shaded. **(B)** HLA-DR and CD86 of five donor compiled MFI over *E.coli* expansion was compared between $\gamma\delta$ T, $\alpha\beta$ T cells and monocytes ($CD3^{neg}CD14^{pos}$ PBMC). Points of *E.coli* stimulation are indicated with black arrows. Bar graphs indicate the mean \pm standard deviation.

Data indicated, moreover, that PBMC stimulation with *E.coli* or zoledronate produced a similar and sustained upregulation of the two pAPC cell surface markers (Fig.4.2).

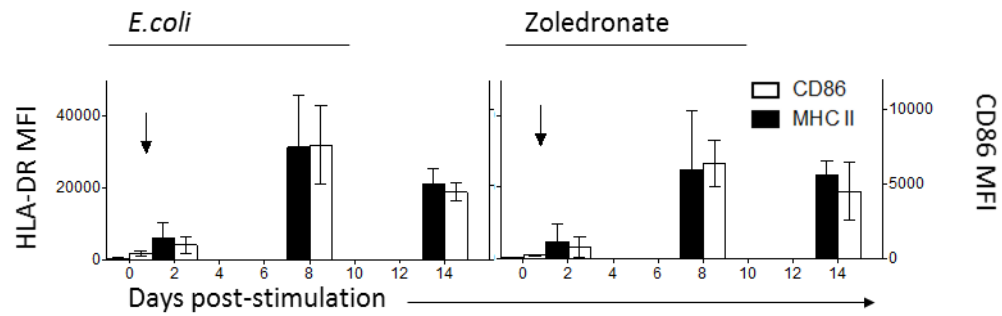


Fig. 4.2. PBMC stimulation with zoledronate leads to similar levels of $\gamma\delta$ T cell upregulation of cell surface HLA-DR and CD86 as stimulation with *E.coli*. Freshly-isolated PBMC (n=5) were expanded for 14 days with irradiated *E.coli*, and stained for cell surface HLA-DR and CD86 throughout expansion. (A) Representative stains of one donor $\gamma\delta$ T cells is shown, with specific antibody in black, unshaded, and isotype-matched control - in gray, shaded. (B) HLA-DR and CD86 MFI over expansion was compared between $\gamma\delta$ T, $\alpha\beta$ T cells and monocytes ($CD3^{neg} CD14^{pos}$ PBMC). Points of *E.coli* stimulation are indicated with black arrows. Bar graphs indicate the mean \pm standard deviation.

4.3. *E.coli* and zoledronate stimulation induces transient $\gamma\delta$ T cell upregulation of CCR7 and downregulation of CD62L

In order to further explore the putative pAPC phenotype of expanded, but not fresh unstimulated $\gamma\delta$ T cells, I set out to document whether $\gamma\delta$ T cell expression of the lymphoid tissue homing markers, CCR7 and CD62L, mirror those of classic $\alpha\beta$ T cells or, rather - those of myeloid APCs, such as DC. Brandes, *et al.* have previously documented $\gamma\delta$ T cells as negative for CCR7 when freshly-isolated, followed by a rapid, potent and transient upregulation of CCR7 on short-term (overnight-36h) endogenous pyrophosphate-stimulated, peripheral human $\gamma\delta$ T cells, which then returned to baseline negativity during short term culture; up to 100% of peripheral $\gamma\delta$ T cells in their culture displayed a CCR7^{pos} phenotype 24h post-stimulation. They specify further that maximal $\gamma\delta$ T cell upregulation of CCR7 took place prior to the initiation of cell proliferation (182). PBMC stimulation with *E.coli* in my model produced a similar result (Fig.4.3).

While Brandes and others interpreted CCR7 upregulation on freshly-isolated $\gamma\delta$ T cells as an indication of migration to lymph nodes as part of putative pAPC function, my data indicate that freshly-isolated $\gamma\delta$ T cells do not engage in en-masse phagocytosis of targets. This is supported by the findings of Wu *et al.*, discussed in the previous chapter, who were able to find only a small minority of short term-activated $\gamma\delta$ T cells engaging in active phagocytosis (50). Moreover, as laid out in this chapter, freshly-isolated or short term-activated $\gamma\delta$ T cells do not appear positive for the APC markers, HLA-DR and CD86. My data indicate that 50+ % of $\gamma\delta$ T cells, expanded with zoledronate or *E.coli*, engage in phagocytosis only upon expansion. Curiously, expanded, phagocytic $\gamma\delta$ T cells did not re-upregulate CCR7 after exposure to *E.coli* (Fig.4.3).

In order to establish whether $\gamma\delta$ T cell expression of CCR7 was similar to that on $\alpha\beta$ T cells during expansion with *E.coli*, CCR7 levels were compared between the two cell populations in parallel. During the transient upregulation by $\gamma\delta$ T cells, CCR7 levels were similar between the two T cell populations (Fig.4.4). Indeed, within 24h of PBMC

stimulation with *E.coli*, a vast majority of $\gamma\delta$ T cells expressed CCR7 at the same level as freshly-isolated $\alpha\beta$ T cells. However, while $\alpha\beta$ T cells – which did not expand after PBMC stimulation with *E.coli* – maintained their expression of CCR7, it was lost entirely on the rapidly-expanding V δ 2 cells, and was not rescued by *E.coli* re-stimulation.

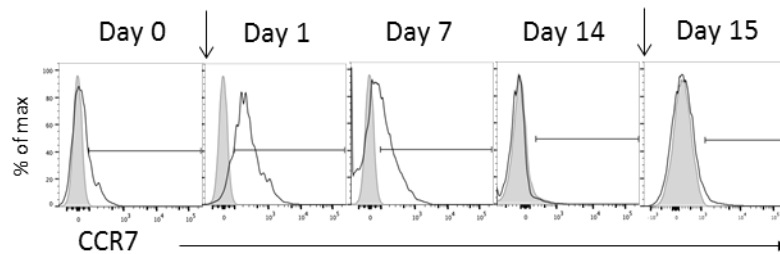


Fig. 4.3. PBMC stimulation with E.coli leads to a transient $\gamma\delta$ T cell upregulation of cell surface CCR7. Freshly-isolated PBMC (n=4) were expanded for 14 days with irradiated *E.coli*, re-stimulated overnight with *E.coli* at D14, and stained for cell surface CCR7. Representative stains of one donor $\gamma\delta$ T cells is shown, with anti-CCR7 antibody in black, unshaded, and isotype-matched control - in gray, shaded. Points of *E.coli* stimulation are indicated with black arrows.

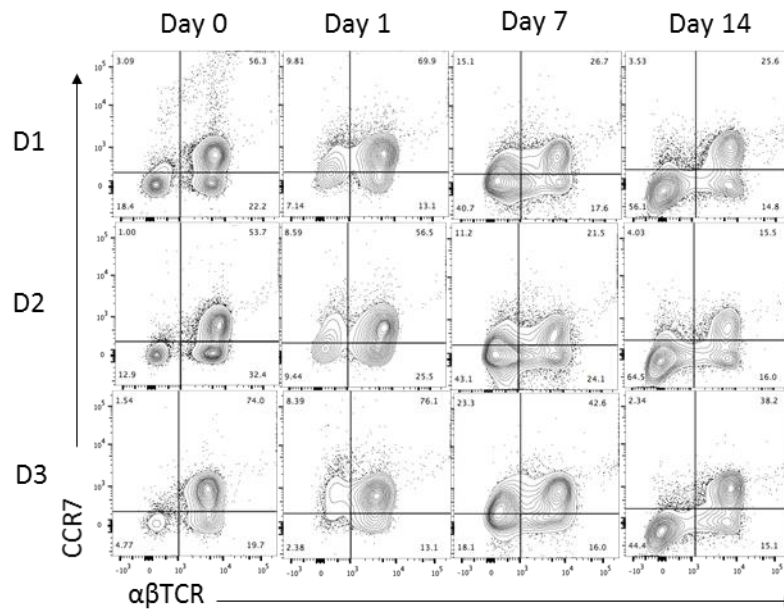


Fig. 4.4. CCR7 expression dynamics after PBMC stimulation with *E.coli* vary between $\alpha\beta$ T and $\gamma\delta$ T cells. Freshly-isolated PBMC (n=4) were expanded for 14 days with irradiated *E.coli*, re-stimulated overnight with *E.coli* at day 14, and stained for cell surface CCR7. CCR7 expression is shown in three representative donor (D1-D3) CD3^{pos} PBMC, and compared in $\alpha\beta$ T versus $\gamma\delta$ T cells over 14 days of expansion.

I concurrently examined $\gamma\delta$ T cell expression of CD62L, which mediates $\alpha\beta$ T cell extravasation from blood into the lymphatic circulation – a step necessary for blood borne cell migration to sites of classic DC antigen presentation. Brandes *et al.* too examined $\gamma\delta$ T cell expression of this lymphoid migratory marker (182). Once again, my data relates closely to their findings. As discussed in their work, and unlike with CCR7, freshly-isolated $\gamma\delta$ T cells appear positive for CD62L (Fig.4.5).

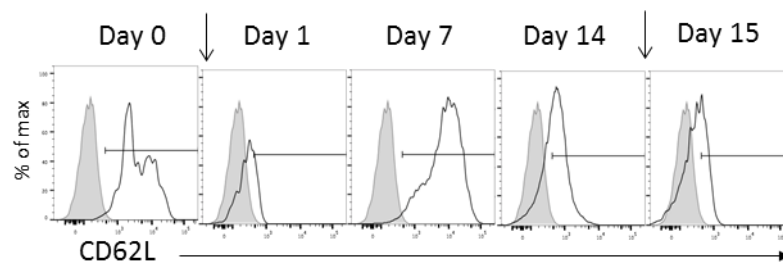


Fig. 4.5. PBMC stimulation with E.coli leads to a transient $\gamma\delta$ T cell downregulation of cell surface CD62L. Freshly-isolated PBMC (n=4) were expanded for 14 days with irradiated E.coli, re-stimulated overnight with E.coli at D14, and stained for cell surface CD62L throughout. Representative stains of one donor $\gamma\delta$ T cells is shown, with anti-CD62L antibody in black, unshaded, and isotype-matched control - in gray, shaded. Points of E.coli stimulation are indicated with black arrows.

PBMC stimulation with *E.coli* produced a transient downregulation of CD62L. Recovered CD62L expression was also decreased upon re-stimulation of *E.coli*-expanded $\gamma\delta$ T cells. In further contrast to CCR7, CD62L levels followed a similar pattern on both cell types, although levels on $\alpha\beta$ T cells were consistently higher than those on $\gamma\delta$ T cells (Fig.4.6).

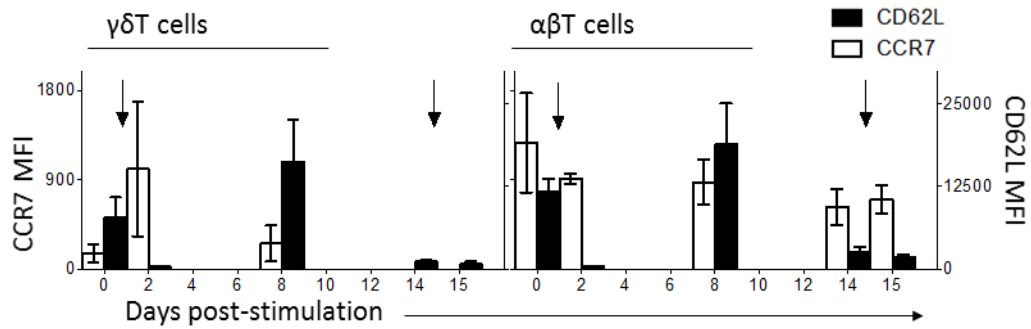


Fig. 4.6. PBMC stimulation with E.coli leads to a transient $\gamma\delta$ T cell upregulation of cell surface CCR7 and downregulation of CD62L. Freshly-isolated PBMC (n=4) were expanded for 14 days with irradiated *E.coli*, re-stimulated overnight with *E.coli* at D14, and stained for cell surface CCR7 and CD62L throughout. Donor CCR7 and CD62L expression MFI was compiled and compared between $\gamma\delta$ T and $\alpha\beta$ T cells throughout expansion and re-stimulation. Points of *E.coli* stimulation are indicated with black arrows. Bar graphs indicate the mean \pm standard deviation.

As with other parameters examined, no significant difference in terms of CCR7 or CD62L expression could be seen between zoledronate and *E.coli*-expanded $\gamma\delta$ T cells (Fig.4.7).

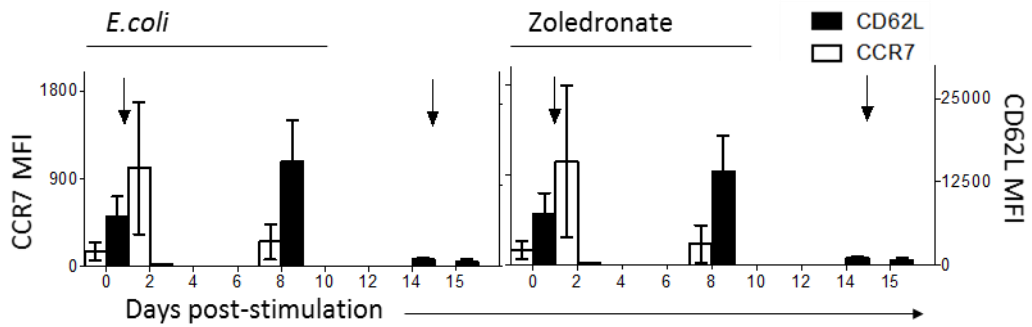


Fig. 4.7. PBMC stimulation with zoledronate leads to similar levels of CCR7 and CD62L on $\gamma\delta$ T cells and stimulation with *E.coli*. Freshly-isolated PBMC (n=4) were expanded for 14 days with irradiated *E.coli*, re-stimulated overnight with *E.coli* at D14, and stained for cell surface CCR7 and CD62L throughout. Donor CCR7 and CD62L expression MFI was compiled and compared between $\gamma\delta$ T and $\alpha\beta$ T cells throughout expansion and re-stimulation. Bar graphs indicate the mean \pm standard deviation.

4.4. *E.coli* and zoledronate stimulation lead to expansion of similar populations of $\gamma\delta$ T cells, as well as $\alpha\beta$ T cells and $CD3^{neg}$ cells

I further endeavored to examine the non-APC effector markers routinely used to distinguish different $\gamma\delta$ T cell populations. As mentioned in the general introduction, peripheral as well as epithelia-resident $\gamma\delta$ T cells display a largely $CD4^{neg}CD8^{neg}$ phenotype, with small single positive $CD8^{pos}$ subpopulations. A similar phenotype was observed upon investigation of both *E.coli* and zoledronate-expanded $\gamma\delta$ T cells (Fig. 4.8).

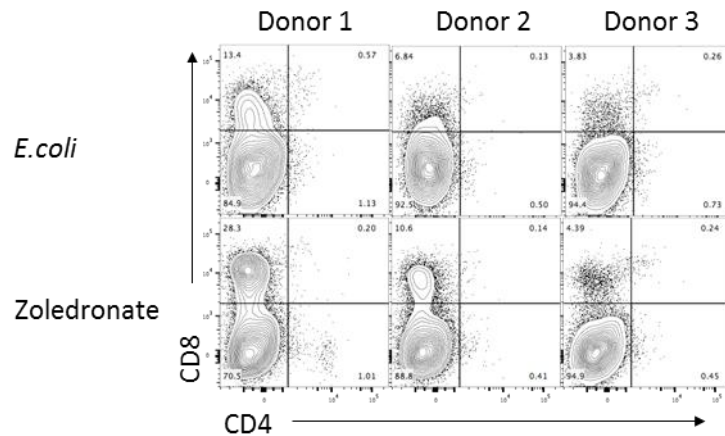


Fig. 4.8. PBMC expansion with *E.coli* or zoledronate leads to proliferation of predominantly $CD4^+ CD8^- \gamma\delta$ T cells. Day 14 *E.coli* and zoledronate-expanded PBMC (n=4) were examined for $\gamma\delta$ T cell surface marker expression via flow cytometry. Shown are representative stains from three donors, gated on total live $\gamma\delta$ T cells.

Similarly, *E.coli* and zoledronate-expanded $\gamma\delta$ T cells exhibited equivalent positivity for the cytotoxic marker CD56 and low affinity phagocytic Fc γ R, CD16, both of which are further classic markers of NK cells and NKT cells (Fig.4.9). Expression of CD16 and CD56 on freshly-isolated peripheral $\gamma\delta$ T cells and V δ 2 cells, in particular, has been documented in the literature previously (183,184). In summary, my data indicate that freshly-isolated peripheral *E.coli* and zoledronate-sensitive V δ 2 cells transition from a non-phagocytic, largely CD4⁻CD8⁻ HLA-DR^{neg} CD86^{neg} CCR7^{neg} CD62L^{pos} CD16^{pos} CD56^{pos} phenotype to a phagocytic, largely CD4⁻CD8⁻ HLA-DR^{pos} CD86^{pos} CCR7^{neg/pos} CD62L^{pos} CD16^{pos} CD56^{pos} phenotype as they expand in response to stimulus.

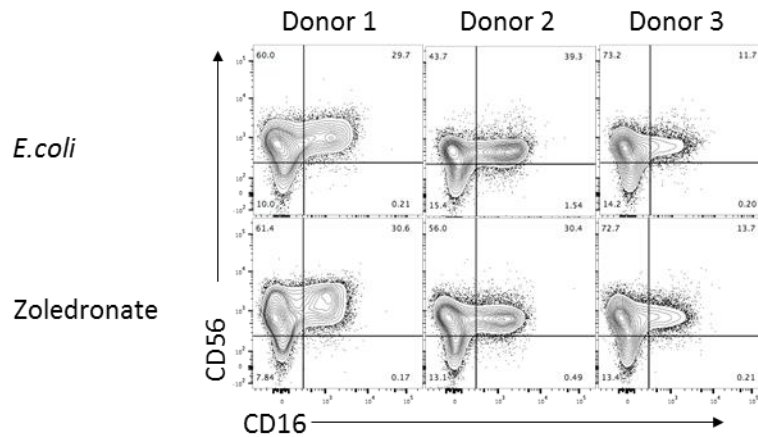


Fig. 4.9. PBMC expansion with *E.coli* or zoledronate leads to proliferation of $\gamma\delta$ T cells that are predominantly CD56^{pos} and CD16^{pos}. Day 14 *E.coli* and zoledronate-expanded PBMC (n=4) were examined for $\gamma\delta$ T cell surface marker expression via flow cytometry. Shown are representative stains from three donors, gated on total live $\gamma\delta$ T cells.

The apparent homogeneity of *E.coli* and zoledronate-expanded $\gamma\delta$ T cells brought my attention to the phenotype of other cell types that may have been expanded or maintained with these expansion protocols. As discussed in the previous results chapter, while both conditions resulted in the preferential expansion of V δ 2 cells, $\alpha\beta$ T cells and a minor population of CD3^{neg} cells persisted in culture throughout stimulation. $\alpha\beta$ T cells remaining in culture after two weeks of PBMC expansion with *E.coli* or zoledronate presented with similar proportions of single positive CD4^{pos}, CD8^{pos} or double negative CD4^{neg}CD8^{neg} T cells – with each phenotype representing roughly a third of all $\alpha\beta$ T cells (Fig.4.10).

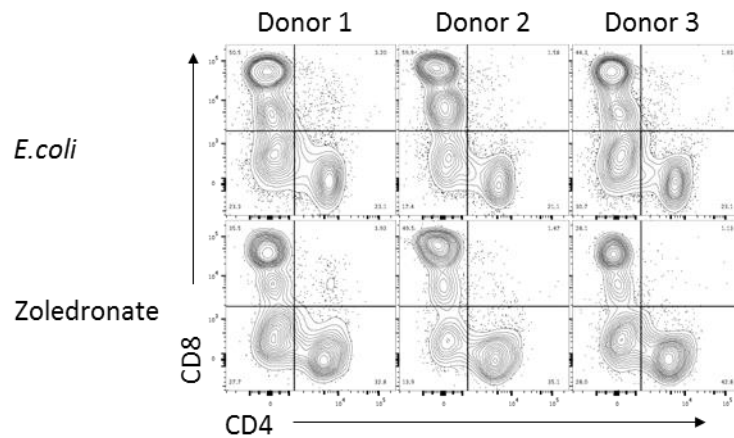


Fig. 4.10. PBMC stimulation with *E.coli* or zoledronate sustains CD4^{pos}, CD8^{pos} and CD4^{neg}CD8^{neg} $\alpha\beta$ T cells. Day 14 *E.coli* and zoledronate-expanded PBMC (n=4) were examined for $\alpha\beta$ T cell content via flow cytometry. Shown are representative stains from three donors, gated on total live $\alpha\beta$ T cells.

A minor difference could be observed between *E.coli* and zoledronate-maintained $\alpha\beta$ T cells in terms of CD56 expression, whence *E.coli*-expanded $\alpha\beta$ T cells contained a ~5% CD56^{pos} subpopulation, whereas zoledronate-expanded $\alpha\beta$ T cells did not (Fig.4.11).

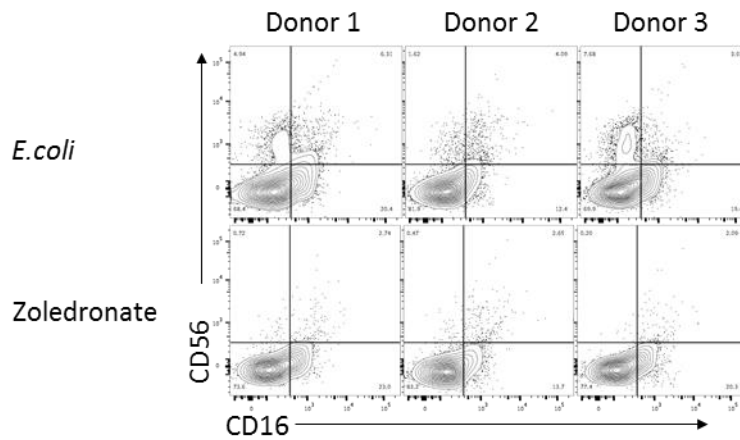


Fig. 4.11. PBMC stimulation with *E.coli* or zoledronate sustains CD16^{neg} CD56^{neg} $\alpha\beta$ T cells. Day 14 *E.coli* and zoledronate-expanded PBMC (n=4) were examined for $\alpha\beta$ T cell content via flow cytometry. Shown are representative stains from three donors, gated on total live $\alpha\beta$ T cells.

Perhaps, most crucial to my examination of non- $\gamma\delta$ T cell populations maintained within *E.coli* or zoledronate-expanded PBMC was to determine whether expanded PBMC cultures contain *bona fide* myeloid, phagocytic APCs. Published data of $\gamma\delta$ T cell APC characteristics have been met with great scepticism from large swaths of the T cell field, informed by justified concern for the effects observed being cause by ‘contaminating’ classic myeloid APC, rather than $\gamma\delta$ T cells. Staining whole, expanded PBMC for CD33 – a general myeloid marker (185) – suggested that both *E.coli* and zoledronate-expanded PBMC contained 0.1-0.8% CD3^{neg} CD33^{pos} cells (Fig.4.12).

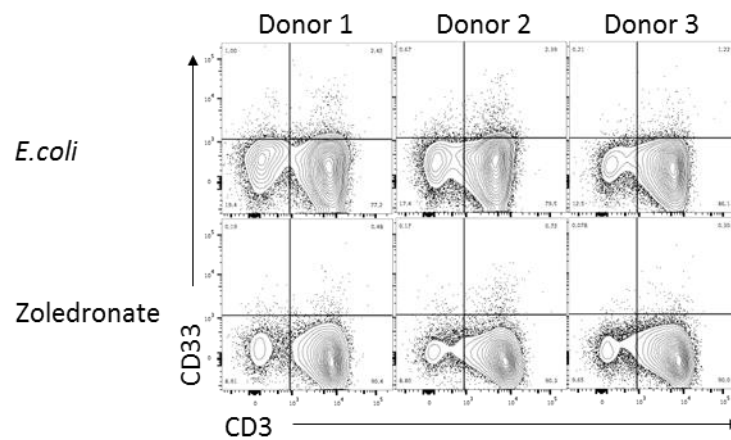


Fig. 4.12. PBMC stimulation with *E.coli* or zoledronate does not expand myeloid cells. Day 14 *E.coli* or zoledronate-expanded PBMC (n=4) were examined for CD3^{neg} cell content via flow cytometry. Shown are representative stains from three donors, gated on total live PBMC.

While such a low proportion of myeloid cells cannot be deemed a significant potential contaminant set against my observation that nearly 100% of expanding $\gamma\delta$ T cells express CD86 and HLA-DR, while ~50% display phagocytic activity, it was further found that the 0.1-0.8% proportion of CD3^{neg} CD33^{pos} cells was not significantly different from that of CD3^{neg} isotype control^{pos} cells. The minor CD33^{pos} population observed is, thus, likely to represent non-specific binding of the antibody, rather than a real subset of CD3^{neg} cells within expanded PBMC. Further staining revealed that these CD3^{neg} cells are also negative for cell surface, CD14 and CD1c, excluding the possibility that expanded PBMC may contain B cells, monocytes or DCs, respectively, all of which possess well-documented pAPC capacity (Fig.4.13).

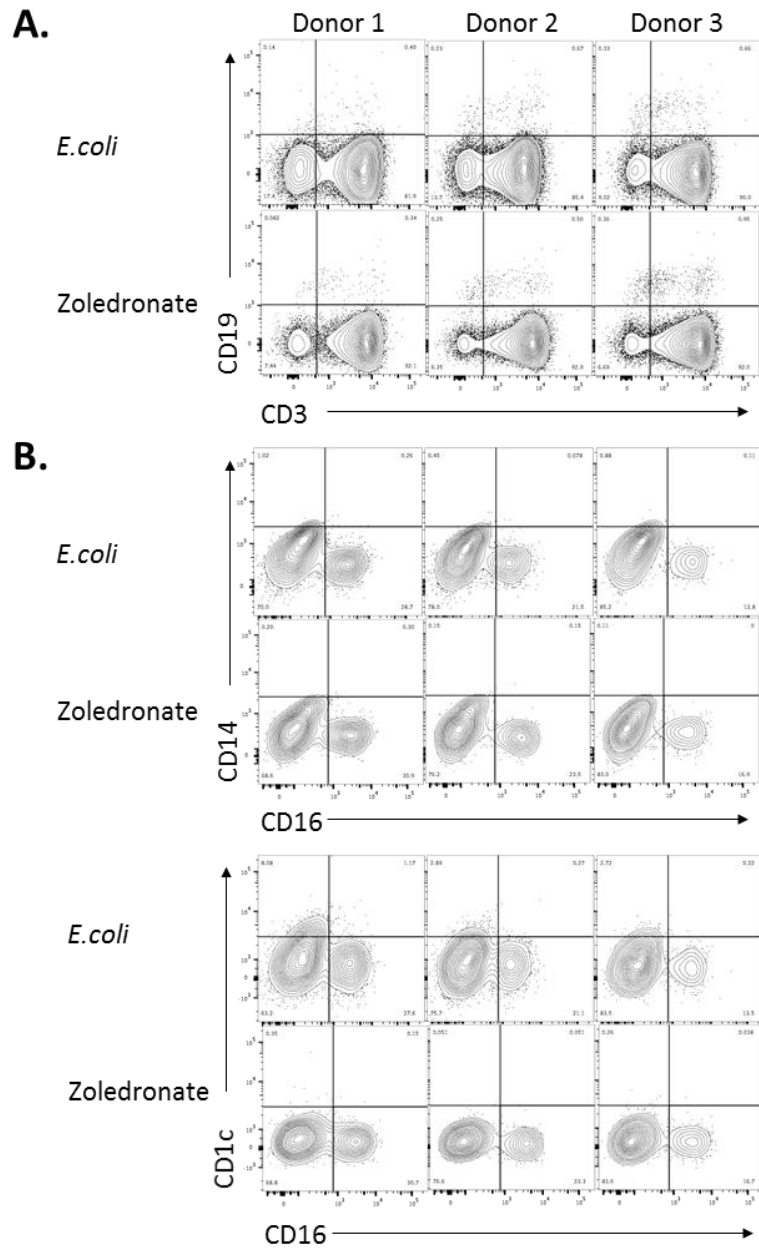


Fig. 4.13. PBMC stimulation with *E. coli* or zoledronate does not expand B cells, dendritic cells or monocytes. Day 14 *E. coli* or zoledronate-expanded PBMC (n=4) were examined for CD3^{neg} cell content via flow cytometry. Shown are representative stains from three donors (A) of total live PBMC expression of CD3 versus CD19, or (B) of CD3^{neg} cell CD14 versus CD16 or CD1c versus CD16 expression.

Notably, however, a significant portion of CD3^{neg} PBMC presented with a CD16^{pos} phenotype. Closer examination revealed that the vast majority of these CD16^{pos} cells were also positive for CD56 (Fig.4.14). I, thus, stipulate that the minor CD3^{neg} population that is sustained during $\gamma\delta$ T cell expansion with *E.coli* or zoledronate consists largely of natural killer (NK) cells.

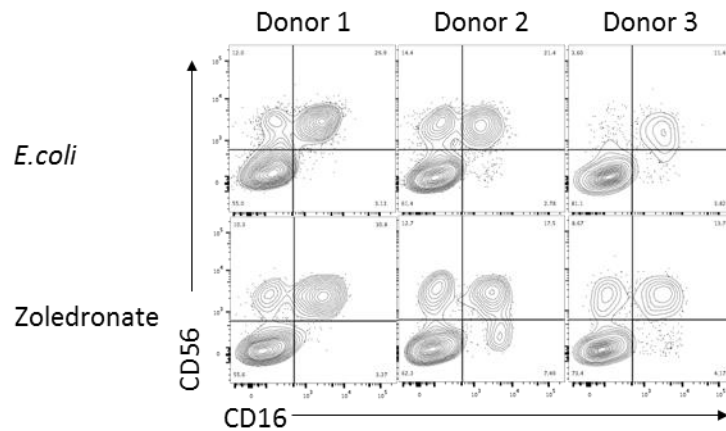


Fig. 4.14. PBMC stimulation with *E.coli* or zoledronate and IL-2 sustains NK cells. Day 14 *E.coli*-expanded PBMC (n=4) were examined for non- $\gamma\delta$ T cell content via flow cytometry. Markers employed in the analysis were: CD3, CD16 and CD56. Shown are representative stains from three donors, gated on total live CD3^{neg} PBMC.

4.5. *E.coli* and zoledronate induce significantly different early cytokine environments within stimulated PBMC

While both *E.coli* and zoledronate have been linked to pAg-mediated activation of $\gamma\delta$ T cells directly and indirectly, respectively, both stimuli nonetheless represent vastly different antigenic challenges to the PBMC compartment (64,103). As covered briefly in the general introduction, zoledronate is a small molecule bisphosphonate drug that inhibits farnesyl pyrophosphate synthase of the eukaryotic cell mevalonate cholesterol synthesis pathway and, consequently, leads to the accumulation of endogenous pyrophosphate metabolic intermediates, such as isopentenyl pyrophosphate (IPP) (180). IPP is then thought to induce conformational changes in the MHC-like butyrophilin (BTN) molecules at the cell surface, signalling cell ‘stress’. T cell receptor (TCR)-engagement of BTN3A.1, specifically, is thought to play a central role in $V\gamma 9V\delta 2$ T cell recognition of transformed or damaged cells (100). Phosphoantigens within *E.coli*, meanwhile, include some of the most potent documented $V\gamma 9V\delta 2$ T cell stimuli, such as (E)-4-hydroxy-3-methyl-but-2-enyl pyrophosphate (known as ‘HMBPP’), which is synthesized by some bacterial and parasitic species via isoprenoid biosynthesis (64). The potency of HMBPP in activating $\gamma\delta$ T cells, by some estimates, exceeds that of IPP by up to a 1000-fold. The structural differences between IPP and HMBPP are briefly addressed in Fig.1.2, while the various routes by which IPP and HMBPP may be activating $\gamma\delta$ T cells – in Fig.1.3.

In addition to HMBPP, *E.coli* expresses a plethora of further immunogenic signals that are thought to be recognized by $\gamma\delta$ T cells via a number of pathogen-sensing mechanisms, such as i) Lipid A, thought to engage the $\gamma\delta$ TCR directly (93), ii) LPS, which triggers $\gamma\delta$ T cell TLR-4 (93) or iii) a series of alkyl amines, including isobutylamine, which too activate $\gamma\delta$ T cells in a TCR-dependent manner (66,124). I note that, while $\gamma\delta$ T cell use and expression of TLRs has been studied and reviewed before (186,187), a comprehensive understanding of the role this receptor family plays in the physiology of various $\gamma\delta$ T cell subsets is lacking.

In addition to *E.coli* representing a significantly different stimulus from zoledronate to $\gamma\delta$ T cells directly, the introduction of a bisphosphonate drug *versus* a bolus of Gram-negative bacteria induces starkly different responses in other non- $\gamma\delta$ T cell PBMCs. To assess the collective early PBMC response to *E.coli*, zoledronate or a non-specific T cell stimulus, such as IL-2, freshly-isolated PBMC were cultured overnight in IL-2 medium (100 IU/mL) with the addition of *E.coli* (MOI 10) or zoledronate (5 μ M), or medium only (mock). After overnight culture, supernatant was collected and analysed for cytokine content via the cytokine multiplex assay, meso scale discovery electrochemiluminescence (MSD) (Fig.4.15). An examination of the lymphocyte growth factors, IL-7 and IL-15, revealed that neither cytokine was produced by zoledronate or *E.coli*-stimulated PBMC. High levels of IL-2 among all conditions served as an internal technical control for MSD, as all cell culture medium in the experiment contained added IL-2 at a pre-specified, equal amount. Significant differences in the cytokine response could be observed in terms of IFN- γ , TNF- α and TNF- β – cytokines associated with a pro-inflammatory Th1-type response. It is, perhaps, unsurprising that PBMC stimulation with *E.coli*, rather than zoledronate, induced a potent Th1 response and production of cytokines linked to activated monocytes. Such responses by PBMC to Gram-negative bacteria have been documented previously (66,102,188–190). Although Th2-type cytokines (IL-4, IL-5 and IL-13) could not be detected at high levels, *E.coli* nonetheless elicited higher levels than zoledronate. Unlike PBMC stimulation with zoledronate, stimulation with *E.coli* induced high levels of pyrogens and systemic inflammatory cytokines, such as IL-6, IL-1 α and IL-1 β , as well as IL-8 and GM-CSF. Interestingly, while the mean amount produced was higher in *E.coli* compared to zoledronate-stimulated PBMC, the same vast differences in statistical significance between the two stimuli couldn't be observed when examining antigen presentation and priming-associated cytokines, such as IL-12p40, IL-12p70 and IL-16. The same was true for the anti-inflammatory, regulatory mediator, IL-10. Freshly-isolated PBMC stimulation with IL-2 medium alone (mock) failed to induce a response in any of the cytokines examined.

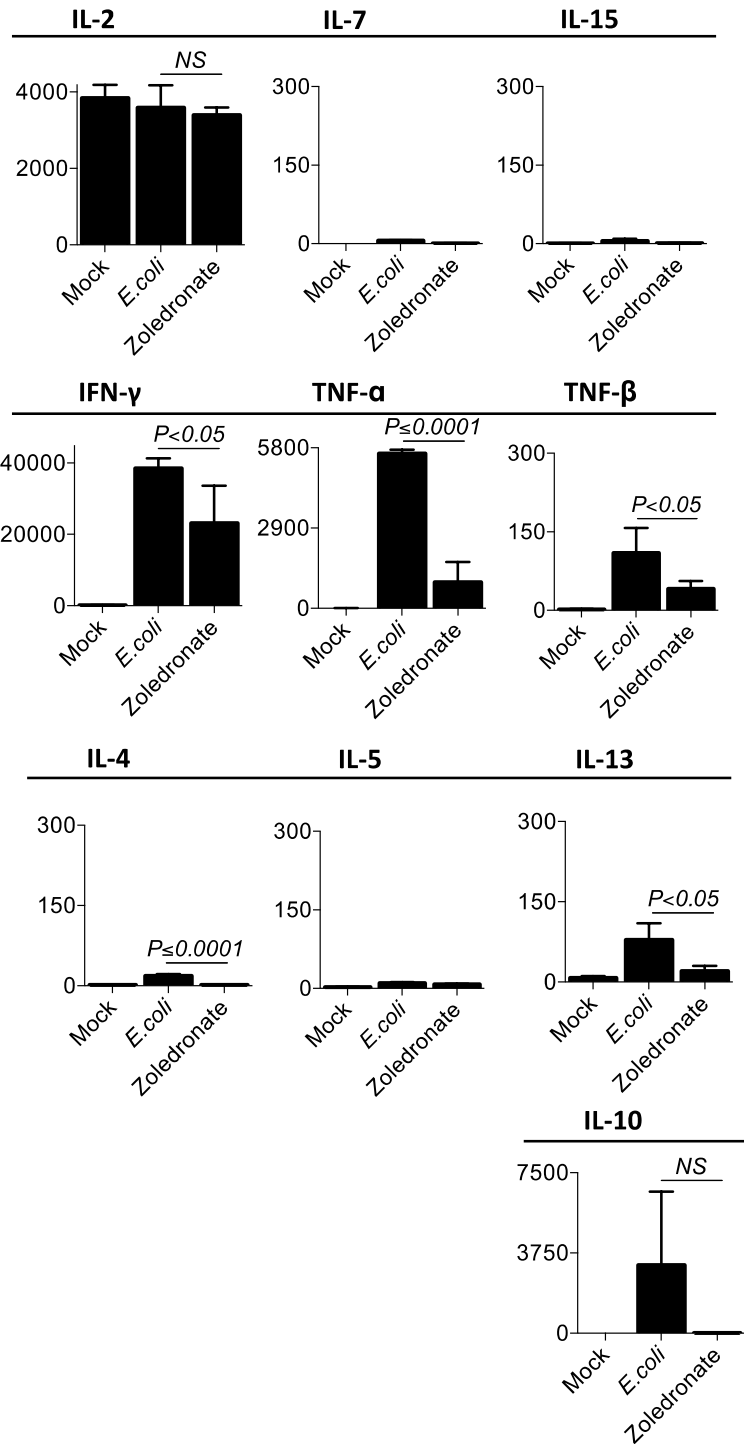


Figure 4.15 is continued on the next page.

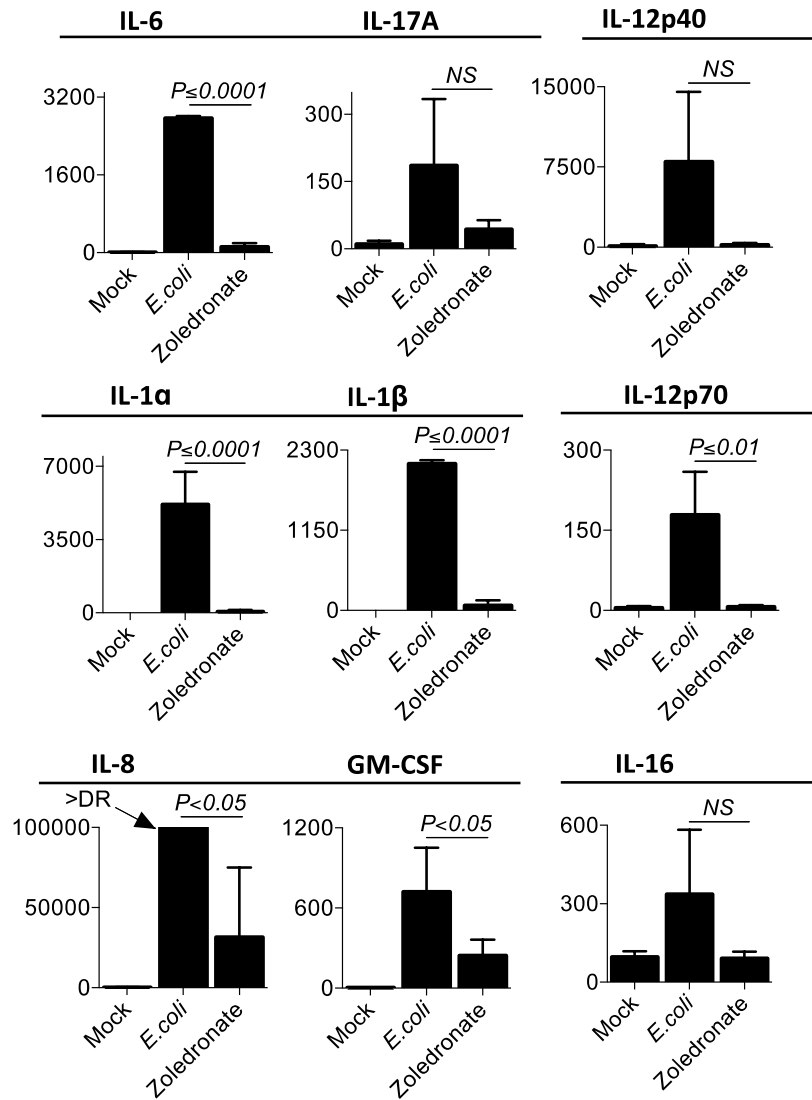


Fig. 4.15. Fresh PBMC stimulation with *E. coli* or zoledronate leads to significantly different early cytokine environments. Freshly-isolated PBMC (n=4) were stimulated overnight with irradiated *E. coli*, zoledronate (5 μ M) or mock-stimulated with IL-2 media alone. Supernatants were collected and analyzed using a meso scale discovery electrochemiluminescence assay (MSD). The x-axis on the graphs indicates the stimulus applied to each set of PBMC; the y-axis indicates the amount of cytokine detected in media (pg/mL). '>DR' denotes that the cytokine amount was above the detection range of the MSD assay. Bar graphs indicate the mean \pm standard deviation.

4.6. *E.coli* and zoledronate induce similar V γ 9V δ 2 TCR repertoires

The observation that *E.coli* and zoledronate stimulation of freshly-isolated PBMC induces largely equivalent $\gamma\delta$ T cell populations in terms of APC marker, homing receptor, CD4 and CD8, as well as CD16 and CD56 expression prompted us to examine the early cytokine environment within stimulated PBMC. Upon noting that the early cytokine environment is vastly different between zoledronate and *E.coli*-stimulated PBMC, I set out to characterise the T cell receptor (TCR) repertoire of the differentially expanded $\gamma\delta$ T cells. As described earlier, zoledronate and *E.coli* are antigenically vastly divergent stimuli – each representing one documented self TCR ligand (i.e. BTN3A) and multiple non-self TCR ligands (e.g. Lipid A, isobutylamine, HMBPP, etc.), respectively.

Freshly-isolated PBMC were expanded with *E.coli* or zoledronate for 14 days, and the resulting TCR repertoire was examined, using an Irepertoire Illumina human gamma delta CDR3 sequencing platform. The TCR CDR3 regions of (a) freshly-isolated unexpanded, (b) *E.coli*-expanded and (c) zoledronate-expanded $\gamma\delta$ T cells from one representative donor were sequenced. *E.coli* and zoledronate-expanded $\gamma\delta$ T cells showed significant overlap of their V γ and V δ CDR3 sequences; both expansions resulted in a predominantly V γ 9V δ 2 $\gamma\delta$ T cell population (Fig.4.16).

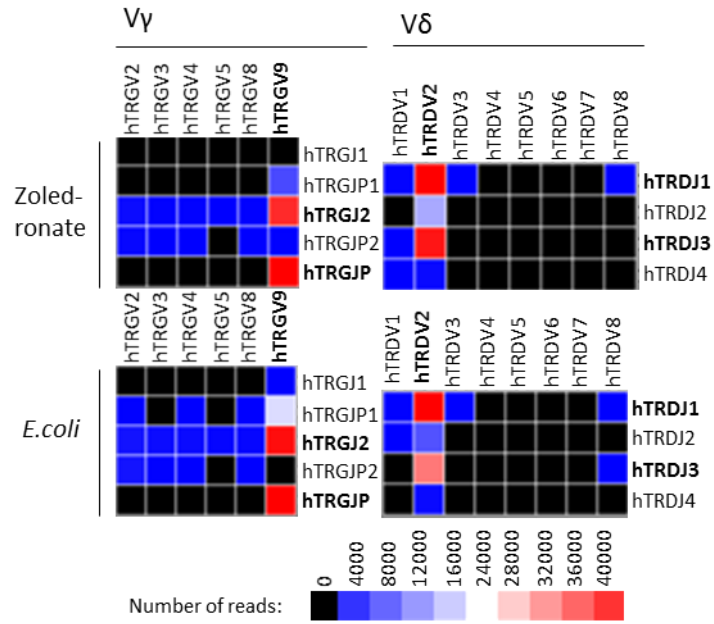


Fig. 4.16. *E.coli* and zoledronate induce proliferation of similar $\gamma\delta T$ cell clones. Freshly-isolated PBMC were expanded with UV-irradiated *E.coli* or zoledronate for 14 days. The resulting $\gamma\delta T$ cell CDR3 repertoire was examined. Representative heat maps of one donor expanded $\gamma\delta T$ cell V γ (VG), V δ (VD) and V \jmath (VJ) chain reads are shown.

CDR3 homology and frequency in selected sequences that represented 5000 or more CDR3 reads were investigated (Fig.4.17). The most prominent group in V γ chain CDR3 sequences was shared between all three expansion conditions, suggesting a largely conserved expansion. The other prominent group was shared between *E.coli* and zoledronate-expanded $\gamma\delta$ T cells, with only low counts exclusive to either group. ~80-90% overlap in the V γ and the V δ chain CDR3 regions was observed between the two expansion protocols. Notably, the single exclusive group of V δ chains was found in freshly isolated $\gamma\delta$ T cells, indicating a significant shift in V δ chain CDR3 repertoire post expansion.

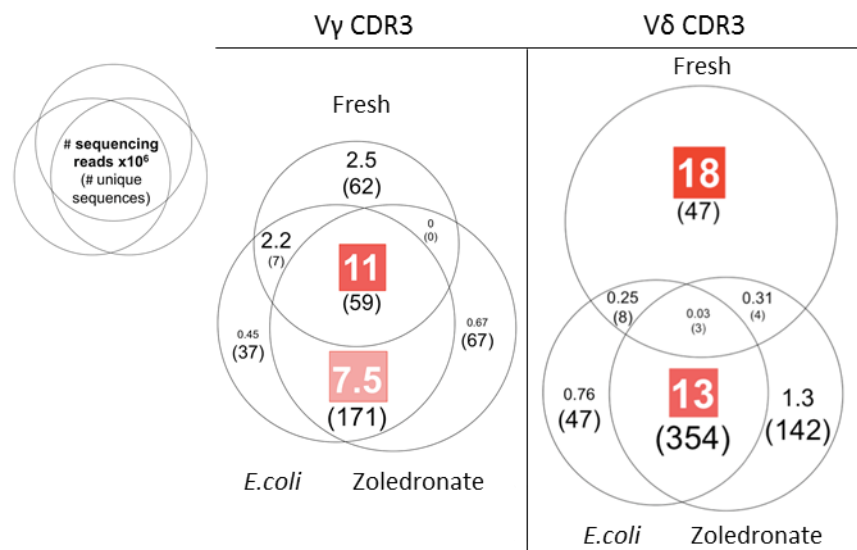


Fig. 4.17. E.coli and zoledronate focus the $\gamma\delta$ T cell CDR3 repertoire in a similar manner. Freshly-isolated PBMC were expanded with UV-irradiated *E.coli* or zoledronate for 14 days. The resulting $\gamma\delta$ T cell CDR3 repertoire was examined. The number of shared TCR CDR3 sequences was tallied and compared in expanded and fresh unexpanded $\gamma\delta$ T cells. A comparison of the number of sequencing reads shared as well as the number of unique sequences in each category is shown for both V γ and V δ TCR chains. For all samples, total depth of sequencing was equivalent. Only sequences with more than 5000 reads were tallied to select for the commonest clones.

To further examine the homology between the TCR repertoires of $\gamma\delta$ T cells expanded with *E.coli* or zoledronate, CDR3 spectratype analysis was performed for both populations. The donor used for spectratype analysis was different to the donor used for sequencing, so as to validate repertoire similarities or differences in more than one donor. Striking homology in CDR3 spectratypes was observed in the V γ 9 and V δ 2 chains of *E.coli* and zoledronate-expanded $\gamma\delta$ T cells, confirming the CDR3 overlap observed in CDR3 sequencing (Fig.4.18).

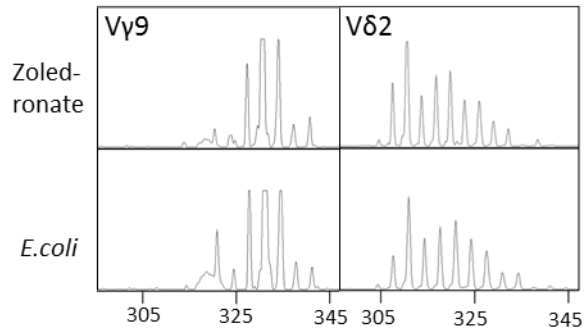


Fig. 4.18. E.coli and zoledronate-expanded $\gamma\delta$ T cells present with similar spectratypes. Freshly-isolated PBMC were expanded with UV-irradiated E.coli or zoledronate for 14 days. The resulting $\gamma\delta$ T cell CDR3 repertoire was examined. TCR CDR3 spectratyping was carried out for expanded V γ 9V δ 2 T cells. Representative spectratypes of one donor are shown.

4.7. Discussion

The experiments described in this chapter were designed to provide a detailed phenotypic analysis of fresh *versus E.coli* and zoledronate-expanded $\gamma\delta$ T cells. Particular focus was placed on expression of the APC molecules, CD86 and MHC class II (HLA-DR, specifically), and lymphoid tissue homing receptors, CCR7 and CD62L. Further analysis was performed on expanded and freshly-isolated V γ 9V δ 2 cell TCR repertoires. Findings included:

- i) Freshly-isolated PBMC stimulation with *E.coli* or zoledronate induces sustained $\gamma\delta$ T cell (including V δ 2 cell) upregulation of HLA-DR and CD86.
- ii) $\gamma\delta$ T cell upregulation of HLA-DR and CD86 is equivalent to that of freshly-isolated monocytes in terms fluorescence intensity.
- iii) $\alpha\beta$ T cells do not significantly upregulate HLA-DR or CD86 in response to PBMC stimulation with *E.coli* or zoledronate.
- iv) Freshly-isolated PBMC stimulation with *E.coli* or zoledronate induces transient $\gamma\delta$ T cell (including V δ 2 cell) upregulation of CCR7.
- v) Expanding $\gamma\delta$ T cells return to a CCR7^{neg} phenotype post-transient upregulation, which is not rescued by expanded $\gamma\delta$ T cell re-stimulation with *E.coli*.
- vi) The period of maximal $\gamma\delta$ T cell surface HLA-DR and CD86 levels does not overlap with that of maximal cell surface CCR7 levels.
- vii) Freshly-isolated $\gamma\delta$ T cells are positive for CD62L.
- viii) Freshly-isolated PBMC stimulation with *E.coli* or zoledronate induces transient $\gamma\delta$ T cell (including V δ 2 cell) downregulation of CD62L.
- ix) Expanding $\gamma\delta$ T cells return to a somewhat CD62L^{pos} phenotype post-transient downregulation, although positivity eventually declines as the expansion progresses.
- x) Some downregulation of $\gamma\delta$ T cell CD62L is still seen upon expanded $\gamma\delta$ T cell re-stimulation with *E.coli*.

- xi) Of the markers examined, fluctuation levels of $\gamma\delta$ T cell surface CD86 and HLA-DR, pre- and post-stimulation, follow a similar pattern. CCR7 levels do not match the pattern of CD86 and HLA-DR positivity. CD62L levels do not match the pattern of either CD86 and HLA-DR, nor CCR7.
- xii) Freshly-isolated PBMC stimulation with *E.coli* or zoledronate leads to the expansion of predominantly CD4^{neg}CD8^{neg} V δ 2 cells that are CD56^{pos} and CD16^{pos}.
- xiii) The same expansions further sustain a mixture of CD4^{pos}, CD8^{pos} and CD4^{neg}CD8^{neg} $\alpha\beta$ T cells that are largely CD56^{neg} and CD16^{neg}.
- xiv) Freshly-isolated PBMC stimulation with *E.coli* or zoledronate does not sustain or expand myeloid cells (including DC and monocytes) or B cells.
- xv) The stimulation does, however, sustain a minor population of CD3^{neg}CD56^{pos}CD16^{pos} PBMC.
- xvi) TCR sequencing of expanded $\gamma\delta$ T cells indicates that both *E.coli* and zoledronate expand V γ 9V δ 2 cells preferentially.
- xvii) Sequencing further indicates that both expansion stimuli expand highly homologous TCR repertoires, in terms of CDR3, which are nonetheless significantly different from freshly-isolated $\gamma\delta$ T cell CDR3.
- xviii) Focusing of the CDR3 repertoires in response to both stimuli compared to freshly-isolated $\gamma\delta$ T cells is largely located in the V δ chain locus and not the V γ chain locus.
- xix) The homology of CDR3 repertoires between *E.coli* versus zoledronate-expanded V γ 9 δ 2 cells is further supported by spectratype analysis.
- xx) Similar populations of $\gamma\delta$ T cells, $\alpha\beta$ T cells and CD3^{neg} cells were expanded or sustained despite divergent early cytokine milieus present in PBMC stimulated with *E.coli* versus zoledronate.

The focus of this chapter was two-fold. Firstly, I aimed to characterize the dynamics of pAPC markers on $\gamma\delta$ T cells expanded with *E.coli* or zoledronate. Secondly, I aimed to establish whether the expansion of V δ 2 cells with apparently equivalent phagocytic

capacity in response to stimulation with *E.coli* or zoledronate, as described in the previous chapter, correlates to further phenotypic similarities in the two cell populations.

As outlined in the chapter introduction, the upregulation of MHC class II (HLA-DR, specifically) and CD86 on activated V δ 2 cells in response to diverse stimuli, ranging from IPP to Gram-negative bacteria as well as mycobacteria, has been described in the literature previously (102,105). I was able to reproduce these results and establish, moreover, that this upregulation is sustained and consistent among the various donors examined. This is strongly indicative of the putative pAPC role of activated, but not resting (i.e. freshly-isolated, unstimulated) peripheral V δ 2 cells. $\gamma\delta$ T cell upregulation of the lymphoid-homing receptor CCR7 in response to stimulation has been previously described by Brandes, Moser and colleagues (51,182). This finding was interpreted as an indication that $\gamma\delta$ T cell APC function is likely to resemble that of classic professional APCs, such as DC, in terms of localisation.

Curiously, I was unable to find an obvious correlation between these lymphoid homing cell surface markers and cell surface levels of HLA-DR and CD86. While transient upregulation of CCR7 could be observed in response to freshly-isolated $\gamma\delta$ T cell stimulation, it did not appear to correlate with maximal $\gamma\delta$ T cell upregulation of HLA-DR nor CD86, nor was I able to detect significant phagocytosis of opsonized *E.coli* by freshly-isolated $\gamma\delta$ T cells. It must be noted that staining for homing receptors on circulating $\gamma\delta$ T cells is significantly complicated by the fact that CCR7 and CD62L are homing markers with dual interpretations of function. On canonical, peripheral $\alpha\beta$ T cells these are markers of a naïve, unstimulated state and continued lymphatic re-circulation in search of cognate antigen. On classic APC, such as DC, meanwhile, these are markers of exit from tissue where an inflammatory target has been encountered, and shuttling to lymph nodes for presentation of phagocytosed antigenic material to naïve T cells. It remains unclear as to what relationship the ‘innate-like’ $\gamma\delta$ T cells bear to canonical $\alpha\beta$ T cell homing markers. The interpretation of Brandes *et al.* regarding $\gamma\delta$ T cell CCR7 ascribes it to the ‘myeloid-like’ properties of these ‘innate T cells’. Due to a lack of obvious correlation and in the

absence of functional studies, I hesitate to make such a conclusion sans further investigation. It remains, moreover, unclear as to whether $\gamma\delta$ T cell antigen presentation occurs in lymph nodes *in vivo*.

Comprehensive further experimental investigation is necessary to determine the homing patterns of activated, phagocytic APC-like peripheral human V δ 2 cells. It cannot be ruled out, for example, that the phagocytic and antigen presenting capacity of these cells peaks at seven days post-stimulation and not the 14 days post-stimulation employed in the study. At seven days post-stimulation CCR7 positivity on stimulated $\gamma\delta$ T cells remained higher than compared to baseline expression. The phagocytic and antigen presenting capacity peak may even occur at any time before the seven-day mark after PBMC stimulation with *E.coli* or zoledronate. Perhaps ‘maturation’ into this phenotype occurs at different rates in a donor-dependent manner. The only way to effectively address this question is to carry out comparative $\gamma\delta$ T cell phagocytic assays and chemokine receptor staining at much shorter time intervals than the experiments described. A more thorough enquiry would warrant investigation of these phenomena every successive day post-stimulation, or even at hour intervals to ensure precision of the data generated. The resources required for such an undertaking are vast, which was a deciding factor in my not pursuing of this strategy. It is curious to note, however, that 14 day expanded $\gamma\delta$ T cells were capable of *E.coli* phagocytosis, but did not re-upregulate CCR7 in response to re-encounter with *E.coli*. CD62L was, furthermore, downregulated upon $\gamma\delta$ T cell re-encounter with *E.coli*. This may be indicative that $\gamma\delta$ T cell phagocytosis does not correlate with $\gamma\delta$ T cell migration to lymphoid tissue – at least in terms of CCR7 and CD62L.

A point of consideration in the context of examining APC phenotype in short term-expanded $\gamma\delta$ T cells concerns my investigative motivation, which is rooted in the potential use of $\gamma\delta$ T cells in the clinic. A requirement in the clinic for a large number of cells available for use, in combination with the relative scarcity of $\gamma\delta$ T cells in the periphery, indicates a likely necessity for clinic-destined $\gamma\delta$ T cells to be expanded *in vitro* for 14 days

or more. The phenotypic characterisation of $\gamma\delta$ T cells expanded for 14 days and more, thus, carries some value in and of itself.

A crucial step in the meaningful exploration of activated peripheral $\gamma\delta$ T cell homing properties is characterisation of homing receptors beyond CCR7 and CD62L. In addition to the above-mentioned CCR7 and CD62L, various groups have addressed $\gamma\delta$ T cell expression of CCR2, CCR5, CCR6, CXCR3 and CXCR4, among others (191,192). There persists, however, an overall lack of consensus on the significance of each of these receptors on $\gamma\delta$ T cells compared to canonical $\alpha\beta$ T cells. It is, moreover, unclear whether these investigations have examined both activated and non-activated $\gamma\delta$ T cells. Comprehensive review on $\gamma\delta$ T cell homing properties is necessary. Such an undertaking is significantly complicated by the ambiguous relationship between human and laboratory animal (*e.g.* mouse) $\gamma\delta$ T cells, making information on *in vivo* human $\gamma\delta$ T cells trafficking scarce. While some review on the subject is available in the literature, it is nearly 15-years-old and likely out of date (193). The chemokine receptors I propose ripe for investigation in the context of $\gamma\delta$ T cell APCs, before and after stimulation, are summarized in Table 4.1.

Table 4.1 | Homing receptors of interest to $\gamma\delta$ T cell APC function

Receptor	Immune cell expression	Key immune function
CXCR3	Th1, CD8 ^{POS} TCM and T _{EM} , Treg, Tfh, NK, NKT, pDC, B cell	Th1-type adaptive immunity
CXCR5	Tfh, Tfr, CD8 ^{POS} T _{EM} , B cells	T and B cell trafficking in lymphoid tissue to B cell zones/follicles
CCR2	Th1, monocyte, macrophage, iDC, basophil, NK	Th1-type adaptive immunity, monocyte trafficking
CCR4	Th2, skin- and lung-homing T, Treg, Th17, CD8 ^{POS} T, monocytes, B cells, iDC	Homing of T cells to skin and lung, Th2-type immune response
CCR6	Th17, iDC, $\gamma\delta$ T, NKT, NK, Treg, Tfh	iDC trafficking, GALT development, Th17 adaptive immune responses
CCR8	Th2, Treg, skin T _{RM} , $\gamma\delta$ T, monocyte, macrophage	Immune surveillance in skin, type 2 adaptive immunity, thymopoiesis
CCR9	Gut-homing T, thymocytes, B cells, DC, pDC	Homing of T cells to gut, GALT development and function, thymopoiesis
CCR10	Skin-homing T, IgA-plasmablasts	Humoral immunity at mucosal sites, immune surveillance in skin
CXCR1	Cross-presenting CD8 ^{POS} DC, thymic DC	Antigen cross-presentation by CD8 ^{POS} DCs
CX3CR1	Resident monocytes, macrophages, microglia, Th1, CD8 ^{POS} T _{EM} , NK $\gamma\delta$ T, DCs	Patrolling monocytes in innate immunity, microglial cell and NK cell migration, Th1-type adaptive immunity

Elements of this table have been adapted from Luster et al. (2014) (103).

Abbreviations: DC, dendritic cell; iDC, immature DC; GALT, gut-associated lymphoid tissue; NK, natural killer cell; NKT, natural killer T cell; T_{CM}, central memory T cell; T_{EM}, effector memory T cell; T_{RM}, resident-memory T cell; Tfh, T follicular helper cell; Tfr, follicular regulatory T cell; Th, T helper cell; Treg, regulatory T cell.

Upon considering non- $\gamma\delta$ T cell populations that were sustained during expansion post PBMC stimulation with *E.coli* or zoledronate, it is perhaps unremarkable that I found these consisted largely of $\alpha\beta$ T cells and $CD3^{neg}CD33^{neg}CD56^{pos}CD16^{pos}$ cells. While finding PBMC in culture that were $CD3^{neg}$ after 14 days of T cell expansion was initially surprising, learning that these are $CD33^{neg}$ (i.e. not of myeloid origin) as well as $CD56^{pos}CD16^{pos}$ leads us to postulate that these cells are likely NK cells. All $\gamma\delta$ T cell expansion media employed in these studies contained high concentrations of IL-2, which is a known mitogen of T cells (with $\gamma\delta$ TCRs or $\alpha\beta$ TCRs) as well as NK cells (194). As indicated by MSD data, PBMC exposure to *E.coli* or zoledronate further induced high levels of potent pro-inflammatory cytokines, such as IFN- γ . An intriguing possibility remains that the $\alpha\beta$ T cells remaining in culture after two weeks of *E.coli* or zoledronate expansion represent antigen-specific outgrowth of $\alpha\beta$ T cell clones rare at baseline, rather than a non-specific bystander effect. Significant further phenotyping and, importantly, functional assays are necessary to determine the nature of the $\alpha\beta$ T cells and likely NK cells remaining in $\gamma\delta$ T cell culture. It cannot be ruled out that these cells play a ‘supportive’ role in their engagement of expanding $\gamma\delta$ T cells. While a skewing of the functional phenotype is possible, expansion protocols with purified $\gamma\delta$ T cells have been published, suggesting that the presence of $\alpha\beta$ T cells or NK cells is not essential for $\gamma\delta$ T cell expansion (195).

The finding that both expansion conditions induced proliferation of predominantly $CD4^{neg}CD8^{neg}$ V δ 2 cells that are $CD56^{pos}$ and $CD16^{pos}$ is, perhaps, also unremarkable. The expansion of $CD56^{pos}$ and $CD16^{pos}$ V δ 2 cells using pAg stimulation has been described previously (184,196). More surprising was the finding that no significant differences could be found in terms of these important functional markers whether PBMC had been exposed to *E.coli* versus zoledronate. I postulated initially that, given the highly divergent stimuli that *E.coli* and zoledronate represent, proliferating V δ 2 cells may be skewed to divergent phenotypic paths. In terms of the parameters that I examined, this did not appear to be the case.

Expanded $\gamma\delta$ T cell TCR sequencing determined that both expansion stimuli induced proliferation of specifically V γ 9V δ 2 cells. CDR3 sequencing and spectratyping further revealed a striking similarity between *E.coli* and zoledronate-expanded V γ 9V δ 2 cell CDR3, which were nonetheless significantly different from freshly-isolated, unexpanded $\gamma\delta$ T cells. These findings are consistent with the focusing of the $\gamma\delta$ TCR repertoire on a common set of TCR ligands, regardless of stimulation with *E.coli* versus zoledronate. As described earlier, it has been proposed that zoledronate activates $\gamma\delta$ T cells by causing accumulation of endogenous pyrophosphates and, consequently, conformational changes in butyrophilin molecules, such as BTN3A. Like zoledronate, *E.coli* too has been documented to cause the accumulation of endogenous pyrophosphates (IPP), which then serve to drive activation and proliferation of V γ 9V δ 2 T cells (101,102). It may have to be considered, therefore, that V γ 9V δ 2 cell proliferation is regulated foremostly by recognition of ‘self-stress’, via *e.g.* BTN molecules, even if the stimulus is exogenous in nature (as addressed briefly in Fig.1.3); even if the stimulus contains a plethora of further pro-inflammatory molecules in and of itself, as is the case with *E.coli*. Related to this is the observation that the recognition of pAg signals appears to occur primarily through germline-encoded regions of the V γ 9V δ 2 TCR, and involves all CDR loops (181). Relative to the $\alpha\beta$ TCR, there are, moreover, relatively few germline genes available for assembly of the $\gamma\delta$ TCR (197). While some have postulated that the expansion of the V γ 9V δ 2 subset in the periphery after birth is driven by exposure to environmental microbial ligands, there remains a lack of consensus on the factors that drive V γ 9V δ 2 cell expansion *in vivo* (198).

Having observed striking similarities between V γ 9V δ 2 cell responses within PBMC stimulated with zoledronate or *E.coli*, I ventured to better characterise the functional responses of both freshly-isolated and expanded $\gamma\delta$ T cells. I set out, moreover, to determine whether the functional shift between a non-phagocytic to a phagocytic cell population pre- and post-expansion correlates with further effector function changes in $\gamma\delta$ T cells pre- and post-stimulation.

4.8. Summary

Data laid out in this chapter lead us to the conclusion that *E.coli* and zoledronate-expanded $\gamma\delta$ T cells bear a close resemblance in terms of functional cell surface marker expression, with both populations presenting with a predominantly HLA-DR^{pos} CD86^{pos} CCR7^{neg} CD62L^{low} CD4^{neg} CD8^{neg} CD16^{pos} CD56^{pos} phenotype. Striking homology could, moreover, be seen in the differentially expanded V γ 9V δ 2 TCR CDR3 sequences, which were similar to one another, but not to freshly-isolated TCR CDR3s. This suggests that PBMC stimulation with *E.coli* and zoledronate leads to V γ 9V δ 2 CDR3 focusing on a similar set of ligands.

5. $\gamma\delta$ T CELL ACQUISITION OF pAPC PHENOTYPE IS CONCURRENT TO A LOSS OF Th1 INFLAMMATORY PHENOTYPE

5.1. Aims

The previous results chapter documents the observation that expanded V δ 2 $\gamma\delta$ T cells acquire an opsonin-dependent phagocytic phenotype that correlates with upregulation of CD86 and MHC class II. This phenotypic shift resulted from PBMC stimulation with either *E.coli* or zoledronate. Surprisingly, in all parameters examined (including TCR repertoire) V δ 2 cells expanded with *E.coli* or zoledronate appeared highly similar. In this chapter I set out to document in further detail the impact of expansion on V δ 2 cell effector phenotype. Parameters such as antigen presentation, cytokine production and cytotoxic capacity were considered.

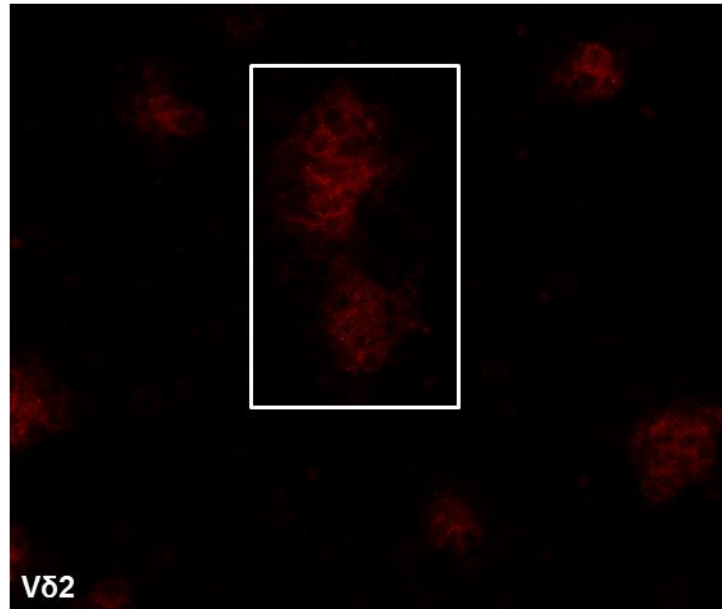
A number of publications describe the *in vitro* pAPC activity of human $\gamma\delta$ T cells (49–51,60). This phenotype has, however, not been correlated to corresponding output of cytokines, memory phenotype, expansion status or cytotoxic capacity of the $\gamma\delta$ T cells in question. In this chapter I set out to determine whether $\gamma\delta$ T cells expanded with *E.coli* or zoledronate do indeed act as APCs to naïve peripheral $\alpha\beta$ T cells. I explored, moreover, how this antigen presentation correlates to more accepted and classic $\gamma\delta$ T cell functions, such as production of IFN- γ and cytotoxicity.

5.2. $\gamma\delta$ T cells expanded with *E.coli* or zoledronate display a pAPC effector phenotype

The previous chapters described my observation that $\gamma\delta$ T cell expansion with *E.coli* or zoledronate produces a population of efficiently phagocytic HLA-DR^{pos}CD86^{pos} V δ 2 cells. While these observations provide evidence toward pAPC function by $\gamma\delta$ T cells, functional assays are necessary to establish whether expanded V δ 2 cells are indeed capable of antigen presentation.

E.coli-expanded PBMC examination with confocal microscopy revealed that, within ~30min of plating, V δ 2 cells had re-formed large, 'grape-like' clusters, observed typically with *in vitro* activated $\gamma\delta$ T and $\alpha\beta$ T cells (Fig.5.1A). These V δ 2 cells further displayed a single, regular, rounded nuclear shape, as indicated by DAPI staining (Fig.5.1B), another classic T cell morphological feature. Inadvertently, such clustering presents a significant technical challenge to imaging. Clear cell images via confocal microscopy require a low cell density and separation of single cells, so as to be able to document cell shape and movement precisely. Thus, detailed information about expanded cell morphology was acquired by examination of non-clustered V δ 2 cells (Fig.5.2). Low density, unclustered expanded V δ 2 cells revealed a shape highly atypical for normally-round and regular T cells - with dendritic-like cell shape and irregular membrane ruffles extending in all directions (Fig.5.2A, B).

A.



B.

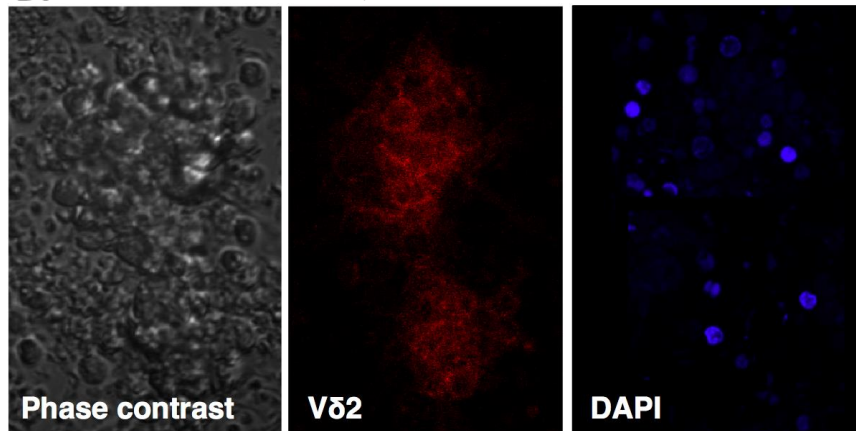


Fig. 5.1. $\gamma\delta T$ cell activation and expansion leads to Vδ2 cell clustering. Day 14 E.coli-expanded PBMC were stained with Vδ2-PE mAb, DAPI and examined via confocal microscopy. (A) Shown is a representative field of vision with Vδ2-PE seen in red. (B) A section of the field of vision, showing a Vδ2 cell cluster, was amplified to provide greater detail of cell membrane and nuclear shape.

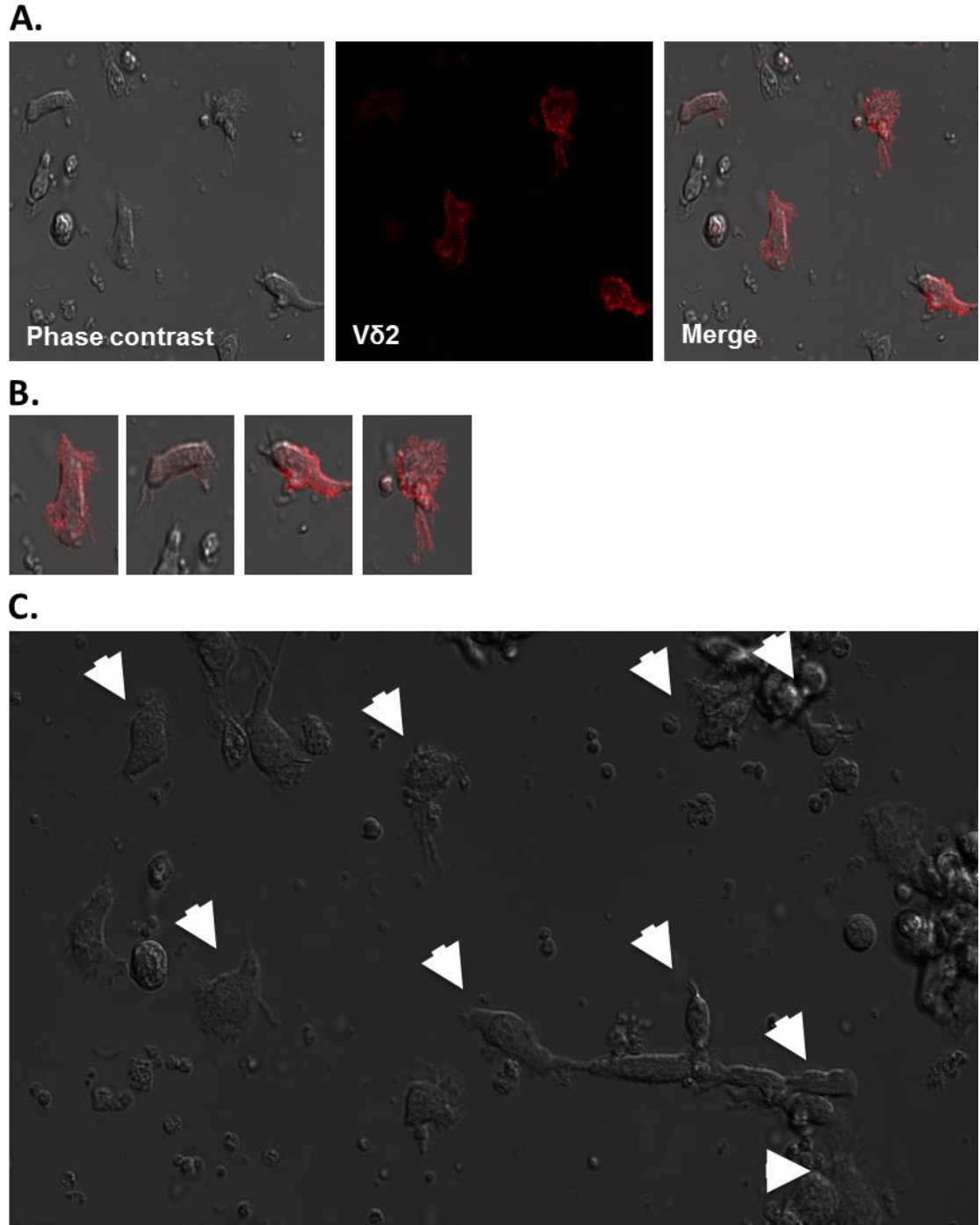


Fig. 5.2. V δ 2 cell expansion leads to their acquisition of a phagocyte-like morphology and probing behaviour. Day 14 *E.coli*-expanded PBMC were stained with V δ 2-PE mAb and examined via confocal microscopy. **(A)** Shown is a representative field of vision, with PBMC in light phase contrast, V δ 2-PE or a merge of the two, with **(B)** magnified V δ 2 PBMC from the representative field of vision. **(C)** Light phase contrast images from the same field of vision as shown in panel **(A)** were collected every 2 seconds for 5 minutes. Shown is a video sequence of the collected images. V δ 2 PBMC are indicated with white arrows. The video material is available for viewing in the CD attached to the thesis as supplementary media material.

Strikingly, the movement of expanded V δ 2 cells was strongly reminiscent of phagocyte probing (a screenshot from the video material is visible in Fig.5.2C; the full video is provided in a CD attached to the thesis in Supplementary Media Material). Every single V δ 2 cell in the field of vision appeared engaged in active, exploratory membrane ruffling. Grinstein and Botelho define ‘probing’ as “membrane extensions enriched in phagocytic receptors flail[-ing] about in an actin-dependent manner, enhancing the likelihood of particle contact and receptor-ligand engagement” (199). Such probing is characteristic of phagocytic cells, including dendritic cells, and constitutes the first stage of phagosome formation. The stages of phagosome formation, as described by Grinstein and Botelho, are i) probing via membrane ruffling followed by receptor-ligand binding, given presence of target, ii) early signalling and cup formation, mediated by receptor clustering and tyrosine kinase activation, iii) pseudopod extension via actin remodelling and localised membrane secretion, and iv) phagosome closure involving phagocytic signal termination.

To test whether expanded V δ 2 cells are capable of activating naïve $\alpha\beta$ T cells, zoledronate-expanded PBMC were FACS-sorted for V δ 2 cells to >98% purity. Zoledronate instead of *E.coli*-expanded PBMC were used to avoid the possibility that *E.coli* debris may be lingering in the cell media or has been internalized by cells. Purified V δ 2 cells were then incubated overnight with IgG-opsonized *E.coli*. In parallel, $\alpha\beta$ T cells were purified from freshly-isolated, unstimulated autologous PBMC. Expanded, opsonized *E.coli*-stimulated V δ 2 cells were then co-cultured for two days with purified $\alpha\beta$ T cells at $\gamma\delta$ T: $\alpha\beta$ T ratios of 1:20, 1:10 and 1:5. The experimental setup is illustrated in the Materials and Methods chapter. Normally, $\alpha\beta$ T cell antigen presentation assays require the use of a cell line with a known TCR specificity or $\alpha\beta$ T cell transduction with TCR of known specificity, and possibly even transduction of the APC with a specific HLA type. I was able to overcome the necessity for HLA transduction by employing ‘responder’ $\alpha\beta$ T cells isolated from the same donor as the ‘stimulator’ expanded V δ 2 cells. As for the necessity for TCR transduction of responder $\alpha\beta$ T cells, I stipulated there may be a relatively high baseline frequency of *E.coli*-reactive $\alpha\beta$ T cells in the peripheral blood of healthy human adults, due to the ubiquitous distribution of *E.coli* as both, a commensal and pathogen. I, therefore, speculated that there may be high-enough numbers of *E.coli*-reactive $\alpha\beta$ T cells

in unstimulated donor PBMC to be detectable using flow cytometry. Indeed, various groups have documented the relatively high numbers of *E.coli*-reactive $\alpha\beta$ T cells in humans at various anatomical sites, ranging from blood to synovial fluid, to lamina propria (200–203). The responders in this antigen presentation assay were, thus, non-transduced, normal adult PBMC $\alpha\beta$ T cells.

$\alpha\beta$ T cells co-cultured with mock-stimulated V δ 2 cells (V δ 2 cells stimulated with medium only) did not produce IFN- γ . Importantly, this indicates that HLA-DR^{pos}CD86^{pos} V δ 2 alone are not sufficient to induce an IFN- γ response from naïve $\alpha\beta$ T cells (Fig.5.3A, B). *E.coli*-stimulated V δ 2 cells, meanwhile, induced $\alpha\beta$ T cell IFN- γ production at all the $\gamma\delta$ T: $\alpha\beta$ T cell ratios examined. $\gamma\delta$ T: $\alpha\beta$ T ratios ranging from 1:5 to 1:20 did not produce a significant difference in the IFN- γ observed. In terms of subset-specificity of the response, IFN- γ production was observable only in CD4+ $\alpha\beta$ T cells (Fig.5.3C).

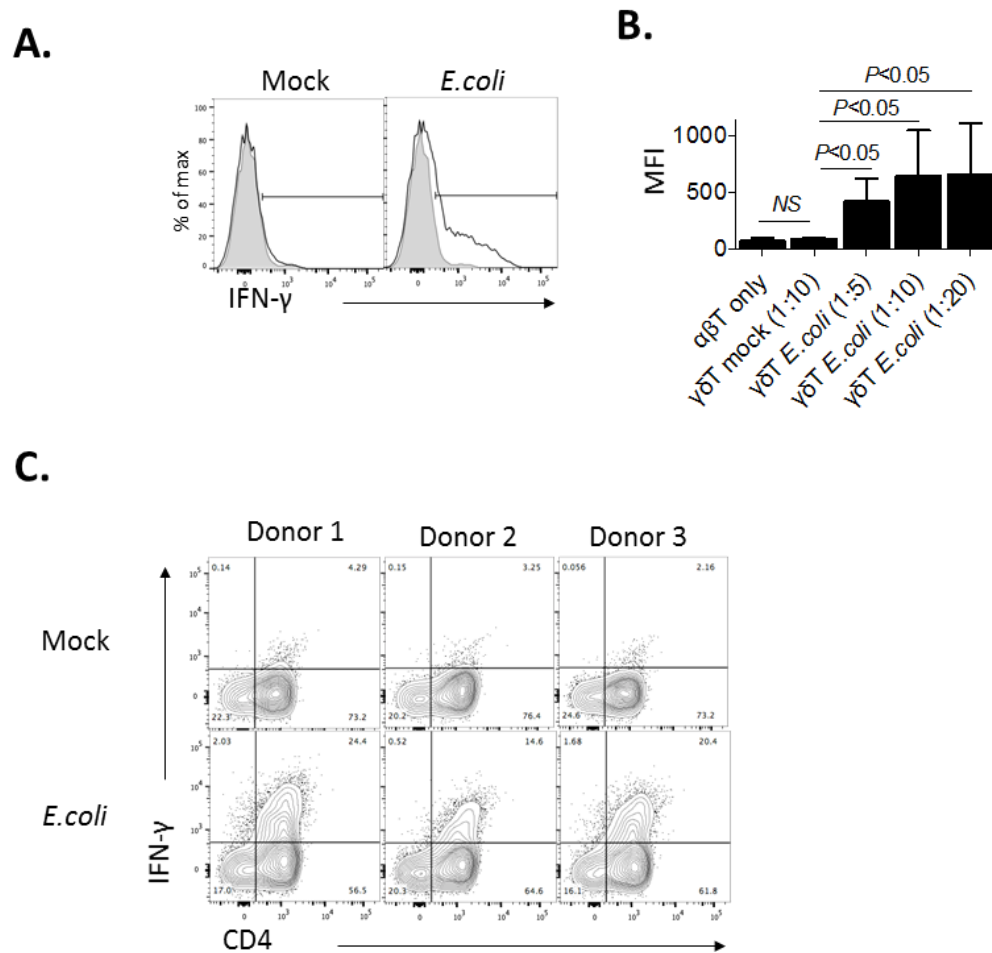
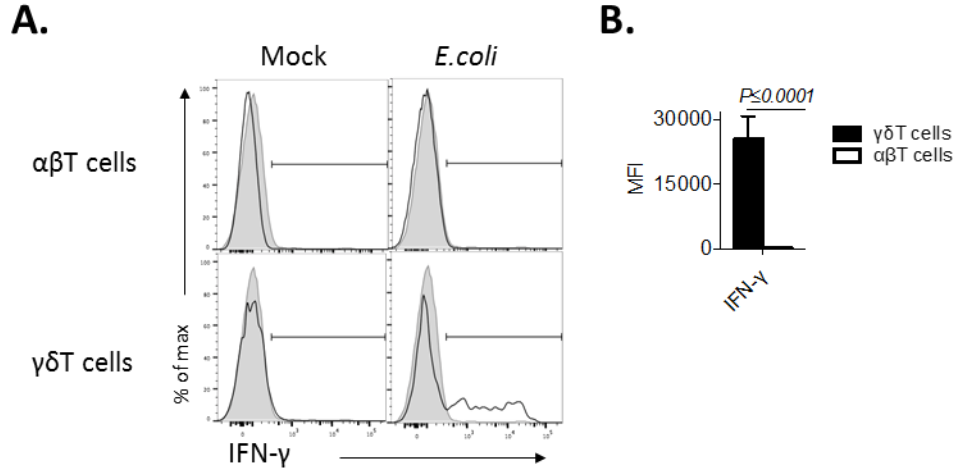


Fig. 5.3. Expanded $\gamma\delta T$ cells, co-cultured with opsonized *E. coli*, induce IFN- γ production in fresh autologous $\alpha\beta T$ cells. $\gamma\delta T$ cells were expanded for 14 days from freshly-isolated PBMC using zoledronate ($5\mu M$). On day 14, $\gamma\delta T$ cells were purified from expanded PBMC using FACS-sorting and rested overnight. Purified $\gamma\delta T$ cells were then incubated overnight with IgG-opsonized, irradiated *E. coli* at MOI 10 and washed thoroughly. In parallel, $\alpha\beta T$ cells were purified via positive magnetic selection from autologous, freshly-isolated PBMC and rested overnight. Purified, *E. coli*-stimulated, expanded $\gamma\delta T$ cells were then co-cultured for 2 days with purified, autologous fresh $\alpha\beta T$ cells. After 2 day co-culture, $\alpha\beta T$ cells were blocked with monensin, permeabilized and stained via FACS for intracellular IFN- γ . **(A)** Representative stains of one donor $\alpha\beta T$ cells is shown comparing co-culture with mock (media only)-stimulated or *E. coli*-stimulated expanded $\gamma\delta T$ cells at a $\gamma\delta T$: $\alpha\beta T$ ratio of 1:10 (anti-IFN- γ antibody in black, unshaded, and isotype-matched control - in gray, shaded). **(B)** Three donor $\alpha\beta T$ cell IFN- γ MFI were compiled and compared between $\alpha\beta T$ cells stimulated with i) media only ($\alpha\beta T$ only), ii) mock-stimulated $\gamma\delta T$ cells at a $\gamma\delta T$: $\alpha\beta T$ ratio of 1:10, iii) *E. coli*-stimulated $\gamma\delta T$ cells at a $\gamma\delta T$: $\alpha\beta T$ ratio of 1:5, iv) *E. coli*-stimulated $\gamma\delta T$ cells at a $\gamma\delta T$: $\alpha\beta T$ ratio of 1:10, v) *E. coli*-stimulated $\gamma\delta T$ cells at a $\gamma\delta T$: $\alpha\beta T$ ratio of 1:20. **(C)** Representative stains of three donor $\alpha\beta T$ cells is shown comparing co-culture with mock (media only)-stimulated or *E. coli*-stimulated expanded $\gamma\delta T$ cells. $\alpha\beta T$ cell IFN- γ production is set against expression of CD4. Bar graphs indicate the mean \pm standard deviation.

$\alpha\beta$ T cells within freshly-isolated, *E.coli*-stimulated whole PBMC did not produce IFN- γ (Fig.5.4). Freshly-isolated V δ 2 cells do not, thus, appear capable of professional antigen presentation to naïve $\alpha\beta$ T cells. Significant further experimental investigation is, however, necessary to draw this conclusion with certainty. The autologous stimulator-responder APC assay setup is experimentally convenient and interesting in some aspects, but is far from an all-encompassing experimental design. Of note, $\gamma\delta$ T cells within freshly-isolated, *E.coli*-stimulated whole PBMC, meanwhile, produced large amounts of IFN- γ (Fig.5.4).



*Fig. 5.4. $\alpha\beta$ T cells within whole, freshly-isolated, *E.coli*-stimulated PBMC do not produce IFN- γ . Freshly-isolated PBMC were stimulated overnight with *E.coli* or mock stimulated (media only). PBMC were then blocked with monensin, stained for cell surface markers, permeabilized and stained for intracellular IFN- γ . (A) Representative stains of intracellular IFN- γ levels from one donor are shown, comparing mock or *E.coli*-stimulated $\gamma\delta$ T cells and $\alpha\beta$ T cells (anti-IFN- γ antibody in black, unshaded, and isotype-matched control - in gray, shaded). (B) Five donor data were compiled, comparing IFN- γ production by $\gamma\delta$ T and $\alpha\beta$ T cells within overnight *E.coli*-stimulated, freshly-isolated PBMC. Bar graphs indicate the mean \pm standard deviation.*

5.3. $\gamma\delta$ T cell expansion leads to a loss of a Th1 inflammatory phenotype

Having documented the phagocytic and pAPC capacity of expanded $\gamma\delta$ T cells, I set out to further explore the *E.coli* response of freshly-isolated $\gamma\delta$ T cells. Freshly-isolated PBMC were co-cultured with irradiated *E.coli* at MOI 10. After overnight stimulation, responses within stimulated PBMC were characterised. *E.coli*, but not mock, stimulation resulted in significant $\gamma\delta$ T cell upregulation of CD69, production of IFN- γ and TNF- α , as well as CD107a-mediated cytotoxic degranulation in a manner that was highly consistent among all donors examined (Fig.5.5A). $\gamma\delta$ T cells presented with high baseline positivity for granulysin, which remained largely unchanged after stimulation. A mean ~50% of $\gamma\delta$ T cells within freshly-isolated PBMC responded to *E.coli* with the upregulation of CD69, production of IFN- γ and cytotoxic degranulation (Fig.5.5B). While $\alpha\beta$ T cells failed to upregulate CD69 or produce cytokines, a cytotoxic response could be observed, albeit at significantly lower levels than that of $\gamma\delta$ T cells (Fig.5.6).

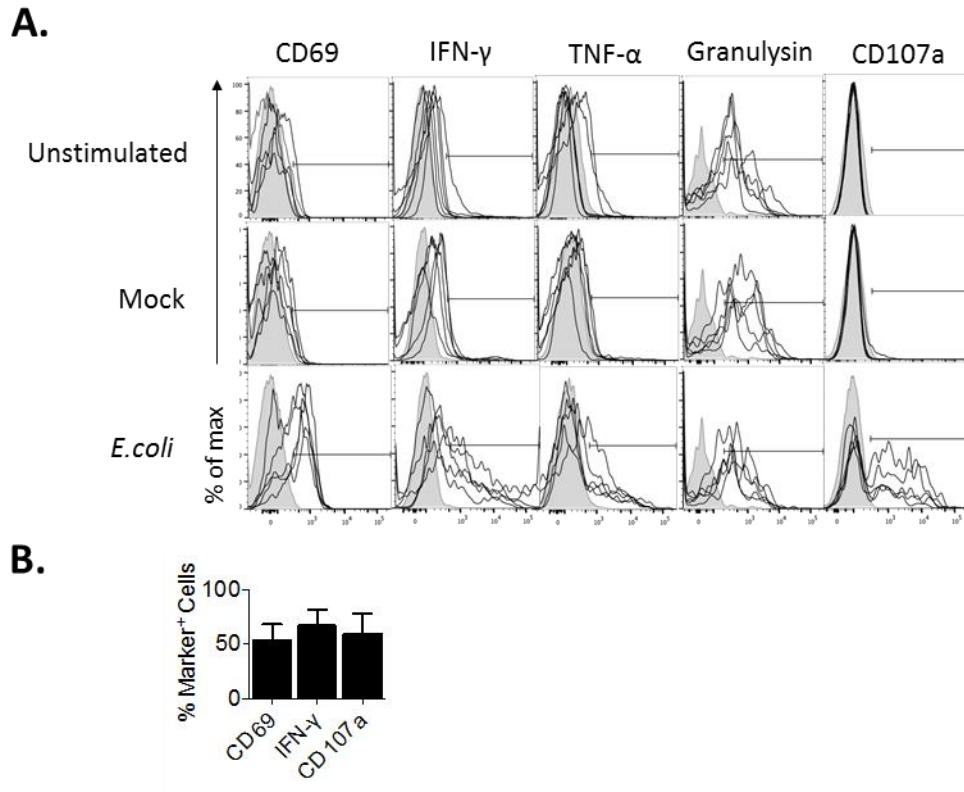


Fig. 5.5. Freshly-isolated PBMC stimulation with *E.coli* leads to potent $\gamma\delta$ T cell activation and effector responses. Freshly-isolated PBMC ($n=5$) were stimulated with irradiated *E.coli* at MOI 10 and analysed after overnight (16-18h) culture. **(A)** Shown are overlaid five donor sample stains of unstimulated, and overnight mock (IL-2 only) or *E.coli*-stimulated PBMC. The parameters examined were $\gamma\delta$ T cell surface CD69 and CD107a, as well as intracellular IFN- γ , TNF- α and granulysin (marker in black, unshaded; isotype control in gray, shaded). **(B)** The proportion of CD69^{pos}, IFN- γ ^{pos} and CD107a^{pos} cells was examined in $\gamma\delta$ T cells of overnight *E.coli*-stimulated PBMC.

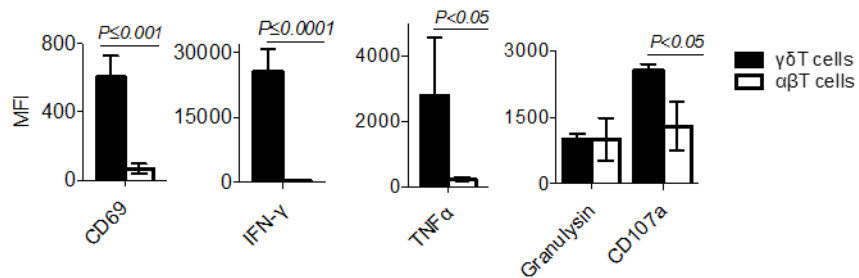


Fig. 5.6. Fresh PBMC stimulation with *E.coli* leads to $\gamma\delta$ T cell, but not $\alpha\beta$ T cell, effector responses. Freshly-isolated PBMC ($n=5$) were stimulated with irradiated *E.coli* at MOI 10 and analysed after overnight (16-18h) culture. The MFI of cell surface CD69, CD107a, as well as intracellular IFN- γ , TNF- α and granulysin were compared in $\gamma\delta$ T and $\alpha\beta$ T cells of overnight *E.coli*-stimulated PBMC. Bar graphs indicate the mean \pm standard deviation.

A majority of $\gamma\delta$ T cells were IFN- γ ^{pos}CD107a^{pos}; a significant fraction, nonetheless, exhibited a single-positive IFN- γ ^{pos} or CD107a^{pos} phenotype (Fig.5.7). These were later found to be V δ 2 and V δ 1 cells, respectively (Fig.5.7B). While V δ 2 and V δ 1^{neg}V δ 2^{neg} $\gamma\delta$ T cell populations were major cytokine producers, V δ 1 cells exhibited a significantly more potent cytotoxic response as measured by granulysin and CD107a expression. CD69 expression was markedly higher on V δ 2 cells compared to other $\gamma\delta$ T cell subsets. No IL-17 or IL-10 production by $\gamma\delta$ T cells could be detected via FACS, ELISA or MSD prior to or after expansion, as indicated in the previous chapter.

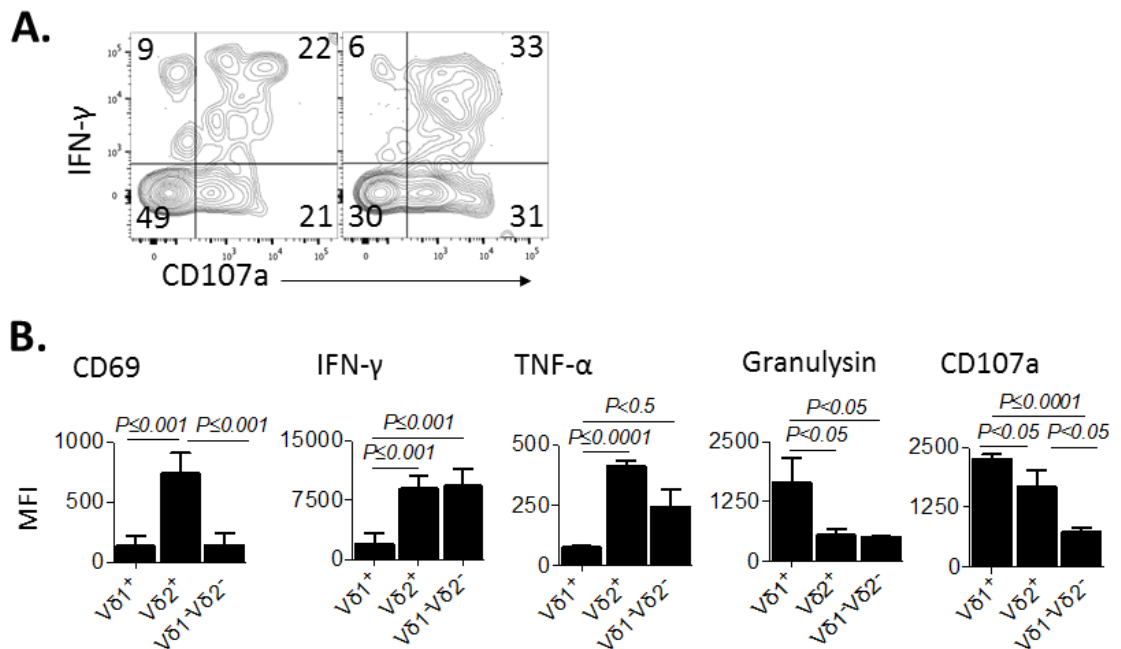


Fig. 5.7. Fresh PBMC stimulation with *E. coli* leads to predominantly V δ 2 cell activation and effector responses. Freshly-isolated PBMC (n=5) were stimulated with irradiated *E. coli* at MOI 10 and analysed after overnight (16-18h) culture. **(A)** Two representative donor stains are shown for *E. coli*-stimulated $\gamma\delta$ T cells, comparing cell surface CD107a and intracellular IFN- γ . **(B)** Cell surface CD69, CD107a, as well as intracellular IFN- γ , TNF- α and granulysin MFI were compared in V δ 1, V δ 2 and V δ 1^{neg}V δ 2^{neg} $\gamma\delta$ T cells. Bar graphs indicate the mean + standard deviation.

I next hypothesized that $\gamma\delta$ T cell expansion with *E.coli* may enhance the anti-*E.coli* response upon re-challenge. Unexpectedly, following expansion with *E. coli*, $\gamma\delta$ T cells exhibited a significantly decreased cytokine (IFN- γ , TNF- α) response to *E.coli*, and decreased CD69 expression compared to that observed in freshly isolated $\gamma\delta$ T cells (Fig.5.8A). *E.coli*-expanded $\gamma\delta$ T cells did, however, continue to exhibit CD107a-mediated cytotoxic degranulation and presence of granulysin, albeit at lower levels compared to freshly isolated $\gamma\delta$ T cells (Fig.5.8A, B). These observations may partially be attributed to the loss of the highly cytotoxic V δ 1 subset after expansion. Further surprising was the finding that $\gamma\delta$ T cell expansion with zoledronate resulted in a similar loss of cytokine production capacity post-expansion (Fig.5.9), ruling out the possibility that the loss of Th1 cytokine production was a specific result of exposure to *E.coli*.

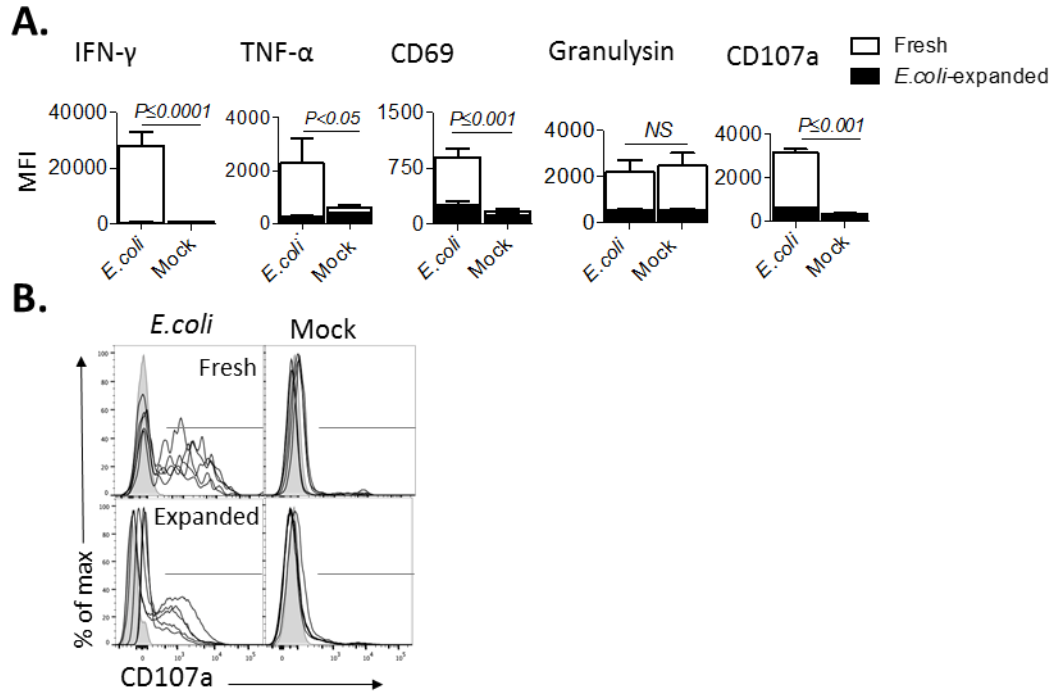


Fig. 5.8. Expanded $\gamma\delta T$ cells lose IFN- γ and TNF- α production capacity, but retain cytotoxicity, upon re-stimulation with *E.coli*. Freshly-isolated PBMC (n=5) were stimulated with *E.coli* and analyzed after overnight (16-18h) culture or left to expand for 14 days, and re-stimulated with *E.coli* or mock-stimulated (media only) overnight on day 14. $\gamma\delta T$ cell accumulation of intracellular IFN- γ , TNF- α , granulysin and cell surface CD69, as well as CD107a were assessed via FACS analysis. **(A)** $\gamma\delta T$ cell MFI in response to *E.coli* or mock stimulation were compared between freshly-isolated and 14 day *E.coli*-expanded $\gamma\delta T$ cells. **(B)** Shown are overlaid five donor sample stains of overnight mock or *E.coli*-stimulated $\gamma\delta T$ cell CD107a in fresh versus *E.coli*-expanded PBMC (marker in black, unshaded; isotype control in gray, shaded). Bar graphs indicate the mean \pm standard deviation.

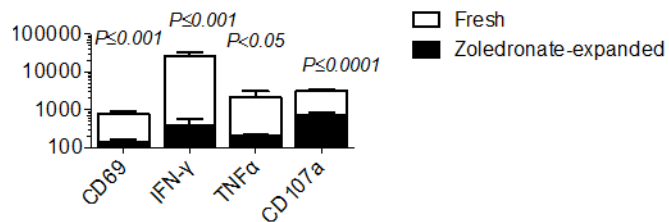


Fig. 5.9. $\gamma\delta T$ cell loss of early Th1 and reduction of cytotoxic phenotype occurs in response to expansion with zoledronate. Freshly-isolated PBMC (n=3) were stimulated with zoledronate, left to expand for 14 days, and re-stimulated with *E.coli* overnight on day 14. $\gamma\delta T$ cell intracellular IFN- γ , TNF- α and cell surface CD69 as well as CD107a were assessed via FACS analysis. Parameter MFI in response to *E.coli* stimulation were compared between freshly-isolated and 14 day zoledronate-expanded $\gamma\delta T$ cells. Bar graphs indicate the mean \pm standard deviation.

The decrease in cytokine production by *E.coli*-expanded compared to freshly-isolated $\gamma\delta$ T cells was not associated with a shift in memory phenotype or exhaustion marker expression (Fig.5.10A-C).

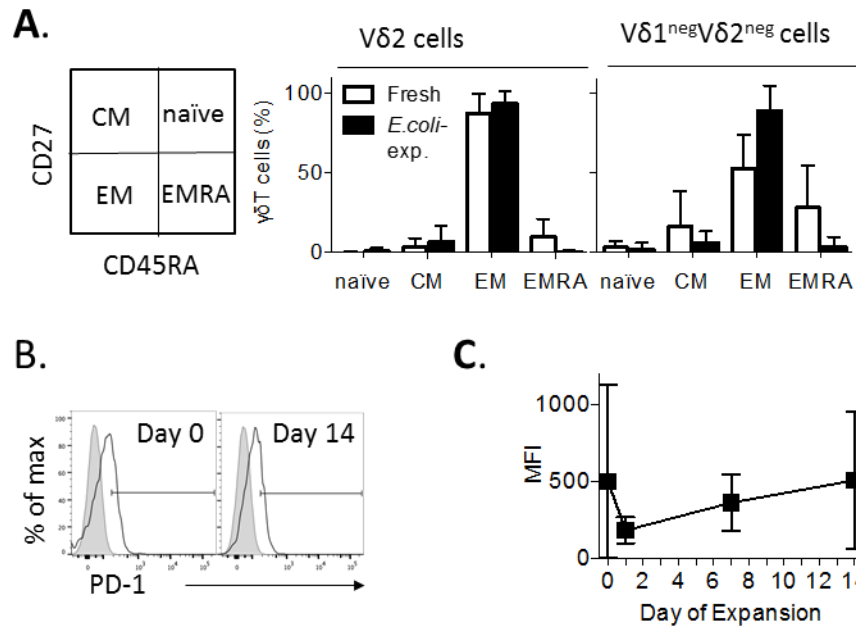


Fig. 5.10. Expansion in response to PBMC stimulation with *E.coli* does not lead to a significant change in $\gamma\delta$ T cell memory phenotype or PD1 expression. (A) $\gamma\delta$ T cell memory phenotype, as determined by cell surface expression of CD27 and CD45RA, was compared between fresh and *E.coli*-expanded V δ 2 and V δ 1^{neg}V δ 2^{neg} $\gamma\delta$ T cells (n=7). (B) Representative donor stains are shown comparing PD-1 expression on fresh (D0) and expanded (D14) $\gamma\delta$ T cells with PD-1 in black, unshaded, overlaid with isotype control in gray, shaded. (C) Cell surface PD-1 MFI on $\gamma\delta$ T cell surface was tracked throughout PBMC expansion with *E.coli* (n=7).

In order to establish whether the failure of *E.coli* re-stimulation to induce Th1-type cytokine production in expanded $\gamma\delta$ T cells is due to a lack of non-T cell ‘helper’ cells, I set up an autologous expanded + freshly-isolated PBMC culture system (described in the materials and methods chapter). Briefly, *E.coli*-expanded $\gamma\delta$ T cells were mixed with autologous, freshly-isolated PBMC at a $\gamma\delta$ T cell:PBMC ratio of 1:10 prior to the addition of *E.coli*. Therefore, if $\gamma\delta$ T cell production of IFN- γ requires, for example, the presence of freshly-isolated monocytes, the presence of such ‘helper’ cells would be provided by autologous PBMC. This addition of autologous PBMC did not rescue the lost expanded $\gamma\delta$ T cell Th1-like phenotype (Fig.5.11). I, thus, concluded that the altered cytokine profile of expanded *versus* freshly isolated $\gamma\delta$ T cells represents a true phenotypic shift.

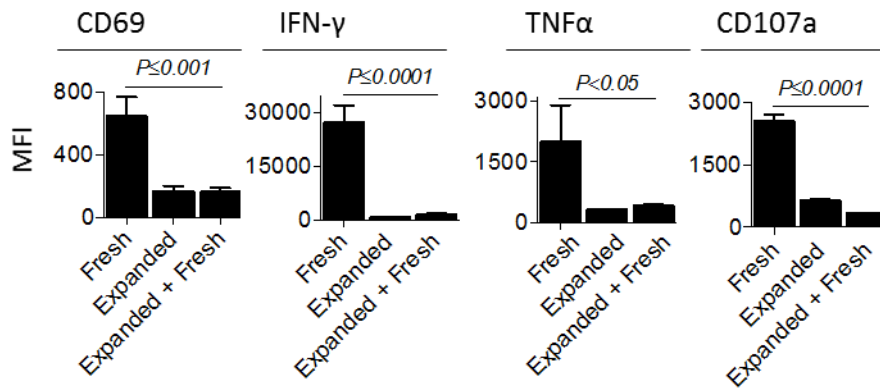
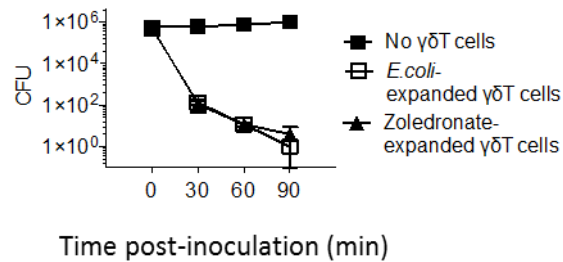


Fig. 5.11. $\gamma\delta$ T cell primary response effector phenotype is not rescued by the addition of fresh PBMC to expanded $\gamma\delta$ T cell culture. 14 day *E.coli*-expanded $\gamma\delta$ T cell culture (n=5) was stained for cell surface markers and supplemented with freshly-isolated, autologous, $\gamma\delta$ T cell-depleted PBMC at a ratio of 1:10 prior to overnight co-culture with *E.coli* at MOI 10. $\gamma\delta$ T cell responses were compared in terms of cell surface CD69, CD107a, as well as intracellular IFN- γ and TNF- α between i) freshly-isolated PBMC, ii) 14 day expanded PBMC, and iii) 14 day expanded PBMC supplemented with freshly-isolated PBMC.

Having established that expanded $\gamma\delta$ T cells do maintain some CD107a-mediated cytotoxic degranulation in response to *E.coli* re-stimulation, I evaluated direct expanded $\gamma\delta$ T cell cytotoxicity against *E.coli*. FACS-sorted *E.coli*-expanded $\gamma\delta$ T cells were exposed to live

bacteria for specified time intervals; cytotoxicity was inferred from residual colony numbers on agar plates. Remarkably, *E.coli* colony forming unit (CFU) count declined by >90% within 30 minutes (Fig.5.12). The high efficiency of bactericidal activity was observed upon use of either *E.coli* or zoledronate-expanded $\gamma\delta$ T cells.



*Fig. 5.12. Expanded $\gamma\delta$ T cells kill *E.coli* rapidly and effectively.* Freshly-isolated PBMC (n=4) were stimulated with *E.coli* or zoledronate and left to expand for 14 days. $\gamma\delta$ T cells were then purified by twice-repeated positive magnetic selection and rested overnight. Rested $\gamma\delta$ T cells were co-cultured with live *E.coli* at MOI 10. At designated time points the co-culture was lysed in H_2O , and plated on agar for overnight growth; resulting *E.coli* CFU were counted.

5.4. Discussion

The data laid out in this chapter explores the pAPC capacity of expanded V δ 2 cells, and attempts to correlate it to more commonly-described $\gamma\delta$ T cell functions, such as Th1-type cytokine production and cytotoxicity. Findings included:

- i) Expanding V δ 2 cells display classic T cell morphological features in terms of clustering and a single, round, regularly sized nucleus.
- ii) Expanding V δ 2 cells also display morphological features characteristic of myeloid phagocytes, such as an irregular cell shape with numerous membrane protrusions, and probing behaviour via guided membrane ruffling and motility.
- iii) Expanded V δ 2 cells, co-cultured with IgG-opsonized *E.coli* (but not medium alone), induce IFN- γ production in naïve, autologous $\alpha\beta$ T cells.
- iv) *E.coli*-pulsed V δ 2 cell-induced IFN- γ production is specific for CD4 $\alpha\beta$ T cells.
- v) IFN- γ production by $\alpha\beta$ T cells is not seen when *E.coli* is added to whole freshly-isolated PBMC. This indicates that expanded (phagocytic, HLA-DR^{pos} CD86^{pos}) V δ 2 cells are necessary for the triggering of an $\alpha\beta$ T cells IFN- γ response.
- vi) Freshly-isolated PBMC stimulation with irradiated *E.coli* induces potent $\gamma\delta$ T cell Th1-like cytokine (IFN- γ and TNF- α) production that is consistent among all donors examined.
- vii) Freshly-isolated $\gamma\delta$ T cells within PBMC are highly positive for granulysin at baseline. While stimulation with *E.coli* induces potent CD107a-mediated cytotoxic degranulation, intracellular granulysin levels are not significantly altered.
- viii) These responses within PBMC are seen in freshly-isolated $\gamma\delta$ T cells, but not $\alpha\beta$ T cells.
- ix) $\gamma\delta$ T cell response to *E.coli* is subset-specific. V δ 2 cells are significantly more activated and are the predominant producers of Th1-type cytokines, while V δ 1 cells display the most potent cytotoxicity.

- x) The potent Th1-type, cytotoxic response to *E.coli* is seen in freshly-isolated $\gamma\delta$ T cells, but not expanded V δ 2 cells. This loss of phenotype does not appear to be due to exhaustion, memory phenotype shift, nor absence of myeloid ‘helper’ cells (*e.g.* monocytes) within expanded PBMC.
- xi) The loss of a Th1-type phenotype to *E.coli* challenge results from $\gamma\delta$ T cell expansion with *E.coli* as well as zoledronate.
- xii) An effector function that is preserved, albeit at lower level than when freshly-isolated, is V δ 2 cell CD107a-mediated cytotoxic degranulation.
- xiii) $\gamma\delta$ T cells expanded with *E.coli* and zoledronate display remarkably effective and rapid anti-*E.coli* bactericidal capacity.

Establishing that HLA-DR^{pos} CD86^{pos} phagocytic V δ 2 cells display myeloid-like morphology and probing behaviour, combined with the observation that *E.coli*-pulsed V δ 2 cells are capable of inducing IFN- γ production in naïve, autologous $\alpha\beta$ T cells in a CD4-dependent manner provides a strong case for the pAPC capacity of peripheral human $\gamma\delta$ T cells. I concede, however, that the antigen presentation assay described in this chapter is non-standard and far from exhaustive. While there are indeed published statistics on the frequency of *E.coli*-reactive $\alpha\beta$ T cell clones in the periphery, they are significantly lower than the proportion of IFN- γ ^{pos} CD4 $\alpha\beta$ T cells I observed in our antigen presentation assay (14-24% of all $\alpha\beta$ T cells). This casts doubt on the reliability of the findings described. I stipulate that the high proportion of activated $\alpha\beta$ T cells observed is likely a consequence of the purification method employed: $\alpha\beta$ T cells were isolated from PBMC using positive magnetic selection, a method known to cross-link the $\alpha\beta$ TCR. A longer ‘resting’ period sans stimulation (*e.g.* two days instead of one) may be necessary to fully mute this initial stimulus. Alternatively, other cell purification methods may be employed, such as FACS sorting for *e.g.* CD3^{pos} $\gamma\delta$ TCR^{neg} PBMC. It is interesting to note, however, that $\alpha\beta$ T cells co-cultured with non-pulsed V δ 2 cells failed to show any IFN- γ production. It is unclear as to why that is. It is conceivable that the high proportion of IFN- γ ^{pos} CD4 $\alpha\beta$ T cells post stimulation with *E.coli*-pulsed V δ 2 cells was the consequence of a necessary double stimulus from anti- $\alpha\beta$ TCR-coated magnetic beads, followed by TCR stimulation via HLA-DR-presented *E.coli* antigen and co-stimulation from $\gamma\delta$ T cells. The data obtained

in these experiments further requires a significant enlargement of the panel of target antigens used. *E.coli* on its own is insufficient as a model to test the pAPC capacity of $\gamma\delta$ T cells. The use of whole bacteria complicates the investigation in a number of manners, including the possibility that the observed $\alpha\beta$ T cell activation is due, in some part, to triggering of TLRs or other PRRs by *E.coli* that have been carried over from the $\gamma\delta$ T cell pulsing co-culture. Such issues may be overcome by the use of protein targets that still require pAPC processing for presentation on MHC class II, as was the case with previous work in my laboratory by Himoudi *et al.* (49). A peptide target stimulus does, however, require $\alpha\beta$ T cell responder cells with a known TCR specificity and, therefore, transduction or the use of a cell line. Microfluidic platforms for the examination of single cell pair Ca^{2+} flux as the result of TCR triggering (as described by Dura, *et al.* (204)) would doubtless provide fascinating insight into V δ 2 cell activation of naïve $\alpha\beta$ T cells. A further matter to be considered in a protein-stimulus experimental setup is the necessity for IgG opsonisation.

Perhaps, most striking of all the findings is the total loss of freshly-isolated V δ 2 cell Th1-type cytokine production during expansion, concurrent with the acquisition of a phagocytic HLA-DR^{pos} CD86^{pos} phenotype. This observation, in combination with IgG-opsonisation as a pre-requisite of phagocytosis (and other pAPC functions), suggests careful regulation of V δ 2 T cell effector function. It is tempting to speculate that, whenever an early immune response is sufficient to neutralize infection, V δ 2 cells are prevented from posing an unnecessary inflammatory threat by amplifying responses further through downregulation of their early cytokine responsiveness. Noteworthy was the finding that, despite the loss of Th1-type cytokine production, V δ 2 cells retained highly efficient bactericidal capacity. It is unusual to consider that T cells are capable of such potent and direct bacterial killing. While significant further study is warranted to establish the exact mechanisms, the data presented in this chapter highlights the plethora of information yet to be learned. V δ 2 cell CD107a-mediated degranulation was decreased with expansion, but not entirely. It is conceivable that the residual CD107a-mediated degranulation was sufficient to kill *E.coli* in culture. It is also possible that the bactericidal functions of expanded V δ 2 cells are not limited to CD107a-mediated cytotoxicity. Mass

spectrometry of *E.coli*-stimulated V δ 2 cell supernatants would provide fascinating insight into the efficient killing of bacteria observed.

$\gamma\delta$ T cell direct killing of cellular and/or microbial targets combined with inflammatory cytokine production followed by uptake of the target into acidifying antigen processing compartments raises a novel paradigm. It is tantalizing to hypothesize that the combination of innate-like recognition and killing followed by myeloid cell-like phagocytosis by a lymphocyte-like cell may evolutionarily have preceded the full development of T lymphocyte-mediated adaptive immunity. Such a hypothesis is supported by previous studies showing that $\gamma\delta$ TCR chain genes may have preceded the development of $\alpha\beta$ TCR chain genes (205). In addition, the existence in jawless fish of three lymphocyte-like cells expressing variable lymphocyte receptors instead of TCR or BCR chain genes also supports this contention, as they otherwise resemble $\gamma\delta$ T, $\alpha\beta$ T and B cells by the expression of other orthologous genes (206).

5.5. Summary

Data examined in this chapter revealed that V δ 2 cell acquisition of a pAPC phenotype during expansion with *E.coli* or zoledronate is accompanied by a loss of a Th1-type pro-inflammatory phenotype, whilst maintaining potent cytotoxicity.

6. V δ 2 $\gamma\delta$ T CELL EFFECTOR FUNCTION DEPENDENCE ON THE TCR

6.1. Aims

Having documented the evolution of peripheral $\gamma\delta$ T cell effector function in response to stimulation by both, *E.coli* and zoledronate, I ventured to explore a mechanistic basis for this transition. The data presented in this chapter addresses the above-described range of effector functions in the context of the $\gamma\delta$ TCR. Blocking with monoclonal antibody was employed to determine $\gamma\delta$ T cell functional dependence on the TCR.

6.2. Phagocytosis by expanded $\gamma\delta$ T cells is TCR-dependent

As described in Chapter III, *E.coli* and zoledronate-expanded $\gamma\delta$ T cells phagocytosed opsonized bacteria with similar dynamics – with a similar level of uptake of beads, and uptake as well as acidification of bacteria. Chapter V, meanwhile, described that *E.coli* and zoledronate-expanded $\gamma\delta$ T cells express highly homologous TCR repertoires. I, thus, hypothesized that both stimuli may lead to $\gamma\delta$ T cell engagement of effector functions in a similar manner in the context of the TCR. To examine the importance of the TCR in $\gamma\delta$ T cell phagocytosis, *E.coli* or zoledronate-expanded $\gamma\delta$ T cells were cultured with anti- $\gamma\delta$ TCR mAb (clone: B1), isotype-matched control mAb of known non-*E.coli* specificity (clone: MG1-45) or media alone, prior to co-culture. Both uptake and acidification of opsonized bacteria by *E.coli*-expanded $\gamma\delta$ T cells were highly sensitive to TCR inhibition (Fig.6.1). Zoledronate-expanded $\gamma\delta$ T cells too displayed TCR-dependence for both measures of phagocytosis, although the sensitivity to inhibition was less marked than that

seen with *E.coli*-expanded cells (Fig.6.1). It remains unclear as to whether this difference between the expansion conditions is a real one or caused by technical discrepancy, *e.g.* better viability of zoledronate- versus *E.coli*-expanded $\gamma\delta$ T cells. I note that all the phagocytosis data presented herein is only that of expanded PBMC culture, as I was unable to detect substantial, and therefore quantifiable, phagocytosis by freshly-isolated $\gamma\delta$ T cells. Measurements of expanded $\gamma\delta$ T cell TCR dependence for phagocytosis are, thus, largely relevant only to the predominant population within expanded $\gamma\delta$ T cells - V γ 9V δ 2 cells.

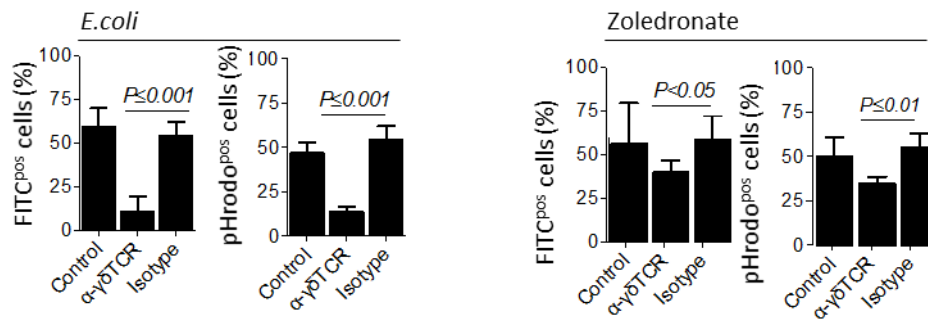


Fig. 6.1. *E.coli* and zoledronate-expanded $\gamma\delta$ T cells phagocytose *E.coli* in a TCR-dependent manner. Freshly-isolated PBMC (n=5) were expanded with UV-irradiated *E.coli* or zoledronate for 14 days, and examined for *E.coli* phagocytosis on day 14. To determine uptake, PBMC were incubated with IgG-opsonized *E.coli* for 60min. PBMC were pre-cultured with normal media (control), anti- $\gamma\delta$ TCR mAb (clone: B1) or isotype-matched control. The effect of pre-culture with anti- $\gamma\delta$ TCR mAb on phagocytosis was examined; data is shown for *E.coli*-expanded (left) or zoledronate-expanded (right) $\gamma\delta$ T cells, incubated with FITC-*E.coli* or pHrodo-*E.coli*. Bar graphs indicate the mean \pm standard deviation.

To further investigate the role of the TCR in V γ 9V δ 2 cell phagocytosis, expanded PBMC were incubated with IgG-opsonized green fluorescent beads for 60 minutes, and analyzed via Trypan Blue quenching and flow cytometry, with or without $\gamma\delta$ TCR blocking (Fig.6.2A). Uptake of opsonized beads by expanded $\gamma\delta$ T cells was significantly inhibited in the presence of anti- $\gamma\delta$ TCR mAb (Fig.6.2B). Bead adherence, as measured in non-quenched PBMC-bead co-culture, was not affected by blocking of the TCR.

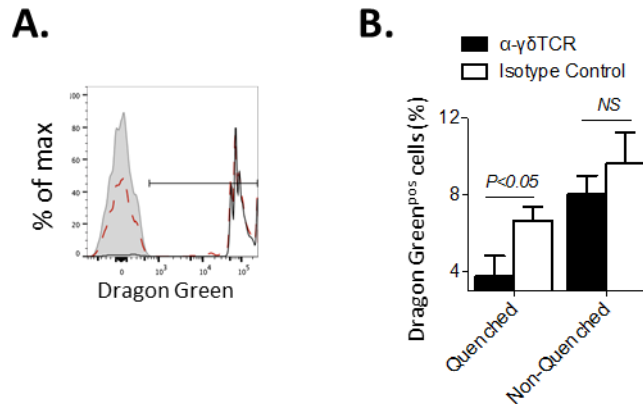
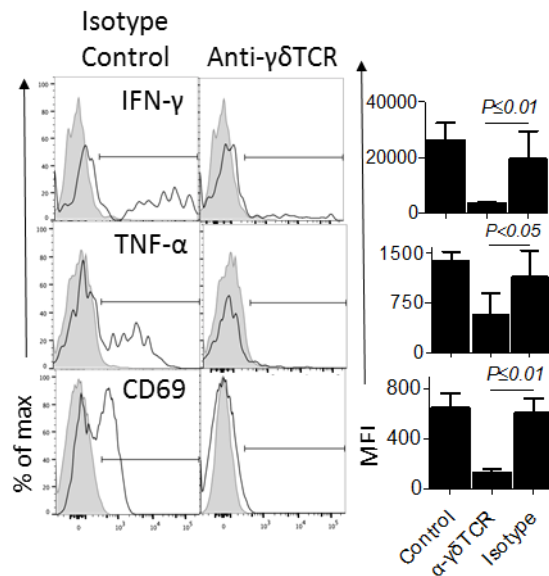


Fig. 6.2. Expanded $\gamma\delta$ T cells take up 1.0 μ m beads in a TCR-dependent manner. Freshly-isolated PBMC (n=5) were expanded with UV-irradiated *E.coli* for 14 days, and examined for uptake of fluorescent green beads on day 14. **(A)** PBMC were incubated with opsonized green fluorescent beads and quenched post-culture with Trypan Blue. Shown are representative stains, gated on $\gamma\delta$ T cells: i) non-quenched co-culture indicating total bead fluorescence (black, solid, unshaded), ii) quenched co-culture indicating intracellular bead fluorescence (red, dotted, unshaded), iii) cells alone (gray, shaded). **(B)** The effect of anti- $\gamma\delta$ TCR mAb was examined on $\gamma\delta$ T cell uptake of opsonized beads in quenched and non-quenched samples (n=3). Bar graphs indicate the mean \pm standard deviation.

6.3. $\gamma\delta$ T cell cytokine production and proliferation in response to *E.coli* are TCR-dependent, whereas TCR dependence of cytotoxicity appears only partial

To assess the TCR dependence of freshly-isolated $\gamma\delta$ T cell cytokine and cytotoxic effector function in response to stimulation with UV-irradiated *E.coli*, freshly-isolated PBMC were stimulated with UV-irradiated *E.coli* at MOI 10 and analyzed after overnight (16-18h) co-culture. Exposure to anti- $\gamma\delta$ TCR mAb prior to co-culture led to abrogation of CD69 upregulation and cytokine production (Fig.6.3)



*Fig. 6.3. Fresh $\gamma\delta$ T cell cytokine response to *E.coli* are TCR-dependent.* Prior to stimulation with *E.coli*, freshly-isolated PBMC (n=5) were cultured for 2h with blocking anti- $\gamma\delta$ TCR mAb or isotype-matched control. PBMC were then stimulated with *E.coli* and analyzed after overnight (16-18h) culture. $\gamma\delta$ T cell accumulation of intracellular IFN- γ , TNF- α and cell surface CD69 were assessed via FACS analysis after overnight stimulation of freshly-isolated PBMC. Shown left are representative stains from one donor (marker in black, unshaded; isotype control in gray, shaded); shown right are donor parameter compilation MFI. Bar graphs indicate the mean \pm standard deviation.

Pre-culture with anti- $\gamma\delta$ TCR mAb further lead to a decrease in the double positive IFN- γ^{pos} CD107a pos but not in single positive CD107a pos $\gamma\delta$ T cell populations (Fig.6.4). The decrease in IFN- γ^{pos} CD107a pos $\gamma\delta$ T cells was subset specific, as only V δ 2 but not V δ 1 $\gamma\delta$ T cell cytotoxic degranulation was sensitive to a pre-blocked TCR (Fig.6.5).

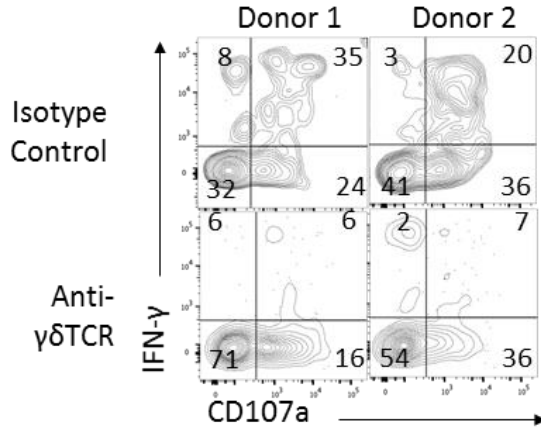


Fig. 6.4. IFN- γ^{pos} CD107a pos and IFN- γ^{neg} CD107a pos $\gamma\delta$ T cells display different sensitivity to TCR inhibition. Prior to stimulation with *E.coli*, freshly-isolated PBMC (n=5) were cultured for 2h with blocking anti- $\gamma\delta$ TCR mAb or isotype-matched control. PBMC were then stimulated with *E.coli* and analyzed after overnight (16-18h). Two representative donor samples, gated on $\gamma\delta$ T cells, are shown correlating intracellular IFN- γ and cell surface CD107a post overnight *E.coli* stimulation of PBMC.

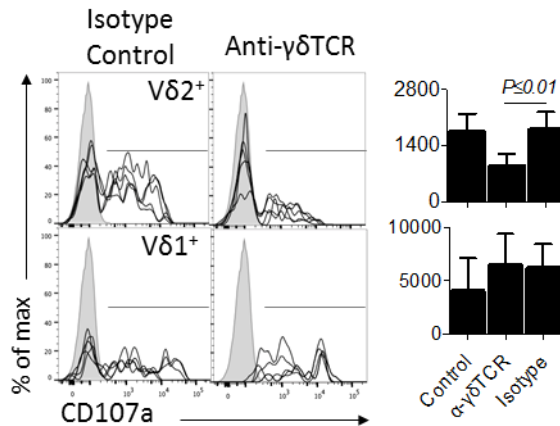
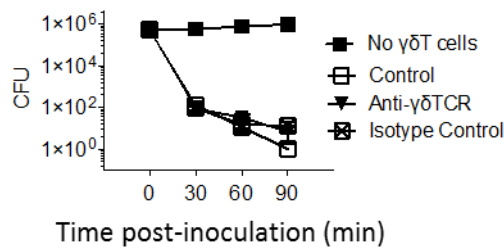
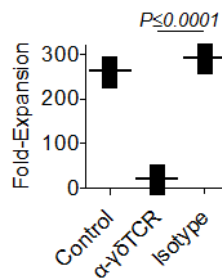


Fig. 6.5. V δ 2 cell, but not V δ 1 cell, CD107a-mediated degranulation is partially TCR-dependent. Prior to stimulation with *E.coli*, freshly-isolated PBMC (n=5) were cultured for 2h with blocking anti- $\gamma\delta$ TCR mAb or isotype-matched control. PBMC were then stimulated with *E.coli* and analyzed after overnight (16-18h) culture. The effect of anti- $\gamma\delta$ TCR mAb on fresh $\gamma\delta$ T cell surface CD107a post-PBMC *E.coli* stimulation is shown for five representative donors, comparing V δ 1 and V δ 2 cells. Bar graphs indicate the mean \pm standard deviation.

To evaluate the impact of TCR blocking on direct $\gamma\delta$ T cell cytotoxicity against *E.coli*, FACS-sorted *E.coli*-expanded $\gamma\delta$ T cells (predominantly with a V δ 2 TCR) were pre-treated with blocking anti- $\gamma\delta$ TCR mAb and exposed to live bacteria; cytotoxicity was inferred from residual colony numbers on agar plates. As described in the previous chapter, *E.coli* colony forming unit (CFU) count declined by >90% within 30 minutes of exposure to purified $\gamma\delta$ T cells. Interestingly, this effect was not dependent upon $\gamma\delta$ TCR engagement (Fig.6.6). Although $\gamma\delta$ TCR blocking showed no significant impact on bactericidal function, it completely blocked $\gamma\delta$ T cell proliferation in response to *E.coli* (Fig.6.7).



*Fig. 6.6. Expanded $\gamma\delta$ T cell killing of live *E.coli* is not significantly TCR-dependent.* Freshly-isolated PBMC (n=4) were stimulated with *E.coli* and left to expand for 14 days. $\gamma\delta$ T cells were then purified by twice-repeated positive magnetic selection and rested overnight. Prior to stimulation with live *E.coli*, $\gamma\delta$ T cells were cultured for 2h with blocking anti- $\gamma\delta$ TCR mAb or isotype-matched control. $\gamma\delta$ T cells were then co-cultured with live *E.coli* at MOI 10. At designated time points the co-culture was lysed in H₂O, and plated on agar for overnight growth; resulting *E.coli* CFU were counted.



*Fig. 6.7. $\gamma\delta$ T cell proliferation in response to *E.coli* is TCR-dependent.* Prior to stimulation with *E.coli*, freshly-isolated PBMC (n=5) were cultured for 2h with blocking anti- $\gamma\delta$ TCR mAb or isotype-matched control. PBMC were then stimulated with *E.coli* and left to expand for 14 days. Proliferation in response to *E.coli* stimulation was assessed.

6.4. Discussion

Data presented in this chapter documents freshly-isolated and expanded $\gamma\delta$ T cell effector function dependency on the TCR. Findings included:

- i) *E.coli* and zoledronate-expanded $\gamma\delta$ T cells take up and acidify IgG-opsonized *E.coli* in a TCR-dependent manner.
- ii) *E.coli*-expanded $\gamma\delta$ T cells take up IgG-opsonized 1.0 μ m beads in a TCR-dependent manner.
- iii) Freshly-isolated $\gamma\delta$ T cell activation (as measured by CD69 upregulation), IFN- γ and TNF- α production in response to *E.coli* is TCR-dependent.
- iv) Freshly-isolated $\gamma\delta$ T cell CD107a-mediated cytotoxic degranulation is partially TCR-dependent for V δ 2 cells, but not V δ 1 cells.
- v) The decrease in viable *E.coli* CFU number after exposure to expanded $\gamma\delta$ T cells was not affected by $\gamma\delta$ T cell pre-culture with anti-TCR mAb.

Prior to engaging in discussions of the physiological implications of the TCR blocking data presented in this chapter, I note that all data herein presented hinges on the use of a particular anti- $\gamma\delta$ TCR mAb, clone B1. There exists some literature on the use of this antibody for the effective blocking of human $\gamma\delta$ T cell effector function, particularly in the context of recognizing tumour (and virus)-associated antigens (207). As in the present thesis, data indicated that anti- $\gamma\delta$ TCR mAb, clone B1, inhibited V δ 2 IFN- γ production. Other $\gamma\delta$ T cell subsets remained unexamined. The question arises, therefore, whether the B1 antibody can be used as a credible, broad blocker of all $\gamma\delta$ TCRs. There are several ways of assessing this question. Firstly, is fluorescent staining with the B1 mAb inclusive of non-V δ 2 cells? Indeed, a number of commercial suppliers provide pan anti- $\gamma\delta$ TCR B1 mAb; numerous peer-reviewed publications cite the use of this antibody clone for fluorescent pan- $\gamma\delta$ T cell staining (49,208–210). Moreover, published protocols describe the use of anti- $\gamma\delta$ TCR B1 mAb for the non-biased expansion of V δ 1, V δ 2 and non-V δ 1/V δ 2 $\gamma\delta$ T cells (211), or the induction of proliferation and IFN- γ of non-V γ 9V δ 2 $\gamma\delta$ T cells (212). Crucially, the difference between using the anti- $\gamma\delta$ TCR B1 mAb as a pan-

stimulator or pan-blocker of peripheral human $\gamma\delta$ T cells appears to lie in the way that the antibody is presented to the cells. Free-floating, monomeric IgG exerts a blocking effect, whereas IgG conjugated to beads or the well of a culture well-plate – a stimulatory one, as resultant from antibody binding to single TCRs or cross-linking multiple TCRs on the same cell, respectively.

Having established the existence of a substantive body of peer-reviewed literature that cites the use of anti- $\gamma\delta$ TCR B1 mAb, it was fascinating to note that pre-incubation with this antibody substantially decreased *E.coli* as well as zoledronate-expanded $\gamma\delta$ T cell phagocytosis of opsonized *E.coli*. Previous chapters present my finding that expansion with either stimulus leads to highly homologous V γ 9V δ 2 TCR repertoires. Knowing that zoledronate activates V γ 9V δ 2 cells via accumulation of endogenous IPP, this observation, thus, alludes strongly to a scenario where *E.coli* is not being engaged by the $\gamma\delta$ TCR directly. It suggests instead that *E.coli* too is inducing accumulation of endogenous pyrophosphates, which is what then drives $\gamma\delta$ T cell effector function and proliferation – possibly via inducing conformational changes in BTN3A molecules, as laid out in previous chapters. If it is indeed stressed self that is engaged upon $\gamma\delta$ T cell exposure to *E.coli* and not *E.coli* directly, TCR dependence of *E.coli* phagocytosis suggests a ‘licensing’-type reaction occurring. I stipulate that 14 day expanded PBMC exposure to *E.coli* – via HMBPP release, endogenous IPP stimulation or otherwise – induces markers of cell stress. It is conceivable, even, that expanded $\gamma\delta$ T cells are recognizing these stress markers on each other, given that they constitute the vast majority of live cells remaining in culture. A signal of self-stress may then ‘license’ HLA-DR^{pos} CD86^{pos} $\gamma\delta$ T cell phagocytic effector function, which is further regulated by the necessity for target opsonisation with IgG.

To test whether phagocytosis of IgG opsonized targets is dependent on TCR engagement, I examined whether expanded $\gamma\delta$ T cell uptake of opsonized 1.0 μ m beads is affected by pre-culture with anti- $\gamma\delta$ TCR B1 mAb. It is conceivable, for example, that TCR blocking impedes *E.coli* adherence to $\gamma\delta$ T cells, but not phagocytosis directly. Upon examination of IgG-coated beads I found, however, that bead adherence to expanded $\gamma\delta$ T cells was not significantly affected, while phagocytosis was. As discussed in Chapter III, I maintain that

further investigation and experimental approaches are necessary to establish the fine details of $\gamma\delta$ T cell phagocytosis. For example, are receptors other than those for IgG opsonin or (possibly) BTN3A involved? Are $\gamma\delta$ T cell TLRs triggered by exposure to *E.coli* and do these interactions modulate the effector function observed? The observation, however, that *E.coli* and zoledronate-expanded $\gamma\delta$ T cell phagocytosis of IgG-opsonized beads or *E.coli* is inhibited by pre-incubation with anti- $\gamma\delta$ TCR B1 mAb lead us to postulate that expanded HLA-DR^{pos} CD86^{pos} V γ 9V δ 2 cell phagocytosis requires an interactive ‘licensing’-type event between the $\gamma\delta$ TCR and Fc γ R. It remains unclear whether the interaction between $\gamma\delta$ TCR and Fc γ R is direct or indirect.

E.coli exposure led to potent TCR-dependent freshly-isolated $\gamma\delta$ T cell IFN- γ and TNF- α production, proliferation as well as substantial cytotoxic degranulation and bacterial killing. Interestingly, freshly-isolated V γ 9V δ 2 cell CD107a-mediated cytotoxicity was only partially TCR-dependent, while *E.coli* killing was entirely unaffected by pre-blocking of the $\gamma\delta$ TCR. The observation that expanded, purified V δ 2 cells exhibited high bactericidal activity despite decreased CD107a-mediated cytotoxic degranulation and blocking of the TCR, may be attributable to the high efficiency of $\gamma\delta$ T cell CD107a-mediated *E.coli* killing, whereupon low level degranulation is sufficient to significantly decrease bacterial viability, or may allude instead to CD107a-independent bactericidal mechanisms. These data suggest differential control for V γ 9V δ 2 cell Th1 responses, proliferation and pAPC function *versus* cytotoxicity. Such a difference is, perhaps, unsurprising in a physiological context. $\gamma\delta$ T cells reside largely at epithelial surfaces populated by billions of commensal and pathogenic microorganisms. Encountering non-self via non-TCR PRRs (*e.g.* TLRs) may trigger an immediate, cytotoxic response. Once the target is killed, however, decisions about further inflammatory processes or even the initiation or regulation of an adaptive immune response are tightly regulated by additional layers of control, involving *e.g.* $\gamma\delta$ TCR and Fc γ R. I note that freshly-isolated V δ 1 cell CD107-mediated cytotoxic degranulation appeared entirely $\gamma\delta$ TCR independent. As discussed in the chapter introduction, similar TCR dependence differences have been observed among mouse $\gamma\delta$ T cell subsets. Significant further experimental probing is necessary to determine the nature and reasons for this difference between human peripheral V δ 1 and V δ 2 $\gamma\delta$ T cells. It would be interesting to examine further whether

intestinal V δ 1 IELs display a similar TCR-independence to PBMC V δ 1 cells with regard to cytotoxicity.

To our knowledge, we are the first group to document direct bactericidal activity of human V γ 9V δ 2 cells. While I've also demonstrated simultaneous CD107a-mediated cytotoxic degranulation, it is unclear whether this is the mechanism by which the remarkably efficient killing took place. Significant further investigation of V γ 9V δ 2 cell direct bactericidal activity is necessary, spanning different microorganisms, strains, from Gram-positive to Gram-negative and intracellular bacteria, plasmodia, fungi, etc. It would be interesting to determine, for example, whether $\gamma\delta$ T cells can distinguish, in the context of bacterial killing, commensal *E.coli* from enteropathogenic *E.coli*. In terms of mechanisms of killing, reproducible mass spectrometry of *E.coli*-V γ 9V δ 2 cell co-culture supernatants would doubtless provide fascinating insight into what are likely multiple modes of bactericidal attack that V γ 9V δ 2 cells engage in.

TCR-engagement as a pre-requisite of V γ 9V δ 2 cell Th1 cytokine production, proliferation and pAPC function suggests careful regulation of the V γ 9V δ 2 T cell compartment. Whenever an early immune response is sufficient to neutralize infection, MHC class II^{pos}CD86^{pos} V γ 9V δ 2 cells expanded in response to encountering self-stress markers may be prevented from posing an unnecessary inflammatory threat by amplifying responses further. This then would be achieved by downregulation of their initial Th1 cytokine responsiveness, as well as imposing a necessity for TCR triggering by stressed-self to exert pAPC function. The requirement for opsonization of a target may be a further safety feature. This could be operative at two levels: i) as herein, when opsonizing with switched target-specific IgG, and ii) in a 'naïve' non-immune situation, where natural antibodies (NAb) of different isotype, including IgG, may be involved.

Further study of the engagement of the V γ 9V δ 2 TCR, possibly with BTN3A targets, is likely to carry significant implications for $\gamma\delta$ T cell anti-tumor immunity by supporting the notion that stress recognition, particularly in combination with Ab-opsonisation, may be sufficient not only for killing of a tumor cell but also for uptake, processing and presentation of tumor-associated antigens (49). Documenting the significance of the TCR

for the engagement of $\gamma\delta$ T cell pAPC function, I set out to determine in the next chapter what relationship this bears to endogenous BTN3A targets. Indeed, is the observed V γ 9V δ 2 cell TCR dependence linked intimately to recognition of self-stress, even upon exposure to such a target-rich stimulus as *E.coli*?

6.5. Summary

Data laid out in this chapter documents that Th1-type cytokine production, proliferation and phagocytic capacity of V γ 9V δ 2 cells is dependent on the TCR. CD107a-mediated cytotoxic degranulation displayed only partial TCR dependency, while V γ 9V δ 2 cell bactericidal activity was unaffected by blocking of the $\gamma\delta$ TCR.

7. V γ 9V δ 2 $\gamma\delta$ T CELL EFFECTOR FUNCTION DEPENDENCE ON BTN3A

7.1. Aims

Finding that freshly-isolated and expanded V δ 2 $\gamma\delta$ T cell activation, cytokine production and pAPC phenotype in response to stimulation with *E.coli* are TCR-dependent, the question arose of what the TCR may be recognizing. The following chapter explores whether the V γ 9V δ 2 TCR ligand in my model is indeed the BTN3A molecule. $\gamma\delta$ T cell responses in the presence or absence of TCR / BTN3A blocking were explored in the context of various ‘self’ and ‘non-self’ stimuli.

7.2. BTN3A is ubiquitously expressed on PBMC

In order to decipher the role of BTN3A (CD277) in $\gamma\delta$ T cell recognition of target cells, I first set out to determine the expression pattern of BTN3A in freshly-isolated and differentially expanded PBMC. FACS-staining revealed that nearly all live, freshly-isolated PBMC were positive for BTN3A, with expression levels largely equivalent among CD3^{pos} and CD3^{neg} cells (Fig.7.1A). Overnight stimulation with irradiated *E.coli* lead to a modest downregulation of BTN3A on all PBMC, although predominant positivity was maintained, with expression levels recovering during expansion. PBMC re-stimulation with *E.coli* on day 14 of the expansion resulted in a less marked downregulation of BTN3A.

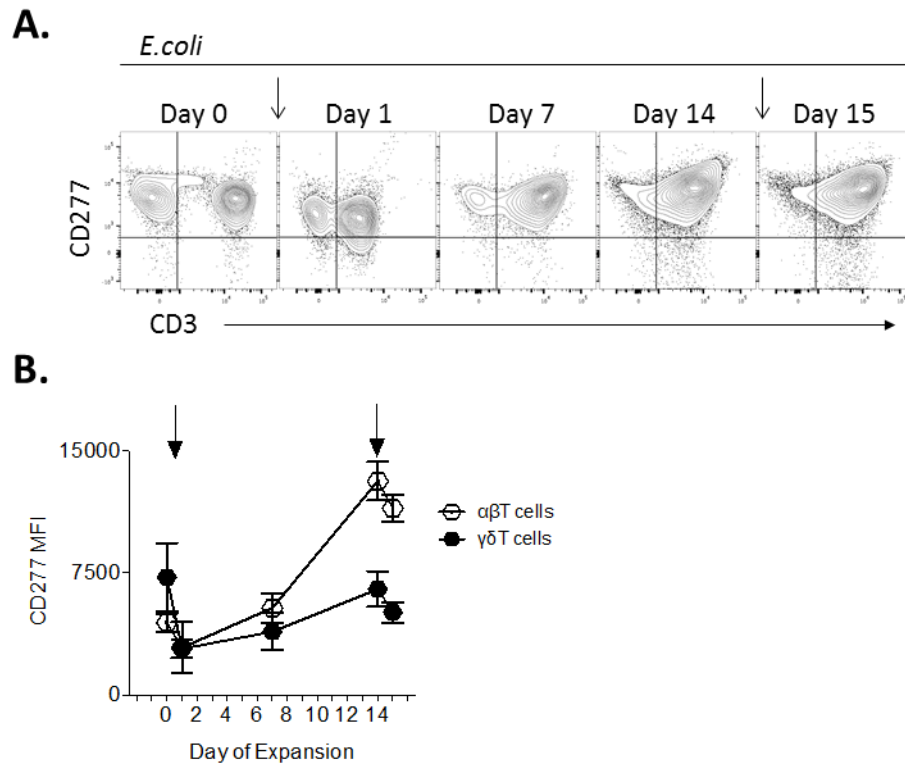
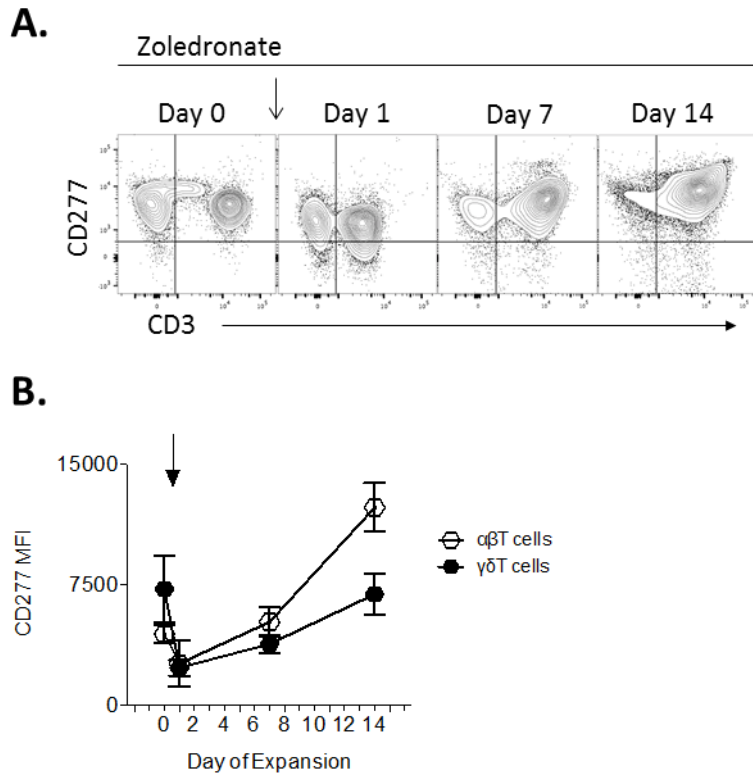


Fig. 7.1. PBMC express high levels of CD277 throughout expansion with E.coli. Freshly-isolated PBMC (n=5) were expanded with UV-irradiated *E.coli* for 14 days. Cell surface CD277 levels were monitored throughout. **(A)** Representative stains of one donor *E.coli*-stimulated PBMC is shown, comparing CD277 levels on CD3^{pos} and CD3^{neg} cells. Points of *E.coli* stimulation are indicated with black arrows. **(B)** Donor CD277 levels in response to *E.coli* were compiled and compared in $\gamma\delta$ T and $\alpha\beta$ T cells.

Interestingly, *E.coli* stimulation resulted in significantly higher BTN3A levels on $\alpha\beta$ T cells than $\gamma\delta$ T cells as the expansion progressed (Fig.7.1B). Similar results were obtained upon freshly-isolated PBMC stimulation with zoledronate (Fig.7.2.).



*Fig. 7.2. PBMC express high levels of CD277 throughout expansion with *E.coli* and zoledronate. Freshly-isolated PBMC (n=4) were expanded with zoledronate for 14 days. Cell surface CD277 levels were monitored throughout. (A) Representative stains of one donor zoledronate-stimulated PBMC is shown, comparing CD277 levels on CD3^{pos} and CD3^{neg} cells. Points of zoledronate stimulation are indicated with black arrows. (B) Donor CD277 levels in response to zoledronate were compiled and compared in $\gamma\delta$ T and $\alpha\beta$ T cells.*

7.3. $\gamma\delta$ T cells are activated by autologous pAg-stimulated PBMC

To determine the role of BTN3A in $\gamma\delta$ T cell antigen recognition, an autologous stimulation experimental system was set up (illustrated in the materials and methods section). Briefly, $\gamma\delta$ T cells were stimulated with autologous PBMC, which in turn had previously been co-cultured overnight with various pAg-inducing and/or –containing stimuli, e.g. zoledronate and irradiated *E.coli*. To test whether such a system may be a viable experimental probe for $\gamma\delta$ T cell activation, $\gamma\delta$ T ‘responder’ cells were stained for various activation markers after overnight co-culture with differentially-stimulated ‘stimulator’ PBMC.

Indeed, overnight co-culture resulted in responder $\gamma\delta$ T cell upregulation of CD69 in response to *E.coli*- and zoledronate- but not mock (medium only)-exposed stimulator PBMC (Fig.7.3).

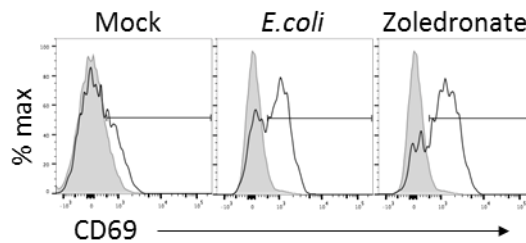
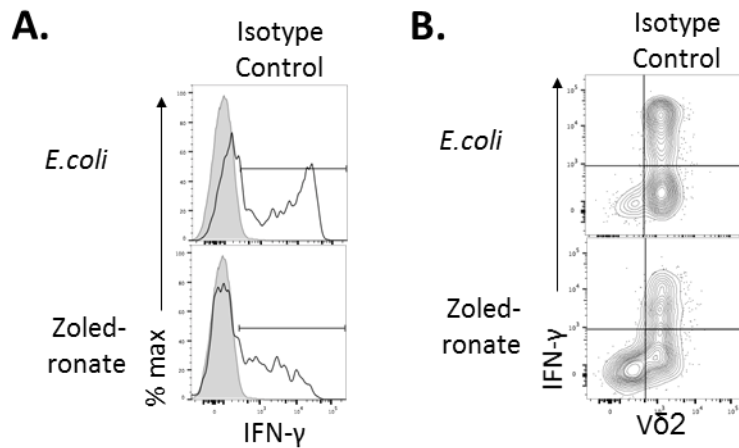


Fig. 7.3. $\gamma\delta$ T cells are activated by autologous zoledronate or E.coli-stimulated PBMC. Freshly-isolated PBMC were co-cultured overnight with autologous, freshly-isolated, $\gamma\delta$ T cell-depleted and overnight *E.coli* or zoledronate-stimulated PBMC. $\gamma\delta$ T cell upregulation of cell surface CD69 in response to differentially-stimulated, autologous PBMC was recorded. PBMC were analyzed via FACS. $\gamma\delta$ T cell surface CD69 was compared post-PBMC O/N co-culture with mock-, *E.coli*- or zoledronate-exposed stimulator cells. Shown are representative stains from one donor (marker in black, unshaded; isotype control in gray, shaded).

A potent IFN- γ response was observed after responder $\gamma\delta$ T cell stimulation with both, *E.coli* and zoledronate-exposed, stimulator cells (Fig.7.4A). As seen with direct PBMC stimulation with *E.coli* or zoledronate (discussed in Chapter V), the IFN- γ response was V δ 2 cell specific (Fig.7.4B).



*Fig. 7.4. V δ 2 $\gamma\delta$ T cells produce IFN- γ in response to autologous *E.coli* or zoledronate-stimulated PBMC. Freshly-isolated PBMC (n=4) were co-cultured overnight with autologous, freshly-isolated, $\gamma\delta$ T cell-depleted and overnight *E.coli* or zoledronate-stimulated PBMC. $\gamma\delta$ T cell responses to differentially-stimulated, autologous PBMC were recorded. PBMC were analyzed via FACS; representative single donor stains are shown (marker in black, unshaded; staining isotype control in gray, shaded). (A) $\gamma\delta$ T cell intracellular IFN- γ was compared post-PBMC O/N co-culture with *E.coli*- or zoledronate-stimulated targets. (B) Intracellular IFN- γ was correlated to $\gamma\delta$ T cell expression of the V δ 2 TCR chain.*

$\gamma\delta$ T cell stimulation with stimulator PBMC further elicited potent CD107a-mediated cytotoxic degranulation. Strikingly, the level of cytotoxicity elicited by direct $\gamma\delta$ T cell stimulation with *E.coli* within whole PBMC was statistically indistinguishable from that elicited by $\gamma\delta$ T cell stimulation with *E.coli*-exposed autologous stimulator PBMC (Fig.7.5).

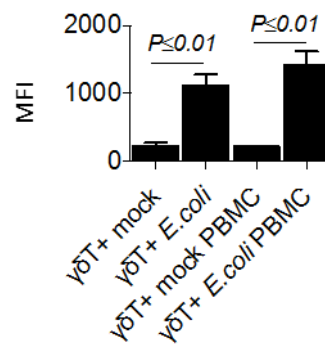


Fig. 7.5. $\gamma\delta$ T cells display equivalent CD107a-mediated cytotoxic degranulation in response to direct *E.coli* stimulation or stimulation with *E.coli*-exposed stimulator PBMC. *E.coli*-expanded PBMC (n=3) were co-cultured overnight with UV-irradiated *E.coli* at MOI 10 or autologous, $\gamma\delta$ T cell-depleted and overnight *E.coli*-stimulated PBMC, or mock-stimulated (media only). Cell surface CD107a was compared between the various stimulated groups. Donor MFI were compiled and compared.

7.4. V γ 9V δ 2 cell effector responses to autologous stimulator PBMC are differentially sensitive to blocking of the $\gamma\delta$ TCR and BTN3A

Having established that $\gamma\delta$ T cells are indeed responsive to differentially stimulated autologous PBMC, I proceeded to examine the sensitivity of this responsiveness to blocking of BTN3A on stimulator PBMC and blocking of the $\gamma\delta$ TCR on responder $\gamma\delta$ T cells (as illustrated in the materials and methods section). Given that BTN3A dependency has been ascribed to V γ 9V δ 2 cells specifically, I first examined V γ 9 chain expression within freshly-isolated peripheral V δ 2 cells. In all donors examined, all freshly isolated V δ 2 also expressed a V γ 9 TCR chain (Fig.7.6).

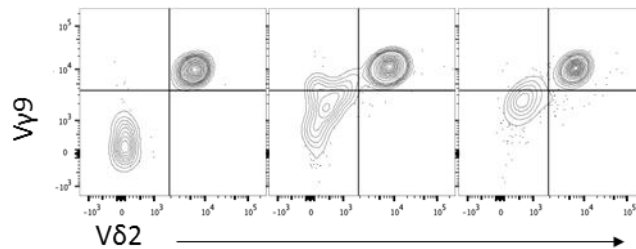
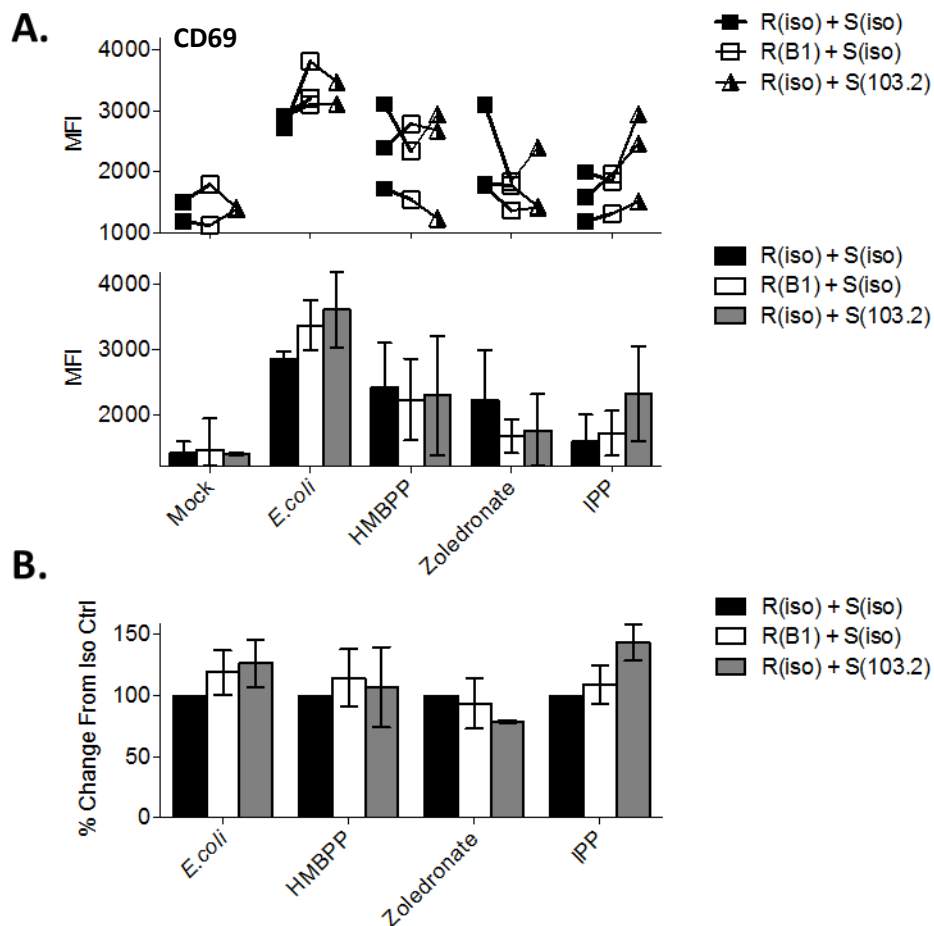


Fig. 7.6. Peripheral V δ 2 cells express a predominantly V γ 9V δ 2 TCR. Freshly-isolated PBMC were stained for CD3, $\alpha\beta$ TCR and the TCR chains V δ 2 and V γ 9. Shown are three representative donor samples, gated on live CD3^{pos} $\alpha\beta$ TCR^{neg} cells.

V γ 9V δ 2 cell responses to various stimuli were then examined in the presence or absence of pre-culture with blocking antibody. Freshly-isolated stimulator PBMC were cultured with medium only (mock), irradiated *E.coli*, HMBPP, IPP or zoledronate. Such a panel was designed to include i) a complex, pAg-expressing non-self target that further includes non-TCR inflammatory stimuli for V γ 9V δ 2 cells, *e.g.* LPS via TLR-4 (*E.coli*), ii) exogenous non-self pAg (HMBPP), iii) exogenous self pAg (IPP) and iv) a pharmacological agent that induces accumulation endogenous pAg, including IPP (zoledronate).

V γ 9V δ 2 cell CD69 upregulation in response to overnight co-culture with these differentially stimulated autologous PBMC was examined (Fig.7.7). Significant CD69 upregulation was seen in response to all stimulator conditions (Fig.7.7A). Donor responses to the various conditions were, however, heterogeneous in potency. Data on the effects of blocking antibodies were, therefore, standardized against each donor's CD69 MFI in the absence of any blocking mAb (i.e. R(iso)+S(iso)), and expressed instead as a percentage change in marker MFI after the addition of blocking antibody (Fig.8.13B). Unexpectedly, it was apparent that responder pre-blocking with anti- $\gamma\delta$ TCR or stimulator pre-blocking with anti-BTN3A exerted no significant effect on V γ 9V δ 2 upregulation of CD69 (Fig.7.7B).

The same assay was repeated with five donors, and measured CD107a-mediated cytotoxic degranulation as well as accumulation of intracellular IFN- γ . Once again, whilst all stimuli elicited V γ 9V δ 2 cell cytotoxicity and IFN- γ production, significant donor-dependent variation could be observed (Fig.7.8A and Fig.7.9A). Standardisation against each condition's cell surface CD107a in the absence of blocking mAb revealed that cytotoxic degranulation too was unaffected by responder or stimulator pre-culture with anti- $\gamma\delta$ TCR or anti-BTN3A mAb, respectively (Fig.7.9A and B). V γ 9V δ 2 intracellular IFN- γ levels, meanwhile, were sensitive to blocking $\gamma\delta$ TCR or anti-BTN3A mAb in response to every stimulus examined (Fig.7.9B). It must be noted that an exception was the IFN- γ response to IPP-stimulated PBMC in the presence of clone B1 mAb, which decreased upon addition of blocking antibody, but failed to acquire meaningful statistical significance at a *p* value of 0.08 (Fig.7.9B). It is possible that statistical significance could have been acquired with an increased donor number. A vast difference was, thus, observed between CD69 upregulation and CD107a-mediated cytotoxic degranulation *versus* IFN- γ production in terms of sensitivity to the blocking mAbs B1 and 103.2.



*Fig. 7.7. Peripheral V γ 9V δ 2 responder cell CD69 upregulation in response to autologous stimulator cells is not sensitive to blocking of BTN3A or $\gamma\delta$ TCR. Freshly-isolated PBMC (n=3) responder cells were stimulated with autologous stimulator PBMC. Stimulator PBMC were prepared by culturing $\gamma\delta$ T cell-depleted, freshly-isolated PBMC overnight with irradiated *E.coli*, HMBPP, zoledronate or IPP. Stimulator PBMC were then pre-blocked with either antagonistic anti-BTN3A mAb (clone: 103.2) or isotype-matched control. Freshly-isolated responder PBMC were, meanwhile, rested overnight, and pre-blocked with anti- $\gamma\delta$ TCR mAb (clone: B1) or isotype-matched control. Responder V γ 9V δ 2 cell upregulation of CD69 in response to co-culture with stimulator PBMC was recorded via FACS. "R(iso)" indicates responder cells pre-incubated with isotype control mAb; "R(B1)" indicates responder cells pre-incubated with B1 mAb; "S(iso)" indicates stimulator cells pre-incubated with isotype control mAb; "S(103.2)" indicates stimulator cells pre-incubated with 103.2 mAb. (A) Shown are donor V γ 9V δ 2 cell CD69 MFI after O/N co-culture in the presence of various blocking conditions. The upper panel shows individual donor points and the lower panel shows a mean and standard deviation of the data compiled. (B) Shown is the percentage change in response to blocking mAb for each donor data point. Each donor's CD69 upregulation in the presence of blocking mAb was compared to that seen with "R(iso)+S(iso)", which represents 100%. Bar graphs indicate the mean \pm standard deviation.*

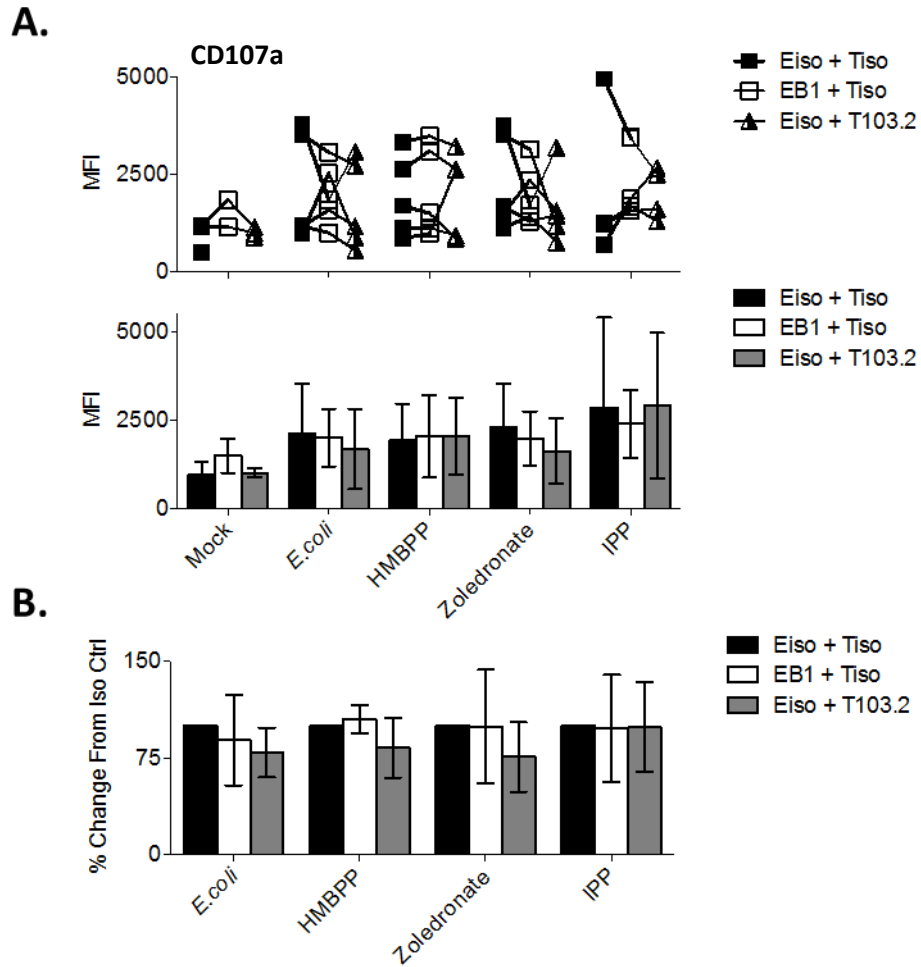
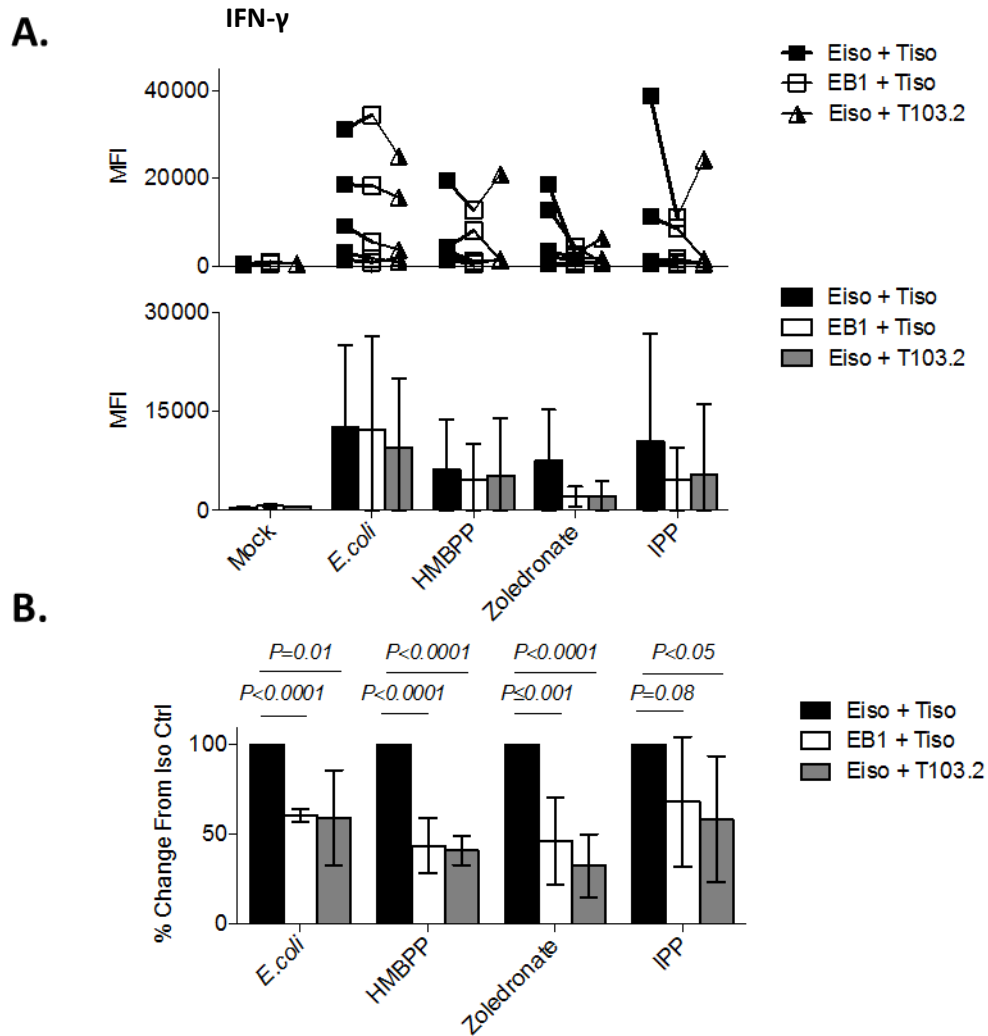


Fig. 7.8. Peripheral V γ 9V δ 2 responder cell CD107a upregulation in response to autologous stimulator cells is not sensitive to blocking of BTN3A or $\gamma\delta$ TCR. Freshly-isolated PBMC (n=5) responder cells were stimulated with autologous stimulator PBMC. Stimulator PBMC were prepared by culturing $\gamma\delta$ T cell-depleted, freshly-isolated PBMC overnight with irradiated *E.coli*, HMBPP, zoledronate or IPP. Stimulator PBMC were then pre-blocked with either antagonistic anti-BTN3A mAb (clone: 103.2) or isotype-matched control. Freshly-isolated responder PBMC were, meanwhile, rested overnight, and pre-blocked with anti- $\gamma\delta$ TCR mAb (clone: B1) or isotype-matched control. Responder V γ 9V δ 2 cell upregulation of CD107a in response to co-culture with stimulator PBMC was recorded via FACS. “R(iso)” indicates responder cells pre-incubated with isotype control mAb; “R(B1)” indicates responder cells pre-incubated with B1 mAb; “S(iso)” indicates stimulator cells pre-incubated with isotype control mAb; “S(103.2)” indicates stimulator cells pre-incubated with 103.2 mAb. **(A)** Shown are donor V γ 9V δ 2 cell CD107a MFI after O/N co-culture in the presence of various blocking conditions. The upper panel shows individual donor points and the lower panel shows a mean and standard deviation of the data compiled. **(B)** Shown is the percentage change in response to blocking mAb for each donor data point. Each donor’s CD107a upregulation in the presence of blocking mAb was compared to that seen with “R(iso)+S(iso)”, which represents 100%. Bar graphs indicate the mean \pm standard deviation.



*Fig. 7.9. Peripheral $V\gamma 9V\delta 2$ responder cell IFN- γ production in response to autologous stimulator cells is sensitive to blocking of *BTN3A* as well as $\gamma\delta TCR$. Freshly-isolated PBMC (n=5) responder cells were stimulated with autologous stimulator PBMC. Stimulator PBMC were prepared by culturing $\gamma\delta T$ cell-depleted, freshly-isolated PBMC overnight with irradiated *E.coli*, HMBPP, zoledronate or IPP. Stimulator PBMC were then pre-blocked with either antagonistic anti-*BTN3A* mAb (clone: 103.2) or isotype-matched control. Freshly-isolated responder PBMC were, meanwhile, rested overnight, and pre-blocked with anti- $\gamma\delta TCR$ mAb (clone: B1) or isotype-matched control. Responder $V\gamma 9V\delta 2$ cell upregulation of IFN- γ in response to co-culture with stimulator PBMC was recorded via FACS. “R(iso)” indicates responder cells pre-incubated with isotype control mAb; “R(B1)” indicates responder cells pre-incubated with B1 mAb; “S(iso)” indicates stimulator cells pre-incubated with isotype control mAb; “S(103.2)” indicates stimulator cells pre-incubated with 103.2 mAb. (A) Shown are donor $V\gamma 9V\delta 2$ cell intracellular IFN- γ MFI after O/N co-culture in the presence of various blocking conditions. The upper panel shows individual donor points and the lower panel shows a mean and standard deviation of the data compiled. (B) Shown is the percentage change in response to blocking mAb for each donor data point. Each donor’s intracellular IFN- γ in the presence of blocking mAb was compared to that seen with “R(iso)+S(iso)”, which represents 100%. Bar graphs indicate the mean \pm standard deviation.*

The majority of published data addressing the interaction between V γ 9V δ 2 cells and BTN3A on target cells (numerous seminal papers included) has been generated using cell lines rather than autologous cells as stimulators (101,152,161,164,213). A likely contributing factor to these experimental setups is the practical difficulty of obtaining and working with large numbers of primary human cells, exacerbated particularly by the usual scarcity of $\gamma\delta$ T cells in human peripheral blood. An additional hurdle of working with primary cells is introduced by the inherent magnitude heterogeneity of $\gamma\delta$ T cell responses. It has been speculated, for example, that $\gamma\delta$ T cell constitution and responsiveness to various stimuli may be significantly impacted by infectious exposure in early life (7). The use of cell line stimulators is a way of standardizing immunogenic targets for all donors within a given study. A number of important $\gamma\delta$ T cell-BTN3A publications have relied on the use of THP-1 cells, specifically (101,164,214).

7.5. $V\gamma 9V\delta 2$ cell effector responses to stimulator THP-1 cells are differentially sensitive to blocking of the $\gamma\delta$ TCR and BTN3A

In a setup that differed from the autologous stimulator-responder system with the use of THP-1 cell line stimulator cells (illustrated in Fig.7.6), $V\gamma 9V\delta 2$ cell responses were tested. In order to validate initial experimental reservations on my part regarding the use of allogeneic ‘non-self’, transformed stimulator cells, I tested $V\gamma 9V\delta 2$ cell activation upon stimulation with THP-1 cells only in the absence of further pAg stimulus. Indeed, $V\gamma 9V\delta 2$ cells upregulated CD69, engaged in CD107a-mediated cytotoxic degranulation and produced IFN- γ in response to overnight co-culture with otherwise unmodified THP-1 cells (Fig.7.10).

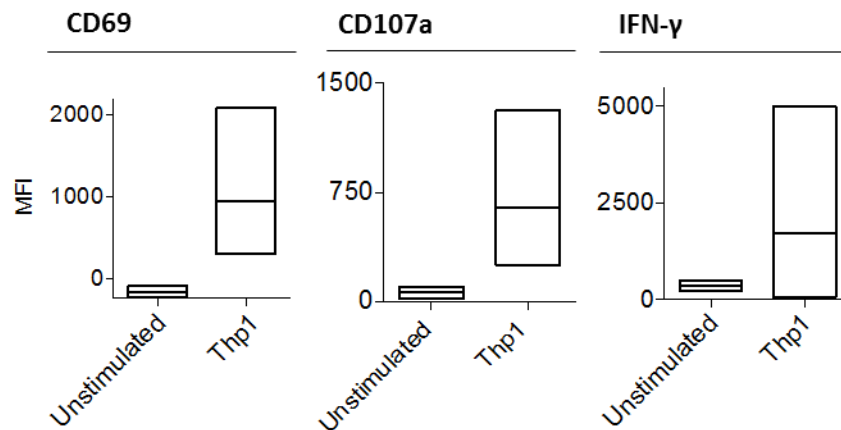


Fig. 7.10. $V\gamma 9V\delta 2$ cells are potently activated by co-culture with THP-1 cells. Freshly-isolated PBMC (n=3) responder cells were stimulated with THP-1 cells. Shown are compilations of donor $V\gamma 9V\delta 2$ cell surface CD69, CD107a and intracellular IFN- γ MFI. The graphs indicate mean and range of the data. Effector responses were compared between unstimulated $V\gamma 9V\delta 2$ cells (unstimulated) and $V\gamma 9V\delta 2$ cells that had undergone O/N co-culture with THP-1 cells.

Having documented a baseline reactivity of freshly-isolated V γ 9V δ 2 cells to unstimulated THP-1 cells, I set out to clarify whether this reactivity can be modified by exposing stimulator THP-1 cells to pAg in the form of *E.coli*, HMBPP, IPP or zoledronate. V γ 9V δ 2 cell CD69 upregulation in response to overnight co-culture with differentially stimulated THP-1 cells was examined (Fig.7.11).

Significant CD69 upregulation upon co-culture with pAg-exposed *versus* pAg-non-exposed (mock) THP-1 cells could be seen with most donor V γ 9V δ 2 cells (Fig.7.11A). Notably, in one of the three examined donors, extremely high CD69 upregulation could be seen even with the addition of only mock-stimulated THP-1 cells. As was the case in the autologous donor PBMC stimulator system, significant donor variation could be observed, if to a lesser extent. As before, the effect of blocking antibodies was calculated as a percentage change set against each donor's CD69 MFI in the absence of any blocking mAb (Fig.7.11B). In contrast to observations from the autologous PBMC system, stimulator pre-culture with anti-BTN3A mAb 103.2 significantly inhibited V γ 9V δ 2 cell CD69 upregulation. Borderline statistical significance, which may have been improved upon increased donor number, was observed for *E.coli*-stimulated ($p=0.06$) as well as mock-stimulated ($p=0.08$) THP-1 cell stimulators. Responder pre-culture with anti- $\gamma\delta$ TCR mAb B1, meanwhile, appeared to exert little to no effect on most V γ 9V δ 2 cell THP-1 responses, save for, interestingly, in the case of IPP-stimulation.

Similar results were obtained when examining CD107a-mediated cytotoxic degranulation (Fig.7.12). V γ 9V δ 2 cell degranulation was inhibited by stimulator pre-culture with anti-BTN3A mAb for every pAg THP-1 stimulus examined, but not mock-stimulated THP-1. Borderline statistical significance could be obtained also for inhibition by responder pre-culture with anti- $\gamma\delta$ TCR mAb (Fig.7.12B). Perhaps the most striking sensitivity to blocking mAbs was obtained upon examining the V γ 9V δ 2 cell IFN- γ response (Fig.7.13). As with cytotoxicity, all responses to pAg-exposed, but not mock, THP-1 stimulators were sensitive to anti-BTN3A mAb (Fig.7.13A). It appeared that anti-BTN3A mAb pre-culture abrogated V γ 9V δ 2 cell IFN- γ production entirely. Significant inhibition could also be achieved with anti- $\gamma\delta$ TCR mAb, when THP-1 stimulators were specifically HMBPP or IPP-exposed. V γ 9V δ 2 cell responses to pAg-stimulated THP-1 cells, thus, appeared

largely sensitive, in terms of activation, cytotoxicity and IFN- γ production, to blocking by the 103.2 and B1 mAbs. It must be noted, however, that the vast inter-donor differences necessitate repeated experiments with increased donor numbers. It is possible that greater statistical significance could be achieved for all pAg stimulation conditions, blocking of the $\gamma\delta$ TCR and even V γ 9V δ 2 cell responses to unmodified THP-1 cells.

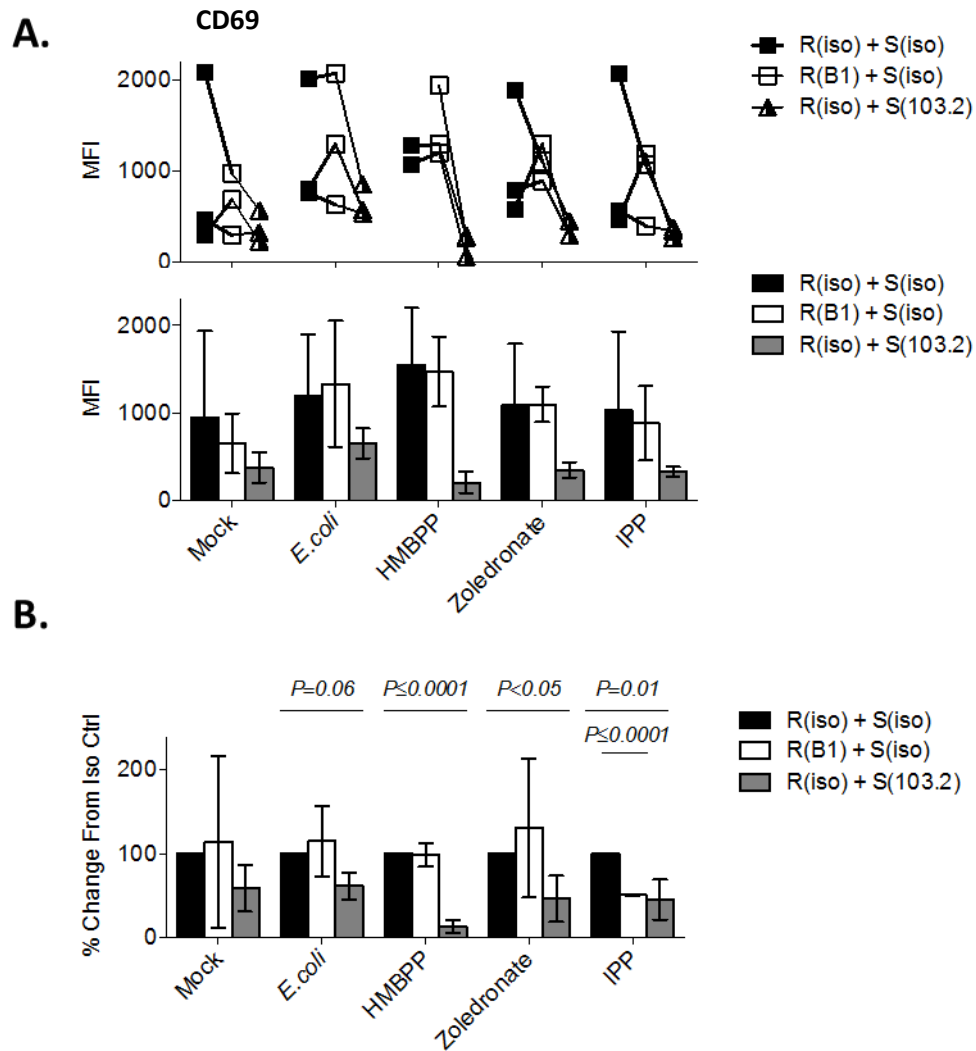


Fig. 7.11. Peripheral $V\gamma 9V\delta 2$ responder cell surface CD69 in response to THP-1 stimulator cells is sensitive to blocking of *BTN3A*. Freshly-isolated PBMC (n=3) responder cells were stimulated with THP-1 stimulator cells. Stimulator THP-1 were prepared by culturing THP-1 cells overnight with irradiated *E. coli*, HMBPP, zoledronate or IPP. Stimulator THP-1 were then pre-blocked with either antagonistic anti-*BTN3A* mAb (clone: 103.2) or isotype-matched control. Freshly-isolated responder PBMC were, meanwhile, rested overnight, and pre-blocked with anti- $\gamma\delta$ TCR mAb (clone: B1) or isotype-matched control. Responder $V\gamma 9V\delta 2$ cell upregulation of CD69 in response to co-culture with stimulator THP-1 was recorded via FACS. “R(iso)” indicates responder cells pre-incubated with isotype control mAb; “R(B1)” indicates responder cells pre-incubated with B1 mAb; “S(iso)” indicates stimulator cells pre-incubated with isotype control mAb; “S(103.2)” indicates stimulator cells pre-incubated with 103.2 mAb. (A) Shown are donor $V\gamma 9V\delta 2$ cell surface CD69 after O/N co-culture in the presence of various blocking conditions. The upper panel shows individual donor points and the lower panel shows a mean and standard deviation of the data compiled. (B) Shown is the percentage change in response to blocking mAb for each donor data point. Each donor’s cell surface CD69 in the presence of blocking mAb was compared to that seen with “R(iso)+S(iso)”, which represents 100%. Bar graphs indicate the mean \pm standard deviation.

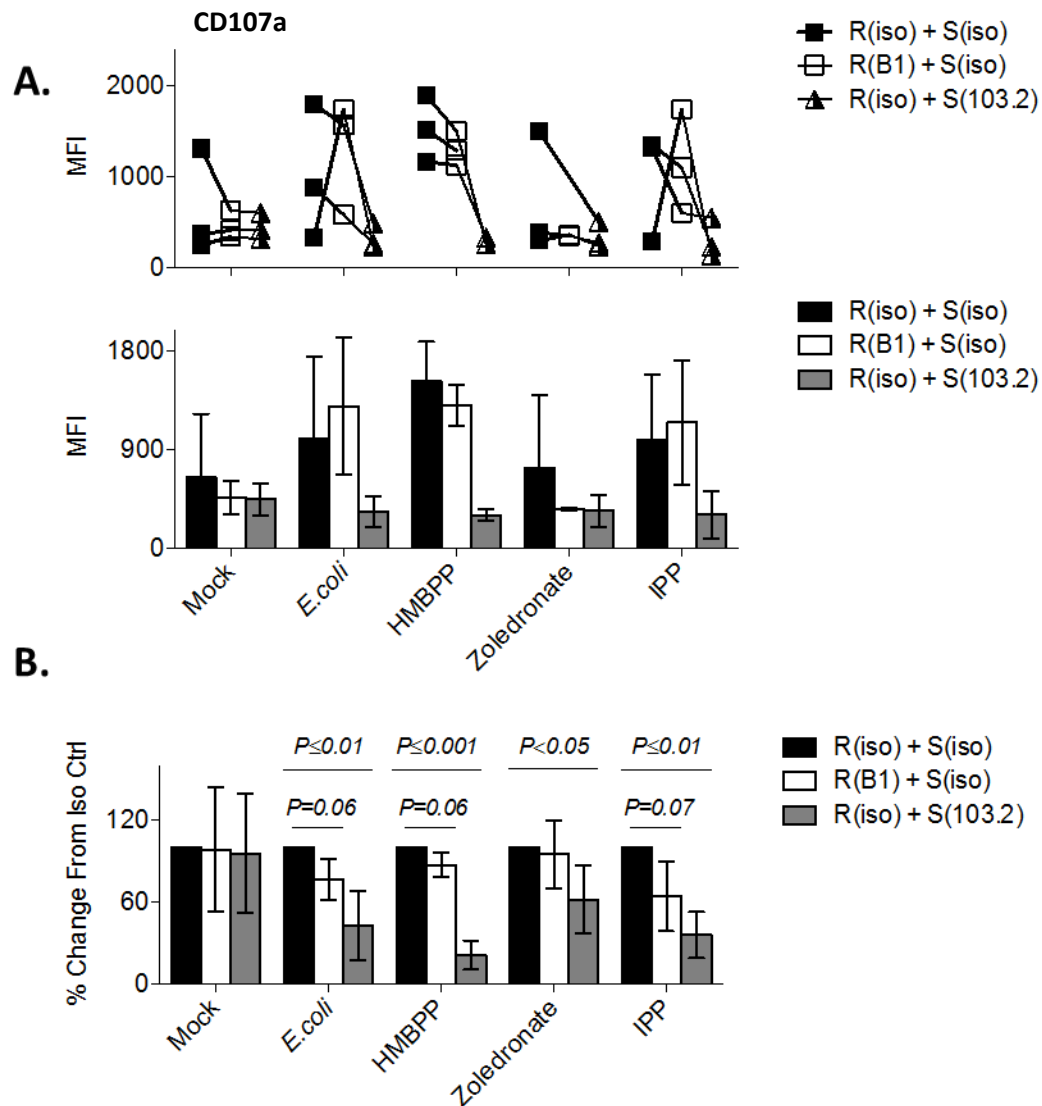


Fig. 7.12. Peripheral $V\gamma 9V\delta 2$ responder cell surface CD107a in response to THP-1 stimulator cells is sensitive to blocking of BTN3A. Freshly-isolated PBMC ($n=3$) responder cells were stimulated with THP-1 stimulator cells. Stimulator THP-1 were prepared by culturing THP-1 cells overnight with irradiated *E.coli*, HMBPP, zoledronate or IPP. Stimulator THP-1 were then pre-blocked with either antagonistic anti-BTN3A mAb (clone: 103.2) or isotype-matched control. Freshly-isolated responder PBMC were, meanwhile, rested overnight, and pre-blocked with anti- $\gamma\delta$ TCR mAb (clone: B1) or isotype-matched control. Responder $V\gamma 9V\delta 2$ cell upregulation of cell surface CD107a in response to co-culture with stimulator THP-1 was recorded via FACS. “R(iso)” indicates responder cells pre-incubated with isotype control mAb; “R(B1)” indicates responder cells pre-incubated with B1 mAb; “S(iso)” indicates stimulator cells pre-incubated with isotype control mAb; “S(103.2)” indicates stimulator cells pre-incubated with 103.2 mAb. (A) Shown are donor $V\gamma 9V\delta 2$ cell surface CD107a after O/N co-culture in the presence of various blocking conditions. The upper panel shows individual donor points and the lower panel shows a mean and standard deviation of the data compiled. (B) Shown is the percentage change in response to blocking mAb for each donor data point. Each donor’s cell surface CD107a in the presence of blocking mAb was compared to that seen with “R(iso)+S(iso)”, which represents 100%. Bar graphs indicate the mean \pm standard deviation.

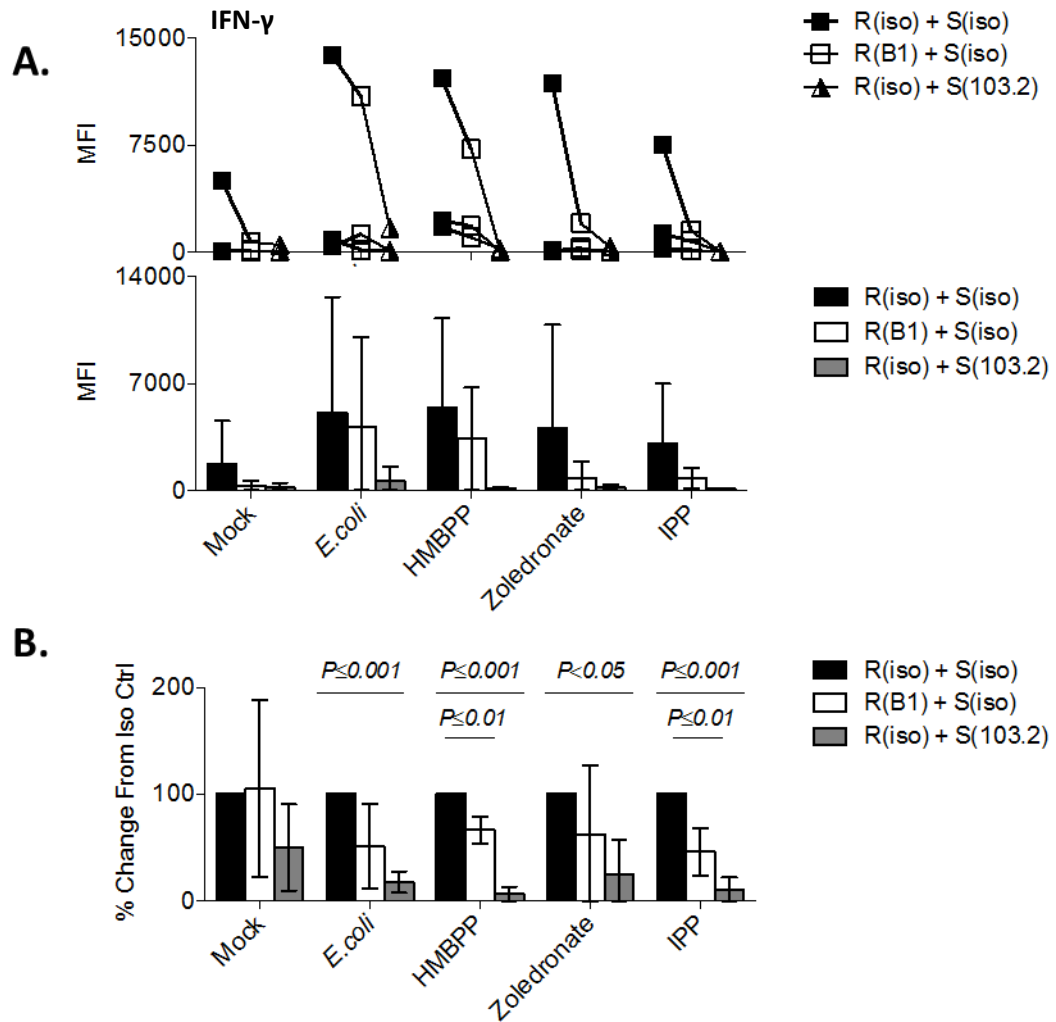


Fig. 7.13. Peripheral $V\gamma 9V\delta 2$ responder $IFN-\gamma$ production in response to THP-1 stimulator cells is sensitive to blocking of BTN3A. Freshly-isolated PBMC (n=3) responder cells were stimulated with THP-1 stimulator cells. Stimulator THP-1 were prepared by culturing THP-1 cells overnight with irradiated *E.coli*, HMBPP, zoledronate or IPP. Stimulator THP-1 were then pre-blocked with either antagonistic anti-BTN3A mAb (clone: 103.2) or isotype-matched control. Freshly-isolated responder PBMC were, meanwhile, rested overnight, and pre-blocked with anti- $\gamma\delta$ TCR mAb (clone: B1) or isotype-matched control. Responder $V\gamma 9V\delta 2$ cell intracellular $IFN-\gamma$ in response to co-culture with stimulator THP-1 was recorded via FACS. “R(iso)” indicates responder cells pre-incubated with isotype control mAb; “R(B1)” indicates responder cells pre-incubated with B1 mAb; “S(iso)” indicates stimulator cells pre-incubated with isotype control mAb; “S(103.2)” indicates stimulator cells pre-incubated with 103.2 mAb. **(A)** Shown are donor $V\gamma 9V\delta 2$ intracellular $IFN-\gamma$ after O/N co-culture in the presence of various blocking conditions. The upper panel shows individual donor points and the lower panel shows a mean and standard deviation of the data compiled. **(B)** Shown is the percentage change in response to blocking mAb for each donor data point. Each donor’s intracellular $IFN-\gamma$ in the presence of blocking mAb was compared to that seen with “R(iso)+S(iso)”, which represents 100%. Bar graphs indicate the mean \pm standard deviation.

7.6. Discussion

Data laid out in this chapter explores freshly-isolated V γ 9V δ 2 cell effector function dependency on the TCR and BTN3A in the context of an autologous and an allogeneic stimulation model. Findings included:

- i) Nearly all freshly-isolated PBMC express BTN3A.
- ii) *E.coli* and zoledronate stimulation of whole PBMC causes mild downregulation of BTN3A, but overall levels are restored throughout expansion with both stimuli.
- iii) Freshly-isolated V γ 9V δ 2 cells upregulate CD69, engage in CD107a-mediated cytotoxicity and produce IFN- γ in response to stimulation with *E.coli*, HMBPP, IPP or zoledronate-exposed autologous PBMC.
- iv) V γ 9V δ 2 cell IFN- γ production, but not CD69 upregulation and CD107a-mediated cytotoxic degranulation, in this autologous stimulation model were sensitive to blocking by both anti-BTN3A mAb (clone: 103.2) and anti- $\gamma\delta$ TCR mAb (clone: B1).
- v) Freshly-isolated V γ 9V δ 2 cells upregulate CD69, engage in CD107a-mediated cytotoxicity and produce IFN- γ in response to stimulation with the otherwise unstimulated, allogeneic THP-1 cell-line, exhibiting baseline reactivity.
- vi) Baseline THP-1-reactivity of V γ 9V δ 2 cells is highly donor-dependent.
- vii) This baseline V γ 9V δ 2 cell activation by THP-1 cells is enhanced by THP-1 cell pre-stimulation with *E.coli*, HMBPP, IPP or zoledronate.
- viii) V γ 9V δ 2 cell IFN- γ production as well as CD69 upregulation and CD107a-mediated cytotoxic degranulation in response to THP-1 stimulators were sensitive to blocking by anti-BTN3A mAb (clone: 103.2). Sensitivity to anti- $\gamma\delta$ TCR mAb (clone: B1) was effector function and stimulus-dependent. As with the autologous stimulator experimental system, IFN- γ production exhibited the highest sensitivity to blocking mAb.

Data laid out in this chapter indicates that freshly-isolated peripheral V γ 9V δ 2 cells respond to pAg-stimulated targets in a BTN3A (and, partially, TCR)-dependent manner. This finding expands and further develops data presented in previous chapters, which outlined that apparently similar factors govern $\gamma\delta$ T cell responses to zoledronate and *E.coli*-stimulated autologous cells. The findings of this chapter are further consistent with the role of BTN3A in V γ 9V δ 2 cell recognition of targets that is described in the literature (152,157,161,213,215).

Despite continuity with previous chapters, I note that the effect of $\gamma\delta$ TCR blocking was far less pronounced in the autologous or THP-1 stimulator systems described in the present chapter than what was observed with direct addition of anti- $\gamma\delta$ TCR mAb to whole PBMC, as described in Chapter VII. The efficacy of blocking mAb pre-culture was, furthermore, dependent on the pAg in use (*e.g.* IPP *versus* HMBPP), the type of stimulator cell (autologous PBMC *versus* allogeneic THP-1) and the donor in consideration. Thus, while general trends could be observed, I emphasize that significant further work is necessary to enhance the reliability and reproducibility of the conclusions drawn.

Foremost, noting the donor-dependence of observed V γ 9V δ 2 cell responses, the number of donors tested needs to be increased substantially. Given the differences between blocking potency in whole PBMC *versus* autologous PBMC stimulator *versus* allogeneic THP-1 stimulator systems, testing the blocking capacity of anti-BTN3A and anti- $\gamma\delta$ TCR mAbs needs to be examined in additional experimental setups. These experimental setups will require careful standardization for factors such as number of washes and culture times. It is possible, for example, that the lower impact of anti- $\gamma\delta$ TCR mAb in the stimulator systems compared to direct PBMC stimulation (as described in Chapter VI) is due to the higher number of washes and extended experimental protocol used in the BTN3A blocking experiments. It is not inconceivable that the anti- $\gamma\delta$ TCR mAb simply detaches from the TCR after a given period of time or is instead removed from the cell surface upon re-cycling of the TCR, as part of normal T cell physiology. A way to potentially mitigate these effects would be to leave the anti- $\gamma\delta$ TCR mAb in culture at a saturating concentration with responder and stimulator cells, so as to permit continuous binding of blocking antibody. A novel danger may be introduced, however, if anti- $\gamma\delta$ TCR mAb is

bound via its Fc portions to cells in culture (*e.g.* THP-1 stimulator cells) and therefore acts instead as an activatory signal by cross-linking the TCR. Anti- $\gamma\delta$ TCR clone B1 is a well-established stimulator to $\gamma\delta$ T cells, if adhered to the surface of beads, well-plates or stimulator cells (211). A troubling recent report that needs to be considered in the context $\gamma\delta$ TCR blocking mAbs has been compiled by Dutta *et al.* (216). They speculate and present supporting data to the notion that decreased effector function (cytotoxicity in this instance) upon pre-culture with anti- $\gamma\delta$ TCR is not necessarily or solely the consequence of functional blocking of the TCR, but alternatively or additionally of mAb-induced cell apoptosis. Lowered functional capacity was, thus, merely a reflection of mAb-related dramatically reduced $\gamma\delta$ T cell viability. While a limited number of experimental setups and readouts were investigated, Dutta *et al.* make the recommendation that B1 and 11F2 anti- $\gamma\delta$ TCR clones be avoided, and replaced instead with the less viability-damaging 5A6.E9 clone. Reasons for the dramatic effect that mAb binding alone can exert on $\gamma\delta$ T cell viability and function remain unclear, but are critically important in evaluating the credibility of a vast number of earlier anti- $\gamma\delta$ TCR mAb-utilizing publications. In the context of the present thesis, I am confident that at a considerable degree of cell viability remained, as continued $\gamma\delta$ T cell proliferation could be observed even post clone B1 mAb treatment. In many cases, as seen in Figures 7.13 and 7.14, for example, anti- $\gamma\delta$ TCR mAb failed to exert any functional effect, even in the context of cytotoxicity. Nonetheless, these experiments need to be repeated with the anti- $\gamma\delta$ TCR clones 11F2 and 5A6.E9, with cell viability tracked closely and carefully.

Similar allowances need to be given to the data presented using anti-BTN3A mAb clone 103.2. As described in the chapter introduction, 103.2 is only one of a number of clones available for agonistic as well as antagonistic BTN3A assays. 103.2 is the only clone documented to act antagonistically on BTN3A, and is stipulated to exert its inhibitory function by 'holding' BTN3A in its inactive, closed conformation (157). Other anti-BTN3A mAb are agonistic and instead hold BTN3A in its active, open conformation, including the clones 19.5, 20.1 and 232.5. Despite a similar effect on BTN3A extracellularly, the functional effect of these clones are vastly different, ranging from strongly activatory to T cells, inducing proliferation, cytokine production and enhancing survival with clone 20.1 and T cell inhibition with clone 232.5. The specific reasons for

the different effects of these mAbs on T cell activation are unclear, but appear to result from epitope location on the extracellular portion of BTN3A, antibody binding affinity, avidity and valency (155–158). In addition to uncertainty of the specific mechanisms of action and physiological relevance of blocking mAbs, also binding of FACS staining mAbs warrants investigation. BTN3A.1 is known to change conformation upon exposure to pAg. It is possible that the decreased positivity of BTN3A seen after PBMC stimulation with *E.coli* and zoledronate (Figures 7.1 and 7.2) was simply reflective of impaired binding of the staining mAb (clone BT3.1) to a conformationally-altered BTN.

Another important yet ambiguous avenue of the data presented in this chapter is the activatory potency of the various target stimuli used, i.e. *E.coli*, HMBPP, IPP and zoledronate. While some trends emerged, overall, all differentially-stimulated stimulator cells (autologous or THP-1) appeared to induce similar V γ 9V δ 2 cell activation, albeit in a strongly donor-dependent manner. It didn't appear to be the case, for example, that *E.coli*-stimulated target cells elicited vastly more CD69 upregulation, cytotoxicity or IFN- γ in V γ 9V δ 2 cells than IPP-stimulated target cells. Such an observation is surprising given that – in contrast to IPP - *E.coli* contain a multitude of immunogenic signals, far in excess of pAg content. Moreover, HMBPP (also found in *E.coli*) has been reported to be a ~10 000 more potent V γ 9V δ 2 cell activator than IPP – a phenomenon that is likely due to its binding affinity to the intracellular B30.2 domain of BTN3A.1 (162). Such an observation appears logical in a physiological context, whereupon endogenous stress-induced IPP has a higher threshold towards activating V γ 9V δ 2 cells than *de facto* non-self HMBPP, which is of obligate microbial origin. Nonetheless, my findings of roughly similar activation levels would be consistent with the supposition that, given saturation of pAg stimulus, the central (if not only) activatory signal V γ 9V δ 2 cells perceive is BTN3A conformational changes. It may be the case that, upon direct exposure to *E.coli*, V γ 9V δ 2 cell activation is further modulated by *e.g.* TLR engagement, but it is clearly not necessary for induction of effector function. Indeed, work by De Libero *et al.* suggests that even HMBPP-expressing *E.coli*-induced activation of V γ 9V δ 2 cells is, in fact, mediated by *E.coli* induction of endogenous stress markers and pyrophosphates (including IPP) (101). Examining such questions in the experimental setups described in this chapter, once again, requires an increased donor number, and, importantly, a titration of pAg stimulus applied to target

cells. An interesting experiment would be autologous (or THP-1) target cell stimulation with a pAg-negative bacterium, *e.g. S.aureus*, and observing how that response compares to that of pAg-positive bacteria, such as *E.coli*, and those, in turn, to the addition of IPP.

Interesting differences in response could be observed between THP-1 *versus* autologous PBMC-stimulated V γ 9V δ 2 cells. Unexpectedly, CD69 upregulation, CD107a-mediated degranulation and IFN- γ were far more sensitive to anti-BTN3A and anti- $\gamma\delta$ TCR blocking in the context of THP-1 cells. THP-1 cells are allogeneic and, therefore, inevitably contain immunogenic signals other than just BTN3A; signals, which include NK cell receptor incompatibilities that are likely to be fortuitously different between donors. V γ 9V δ 2 cells are known to express a number of NK cell receptors, which one would expect to be triggered by allogeneic cells – particularly transformed allogeneic cells, as is the case with THP-1 cells (44,211). It is possible, however, that the standardization of stimulus cell type (i.e. all donor $\gamma\delta$ T cells being treated with the same THP-1 cells and not with corresponding autologous PBMC) improved reproducibility of data and, thus, improved the statistical significance of inhibitor effects observed. It is difficult to compare results from the two experimental systems, however, due to the earlier mentioned protocol differences and technical considerations of working with blocking antibodies. For example, it may be the case that BTN3A cycles from the cell surface more readily in freshly-isolated PBMC than THP-1 cells, therefore, making it appear that anti-BTN3A mAb exerts a greater effect on THP-1 cell recognition than recognition of autologous PBMC. As mentioned earlier, extensive standardization of various experimental setups with titration of antibody as well as pAg is imperative to determine whether such conclusions can indeed be drawn.

It was interesting to note, nevertheless, that the effector function consistently sensitive to blocking mAb across stimulator systems was production of IFN- γ . Unlike CD69 upregulation, induction of IFN- γ production requires overcoming a relatively high activation threshold (217). It may be the case, for example, that cell surface receptor cycling has removed a portion of the blocking anti-BTN3A or anti- $\gamma\delta$ TCR mAbs exposing sufficient ‘active’ BTN3A and ‘free’ $\gamma\delta$ TCR for the induction of CD69 but not IFN- γ . Cell surface CD107a, meanwhile, presents a more perplexing case. Even in previous chapters

that described a near total loss of V δ 2 cell IFN- γ production upon whole PBMC pre-culture with B1 mAb, these same cells maintained a degree of CD107a-mediated cytotoxic degranulation. The factors that regulate V γ 9V δ 2 cell cytotoxicity appear to include the TCR, FcR and NK-like receptors (*e.g.* killer-immunoglobulin-like receptors and NKG2D) as well as TLRs (44,211,218), but remain to be elucidated completely. Determinants of non-V δ 2 $\gamma\delta$ T cell cytotoxicity and activation remain even more poorly understood.

One V γ 9V δ 2 cell effector function that would be interesting to explore in the context of BTN3A-dependency is phagocytosis and pAPC function. In Chapter VII, I documented that expanded V δ 2 cell phagocytosis of IgG opsonized *E.coli* is TCR-dependent. Such TCR and IgG-dependence was observed for both *E.coli* and zoledronate-expanded V δ 2 cells, which were subsequently found to express almost identical V γ 9V δ 2 TCR repertoires. The conclusion drawn from this data was that the V γ 9V δ 2 TCR is unlikely to engage *E.coli* directly, but recognize instead a self-molecule that is present also on zoledronate-stimulated PBMC. Most likely this molecule is BTN3A and its conformational changes. I speculate, therefore, that V γ 9V δ 2 cell phagocytosis is regulated by a ‘licensing’-type interaction between the TCR and BTN3A, as well as Fc γ R. It cannot be ruled out that further undetected interactions between V γ 9V δ 2 cells and neighboring PBMC are taking place, required for the successful engagement of phagocytic effector function. If indeed phagocytosis of target material is TCR and BTN3A-dependent, V γ 9V δ 2 cell pAPC function is likely to be as well.

Significant insight could be gained from a repeat of the above-mentioned *E.coli* phagocytosis assays in the presence of BTN3A blocking mAb, clone 103.2. To address specific mechanistic questions, however, perhaps the most valuable source of data may be bead-uptake experiments. Does V γ 9V δ 2 cell pre-culture with mAb 103.2-coated stimulator cells prevent the uptake of IgG-opsonized beads? Is this uptake in the presence of 103.2-blocked cells restored if the beads further contain stimulatory anti- $\gamma\delta$ TCR mAb? Does pre-culture with the BTN3A agonistic mAb clone 20.1 enhance V γ 9V δ 2 cell phagocytosis of beads? Such a reductionist experimental setup may have questionable direct *in vivo* relevance, but may provide insight into some of the basic questions regarding the mode of action BTN3A, and its role in V γ 9V δ 2 cell. As laid out in the chapter

introduction and Figure 7.3, it is unclear, as of yet, how exactly BTN3A enhances V γ 9V δ 2 cell activation. Is it engaged directly by the TCR? Does it act more as a B7 molecule instead, and bind a homotypic, unknown CTLA-4-like or CD28-like molecule on V γ 9V δ 2 cells? Is 'active' BTN3A instead a crucial adhesion molecule, which is not directly engaged by the TCR, but is necessary to stabilize TCR engagement with another target? Simplistic bead experiments in the presence of stimulator cells, anti- $\gamma\delta$ TCR mAb and agonistic, as well as antagonistic BTN3A mAbs may shed some light on these questions.

7.7. Summary

Data compiled in this chapter documents that V γ 9V δ 2 cell activation, cytokine production and cytotoxicity in response to pAg-exposed stimulator cells is BTN3A-dependent, in a manner that appears to be linked to TCR-dependency. Such dependency is, however, experimental setup, pAg stimulus and donor-dependent, and requires detailed further investigation.

8. DISCUSSION

The primary driver of scientific interest in human $\gamma\delta$ T cells derives from their potential as effectors in cancer and infectious disease immunotherapy (7,9,10,219,220). As the literature suggests, and indeed my data supports, peripheral $\gamma\delta$ T cells are highly effective cytotoxic killers and producers of pro-inflammatory cytokines, yet exhibit high, lymphoid-like specificity for targets, and appear tightly regulated by the need for detection of cellular stress and IgG opsonisation. Moreover, $\gamma\delta$ T cells appear capable of significant immune regulation and perhaps even initiation of $\alpha\beta$ T cell responses in a manner reminiscent of DCs. Unlike DCs, however, V γ 9V δ 2 cells can be accessed in the human periphery with relative ease, and amplified exponentially *in vitro* in an antigen-specific context. Strikingly, infiltrating $\gamma\delta$ T cells have been identified as the single most positive predictive factor in human cancer survival in both pan-cancer and solid-tumour analysis (221).

As approach to the clinic of $\gamma\delta$ T cell-based therapies for cancer and infectious disease gathers momentum, crucial basic biology questions about the nature of these enigmatic lymphocytes remain. How do $\gamma\delta$ T cells recognize self- and non-self antigen en masse in an apparently similar manner? How, if at all, do $\gamma\delta$ T cells differentiate between self- and non-self targets? How are $\gamma\delta$ T cell responses generated so rapidly? How exactly do $\gamma\delta$ T cells kill virally infected and transformed self-cells, and how does this compare to their direct killing of microorganisms? Are $\gamma\delta$ T cells truly capable of DC-like professional antigen presentation? Is their pAPC function important in the initiation of an immune response, or, rather, in the regulation of an existing response? How is $\gamma\delta$ T cell phagocytosis carried out? What are the molecular interactions that govern $\gamma\delta$ T cell effector function and proliferation in response to stimulation? Do the same $\gamma\delta$ T cells engage in cytotoxicity and pro-inflammatory cytokine production, as well as antigen presentation

and immune regulation? How do these disparate functional phenotypes relate to one another during acute immune activation events, such as sepsis?

The examination of these questions is hugely complicated by the physiological differences between human and rodent $\gamma\delta$ T cells. A lack of cheap and easily modifiable animal models has presented a significant hurdle to the dissection of $\gamma\delta$ T cell function and clinical potential. Given the near-necessity for work with human $\gamma\delta$ T cells when attempting to decipher $\gamma\delta$ T cell clinical potential, an important consideration emerges: Are *in vitro* observations regarding $\gamma\delta$ T cell functionality, including pAPC function, relevant *in vivo*? While this question remains acutely present in my evaluation of data output from the $\gamma\delta$ T cell field, an increasing body of clinical data is adding credibility to the notion that conclusions from *in vitro* study of human $\gamma\delta$ T cells bear resemblance to what is happening *in vivo* during the early stages of infection. Significant increases in systemic (and mucosal) $\gamma\delta$ T cell numbers are seen during acute infection with a wide variety of viral, parasitic and bacterial infections, ranging from HCMV and *Escherichia* to *Plasmodium* and *Mycobacterium* (19,62–64,102,134,208,222,223). Data indicates that these $\gamma\delta$ T cells display an activated phenotype (as evidenced by cell surface CD69), are positive for MHC class II and CD86, and correlate negatively with mortality during sepsis and acute systemic inflammatory response syndrome (21,22,24–26,28). Furthermore, natural or experimental elevation of $\gamma\delta$ T cell numbers in human, non-human primate and murine models has correlated with improved prognosis or even protection from a range of infections, including *M. tuberculosis*, HCMV, *T. gondii* and *L. monocytogenes* (28–36).

The present thesis describes an attempt at *ex vivo* modelling of peripheral human $\gamma\delta$ T cell behavior during acute *in vivo* microbial exposure as is seen during *e.g.* sepsis. Cell responses were examined and tracked after whole freshly isolated PBMC stimulation with irradiated *E. coli*. While the data describes $\gamma\delta$ T cell phenotypic and functional shift in response to *in vitro* stimulation with *E. coli*, ultimately, the themes and findings of the work extended beyond a description of $\gamma\delta$ T cell interaction with *E.coli*. At its core, the experimental setup is an exploration of the factors that govern peripheral $\gamma\delta$ T cell

(V γ 9V δ 2 cell, specifically) recognition of target, behaviour after encounter with target and subsequent functional evolution – whether the inflammatory context is of non-self (*e.g.* *E.coli*) or self (*e.g.* IPP) origin. The main experimental findings of the present thesis were as follows:

- i. *E.coli* as well as zoledronate-expanded $\gamma\delta$ T cells are capable of effective phagocytosis of IgG-opsonized targets, including *E.coli*, while freshly-isolated $\gamma\delta$ T cells are not.
- ii. *E.coli* and zoledronate-expanded $\gamma\delta$ T cells bear a close resemblance to one another in terms of functional cell surface marker expression, with both populations presenting with a predominantly V γ 9V δ 2 TCR^{pos} HLA-DR^{pos} CD86^{pos} CCR7^{neg} CD62L^{low} CD4^{neg} CD8^{neg} CD16^{pos} CD56^{pos} phenotype.
- iii. Further homology in the differentially expanded cells is seen with TCR CDR3 sequences, which are similar to one another, but different to freshly-isolated TCR CDR3s. This suggests that PBMC stimulation with *E.coli* and zoledronate leads to V γ 9V δ 2 CDR3 focusing on a similar set of ligands.
- iv. V γ 9V δ 2 cell acquisition of a pAPC phenotype during expansion with *E.coli* or zoledronate is accompanied by a loss of a Th1-type pro-inflammatory phenotype, whilst maintaining potent cytotoxicity.
- v. Expansion does not alter $\gamma\delta$ T cell memory phenotype, which remains effector memory (CD27^{neg} CD45RA^{neg}) prior to, during and after 14 day expansion. Almost no naïve V γ 9V δ 2 cell can be detected at any time.
- vi. Th1-type cytokine production, proliferation and phagocytic capacity of V γ 9V δ 2 cells are all dependent on the TCR. CD107a-mediated cytotoxic degranulation appears only partially TCR dependent, while bactericidal activity appears unaffected by blocking of the $\gamma\delta$ TCR.
- vii. V γ 9V δ 2 cell activation, cytokine production and cytotoxicity in response to pAg-exposed stimulator cells are BTN3A-dependent, in a manner that appears linked to TCR-dependency. Whether this dependency is indeed consistent among various pAg stimuli and donors remains to be determined.

Altogether, the data permit development of an intriguing hypothesis as to the unique role of $\gamma\delta$ T cells (with a V γ 9V δ 2 TCR, specifically) in inflammation related to acute peripheral infection and/or cellular stress. I form the following narrative with published $\gamma\delta$ T cell literature in mind, expanded by the laboratory findings described in this thesis. A summary of my hypothesis of V γ 9V δ 2 cell functional evolution after exposure to antigen can be viewed in figure 8.1.

I postulate that circulating V γ 9V δ 2 cells, of an effector memory phenotype, surveil peripheral blood (and possibly mucosal epithelial sites) for evidence of cellular stress. This stress, manifesting itself as BTN3A conformational changes, can be induced by a wide variety of stimuli, all of which result in the rapid intracellular accumulation of pAg. Such stimuli include abnormally rapid cell proliferation, mutagenic transformation, infection with virus, intracellular bacteria, extracellular bacteria or parasites (64,135,164,165,179,195,224). While it may be the case that some microorganisms, such as *M. tuberculosis*, *P. falciparum* and *E.coli*, express pAgs that are exclusively microbial in origin (*e.g.* HMBPP), it remains unclear whether these induce BTN3A conformational changes directly or act instead by inducing accumulation of endogenous pAg, or both (64,101). Upon encounter with BTN3A in its 'active' conformation, effector memory V γ 9V δ 2 cells are activated in a TCR-dependent manner, and respond with production of Th1-type cytokines (*e.g.* IFN- γ , TNF- α) as well as potent cytotoxicity. Given the apparent broad specificity of the V γ 9V δ 2 TCR for BTN3A (or cells that express 'active' BTN3A, rather), $\gamma\delta$ T cells are activated en masse, thus, mounting a rapid and vigorous pro-inflammatory response.

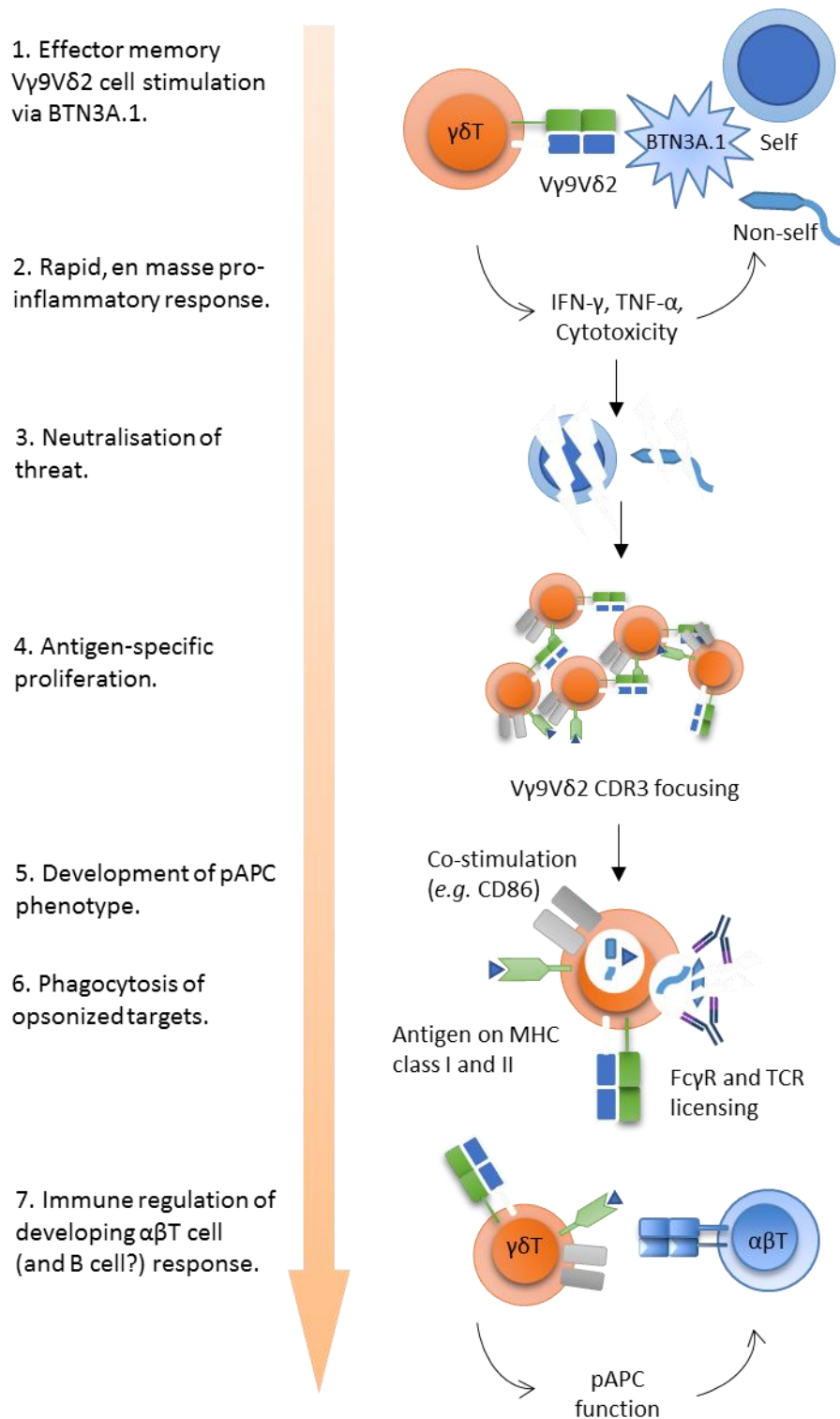


Fig. 8.1. A model of peripheral Vγ9Vδ2 T cell functional evolution following antigenic challenge. Informed by the laboratory data gathered throughout the progression of this thesis, and placed within a context of existing literature on γδT cell physiology, I postulate that, during acute infection-driven cellular stress, Vγ9Vδ2 cell effector phenotype is plastic, and transitions from a Th1-type to a pAPC phenotype following exposure to target antigen.

Through direct, en masse target lysis, as well as activation of downstream immune effectors, V γ 9V δ 2 cells form a widely-acting bulwark against a variety of environmental, infectious or mutagenic threats. Upon neutralizing the immediate threat, activated V γ 9V δ 2 cells proliferate, and undergo a profound functional evolution. Shedding their initial Th1-type pro-inflammatory phenotype, expanding V γ 9V δ 2 cells acquire in its stead a regulatory pAPC phenotype. The loss of canonical T cell capacities, such as IFN- γ production, is paralleled by acquisition of phagocytic capacity, expression of MHC class II and co-stimulatory molecules, necessary for the initiation and/or regulation of the developing adaptive immune response. While my data and data published by others indicates that V γ 9V δ 2 cells can act as pAPCs to $\alpha\beta$ T cells (60,178,225), $\gamma\delta$ T cells have also been implicated in regulation of humoral immunity (225). Such a narrative places peripheral V γ 9V δ 2 cells squarely at the interface between the innate and adaptive immune systems. An almost PRR-like TCR with apparently limited specificity, rapid, en masse reactivity, phagocytic capacity and antigen presenting properties allude to the many myeloid-like characteristics of these cells. The maintenance, nonetheless, of an oligoclonal TCR repertoire, expansion and early Th1-like reactivity place V γ 9V δ 2 cells in the lymphoid branch of the immune system.

One functional hallmark that my data indicates as sustained throughout $\gamma\delta$ T cell functional transition is potent cytotoxicity. While the rapid and efficient killing of *E. coli* by expanded MHC class II^{pos} CD86^{pos} V γ 9V δ 2 cells I report is atypical of most classic pAPCs, such as DCs, it may allude to the unique effector phenotype of activated $\gamma\delta$ T cells. It appears that even V γ 9V δ 2 cell pAPCs retain a highly cytotoxic phenotype. Such potent cytotoxic capacity is well beyond what is required for the killing of a phagocytosis or antigen presentation target. It is known, for example, that DCs can effectively present antigens of internalized cell debris, revealing that killing of targets is not a pre-requisite for professional antigen presentation (226). It is unlikely, therefore, that activated, expanding V γ 9V δ 2 cells retain cytotoxicity in service of pAPC function. The purpose of $\gamma\delta$ T pAPC cytotoxicity remains to be determined. It is, moreover, an important consideration in the design of $\gamma\delta$ T cell-based immunotherapies. Almost all current immunotherapeutic strategies involve *ex vivo* expansion of V γ 9V δ 2 cells, and is, thus,

likely to induce the above-described functional shift, which is accompanied throughout by potent cytotoxic capacity.

Given the plethora of effector functions at the disposal of peripheral V γ 9V δ 2 cells and their plasticity in employing these functions, careful control of the $\gamma\delta$ T cell compartment appears necessary. TCR-engagement as a pre-requisite for activation, proliferation, cytokine production, phagocytosis (and other pAPC functions) paired with a dependence on stress-induced BTN3A conformational changes suggests an elegant mode of regulation. Potentially dangerous pro-inflammatory effector functions of V γ 9V δ 2 cells are prevented from occurring in the absence of cellular stress through the dependence on 'active' BTN3A. Moreover, whenever an early immune response is sufficient to neutralize infection, MHC class II^{pos} CD86^{pos} V γ 9V δ 2 cells may be prevented from posing an unnecessary inflammatory threat through downregulation of their early cytokine (*e.g.* IFN- γ , TNF- α) responsiveness. Even in the event that the infectious ('stressful') threat is sustained throughout V γ 9V δ 2 cell functional transit after encounter with antigen, IgG opsonisation of target is required for such effector functions as phagocytosis and consequent antigen presentation. This could be operative at two levels: i) as herein, when opsonizing with isotype-switched target-specific IgG, ii) in a 'naïve' non-immune situation, where natural antibodies (NAb) of different isotype, including IgG, may be involved. It has previously been demonstrated that NAb can enhance DC uptake and antigen presentation of viruses (227). Numerous, inter-connected layers of regulation, thus, exist to guide V γ 9V δ 2 cell activity. In addition, while dependence on stress-induced BTN3A conformational changes and IgG opsonin restricts their functionality, it permits broad and rapid en masse activation of V γ 9V δ 2 cells if the appropriate conditions are met.

A curious issue with this narrative, nonetheless, persists. Namely, if V γ 9V δ 2 cells do indeed specialize in the recognition of stress-induced BTN3A conformational changes, then why is an oligoclonal (or even polyclonal) V γ 9V δ 2 TCR repertoire maintained? Data presented in this thesis suggests that expansion in response to *E. coli* or zoledronate lead to a focusing of V γ 9V δ 2 CDR3 sequences. Even though the freshly-isolated V γ 9V δ 2

repertoire was dominated by several, highly numerous clones, almost no overlap could be seen between the freshly-isolated *versus E.coli* or zoledronate-expanded repertoire delta chain CDR3 (Fig.4.17). The suggestion is, therefore, that V γ 9V δ 2 cells do indeed have a baseline oligoclonal repertoire, but that it is *not*, in fact, finely-tuned to recognize *E.coli* or zoledronate-induced antigens, which are, presumably, BTN3A conformational changes. Perhaps an even more obvious question emerges upon considering why V γ 9V δ 2 cells need have a varied TCR repertoire at all. If V γ 9V δ 2 cells act primarily as surveyors of cellular stress that manifests itself via pre-determined BTN3A conformational changes, then why maintain such TCR CDR3 diversity? While an argument could be made for physiological redundancy, TCR re-arrangements are, nevertheless, a life-long energy expenditure. Moreover, if $\gamma\delta$ T cells are indeed as evolutionarily ancient as has been suggested by the study of lampreys (206), then their maintenance of a resource-intensive but unnecessary feature over millions of generations seems unlikely. It is known, for example, that mouse dendritic epidermal $\gamma\delta$ T cells bind a murine B7-homologue on keratinocytes, SKINT1, that is crucial for their organ-specificity and survival, in a manner that may parallel human V γ 9V δ 2 cell-BTN3A interactions (141,228,229). These mouse dendritic epidermal $\gamma\delta$ T cells do, however, express an almost entirely homogeneous, invariant TCR repertoire, consistent with their TCR-dependent recognition of a totally restricted set of target antigens focused on the SKINT1 molecule (69,141,229,230). As the literature and my own data indicates, such baseline TCR focus is not seen with peripheral human V γ 9V δ 2 cells (6,32,210).

I note that none of the data presented in this thesis sheds light on whether the V γ 9V δ 2 TCR engages BTN3A directly or whether BTN3A leads to TCR-mediated activation via other means, *e.g.* by binding to a co-stimulatory molecule on V γ 9V δ 2 cells. Perhaps, the maintenance of an oligoclonal (or even polyclonal) V γ 9V δ 2 repertoire indicates that the TCR binds a diverse set of target antigens that are not merely BTN3A conformational changes, even if it is done so in a BTN3A-dependent manner. Significant ambiguity and controversy on the details of V γ 9V δ 2 cell antigen recognition persists. A recent publication by Starick *et al.* suggests that V γ 9V δ 2 cells exhibit differential pAg *versus* agonistic anti-BTN3A mAb reactivity depending on fine CDR3 differences, implicating

the TCR in direct recognition of the conformational changes therein (231). They further postulate that V γ 9V δ 2 cells may also recognize pAg in a BTN3A-independent manner, given particular TCR specificity. These postulates were, however, formed using reductionist animal transductant models, inter-species hybrid cell lines and anti-BTN3A mAbs. The *in vivo* relevance of these findings is yet to be confirmed experimentally. In this respect, for now, V γ 9V δ 2 cells remain a quandary.

Despite a lack of clarity regarding the exact mode of antigen recognition and engagement, clues as to the physiological role of peripheral V γ 9V δ 2 cells can be drawn from their species specificity. Absent in rodents, V γ 9V δ 2 cells are present in such animals as humans and non-human primates. They have been ascribed a particularly important role in the life of young animals, with a disproportionate reactivity to infectious challenge by pAg-expressing pathogens, *M. tuberculosis* and *P. falciparum*, that are further pathogens of high significance in humans as well as non-human primates, but not rodents (7). Indeed, animal models and clinical human data have implicated V γ 9V δ 2 cells in anti-malarial and tuberculosis responses (19,31,34,62,134,223,224,232). Both *M. tuberculosis* and *P. falciparum* are a frequent cause of serious and chronic infection in humans that is often exacerbated by inappropriate immune responses. It is, perhaps, the ever-present threat of *M. tuberculosis* and *P. falciparum* infection that has shaped the human peripheral $\gamma\delta$ T cell compartment. It is, perhaps, a co-evolutionary context in which V γ 9V δ 2 cells developed a plastic and transitory effector phenotype. Potent, Th1-type pro-inflammatory reactions upon encounter with *M. tuberculosis* and *P. falciparum* may be mounted in an attempt to prevent productive infection. These are then followed by the development of a regulatory phenotype upon triggering of the adaptive response, and when the disease enters its chronic stages. Importantly, such a physiological role would account for the highly potent cytotoxicity that V γ 9V δ 2 cells retain even upon acquiring an apparently regulatory phenotype. Cytotoxic killing of *M. tuberculosis* or *P. falciparum*-infected cells by immune effectors is likely crucial during the acute as well as chronic stages of disease.

Further study of the engagement of the V γ 9V δ 2 TCR, possibly with BTN3A targets or co-receptors, will carry significant implications for $\gamma\delta$ T cell anti-tumor immunity. Data is increasingly supportive of the notion that stress recognition, particularly in combination with Ab-opsonisation, may be sufficient not only for killing of a tumor cell but also for uptake, processing and presentation of tumor-associated antigens (49). $\gamma\delta$ T cell direct killing of cellular and/or microbial targets combined with inflammatory cytokine production followed by uptake of the target into acidifying antigen processing compartments raises a novel paradigm. It is tempting to hypothesize that the combination of innate-like recognition and killing followed with myeloid-like phagocytosis by a lymphocyte-like cell may evolutionarily have preceded the full development of T lymphocyte-mediated adaptive immunity. Interestingly, the raised hypothesis is supported by previous studies showing that $\gamma\delta$ TCR chain genes may have preceded the development of $\alpha\beta$ TCR chain genes (205). In addition, the existence in jawless fish of three lymphocyte-like cells expressing variable lymphocyte receptors instead of TCR or BCR chain genes also supports this contention, since they otherwise resemble $\alpha\beta$ T, $\gamma\delta$ T and B cells by the expression of other orthologous genes (206).

Detailed further study of $\gamma\delta$ T cell antigen recognition, engagement and responses in human and humanized animal models is key to unlocking the vast immunotherapeutic potential of these enigmatic lymphocytes. If current suppositions on the physiology of human $\gamma\delta$ T cells are confirmed and clarified in the laboratory, their clinical application is likely to extend well beyond treatment for malignancy, and expand into therapy development for infectious and even immunopathological diseases.

REFERENCES

1. Ferreira LMR. Gammadelta T Cells: Innately Adaptive Immune Cells? *Int Rev Immunol.* 2013 Jun;32(3):223–48.
2. De Rosa, S. C., Mitra, D. K., Watanabe, N., Herzenberg, L A, Herzenberg, L A, Roeder, M. Vd1 and Vd2 gdT cells express distinct surface markers and might be developmentally distinct lineages. *J Leukoc Biol.* 2001 Oct;70:518–26.
3. Hedges JF, Lubick KJ, Jutila MA. T Cells Respond Directly to Pathogen-Associated Molecular Patterns. *J Immunol.* 2005 May 15;174(10):6045–53.
4. Siegers GM, Ribot EJ, Keating A, Foster PJ. Extensive expansion of primary human gamma delta T cells generates cytotoxic effector memory cells that can be labeled with Feraheme for cellular MRI. *Cancer Immunol Immunother.* 2013 Mar;62(3):571–83.
5. Kalyan, S, Kabelitz, D. Defining the nature of human gdT cells: a biographical sketch of the highly empathetic. *Cell Mol Immunol.* 2013;10:21–9.
6. Holtmeier, W., Chowets, Y., Lumeng, A., Morzycka-Wroblewska, E., Kagnoff, M. F. The Delta T Cell Receptor Repertoire in Human Colon and Peripheral Blood Is Oligoclonal Irrespective of V Region Usage. *J Clin Invest.* 1995 Aug;96:1108–17.
7. Vantourout P, Hayday A. Six-of-the-best: unique contributions of $\gamma\delta$ T cells to immunology. *Nat Rev Immunol.* 2013 Jan 25;13(2):88–100.
8. Carding SR, Egan PJ. gdT CELLS: FUNCTIONAL PLASTICITY AND HETEROGENEITY. *Nat Rev Immunol.* 2002 May;2(5):336–45.
9. Silva-Santos B, Serre K, Norell H. $\gamma\delta$ T cells in cancer. *Nat Rev Immunol.* 2015 Oct 9;15(11):683–91.
10. Casetti R, Martino A. The plasticity of gamma delta T cells: innate immunity, antigen presentation and new immunotherapy. *Cell Mol Immunol.* 2008;5(3):161–70.
11. Gogoi D, Chiplunkar SV. Targeting gamma delta T cells for cancer immunotherapy: bench to bedside. *Indian J Med Res.* 2013;138(5):755.

12. Pang DJ, Neves JF, Sumaria N, Pennington DJ. Understanding the complexity of $\gamma\delta$ T-cell subsets in mouse and human: $\gamma\delta$ T-cell subsets in mouse and human. *Immunology*. 2012 Jul;136(3):283–90.
13. Thompson K, Roelofs AJ, Jauhiainen M, Mönkkönen H, Mönkkönen J, Rogers MJ. Activation of $\gamma\delta$ T Cells by Bisphosphonates. In: Choi Y, editor. *Osteoimmunology* [Internet]. Boston, MA: Springer US; 2009 [cited 2015 Oct 22]. p. 11–20. Available from: http://link.springer.com/10.1007/978-1-4419-1050-9_2
14. Wang L, Kamath A, Das H, Li L, Bukowski JF. Antibacterial effect of human V γ 2V δ 2 T cells in vivo. *J Clin Invest*. 2001 Nov 1;108(9):1349–57.
15. Andreu-Ballester JC, Tormo-Calandin C, Garcia-Ballesteros C, Perez-Griera J, Amigo V, Almela-Quilis A, et al. Association of T Cells with Disease Severity and Mortality in Septic Patients. *Clin Vaccine Immunol*. 2013 May 1;20(5):738–46.
16. Vaccaro, R. B A, Gerli, R., Spinozzi, F., Muscat, C., Scalise, F., Castellucci, G., et al. Lymphocytes bearing the gamma delta T cell receptor in acute Brucella melitensis infection. *Eur J Immunol*. 1993;23:1177–80.
17. Galley HF, Lowes DA, Thompson K, Wilson ND, Wallace CA, Webster NR. Characterisation of gamma delta ($\gamma\delta$) T cell populations in patients with sepsis: Gamma delta ($\gamma\delta$) T cells in sepsis. *Cell Biol Int*. 2015 Feb;39(2):210–6.
18. Islam D, Christensson B. Disease-dependent changes in T-cell populations in patients with shigellosis. *Apmis*. 2000;108(4):251–60.
19. Ho M, Tongtawe P, Kriangkum J, Wimonwattrawatee T, Pattanapanyasat K, Bryant L, et al. Polyclonal expansion of peripheral gamma delta T cells in human Plasmodium falciparum malaria. *Infect Immun*. 1994;62(3):855–62.
20. Hara T, Mizuno Y, Takaki K, Takada H, Akeda H, Aoki T, et al. Predominant activation and expansion of V gamma 9-bearing gamma delta T cells in vivo as well as in vitro in Salmonella infection. *J Clin Invest*. 1992 Jul 1;90(1):204–10.
21. Arvand M, Schneider T, Jahn H-U, Hahn H. Streptococcal toxic shock syndrome associated with marked $\gamma\delta$ T cell expansion: case report. *Clin Infect Dis*. 1996;22(2):362–5.
22. Schneider T, Jahn H-U, Liesenfeld O, Steinhoff D, Riecken E-O, Zeitz M, et al. The Number and Proportion of VY9V δ 2 T Cells Rise Significantly in the Peripheral Blood of Patients After the Onset of Acute Coxiella burnetii Infection. *Clin Infect Dis*. 1997;24(2):261–4.
23. Kroca M, Johansson A, Sjostedt A, Tarnvik A. V 9V 2 T Cells in Human Legionellosis. *Clin Vaccine Immunol*. 2001 Sep 1;8(5):949–54.

24. Pinheiro MB, Antonelli LR, Sathler-Avelar R, Vitelli-Avelar DM, Spindola-de-Miranda S, Guimarães TMPD, et al. CD4-CD8- $\alpha\beta$ and $\gamma\delta$ T Cells Display Inflammatory and Regulatory Potentials during Human Tuberculosis. Khader S, editor. PLoS ONE. 2012 Dec 11;7(12):e50923.
25. Matsushima A, Ogura H, Fujita K, Koh T, Tanaka H, Sumi Y, et al. EARLY ACTIVATION OF $\gamma\delta$ T LYMPHOCYTES IN PATIENTS WITH SEVERE SYSTEMIC INFLAMMATORY RESPONSE SYNDROME: Shock. 2004 Jul;22(1):11–5.
26. Zhu, H., Xu, Y., Wang, H., Hu, Y., Chen, H., Cui, L., et al. Human $\gamma\delta$ T cells augment antigen presentation in *Listeria Monocytogenes* infection. Mol Med. 2016;
27. Venet F, Bohé J, Debard A-L, Bienvenu J, Lepape A, Monneret G. Both percentage of $\gamma\delta$ T lymphocytes and CD3 expression are reduced during septic shock: Crit Care Med. 2005 Dec;33(12):2836–40.
28. Long KM, Ferris MT, Whitmore AC, Montgomery SA, Thurlow LR, McGee CE, et al. $\gamma\delta$ T Cells Play a Protective Role in Chikungunya Virus-Induced Disease. Perlman S, editor. J Virol. 2016 Jan 1;90(1):433–43.
29. Khairallah C, Netzer S, Villacreces A, Juzan M, Rousseau B, Dulanto S, et al. $\gamma\delta$ T Cells Confer Protection against Murine Cytomegalovirus (MCMV). Jameson SC, Jung JU, editors. PLOS Pathog. 2015 Mar 6;11(3):e1004702.
30. Sheridan BS, Romagnoli PA, Pham Q-M, Fu H-H, Alonzo F, Schubert W-D, et al. $\gamma\delta$ T Cells Exhibit Multifunctional and Protective Memory in Intestinal Tissues. Immunity. 2013 Jul;39(1):184–95.
31. Chen, Z W. Multifunctional immune responses of HMBPP-specific Vg2Vd2 T cells in *M. tuberculosis* and other infections. Cell Mol Immunol. 2013;10:58–64.
32. Hisaeda H, Sakai T, Nagasawa H, Ishikawa H, Yasutomo K, Maekawa Y, et al. Contribution of extrathymic $\gamma\delta$ T cells to the expression of heat-shock protein and to protective immunity in mice infected with *Toxoplasma gondii*. Immunology. 1996;88(4):551–7.
33. Hiromatsu K, Yoshikai Y, Matsuzaki G, Ohga S, Muramori K, Matsumoto K, et al. A protective role of gamma/delta T cells in primary infection with *Listeria monocytogenes* in mice. J Exp Med. 1992;175(1):49–56.
34. Spencer, C T, Abate, G, Blazevic, A, Hoft, D F. Only a Subset of Phosphoantigen-Responsive gdT Cells Mediate Protective Tuberculosis Immunity.pdf. J Immunol. 2008;181:4471–84.
35. Chen CY, Yao S, Huang D, Wei H, Sicard H, Zeng G, et al. Phosphoantigen/IL2 Expansion and Differentiation of V γ 2V δ 2 T Cells Increase Resistance to

Tuberculosis in Nonhuman Primates. Lewinsohn DM, editor. PLoS Pathog. 2013 Aug 15;9(8):e1003501.

36. T. NINOMIYA, H. TAKIMOTO, G. MATSUZAKI, S. HAMANO, H. YOSHIDA, Y. YOSHIKAI, I. G. KIMURA & K. NOMOTO. Vg1+ gd T cells play protective roles at an early phase of murine cytomegalovirus infection through production of interferon-g. *Immunology*. 2000;99:187–94.
37. Lo Presti E, Dieli F, Meraviglia S. Tumor-Infiltrating gdT Lymphocytes: Pathogenic Role, Clinical Significance, and Differential Programing in the Tumor Microenvironment. *Front Immunol* [Internet]. 2014 Nov 24 [cited 2016 Feb 1];5. Available from: <http://journal.frontiersin.org/article/10.3389/fimmu.2014.00607/abstract>
38. Wu P, Wu D, Ni C, Ye J, Chen W, Hu G, et al. $\gamma\delta$ T17 Cells Promote the Accumulation and Expansion of Myeloid-Derived Suppressor Cells in Human Colorectal Cancer. *Immunity*. 2014 May;40(5):785–800.
39. Rei M, Goncalves-Sousa N, Lanca T, Thompson RG, Mensurado S, Balkwill FR, et al. Murine CD27(-) V 6(+) T cells producing IL-17A promote ovarian cancer growth via mobilization of protumor small peritoneal macrophages. *Proc Natl Acad Sci*. 2014 Aug 26;111(34):E3562–70.
40. Carmi Y, Rinott G, Dotan S, Elkabets M, Rider P, Voronov E, et al. Microenvironment-Derived IL-1 and IL-17 Interact in the Control of Lung Metastasis. *J Immunol*. 2011 Mar 15;186(6):3462–71.
41. Ma C, Zhang Q, Ye J, Wang F, Zhang Y, Wevers E, et al. Tumor-Infiltrating T Lymphocytes Predict Clinical Outcome in Human Breast Cancer. *J Immunol*. 2012 Nov 15;189(10):5029–36.
42. Gentles AJ, Newman AM, Liu CL, Bratman SV, Feng W, Kim D, et al. The prognostic landscape of genes and infiltrating immune cells across human cancers. *Nat Med*. 2015 Jul 20;21(8):938–45.
43. Cheng P, Liu T, Zhou W-Y, Zhuang Y, Peng L, Zhang J, et al. Role of gamma-delta T cells in host response against *Staphylococcus aureus*-induced pneumonia. *BMC Immunol*. 2012;13(1):38.
44. Dandekar AA, O'Malley K, Perlman S. Important Roles for Gamma Interferon and NKG2D in gdT-Cell-Induced Demyelination in T-Cell Receptor -Deficient Mice Infected with a Coronavirus. *J Virol*. 2005 Aug 1;79(15):9388–96.
45. Roberts, S J, Smith, A :, West, A B, Wen, L, Findly, R C, Owen, M J, et al. T-cells ab+ and gdT+ deficient mice display abnormal but distinct phenotypes toward a natural, widespread infection of the intestinal epithelium. *PNAS*. 1996 Oct;93:11774–9.

46. Ke Y, Pearce K, Lake JP, Ziegler HK, Kapp JA. Gamma delta T lymphocytes regulate the induction and maintenance of oral tolerance. *J Immunol.* 1997;158(8):3610–8.
47. Colburn NT, Zaal KJM, Wang F, Tuan RS. A role for γ/δ T cells in a mouse model of fracture healing. *Arthritis Rheum.* 2009 Jun;60(6):1694–703.
48. Fujihashi K, McGhee JR, Kweon M-N, Cooper MD, Tonegawa S, Takahashi I, et al. gamma/delta T cell-deficient mice have impaired mucosal immunoglobulin A responses. *J Exp Med.* 1996;183(4):1929–35.
49. Himoudi N, Morgenstern DA, Yan M, Vernay B, Saraiva L, Wu Y, et al. Human T Lymphocytes Are Licensed for Professional Antigen Presentation by Interaction with Opsonized Target Cells. *J Immunol.* 2012 Feb 15;188(4):1708–16.
50. Wu Y, Wu W, Wong WM, Ward E, Thrasher AJ, Goldblatt D, et al. Human gdT Cells: A Lymphoid Lineage Cell Capable of Professional Phagocytosis. *J Immunol.* 2009 Nov 1;183(9):5622–9.
51. Brandes M, Willmann K, Moser B. Professional antigen-presentation function by human $\gamma\delta$ T cells. *Science.* 2005;309(5732):264–8.
52. Huang Y, Getahun A, Heiser RA, Detanico TO, Aviszus K, Kirchenbaum GA, et al. T Cells Shape Preimmune Peripheral B Cell Populations. *J Immunol.* 2016 Jan 1;196(1):217–31.
53. Oykman P, Mody CH. Direct Microbicidal Activity of Cytotoxic T-Lymphocytes. *J Biomed Biotechnol.* 2010;2010:1–9.
54. Zeng X, Wei Y-L, Huang J, Newell EW, Yu H, Kidd BA, et al. $\gamma\delta$ T Cells Recognize a Microbial Encoded B Cell Antigen to Initiate a Rapid Antigen-Specific Interleukin-17 Response. *Immunity.* 2012 Sep;37(3):524–34.
55. Rezende RM, da Cunha AP, Kuhn C, Rubino S, M'Hamdi H, Gabriely G, et al. Identification and characterization of latency-associated peptide-expressing $\gamma\delta$ T cells. *Nat Commun.* 2015 Dec 8;6:8726.
56. Cheng L, Cui Y, Shao H, Han G, Zhu L, Huang Y, et al. Mouse $\gamma\delta$ T cells are capable of expressing MHC class II molecules, and of functioning as antigen-presenting cells. *J Neuroimmunol.* 2008 Oct;203(1):3–11.
57. Takamatsu, H H, Denyer, M S, Wileman, T E. A sub-population of circulating porcine gd T cells can act as professional antigen presenting cells. *Vet Immunol Immunopathol.* 2002;87:223–4.
58. Takamatsu H-H, Denyer MS, Stirling C, Cox S, Aggarwal N, Dash P, et al. Porcine $\gamma\delta$ T cells: Possible roles on the innate and adaptive immune responses

- following virus infection. *Vet Immunol Immunopathol*. 2006 Jul;112(1-2):49–61.
59. Rhodes SG, Hewinson RG, Vordermeier HM. Antigen Recognition and Immunomodulation by T Cells in Bovine Tuberculosis. *J Immunol*. 2001 May 1;166(9):5604–10.
 60. Brandes M, Willimann K, Bioley G, Lévy N, Eberl M, Luo M, et al. Cross-presenting human $\gamma\delta$ T cells induce robust CD8+ $\alpha\beta$ T cell responses. *Proc Natl Acad Sci*. 2009;106(7):2307–12.
 61. Coffelt SB, Kersten K, Doornebal CW, Weiden J, Vrijland K, Hau C-S, et al. IL-17-producing $\gamma\delta$ T cells and neutrophils conspire to promote breast cancer metastasis. *Nature*. 2015 Mar 30;522(7556):345–8.
 62. Huang D, Chen CY, Zhang M, Qiu L, Shen Y, Du G, et al. Clonal Immune Responses of Mycobacterium-Specific $\gamma\delta$ T Cells in Tuberculous and Non-Tuberculous Tissues during *M. tuberculosis* Infection. Briken V, editor. *PLoS ONE*. 2012 Feb 1;7(2):e30631.
 63. Shen Y. Adaptive Immune Response of Vgamma 2Vdelta 2+ T Cells During Mycobacterial Infections. *Science*. 2002 Mar 22;295(5563):2255–8.
 64. Feurle J, Espinosa E, Eckstein S, Pont F, Kunzmann V, Fournie J-J, et al. *Escherichia coli* Produces Phosphoantigens Activating Human gdT Cells. *J Biol Chem*. 2002 Jan 4;277(1):148–54.
 65. Guzy C, Paclik D, Schirbel A, Sonnenborn U, Wiedenmann B, Sturm A. The probiotic *Escherichia coli* strain Nissle 1917 induces gdT cell apoptosis via caspase- and FasL-dependent pathways. *Int Immunol*. 2008 Apr 25;20(7):829–40.
 66. Wang L, Das H, Kamath A, Bukowski JF. Human V 2V 2 T Cells Produce IFN- and TNF- with an On/Off/On Cycling Pattern in Response to Live Bacterial Products. *J Immunol*. 2001 Dec 1;167(11):6195–201.
 67. Moretto M, Durell B, Schwartzman JD, Khan IA. T Cell-Deficient Mice Have a Down-Regulated CD8+ T Cell Immune Response Against *Encephalitozoon cuniculi* Infection. *J Immunol*. 2001 Jun 15;166(12):7389–97.
 68. Girardi M, Oppenheim DE, Steele CR, Lewis JM, Glusac E, Filler R, et al. Regulation of Cutaneous Malignancy by $\gamma\delta$ T Cells. *Science*. 2001 Oct 19;294(5542):605–9.
 69. Barbee SD, Woodward MJ, Turchinovich G, Mention J-J, Lewis JM, Boyden LM, et al. Skint-1 is a highly specific, unique selecting component for epidermal T cells. *Proc Natl Acad Sci*. 2011 Feb 22;108(8):3330–5.

70. Kaminski MJ, Mroczkowski TF, Krotoski WA. Dendritic epidermal γ/δ T cells (DETC) activated in vivo proliferate in vitro in response to Mycobacterium leprae antigens. *Int J Dermatol*. 2000;39(8):603–8.
71. MacLeod AS, Hemmers S, Garijo O, Chabod M, Mowen K, Witherden DA, et al. Dendritic epidermal T cells regulate skin antimicrobial barrier function. *J Clin Invest*. 2013 Oct 1;123(10):4364–74.
72. Jameson JM, Sharp LL, Witherden DA, Havran WL. Regulation of skin cell homeostasis by gamma delta T cells. *Front Biosci J Virtual Libr*. 2004 Sep 1;9:2640–51.
73. Khanna R, Burrows SR. Human immunology: a case for the ascent of non-furry immunology. *Immunol Cell Biol*. 2011 Mar;89(3):330–1.
74. Zschaler J, Schlorke D, Arnhold J. Differences in innate immune response between man and mouse. *Crit Rev Immunol [Internet]*. 2014 [cited 2017 Jun 19]; Available from: <http://dl.begellhouse.com/journals/2ff21abf44b19838,forthcoming,11600.html>
75. Mestas J, Hughes CCW. Of Mice and Not Men: Differences between Mouse and Human Immunology. *J Immunol*. 2004 Mar 1;172(5):2731–8.
76. Flannagan RS, Jaumouillé V, Grinstein S. The Cell Biology of Phagocytosis. *Annu Rev Pathol Mech Dis*. 2012 Feb 28;7(1):61–98.
77. Underhill DM, Goodridge HS. Information processing during phagocytosis. *Nat Rev Immunol*. 2012 Jun 15;12(7):492–502.
78. Kerr MC, Teasdale RD. Defining Macropinocytosis. *Traffic*. 2009 Apr;10(4):364–71.
79. Dopfer EP, Minguet S, Schamel WWA. A New Vampire Saga: The Molecular Mechanism of T Cell Trophocytosis. *Immunity*. 2011 Aug;35(2):151–3.
80. Overholtzer M, Brugge JS. The cell biology of cell-in-cell structures. *Nat Rev Mol Cell Biol*. 2008 Oct;9(10):796–809.
81. Paul D, Achouri S, Yoon Y-Z, Herre J, Bryant CE, Cicuta P. Phagocytosis Dynamics Depends on Target Shape. *Biophys J*. 2013 Sep;105(5):1143–50.
82. Ravetch JV, Bolland S. IgG fc receptors. *Annu Rev Immunol*. 2001;19(1):275–90.
83. van Lookeren Campagne M, Wiesmann C, Brown EJ. Macrophage complement receptors and pathogen clearance. *Cell Microbiol*. 2007 Sep;9(9):2095–102.

84. Dupuy AG, Caron E. Integrin-dependent phagocytosis - spreading from microadhesion to new concepts. *J Cell Sci.* 2008 May 6;121(11):1773–83.
85. Brown GD. Dectin-1: a signalling non-TLR pattern-recognition receptor. *Nat Rev Immunol.* 2006 Jan;6(1):33–43.
86. Elomaa O, Kangas M, Sahlberg C, Tuukkanen J, Sormunen R, Liakka A, et al. Cloning of a novel bacteria-binding receptor structurally related to scavenger receptors and expressed in a subset of macrophages. *Cell.* 1995;80(4):603–9.
87. Bowdish DM, Gordon S. Conserved domains of the class A scavenger receptors: evolution and function. *Immunol Rev.* 2009;227(1):19–31.
88. Li FJ, Kubagawa Y, McCollum MK, Wilson L, Motohashi T, Bertoli LF, et al. Enhanced levels of both the membrane-bound and soluble forms of IgM Fc receptor (Fc R) in patients with chronic lymphocytic leukemia. *Blood.* 2011 Nov 3;118(18):4902–9.
89. Kambayashi T, Laufer TM. Atypical MHC class II-expressing antigen-presenting cells: can anything replace a dendritic cell? *Nat Rev Immunol.* 2014 Oct 17;14(11):719–30.
90. Rabinovitch M. Professional and non-professional phagocytes: an introduction. *Trends Cell Biol.* 1995;5(3):85–7.
91. Janeway, CA Jr, Travers, P, Walport, M. Immunological Memory. In: *Immunobiology: The Immune System in Health and Disease* [Internet]. 5th Edition. New York: Garland Science; 2001. Available from: <http://www.ncbi.nlm.nih.gov/books/NBK27158/>
92. Ramírez-Valle F, Gray EE, Cyster JG. Inflammation induces dermal V γ 4+ γ δ T17 memory-like cells that travel to distant skin and accelerate secondary IL-17-driven responses. *Proc Natl Acad Sci.* 2015 Jun 30;112(26):8046–51.
93. Cui Y, Kang L, Cui L, He W. Human γ δ T cell Recognition of lipid A is predominately presented by CD1b or CD1c on dendritic cells. *Biol Direct.* 2009;4(1):47.
94. Komori HK, Witherden DA, Kelly R, Sendaydiego K, Jameson JM, Teyton L, et al. Cutting Edge: Dendritic Epidermal T Cell Ligands Are Rapidly and Locally Expressed by Keratinocytes following Cutaneous Wounding. *J Immunol.* 2012 Apr 1;188(7):2972–6.
95. Xu B, Pizarro JC, Holmes MA, McBeth C, Groh V, Spies T, et al. Crystal structure of a T-cell receptor specific for the human MHC class I homolog MICA. *Proc Natl Acad Sci.* 2011 Feb 8;108(6):2414–9.

96. Chien, Y, Konigshofer, Y. Antigen recognition by gd T cells. *Immunol Rev.* 215:46–58.
97. Bhagat G, Naiyer AJ, Shah JG, Harper J, Jabri B, Wang TC, et al. Small intestinal CD8+TCR $\gamma\delta$ +NKG2A+ intraepithelial lymphocytes have attributes of regulatory cells in patients with celiac disease. *J Clin Invest.* 2008 Jan 2;118(1):281–93.
98. Szalai, A. J, Hu, X, Raman, C, Barnum, S R. Requirement of the Fc receptor common c-chain for gd T cell-mediated promotion of murine experimental autoimmune encephalomyelitis. *Eur J Immunol.* 2005;35:3487–92.
99. Ismail AS, Behrendt CL, Hooper LV. Reciprocal Interactions between Commensal Bacteria and Intraepithelial Lymphocytes during Mucosal Injury. *J Immunol.* 2009 Mar 1;182(5):3047–54.
100. Wang H, Henry O, Distefano MD, Wang Y-C, Raikkonen J, Monkkonen J, et al. Butyrophilin 3A1 Plays an Essential Role in Prenyl Pyrophosphate Stimulation of Human V 2V 2 T Cells. *J Immunol.* 2013 Aug 1;191(3):1029–42.
101. Kistowska M, Rossy E, Sansano S, Gober H-J, Landmann R, Mori L, et al. Dysregulation of the host mevalonate pathway during early bacterial infection activates human TCR $\gamma\delta$ cells. *Eur J Immunol.* 2008 Aug;38(8):2200–9.
102. Davey MS, Lin C-Y, Roberts GW, Heuston S, Brown AC, Chess JA, et al. Human Neutrophil Clearance of Bacterial Pathogens Triggers Anti-Microbial $\gamma\delta$ T Cell Responses in Early Infection. Wherry EJ, editor. *PLoS Pathog.* 2011 May 12;7(5):e1002040.
103. Kondo M, Izumi T, Fujieda N, Kondo A, Morishita T, Matsushita H, et al. Expansion of Human Peripheral Blood $\gamma\delta$ T Cells using Zoledronate. *J Vis Exp [Internet].* 2011 Sep 9 [cited 2016 Feb 15];(55). Available from: <http://www.jove.com/details.php?id=3182>
104. Espinosa E, Belmant C, Pont F, Luciani B, Poupot R, Romagné F, et al. Chemical Synthesis and Biological Activity of Bromohydrin Pyrophosphate, a Potent Stimulator of Human $\gamma\delta$ T Cells. *J Biol Chem.* 2001 May 25;276(21):18337–44.
105. Thompson K, Roelofs AJ, Jauhiainen M, Mönkkönen H, Mönkkönen J, Rogers MJ. Activation of $\gamma\delta$ T Cells by Bisphosphonates. In: Choi Y, editor. *Osteoimmunology [Internet].* Boston, MA: Springer US; 2009 [cited 2015 Oct 22]. p. 11–20. Available from: http://link.springer.com/10.1007/978-1-4419-1050-9_2
106. Ryan PL, Sumaria N, Holland CJ, Bradford CM, Izotova N, Grandjean CL, et al. Heterogeneous yet stable V δ 2⁽⁺⁾ T-cell profiles define distinct cytotoxic effector

- potentials in healthy human individuals. *Proc Natl Acad Sci*. 2016 Dec 13;113(50):14378–83.
107. Sallusto, F., Lenig, D., Forster, R., Lipp, M., Lanzavecchia, A. Two subsets of memory T lymphocytes with distinct homing potentials and effector functions. *Nature*. 1999;401:708–12.
 108. Hansson M, Lundgren A, Elgbratt K, Quiding-Järbrink M, Svennerholm A-M, Johansson E-L. Dendritic cells express CCR7 and migrate in response to CCL19 (MIP-3 β) after exposure to *Helicobacter pylori*. *Microbes Infect*. 2006 Mar;8(3):841–50.
 109. Riol-Blanco L, Sanchez-Sanchez N, Torres A, Tejedor A, Narumiya S, Corbi AL, et al. The Chemokine Receptor CCR7 Activates in Dendritic Cells Two Signaling Modules That Independently Regulate Chemotaxis and Migratory Speed. *J Immunol*. 2005 Apr 1;174(7):4070–80.
 110. Griffith JW, Sokol CL, Luster AD. Chemokines and Chemokine Receptors: Positioning Cells for Host Defense and Immunity. *Annu Rev Immunol*. 2014 Mar 21;32(1):659–702.
 111. van der Merwe PA, Dushek O. Mechanisms for T cell receptor triggering. *Nat Rev Immunol*. 2010 Jan;11(1):47–55.
 112. Chakraborty AK, Weiss A. Insights into the initiation of TCR signaling. *Nat Immunol*. 2014 Aug 19;15(9):798–807.
 113. Navarro MN, Cantrell DA. Serine-threonine kinases in TCR signaling. *Nat Immunol*. 2014 Aug 19;15(9):808–14.
 114. Malissen B, Grégoire C, Malissen M, Roncagalli R. Integrative biology of T cell activation. *Nat Immunol*. 2014 Aug 19;15(9):790–7.
 115. Groh V, Rhinehart R, Secrist H, Bauer S, Grabstein KH, Spies T. Broad tumor-associated expression and recognition by tumor-derived $\gamma\delta$ T cells of MICA and MICB. *Proc Natl Acad Sci*. 1999;96(12):6879–84.
 116. Vincent MS, Roessner K, Lynch D, Wilson D, Cooper SM, Tschopp J, et al. Apoptosis of Fas-high CD4+ synovial T cells by *Borrelia*-reactive Fas-ligand-high $\gamma\delta$ T cells in Lyme arthritis. *J Exp Med*. 1996;184(6):2109–18.
 117. Vincent MS, Roessner K, Sellati T, Huston CD, Sigal LH, Behar SM, et al. Lyme arthritis synovial $\gamma\delta$ T cells respond to *Borrelia burgdorferi* lipoproteins and lipidated hexapeptides. *J Immunol*. 1998;161(10):5762–71.
 118. H Spits, X Paliard, V H Engelhard and J E de Vries. Cytotoxic activity and lymphokine production of T cell receptor (TCR)-alpha beta+ and TCR-gamma

- delta+ cytotoxic T lymphocyte (CTL) clones recognizing HLA-A2 and HLA-A2 mutants. Recognition of TCR-gamma delta+ CTL clones is affected by mutations at positions 152 and 156. *J Immunol.* 1990;144:4156-62.
119. Ciccone E, Viale O, Pende D, Malnati M, Ferrara GB, Barocci S, et al. Specificity of human T lymphocytes expressing a γ/δ T cell antigen receptor. Recognition of a polymorphic determinant of HLA class I molecules by a γ/δ clone. *Eur J Immunol.* 1989;19(7):1267-71.
 120. Procelli, S., Brenner, M. B., Greenstein, J. L., Balk, S. P., Terhorst, C., Bleicher, P. A. Recognition of cluster of differentiation 1 antigens by human CD4-CD8-cytolytic T lymphocytes. *Nature.* 1989;(341):447-50.
 121. Faure F, Jitsukawa S, Miossec C, Hercend T. CD1c as a target recognition structure for human T lymphocytes: analysis with peripheral blood γ/δ cells. *Eur J Immunol.* 1990;20(3):703-6.
 122. Constant, P., Davodeu, F., Peyrat, M. A., Poquet, Y., Puzo, G., Bonneville, M., Fournie, J. J. Stimulation of Humany gamma delta T Cells by Nonpeptidic Mycobacterial Ligands. *Science.* 1994;264(5156):267-70.
 123. Tanaka, Y., Morita, C. T., Tanaka, Y., Nieves, E., Brenner, M. B., Bloom, B. R. Natural and synthetic non-peptide antigens recognized by human gamma delta T cells. *Nature.* 1995;375:155-9.
 124. Bukowski JF, Morita CT, Brenner MB. Human $\gamma\delta$ T cells recognize alkylamines derived from microbes, edible plants, and tea: implications for innate immunity. *Immunity.* 1999;11(1):57-65.
 125. Miyagawa F, Tanaka Y, Yamashita S, Minato N. Essential Requirement of Antigen Presentation by Monocyte Lineage Cells for the Activation of Primary Human ?? T Cells by Aminobisphosphonate Antigen. *J Immunol.* 2001 May 1;166(9):5508-14.
 126. Koning, F., Vietor, H., Verreck, F., Rust, J. J. C. Specific recognition of staphylococcal enterotoxin A by human T cells bearing receptors with the V gamma 9 region. *Nature.* 1990;346:572-4.
 127. Loh EY, Wang M, Bartkowiak J, Wiaderkiewicz R, Hyjek E, Wang Z, et al. Gene transfer studies of T cell receptor-gamma delta recognition. Specificity for staphylococcal enterotoxin A is conveyed by V gamma 9 alone. *J Immunol.* 1994;152(7):3324-32.
 128. Holoshitz J. Activation of $\gamma\delta$ T cells by mycobacterial antigens in rheumatoid arthritis. *Microbes Infect.* 1999;1(3):197-202.

129. Joseph Holoshitz, Luis M. Vila, Brian J. Keroack, Dawn R. McKinley, and Nancy K. Bayne. Dual Antigenic Recognition by Cloned Human gamma delta T Cells. *J Clin Invest.* 1992;89:308–14.
130. Fisch, P., Malkovsky, M., Kovats, S., Sturm, E., Braakman, E., Klein, B. S., Vos, S. D., Morrissey, L. W., DeMars, R., Welch, W. J., Bolhuis, R. L. H., Sondel, P. M. Recognition by Human V gamma 9 / V delta 2 T Cells of a GroEL Homolog on Daudi Burkitt's Lymphoma Cells. *Science.* 1990;250(4985):1269–73.
131. Hogquist KA, Jameson SC. The self-obsession of T cells: how TCR signaling thresholds affect fate “decisions” and effector function. *Nat Immunol.* 2014 Aug 19;15(9):815–23.
132. Sutton CE, Lalor SJ, Sweeney CM, Brereton CF, Lavelle EC, Mills KHG. Interleukin-1 and IL-23 Induce Innate IL-17 Production from ?? T Cells, Amplifying Th17 Responses and Autoimmunity. *Immunity.* 2009 Aug;31(2):331–41.
133. Ribot JC, deBarros A, Pang DJ, Neves JF, Peperzak V, Roberts SJ, et al. CD27 is a thymic determinant of the balance between interferon-?- and interleukin 17-producing ?? T cell subsets. *Nat Immunol.* 2009 Apr;10(4):427–36.
134. Lockhart E, Green AM, Flynn JL. IL-17 Production Is Dominated by ?? T Cells rather than CD4 T Cells during Mycobacterium tuberculosis Infection. *J Immunol.* 2006 Oct 1;177(7):4662–9.
135. Hamada S, Umemura M, Shiono T, Tanaka K, Yahagi A, Begum MD, et al. IL-17A Produced by $\gamma\delta$ T Cells Plays a Critical Role in Innate Immunity against *Listeria monocytogenes* Infection in the Liver. *J Immunol Baltim Md 1950.* 2008 Sep 1;181(5):3456–63.
136. Petermann F, Rothhammer V, Claussen MC, Haas JD, Blanco LR, Heink S, et al. ?? T Cells Enhance Autoimmunity by Restraining Regulatory T Cell Responses via an Interleukin-23-Dependent Mechanism. *Immunity.* 2010 Sep;33(3):351–63.
137. Sumaria N, Roediger B, Ng LG, Qin J, Pinto R, Cavanagh LL, et al. Cutaneous immunosurveillance by self-renewing dermal ?? T cells. *J Exp Med.* 2011 Mar 14;208(3):505–18.
138. Cai Y, Shen X, Ding C, Qi C, Li K, Li X, et al. Pivotal Role of Dermal IL-17-Producing ?? T Cells in Skin Inflammation. *Immunity.* 2011 Oct;35(4):596–610.
139. Michel, M. L., Pang, D. J., Haque, S. F. Y., Potocnik, A. J., Pennington, D. J., Hayday, A. C. Interleukin 7 (IL-7) selectively promotes mouse and human IL-17-producing $\gamma\delta$ cells. *PNAS.* 2012;109(43):17549–54.

140. Jensen KDC, Su X, Shin S, Li L, Youssef S, Yamasaki S, et al. Thymic Selection Determines ?? T Cell Effector Fate: Antigen-Naive Cells Make Interleukin-17 and Antigen-Experienced Cells Make Interferon ? Immunity. 2008 Jul;29(1):90–100.
141. Turchinovich G, Hayday AC. Skint-1 Identifies a Common Molecular Mechanism for the Development of Interferon- γ -Secreting versus Interleukin-17-Secreting $\gamma\delta$ T Cells. Immunity. 2011 Jul;35(1):59–68.
142. Haas JD, González FHM, Schmitz S, Chennupati V, Föhse L, Kremmer E, et al. CCR6 and NK1.1 distinguish between IL-17A and IFN- γ -producing $\gamma\delta$ effector T cells. Eur J Immunol. 2009 Dec 1;39(12):3488–97.
143. Wencker M, Turchinovich G, Di Marco Barros R, Deban L, Jandke A, Cope A, et al. Innate-like T cells straddle innate and adaptive immunity by altering antigen-receptor responsiveness. Nat Immunol. 2014 Jan;15(1):80–7.
144. Chodaczek G, Papanna V, Zal MA, Zal T. Body-barrier surveillance by epidermal ?? TCRs. Nat Immunol. 2012 Feb 12;13(3):272–82.
145. Heid HW, Winter S, Bruder G, Keenan TW, Jarasch E-D. Butyrophilin, an apical plasma membrane-associated glycoprotein characteristic of lactating mammary glands of diverse species. Biochim Biophys Acta BBA-Biomembr. 1983;728(2):228–38.
146. Smith IA, Knezevic BR, Ammann JU, Rhodes DA, Aw D, Palmer DB, et al. BTN1A1, the Mammary Gland Butyrophilin, and BTN2A2 Are Both Inhibitors of T Cell Activation. J Immunol. 2010 Apr 1;184(7):3514–25.
147. Arnett HA, Viney JL. Immune modulation by butyrophilins. Nat Rev Immunol. 2014 Jul 25;14(8):559–69.
148. Ikemizu, S., Gilbert, R. J. C., Fennelly, J. A., Collins, A. V., Harlos, K., Jones, E. Y., et al. Structure and Dimerization of a Soluble Form of B7-1. Immunity. 2000;12:51–60.
149. Compte E, Pontarotti P, Collette Y, Lopez M, Olive D. Frontline: Characterization of BT3 molecules belonging to the B7 family expressed on immune cells. Eur J Immunol. 2004 Aug 1;34(8):2089–99.
150. Chapoval AI, Smithson G, Brunick L, Mesri M, Boldog FL, Andrew D, et al. BTNL8, a butyrophilin-like molecule that costimulates the primary immune response. Mol Immunol. 2013 Dec;56(4):819–28.
151. Jeong J, Rao AU, Xu J, Ogg SL, Hathout Y, Fenselau C, et al. The PRY/SPRY/B30.2 Domain of Butyrophilin 1A1 (BTN1A1) Binds to Xanthine Oxidoreductase. J Biol Chem. 2009 Aug 14;284(33):22444–56.

152. Sandstrom A, Peigné C-M, Léger A, Crooks JE, Konczak F, Gesnel M-C, et al. The Intracellular B30.2 Domain of Butyrophilin 3A1 Binds Phosphoantigens to Mediate Activation of Human V γ 9V δ 2 T Cells. *Immunity*. 2014 Apr;40(4):490–500.
153. Rhodes DA, De Bono B, Trowsdale J. Relationship between SPRY and B30.2 protein domains. Evolution of a component of immune defence? *Immunology*. 2005 Dec 1;116(4):411–7.
154. Perfetto L, Gherardini PF, Davey NE, Diella F, Helmer-Citterich M, Cesareni G. Exploring the diversity of SPRY/B30.2-mediated interactions. *Trends Biochem Sci*. 2013 Jan;38(1):38–46.
155. Simone R, Barbarat B, Rabellino A, Icardi G, Bagnasco M, Pesce G, et al. Ligation of the BT3 molecules, members of the B7 family, enhance the proinflammatory responses of human monocytes and monocyte-derived dendritic cells. *Mol Immunol*. 2010 Nov;48(1-3):109–18.
156. Messal N, Mamessier E, Sylvain A, Celis-Gutierrez J, Thibult M-L, Chetaille B, et al. Differential role for CD277 as a co-regulator of the immune signal in T and NK cells. *Eur J Immunol*. 2011 Dec 1;41(12):3443–54.
157. Palakodeti A, Sandstrom A, Sundaresan L, Harly C, Nedellec S, Olive D, et al. The Molecular Basis for Modulation of Human V γ 9V δ 2 T Cell Responses by CD277/Butyrophilin-3 (BTN3A)-specific Antibodies. *J Biol Chem*. 2012 Sep 21;287(39):32780–90.
158. Yamashiro H, Yoshizaki S, Tadaki T, Egawa K, Seo N. Stimulation of human butyrophilin 3 molecules results in negative regulation of cellular immunity. *J Leukoc Biol*. 2010 Oct 1;88(4):757–67.
159. Rhodes DA, Stammers M, Malcherek G, Beck S, Trowsdale J. The Cluster of BTN Genes in the Extended Major Histocompatibility Complex. *Genomics*. 2001 Feb;71(3):351–62.
160. Rhodes DA, Reith W, Trowsdale J. Regulation of Immunity by Butyrophilins. *Annu Rev Immunol*. 2016 May 20;34(1):151–72.
161. Rhodes DA, Chen H-C, Price AJ, Keeble AH, Davey MS, James LC, et al. Activation of Human $\gamma\delta$ T Cells by Cytosolic Interactions of BTN3A1 with Soluble Phosphoantigens and the Cytoskeletal Adaptor Periplakin. *J Immunol*. 2015 Mar 1;194(5):2390–8.
162. Harly C, Peigné C-M, Scotet E. Molecules and Mechanisms Implicated in the Peculiar Antigenic Activation Process of Human V γ 9V δ 2 T Cells. *Front Immunol* [Internet]. 2015 Jan 5 [cited 2017 Jul 7];5. Available from: <http://journal.frontiersin.org/article/10.3389/fimmu.2014.00657/abstract>

163. Esser C. A fat story—antigen presentation by butyrophilin 3A1 to $\gamma\delta$ T cells. *Cell Mol Immunol*. 2014;11(1):5.
164. Vavassori S, Kumar A, Wan GS, Ramanjaneyulu GS, Cavallari M, El Daker S, et al. Butyrophilin 3A1 binds phosphorylated antigens and stimulates human $\gamma\delta$ T cells. *Nat Immunol*. 2013 Jul 21;14(9):908–16.
165. Kabelitz D. Critical role of butyrophilin 3A1 in presenting prenyl pyrophosphate antigens to human $\gamma\delta$ T cells. *Cell Mol Immunol*. 2014;11(2):117.
166. Vermijlen D, Prinz I. Ontogeny of Innate T Lymphocytes “Some Innate Lymphocytes are More Innate than Others. *Front Immunol* [Internet]. 2014 Oct 10 [cited 2017 Nov 5];5. Available from: <http://journal.frontiersin.org/article/10.3389/fimmu.2014.00486/abstract>
167. Le Goff B, Soltner E, Charrier C, Maugars Y, R dini F, Heymann D, et al. A combination of methotrexate and zoledronic acid prevents bone erosions and systemic bone mass loss in collagen induced arthritis. *Arthritis Res Ther*. 2009;11(6):R185.
168. Busetto S, Trevisan E, Patriarca P, Menegazzi R. A single-step, sensitive flow cytofluorometric assay for the simultaneous assessment of membrane-bound and ingested *Candida albicans* in phagocytosing neutrophils. *Cytometry*. 2004 Apr;58A(2):201–6.
169. Dabita D, Margolick JB, Lopez J, Bream JH. Multiplex measurement of proinflammatory cytokines in human serum: Comparison of the Meso Scale Discovery electrochemiluminescence assay and the Cytometric Bead Array. *J Immunol Methods*. 2011 Sep;372(1-2):71–7.
170. Correia DV, Fogli M, Hudspeth K, da Silva MG, Mavilio D, Silva-Santos B. Differentiation of human peripheral blood V 1+ T cells expressing the natural cytotoxicity receptor NKp30 for recognition of lymphoid leukemia cells. *Blood*. 2011 Jul 28;118(4):992–1001.
171. Russell DG, VanderVen BC, Glennie S, Mwandumba H, Heyderman RS. The macrophage marches on its phagosome: dynamic assays of phagosome function. *Nat Rev Immunol*. 2009;9(8):594–600.
172. Tollis, S., Dart, A. E., Tzircotis, G., Endres, R. G. The zipper mechanism in phagocytosis: energetic requirements and variability in phagocytic cup shape. *BMC Syst Biol* [Internet]. 2010;4(149). Available from: <http://www.biomedcentral.com/1752-0509/4/149>

173. Tse SML, Furuya W, Gold E, Schreiber AD, Sandvig K, Inman RD, et al. Differential Role of Actin, Clathrin, and Dynamin in Fc Receptor-mediated Endocytosis and Phagocytosis. *J Biol Chem*. 2003 Jan 31;278(5):3331–8.
174. Wu J, Pugh R, Laughlin RC, Andrews-Polymenis H, McClelland M, Bäumlner AJ, et al. High-throughput Assay to Phenotype *Salmonella enterica* Typhimurium Association, Invasion, and Replication in Macrophages. *J Vis Exp JoVE* [Internet]. 2014 Aug 11;(90). Available from: <http://www.ncbi.nlm.nih.gov/pmc/articles/PMC4500590/>
175. Backert S, Hofreuter D. Molecular methods to investigate adhesion, transmigration, invasion and intracellular survival of the foodborne pathogen *Campylobacter jejuni*. *J Microbiol Methods*. 2013 Oct;95(1):8–23.
176. Koziel J, Maciag-Gudowska A, Mikolajczyk T, Bzowska M, Sturdevant DE, Whitney AR, et al. Phagocytosis of *Staphylococcus aureus* by Macrophages Exerts Cytoprotective Effects Manifested by the Upregulation of Antiapoptotic Factors. Ratner AJ, editor. *PLoS ONE*. 2009 Apr 21;4(4):e5210.
177. Amiel E, Lovewell RR, O'Toole GA, Hogan DA, Berwin B. *Pseudomonas aeruginosa* Evasion of Phagocytosis Is Mediated by Loss of Swimming Motility and Is Independent of Flagellum Expression. *Infect Immun*. 2010 Jul;78(7):2937–45.
178. Himoudi N, Morgenstern DA, Yan M, Vernay B, Saraiva L, Wu Y, et al. Human $\gamma\delta$ T Lymphocytes Are Licensed for Professional Antigen Presentation by Interaction with Opsonized Target Cells. *J Immunol*. 2012 Feb 15;188(4):1708–16.
179. Ryan-Payseur B, Frencher J, Shen L, Chen CY, Huang D, Chen ZW. Multieffector-Functional Immune Responses of HMBPP-Specific V 2V 2 T Cells in Nonhuman Primates Inoculated with *Listeria monocytogenes actA prfA**. *J Immunol*. 2012 Aug 1;189(3):1285–93.
180. Kondo M, Izumi T, Fujieda N, Kondo A, Morishita T, Matsushita H, et al. Expansion of Human Peripheral Blood $\gamma\delta$ T Cells using Zoledronate. *J Vis Exp* [Internet]. 2011 Sep 9 [cited 2016 Feb 15];(55). Available from: <http://www.jove.com/details.php?id=3182>
181. Wang H, Fang Z, Morita CT. V 2V 2 T Cell Receptor Recognition of Prenyl Pyrophosphates Is Dependent on All CDRs. *J Immunol*. 2010 Jun 1;184(11):6209–22.
182. Brandes M. Flexible migration program regulates T-cell involvement in humoral immunity. *Blood*. 2003 Jul 31;102(10):3693–701.

183. Chen Z, Freedman MS. Correlation of specialized CD16+ $\gamma\delta$ T cells with disease course and severity in multiple sclerosis. *J Neuroimmunol*. 2008 Feb;194(1-2):147–52.
184. Alexander AAZ, Maniar A, Cummings J-S, Hebbeler AM, Schulze DH, Gastman BR, et al. Isopentenyl Pyrophosphate-Activated CD56+ T Lymphocytes Display Potent Antitumor Activity toward Human Squamous Cell Carcinoma. *Clin Cancer Res*. 2008 Jul 1;14(13):4232–40.
185. Garnache-Ottou F, Chaperot L, Biichle S, Ferrand C, Remy-Martin J-P, Deconinck E, et al. Expression of the myeloid-associated marker CD33 is not an exclusive factor for leukemic plasmacytoid dendritic cells. *Blood*. 2005;105(3):1256–64.
186. Wesch D, Peters C, Oberg H-H, Pietschmann K, Kabelitz D. Modulation of $\gamma\delta$ T cell responses by TLR ligands. *Cell Mol Life Sci*. 2011 Jul;68(14):2357–70.
187. Dar AA, Patil RS, Chiplunkar SV. Insights into the Relationship between Toll Like Receptors and Gamma Delta T Cell Responses. *Front Immunol* [Internet]. 2014 Jul 31 [cited 2015 Apr 16];5. Available from: <http://journal.frontiersin.org/article/10.3389/fimmu.2014.00366/abstract>
188. Lang KS, Lang PA, Meryk A, Pandyra AA, Boucher L-M, Pozdeev VI, et al. Involvement of Toso in activation of monocytes, macrophages, and granulocytes. *Proc Natl Acad Sci*. 2013 Feb 12;110(7):2593–8.
189. Bouwman LI, de Zoete MR, Bleumink-Pluym NMC, Flavell RA, van Putten JPM. Inflammasome Activation by *Campylobacter jejuni*. *J Immunol*. 2014 Nov 1;193(9):4548–57.
190. Siegesmund AM. *Campylobacter jejuni* infection of differentiated THP-1 macrophages results in interleukin 1 release and caspase-1-independent apoptosis. *Microbiology*. 2004 Mar 1;150(3):561–9.
191. Glatzel A, Wesch D, Schiemann F, Brandt E, Janssen O, Kabelitz D. Patterns of Chemokine Receptor Expression on Peripheral Blood T Lymphocytes: Strong Expression of CCR5 Is a Selective Feature of V α 2/V β 9 T Cells. *J Immunol*. 2002 May 15;168(10):4920–9.
192. Penido C, Costa MFS, Souza MC, Costa KA, Candea ALP, Benjamim CF, et al. Involvement of CC chemokines in T lymphocyte trafficking during allergic inflammation: the role of CCL2/CCR2 pathway. *Int Immunol*. 2008 Jan 1;20(1):129–39.
193. Kabelitz D, Wesch D. Features and functions of gamma delta T lymphocytes: focus on chemokines and their receptors. *Crit Rev Immunol*. 2003;23(5-6):339–70.

194. Yu T-K, Caudell EG, Smid C, Grimm EA. IL-2 Activation of NK Cells: Involvement of MKK1/2/ERK But Not p38 Kinase Pathway. *J Immunol.* 2000 Jun 15;164(12):6244–51.
195. Schilbach K, Geiselhart A, Handgretinger R. Induction of proliferation and augmented cytotoxicity of $\gamma\delta$ T lymphocytes by bisphosphonate clodronate. *Blood.* 2001;97(9):2917–2917.
196. Fowler DW, Copier J, Dagleish AG, Bodman-Smith MD. Zoledronic acid causes $\gamma\delta$ T cells to target monocytes and down-modulate inflammatory homing. *Immunology.* 2014 Dec;143(4):539–49.
197. Porcelli S, Brenner MB, Band H. Biology of the Human γ T-Cell Receptor. *Immunol Rev.* 1991;120(1):137–83.
198. Parker CM, Groh V, Band H, Porcelli SA, Morita C, Fabbi M, et al. Evidence for extrathymic changes in the T cell receptor gamma/delta repertoire. *J Exp Med.* 1990;171(5):1597–612.
199. Botelho, R. J. G S. Phagocytosis. *Curr Biol.* 2011;21(14):R532–3.
200. Dellabona P, Casorati G, Friedli B, Angman L, Sallusto F, Tunnacliffe A, et al. In vivo persistence of expanded clones specific for bacterial antigens within the human T cell receptor alpha/beta CD4-8-subset. *J Exp Med.* 1993;177(6):1763–71.
201. Olsen I, Lundin KE, Sollid LM. Increased frequency of intestinal CD4+ T cells reactive with mycobacteria in patients with Crohn's disease. *Scand J Gastroenterol.* 2013 Nov;48(11):1278–85.
202. Howe R, Dillon S, Rogers L, McCarter M, Kelly C, Gonzalez R, et al. Evidence for Dendritic Cell-Dependent CD4+ T Helper-1 Type Responses to Commensal Bacteria in Normal Human Intestinal Lamina Propria. *Clin Immunol Orlando Fla.* 2009 May;131(2):317–32.
203. Syrbe U, Scheer R, Wu P, Sieper J. Differential synovial Th1 cell reactivity towards *Escherichia coli* antigens in patients with ankylosing spondylitis and rheumatoid arthritis. *Ann Rheum Dis.* 2012;71(9):1573–6.
204. Dura B, Dougan SK, Barisa M, Hoehl MM, Lo CT, Ploegh HL, et al. Profiling lymphocyte interactions at the single-cell level by microfluidic cell pairing. *Nat Commun.* 2015 Jan 13;6:5940.
205. Richards MH, Nelson JL. The evolution of vertebrate antigen receptors: a phylogenetic approach. *Mol Biol Evol.* 2000;17(1):146–55.

206. Hirano M, Guo P, McCurley N, Schorpp M, Das S, Boehm T, et al. Evolutionary implications of a third lymphocyte lineage in lampreys. *Nature*. 2013 Aug 11;501(7467):435–8.
207. Dai Y, Chen H, Mo C, Cui L, He W. Ectopically Expressed Human Tumor Biomarker MutS Homologue 2 Is a Novel Endogenous Ligand That Is Recognized by Human ?? T Cells to Induce Innate Anti-tumor/Virus Immunity. *J Biol Chem*. 2012 May 11;287(20):16812–9.
208. Owens GC, Erickson KL, Malone CC, Pan C, Huynh MN, Chang JW, et al. Evidence for the involvement of gamma delta T cells in the immune response in Rasmussen encephalitis. *J Neuroinflammation* [Internet]. 2015 Dec [cited 2017 Jul 3];12(1). Available from: <http://www.jneuroinflammation.com/content/12/1/134>
209. Glanville N, Message SD, Walton RP, Pearson RM, Parker HL, Laza-Stanca V, et al. $\gamma\delta$ T cells suppress inflammation and disease during rhinovirus-induced asthma exacerbations. *Mucosal Immunol* [Internet]. 2013 Feb 6 [cited 2017 Jul 3]; Available from: <http://www.nature.com/doi/10.1038/mi.2013.3>
210. Davey MS, Willcox CR, Joyce SP, Ladell K, Kasatskaya SA, McLaren JE, et al. Clonal selection in the human V δ 1 T cell repertoire indicates $\gamma\delta$ TCR-dependent adaptive immune surveillance. *Nat Commun*. 2017 Mar 1;8:14760.
211. Fisher JPH, Yan M, Heuwerkerk J, Carter L, Abolhassani A, Frosch J, et al. Neuroblastoma killing properties of V-delta 2 and V-delta2 negative gamma delta T cells following expansion by artificial antigen presenting cells. *Clin Cancer Res Off J Am Assoc Cancer Res*. 2014 Nov 15;20(22):5720–32.
212. Deetz CO, Hebbeler AM, Propp NA, Cairo C, Tikhonov I, Pauza CD. Gamma Interferon Secretion by Human V γ 2V δ 2 T Cells after Stimulation with Antibody against the T-Cell Receptor plus the Toll-Like Receptor 2 Agonist Pam3Cys. *Infect Immun*. 2006 Aug 1;74(8):4505–11.
213. Peigné C-M, Léger A, Gesnel M-C, Konczak F, Olive D, Bonneville M, et al. The Juxtamembrane Domain of Butyrophilin BTN3A1 Controls Phosphoantigen-Mediated Activation of Human V γ 9V δ 2 T Cells. *J Immunol*. 2017 Jun 1;198(11):4228–34.
214. Lena H-JGMK, Jenö AP, Mori L, De Libero G. Human T Cell Receptor Cells Recognize Endogenous Mevalonate Metabolites in Tumor Cells. 2015 Oct 22 [cited 2015 Oct 22]; Available from: <http://journal.9med.net/qikan/article.php?id=56556>
215. Nguyen K, Li J, Puthenveetil R, Lin X, Poe MM, Hsiao C-HC, et al. The butyrophilin 3A1 intracellular domain undergoes a conformational change involving the juxtamembrane region. *FASEB J*. 2017 Jul 13;31(13):201601370RR.

216. Dutta I, Postovit L-M, Siegers GM. Apoptosis Induced via Gamma Delta T Cell Antigen Receptor “Blocking” Antibodies: A Cautionary Tale. *Front Immunol* [Internet]. 2017 Jun 30 [cited 2017 Jul 27];8. Available from: <http://journal.frontiersin.org/article/10.3389/fimmu.2017.00776/full>
217. Pfeffer LM. The Role of Nuclear Factor κ B in the Interferon Response. *J Interferon Cytokine Res*. 2011 Jul;31(7):553–9.
218. Wesch D, Peters C, Oberg H-H, Pietschmann K, Kabelitz D. Modulation of $\gamma\delta$ T cell responses by TLR ligands. *Cell Mol Life Sci*. 2011 Jul;68(14):2357–70.
219. Gogoi D, Chiplunkar SV. Targeting gamma delta T cells for cancer immunotherapy: bench to bedside. *Indian J Med Res*. 2013;138(5):755.
220. Riganti C, Massaia M, Davey MS, Eberl M. Human $\gamma\delta$ T-cell responses in infection and immunotherapy: Common mechanisms, common mediators?: HIGHLIGHTS. *Eur J Immunol*. 2012 Jul;42(7):1668–76.
221. Gentles AJ, Newman AM, Liu CL, Bratman SV, Feng W, Kim D, et al. The prognostic landscape of genes and infiltrating immune cells across human cancers. *Nat Med*. 2015 Jul 20;21(8):938–45.
222. Dechanet J, Merville P, Berge F, Bone-Mane G, Taupin J L, Michel P, et al. Major Expansion of $\gamma\delta$ T Lymphocytes following Cytomegalovirus Infection in Kidney Allograft Recipients. *J Infect Dis*. 1999;179:1–8.
223. Worku S, Bjorkman A, Troye-Blomberg M, Jemaneh L, Farnert A. Lymphocyte activation and subset redistribution in the peripheral blood in acute malaria illness: distinct gamma delta + T cell patterns in *Plasmodium falciparum* and *P. vivax* infections. *J Clin Exp Immunol*. 1997;108:34–41.
224. D’Ombrian M C, Hansen D S, Simpson K M, Schofield L. $\gamma\delta$ -T cells expressing NK receptors predominate over NK cells and conventional T cells in the innate IFN- γ response to *Plasmodium falciparum* malaria. *Eur J Immunol*. 2007;37:1864–73.
225. Brandes M, Willimann K, Moser B. Professional antigen-presentation function by human $\gamma\delta$ T cells. *Science*. 2005;309(5732):264–8.
226. Alfaro C, Suarez N, Oñate C, Perez-Gracia JL, Martinez-Forero I, Hervas-Stubbs S, et al. Dendritic Cells Take up and Present Antigens from Viable and Apoptotic Polymorphonuclear Leukocytes. *PLoS ONE* [Internet]. 2011 Dec 20;6(12). Available from: <http://www.ncbi.nlm.nih.gov/pmc/articles/PMC3243708/>

227. Dürrbach A, Baple E, Preece AF, Charpentier B, Gustafsson K. Virus recognition by specific natural antibodies and complement results in MHC I cross-presentation. *Eur J Immunol.* 2007;37(5):1254–65.
228. Jameson JM, Cauvi G, Witherden DA, Havran WL. A Keratinocyte-Responsive TCR Is Necessary for Dendritic Epidermal T Cell Activation by Damaged Keratinocytes and Maintenance in the Epidermis. *J Immunol.* 2004 Mar 15;172(6):3573–9.
229. Minagawa, M., Ito, A., Shimura, H., Tomiyama, K., Ito, M., Kawai, K. Homogeneous epithelial gamma delta T cell repertoire of the skin is shaped through peripheral selection. *J Dermatol Sci.* 2001;25:150–5.
230. Ferrero, I., Wilson, A., Beerman, F., Held, W., MacDonald, H. R. T Cell Receptor Specificity Is Critical for the Development of Epidermal gamma delta T Cells. *J Exp Med.* 2001;194(10):1473–83.
231. Starick L, Riano F, Karunakaran MM, Kunzmann V, Li J, Kreiss M, et al. Butyrophilin 3A (BTN3A, CD277)-specific antibody 20.1 differentially activates V γ 9V δ 2 TCR clonotypes and interferes with phosphoantigen activation. *Eur J Immunol.* 2017 Jun;47(6):982–92.
232. Farrington LA, Jagannathan P, McIntyre TI, Vance HM, Bowen K, Boyle MJ, et al. Frequent Malaria Drives Progressive V δ 2 T-Cell Loss, Dysfunction, and CD16 Up-regulation During Early Childhood. *J Infect Dis.* 2015 Dec 13;jiv600.

SUPPLEMENTARY MEDIA MATERIAL

Fig. 5.4. V δ 2 cell expansion leads to their acquisition of a phagocyte-like morphology and probing behaviour.

Panel (C). Day 14 *E.coli*-expanded PBMC were stained with V δ 2-PE mAb and examined via confocal microscopy. Shown is a representative field of vision, with PBMC in light phase contrast. Light phase contrast images from the same field of vision as shown in Fig.5.4 panel (A) were collected every 2 seconds for 5 minutes. Shown is a video sequence of the collected images. V δ 2 PBMC are indicated with white arrows.

APPENDIX

***E.coli* promotes human V γ 9 δ 2 T cell transition from cytokine-producing bactericidal effectors to professional phagocytic killers in a TCR-dependent manner**

Nature Scientific Reports. DOI:10.1038/s41598-017-02886-8.